

LEGISLATIVE REFERENCE LIBRARY
QE128.L4 L39 1991

Lawler, T. L. - Aeromagnetic interpretation pseudo



3 0307 00042 8592

This document is made available electronically by the Minnesota Legislative Reference Library as part of an ongoing digital archiving project. <http://www.leg.state.mn.us/lrl/lrl.asp>
(Funding for document digitization was provided, in part, by a grant from the Minnesota Historical & Cultural Heritage Program.)

Report 290

Aeromagnetic Interpretation Pseudo-Geologic Maps, with Evaluation, in Lake of the Woods and Lake Counties, Minnesota

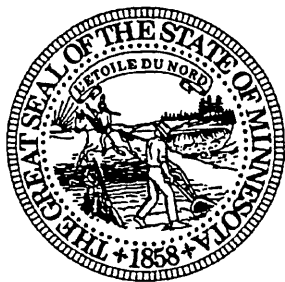


RECEIVED
SEP 10 1991
SECRETARY OF
THE SENATE

**Minnesota Department of
Natural Resources
Division of Minerals**

1991

QE
128
.L4
L39
1991



Minnesota Department of Natural Resources
Division of Minerals
William C. Brice, Director

Report 290

**Aeromagnetic Interpretation Pseudo-Geologic Maps,
with Evaluation, in Lake of the Woods and Lake Counties,
Minnesota**

By:
T. L. Lawler and E. A. Venzke

RECEIVED

MAR 9 1993

LEGISLATIVE REFERENCE LIBRARY
STATE CAPITOL
ST. PAUL, MN. 55155

A Minerals Diversification Project

1991

Publication Notification

Equal opportunity to participate in and benefit from programs of the Minnesota Department of Natural Resources is available to all individuals regardless of race, color, national origin, sex, age or disability. Discrimination inquiries should be sent to MN-DNR, 500 Lafayette Road, St. Paul, MN 55155-4049 or the Equal Opportunity Office, Department of the Interior, Washington, D.C. 20240.

This report is available at selected libraries in Minnesota. It may be purchased at the Hibbing Office, DNR Minerals Division. For further information contact Minerals Resource Geologist at (218) 262-6767.

Neither the State of Minnesota nor the Department of Natural Resources, nor any of their employees, nor any of their contractors, subcontractors, nor their employees, makes any warranty, express or implied, or assumes any legal liability or responsibility for the accuracy, completeness or usefulness of any information, apparatus, product or process disclosed, or represents that its use would not infringe on privately owned rights.

Reference to a Company or Product name does not imply approval or recommendation of the product by the State of Minnesota or the Department of Natural Resources to the exclusion of others that may meet specifications.

Table of Contents

Table of Contents	i
List of Figures	iii
List of Tables	iv
List of Plates	iv
Executive Summary	1
Introduction	3
Purpose and Scope	3
Objectives	3
Structure of the Report	4
Acknowledgements	4
Baudette Area	5
Location and Access Baudette Area	5
Regional Geologic Setting	5
Previous Work and Exploration History	5
Methodology - Baudette Area	9
Drill Hole Data	9
Ground Geophysical Profile Data	9
Results and Discussion - Baudette Area	10
Comparison of Map and Drill Hole Data	10
Tests of Map with Ground Geophysical Profiles	11
Summary	13
McDougal Lakes Area	19
Introduction	19
Location and Access	19
Geologic Setting	21
Previous Work and Exploration History	21
Methodology - McDougal Lakes Area	23
New Drill Holes	23
Outcrops and Pebble Counts	23
Lithochemistry	24
Ground Geophysical Surveys	24
Additional Data Generated	24
Results and Discussion - McDougal Lakes Area	25
Comparison of Pseudo-Geologic and Geologic Maps	25
Structure	25
South Kawishiwi Intrusion	28
Bald Eagle Intrusion	28
Troctolite	28
Anorthosite	28

Oxide-rich Rocks	29
Granophyre	29
Geophysical Measurements of Drill Core	29
Lithochemistry of Drill Core and Outcrops	33
Anorthositic Rocks	33
Bald Eagle Intrusion	33
Oxide Gabbros	36
Ground Geophysical Surveys	36
Summary	37
Conclusions	43
Baudette Area	43
McDougal Lakes Area	43
Recommendations	44
References	45
Appendix 290-A. Project Chronology	A-1
Appendix 290-B. TH Drill Core Summary Information	B-1
Lithologic Log for DDH TH-1	B-2
Lithologic Log for DDH TH-2	B-3
Lithologic Log for DDH TH-3	B-4
Lithologic Log for DDH TH-4	B-5
Lithologic Log for DDH TH-5	B-6
Lithologic Log for DDH TH-6	B-7
Appendix 290-C. Density and Magnetic Susceptibility Measurements on TH Drillholes	C-1
Appendix 290-D. Report on Aeromagnetic Data Interpretation, Baudette Area, Minnesota	D-1
Appendix 290-E. Aeromagnetic Data Interpretation for the McDougal Lakes Area, Duluth Complex, Lake County, Minnesota	E-1
Appendix 290-F. Drift Pebble Lithology of the Tomahawk Road Area, Lake County, Minnesota: Can it be used to infer local bedrock?	F-1
Appendix 290-G. Drill Core and Outcrop Assay Data	G-1
Addendum	Pocket 4

List of Figures

	Page
Figure 290-1. Pseudo-geologic map of the original four-township Baudette Area (simplified from Spector, Plate 2) showing drillhole locations and geophysics traverses.	6
Figure 290-2. Regional geology of northern Minnesota (after Southwick and Morey, 1990) showing the original Baudette pseudo-geologic map area and the extended area.	7
Figure 290-3. VLF-EM profile from station 36,400S to 37,450S (Section 18, T157N, R33W).	14
Figure 290-4. Magnetic susceptibility profile from station 20,750S to 22,600S (Section 31, T158N, R33W).	14
Figure 290-5. Magnetic susceptibility profile from station 4,150E to 4,500E (Section 36, T159N, R33W).	15
Figure 290-6. Magnetic susceptibility profile from station 5,900 to 7,400 (Section 36, T159N, R33W) showing both Magnetic Total Field and Magnetic Gradient measurements.	15
Figure 290-7. Magnetic susceptibility profile from stations 2,600E to 4,000E (Section 17, T160N, R33W).	16
Figure 290-8. VLF-EM profile from station 1,500S to 3,200S (Section 1, T160N, R33W).	16
Figure 290-9. Magnetic susceptibility profile from station 1,500S to 3,200S (Section 1, T160N, R33W). . .	17
Figure 290-10. Pseudo-geologic map of the McDougal Lakes Area (simplified from Ferderer, Plate 3) with drillhole locations. See Plate 3 for explanation of legend.	20
Figure 290-11. Regional geologic map of northeastern Minnesota (from Buchheit and others, 1989) showing the geochemical till survey area and the McDougal Lakes pseudo-geologic map area.	22
Figure 290-12. Forward modeling profile H-H' (modified from Ferderer, 1989).	27
Figure 290-13. Summary of magnetic susceptibility measurements on drill core.	31
Figure 290-14. Summary of density measurements on drill core.	32
Figure 290-15. MgO vs. FeO* variation diagram showing geochemical fields with associated lithologic names of samples. Project 290 data from this study; Project 255 data from Dahlberg and others (1989).	34
Figure 290-16. CaO vs. TiO ₂ variation diagram showing geochemical fields with associated lithologic names of samples. Project 290 data from this study; Project 255 data from Dahlberg and others (1989).	34
Figure 290-17. AFM diagram of McDougal Lakes Area analyses.	35
Figure 290-18. Variation diagram of MG# vs. Ni showing varieties of Troctolite-Picrite.	35
Figure 290-19. VLF-EM profile from station 600W to 3,000W (Section 30, T61N, R9W).	38
Figure 290-20. Magnetic susceptibility profile from station 600W to 3,000W (Section 30, T61N, R9W). . .	38
Figure 290-21. VLF-EM profile from station 2,000N to 3,350N (Section 25, T61N, R10W).	39
Figure 290-22. Magnetic susceptibility profile from station 2,000N to 3,350N (Section 25, T61N, R10W). . .	39
Figure 290-23. VLF-EM profile from station 8,200W to 10,000W (Section 26, T61N, R10W).	40
Figure 290-24. Magnetic susceptibility profile from station 8,200W to 10,000W (Section 26, T61N, R10W).	40
Figure 290-25. Magnetic susceptibility and VLF-EM profile from station 1,100S to 2,700S (Section 32, T61N, R9W).	41
Figure 290-26. VLF-EM profile from station 2,000S to 3,600S (Section 3, T61N, R10W).	41

List of Tables

	Page
Table 290-1. Comparison of Drillhole Data and Baudette Area Pseudo-Geologic Map.	11
Table 290-2. Tests with Ground Geophysical Profiles in the Baudette Area.	13
Table 290-3. Comparison of Drillholes, Core Analyses, and Outcrops with the McDougal Lakes Area Pseudo-Geologic Map.	26

List of Plates

	Pocket
Plate 290-1. Flight Path Plot Baudette Area.	1
Plate 290-2. Aeromagnetic Interpretation Baudette Area.	2
Plate 290-3. Aeromagnetic Data Interpretation for the McDougal Lakes Area, Duluth Complex	3
Plate 290-4. Aeromagnetic Data Interpretation of a 12 township block near Baudette.	4

Executive Summary

Recent improvements in the quality of geophysical surveys, combined with sophisticated computer enhancement techniques, now provide the capability to infer geologic features based on geophysical studies. Maps showing geologic information inferred from remote measurements of physical properties are called pseudo-geologic maps. For accurate and detailed interpretations, these maps require high resolution aeromagnetic and regional gravity surveys. In Minnesota these are available due to the efforts of the Minnesota Geological Survey and the United States Geological Survey. Most of the aeromagnetic survey work was funded by the Legislative Commission on Minnesota Resources (LCMR).

Conventional geologic maps are a reflection of the quantity and quality of available geologic information. A paucity of geologic data results in simple maps showing only major lithologic units and structural features. Obtaining more geologic data with traditional drilling methods is expensive, particularly in areas of deep overburden. Geophysical interpretations, when combined with known geology, can result in more detailed geologic maps. These maps display detailed geologic information which includes lithologic units, structural features, and depths to magnetic source not available on standard geologic maps. These details, combined with geochemical and geophysical data, can reveal areas of economic mineral potential and help plan effective programs to locate such mineral potential. Accurate, detailed, geologic maps are a valuable resource essential for making good land management decisions and encouraging exploration by private industry. Pseudo-geologic maps are a relatively inexpensive way of providing these maps in areas with deep overburden and few outcrops.

The Department of Natural Resources (DNR), in a pilot program designed to test the practicality and accuracy of pseudo-geologic maps, selected two areas and contracted with private consultants to interpret the geophysical data and make maps of these areas. The DNR then evaluated these maps using a variety of methods to determine if they were accurate. The two areas were selected where previous work indicated good mineral potential and there is considerable state mineral ownership, but little or no current activity by private industry. One strip of four townships near Baudette, Minnesota, is in a faulted, Archean, granite-greenstone terrain where there are deep glacial deposits and good potential for gold or base metal deposits. The other four township block is in the McDougal Lakes area of Lake County, within the central Duluth Complex where geochemical surveys showed elevated base and platinum group mineral trends in glacial overburden. Glacial cover is not too deep over most of the area (the deepest glacial drift intersected in drill holes is sixty-one feet), and there are some outcrops.

The Baudette Area was mapped by Dr. Allan Spector from Toronto, Canada, who has a broad background in Archean granite-greenstone terranes having gold or base metal mineral potential. Dr. Robert Ferderer of Eagan, Minnesota, who has expertise in geophysical studies of the Duluth Complex, mapped the McDougal Lakes Area. These consultants both have the experience necessary to create pseudo-geologic maps and are familiar with the advanced computerized methodologies that are used.

The Baudette Area pseudo-geologic map was tested using drill hole data not provided to the consultant, ground geophysical traverses over selected features, and independent depth estimates. By withholding some drill hole data, we made the task more difficult and lowered the quality of the product to allow a comprehensive test of the method.

The pseudo-geologic map in the McDougal Lakes Area was tested using a variety of different methods. Six new drill holes were completed in six different map units. These holes were logged and described using thin sections and lithochemistry. Magnetic susceptibility and density measurements were also taken on the core, which has started a database of physical properties of Minnesota lithologies at the DNR. Ground geophysical traverses were done to test selected features. Reconnaissance outcrop mapping with assays was completed in a portion of the map area where a glacial drift pebble count study was also undertaken. The pebble count work was intended to determine if glacial drift pebble composition could be used to infer the lithology of the underlying bedrock in drift-covered areas. The pebble count, thin section, outcrop studies, and drill core logging were done by, or under the direction, of Dr. John C. Green, University of Minnesota - Duluth.

This work demonstrates numerous methods that can be integrated to evaluate bedrock geology areas where there is a paucity of geologic data. Drill holes test lithologic units and structures to the depth of the hole with strong confidence in the results. Ground geophysics combined with outcrop or drilling can be used to confidently map near surface lithologic units and structural features. Pebble counts and till geochemistry provide an interpretation of the underlying bedrock which is much less confident, especially where subglacial tills are found

and where rock boundaries are at large angles to ice transport direction. Geophysical forward modelling provides an interpretation of geophysical data to a depth of two kilometers. These methods are complementary and provide information at different scales and stratigraphic levels, which allows for a better evaluation of the mineral potential of each area. Wherever tested, the pseudo-geologic maps proved to be reasonably accurate. Map detail and accuracy could be increased by providing the contractor with low cost ground geophysical data taken along roads in areas to be mapped. Airborne electromagnetic data would also aid in making comprehensive pseudo-geologic maps.

Introduction

Purpose and Scope

The Department of Natural Resources (DNR) is responsible for managing state and county mineral interests on more than 12,000,000 acres of land. The Division of Minerals is also interested in diversifying Minnesota's mineral industry. To meet these objectives, the DNR provides libraries of geologic data and drill core and conducts a number of projects concerned with improving the mineral potential database. The geodrilling program is used in those areas where economic mineral potential is suspected, but data is lacking and there is little or no industry leasing of State mineral lands.

Accurate, detailed, geologic maps are essential for both the land management function and the encouragement of mineral potential investigations by private industry. Detailed, accurate maps reflect an abundance of available geologic information. Where there is a paucity of geologic data, geologic maps lack detail and provide a simple display of major lithologic units and structural features. Such maps are made using sparse drill holes and outcrops supplemented by regional geophysical surveys where geology is inferred from gross features on geophysical maps. Detailed maps are desirable, but in many places, such as areas of deep overburden, obtaining the data by traditional drilling methods is expensive. The problem is producing the most practical geologic map for the least cost, using available data.

Better resolution of lithologic units and structural features is achieved using recently improved geophysical equipment, methods of locating survey lines, computer enhancement of data, and integration of data from various geophysical methods. Inferred geology from these relatively low cost measurements of the physical properties of lithologic units and geologic features can be used to supplement available geologic data in the construction of what are called pseudo-geologic maps. These maps display lithologic units, structural features, and depth of burial to the measured geophysical parameter. There are some lithologic units, or mixtures of lithologies, which produce similar geophysical responses. Therefore, the methods are not perfect, but they do produce maps much closer to the true geology and with greater detail than older maps made from sparse geologic information and gross geophysical interpretations. Most of the geophysical data computer enhancement

methods available require computer equipment, software and expertise not available within the DNR.

Objectives

The overall objective of this project over the last biennium has been to produce and evaluate two pseudo-geologic maps as a pilot project. The two test areas selected have geologic conditions which make it difficult and expensive to produce detailed maps using traditional methods. Deep glacial deposits present problems in one area. Mapping lithologic units having a horizontal or layered orientation presents problems in the other area. The areas mapped must be large enough to test a variety of lithologic units and geologic features. It was also important to select areas which have a good potential for economic mineral deposits and have a good geophysical database.

The first area is an Archean, granite-greenstone terrain in Lake of the Woods County, which has in the past received considerable attention as having potential for massive base metal sulfide deposits and/or Archean, Superior Province type, lode gold deposits. This is an area of deep glacial deposits, generally over 100 feet. There is a good regional geophysical database available and considerable State mineral ownership. To cover a wide variety of lithologic units and geologic features, a four township strip west of Baudette (T157N, R33W - T160N, R33W) was mapped perpendicular to the regional structural grain.

In the Baudette area the objectives are to: 1) Produce a relatively detailed bedrock geologic map in an area of deep glacial drift; 2) Produce a depth to bedrock map which will help plan further mineral potential evaluation work and aid in land management decisions; and 3) Test the veracity of the map making methods used.

The second area chosen for construction of a pseudo-geologic map is a four township block in the McDougal Lakes area, Lake County. The block covers all or parts of T59-61N, R9-11W, centered on T60N, R10W, within the Proterozoic, layered mafic intrusive Duluth Complex. It was selected because: 1) There were encouraging geochemical results from glacial drift geochemistry (Buchheit and others, 1989), and also a need to further investigate the source of these geochemical values. 2) Duluth Complex rocks are younger than the Archean rocks underlying much of northern Minnesota and are expected to have geologic units with a more nearly horizontal rather than vertical orientation. 3) The area has widespread

interest among industry and academia, as judged from comments at various meetings and academic research done. In spite of this interest there hasn't been much activity (leasing) by industry and the DNR would like to encourage private investigations of the inner portions of the Duluth Complex. 4) There is moderate glacial drift overburden with some outcrop.

The objectives of the McDougal Lakes Area investigation were to: 1) Produce a relatively detailed three dimensional geologic map in an area of complex layered geologic units and structures; 2) Relate geochemical results to geologic units; 3) Describe geophysical responses to Proterozoic geologic units and features; and 4) Test the veracity of the map making methods used and thus encourage industry to use these methods.

Structure of the Report

This study has produced two types of results: pseudo-geologic maps and the data generated to evaluate the maps. Selected pseudo-geologic map areas are on very different geologic terrains and the maps were produced by independent contractors. Their reports are reproduced here as appendices, and the maps as plates. The main focus of the text is on the evaluation aspects of the project. Also, since each area was interpreted by different contractors and evaluated using different methods, they will be discussed separately.

Following a short introduction to each area, the methods used to evaluate the maps and test specific features will be described. The discussion sections will then present the data produced by each method and evaluate the map accordingly. A brief summary discussion is included for each area. It will attempt to synthesize the data and evaluations. At the end of the report, under the conclusions heading, there is a brief summary of the evaluations for each area as well as conclusions regarding aeromagnetic interpretation pseudo-geologic maps in general. Recommendations for future work close the report.

Acknowledgements

The authors wish to thank all the people who made contributions to the successful completion of this project and report. Particularly we want to thank our colleagues at the Department of Natural Resources, Minerals Division, with special thanks to E. Henk Dahlberg and Dennis Martin for their help with many aspects of the study, Kathy Lewis and Mark Kotz for land ownership reviews, Jacki Jiran and Rick Ruhanen for computer services, Diane Melchert and Dorothy Cencich for word processing, accounting by

Sue Saban and Helen Koslucher, drafting by Pat Geiselman and Gregory Walsh. Also Dr. Tuomo Alapieti, on sabbatical leave from the Geology Department of the University at Oulu, Finland, who assisted with thin section and lithologic interpretations.

Dr. Allan Spector and Associates Ltd. from Toronto, Canada was selected to map the Baudette Area. Dr. Spector has extensive experience with massive sulfide and gold deposits in granite-greenstone belts, and has the computer expertise and equipment available to make the desired map.

Dr. Robert J. Ferderer produced the map of the McDougal Lakes Area, Lake County. His background with the Duluth Complex and studies of computer enhancement methods applicable to the geologic problems of this area are apparent in his report.

Dr. John Green, with the help of Ed Venzke, did a glacial till pebble count study to determine if such a method could be used to infer local bedrock in a portion of the McDougal Lake Area, which is included as a part of this report. Dr. Green also logged the holes drilled for this project and described thin sections from drill core and outcrops in the area.

The pseudo-geologic maps were made using a geophysical database available due to the efforts of the Minnesota Geological Survey (MGS) and the U. S. Geological Survey (USGS). Particularly helpful are recently flown high resolution aeromagnetic surveys of the Baudette area where the aeromagnetic map was compiled by the USGS in cooperation with the MGS and the Geological Survey of Canada (GSC). It was done as part of the Roseau Conterminous United States Mineral Assessment Program (CUSMAP). In the McDougal Lakes Area these surveys were done by the MGS. The aeromagnetic data was acquired with funds provided by the Legislative Commission on Minnesota Resources (LCMR).

The McDougal Lakes Area is within the Superior National Forest and the cooperation rendered by U.S. Forest Service personnel was critical to the execution of field work in that area. Especially helpful were Stuart Behling, Zone Geologist in Duluth, and the people in the district offices, Paul Butler (Isabella District) and Robert Kari (Kawishiwi District).

Most important to the success of the project were William Brice Director of the Division of Minerals, and Marty Vadis, Assistant Director. Without their support there would be no project.

Baudette Area

Location and Access Baudette Area

In the Baudette Area a north-south strip of four townships (T157N, R33W, - T160N, R33W) was mapped. Figure 1 shows the map area location and Dr. Spector's map (Spector, 1989) modified to show locations of all drill holes, also profiles of ground geophysical traverses. The northeast corner of T160N, R33W is eleven miles west of the town of Baudette, the closest location of suitable quarters for field crews. This township has fair access, with County Road 2 on the west township line, County Road 3 running east-west across the center of the township, and several section line roads. Most of the area is within a mile of a good road with the exception of the southeast quarter of the township where the farthest point from a road is about three miles.

The other three townships (T157N, R33W - T159N, R33W) have poor access. County Road 2 continues south to the west one-quarter corner of Section 19, T157N, R33W, where it turns west. Three gravel roads, one in each township, wander across the area in an easterly direction from their juncture with County Road 2. Two of these follow the course of the north and south branches of the Rapid River. The third, the Faunce-Butterfield Road, crosses T159N. About a third of the area is within a mile of a road, the rest is a distance of two miles or more. The roads are mostly sand and gravel in pine forest and should be accessible throughout the year. There is a lot of swamp or wet lands away from the roads which are accessible when frozen during the cold months using snowshoes or all terrain vehicles.

Regional Geologic Setting

The Baudette Area is an Archean granite-greenstone complex of the Wabigoon Subprovince. Figure 2 shows both the original pseudo-geologic map area and the extended map area in relation to geologic subprovinces and structural features (Southwick and Morey, 1990). There is a brief description of the extended map area along with the map in the Addendum (Pocket 4). Frey and Venzke (1991) describe this area as being "made up of variably deformed and metamorphosed supracrustal volcanic and sedimentary rocks intruded by mafic (perhaps ultramafic?) to felsic intrusions. The rocks are metamorphosed to greenschist (upper?) or amphibolite facies, with local

punctuated contact metamorphism and intrusions. The supracrustals may be partially melted locally."

Interflow metasediments are present within the volcanic rocks, including Algoma-type sulfide and oxide facies iron formations which are conductive and were defined by airborne electromagnetic surveys. The youngest rock units are northwest-southeast trending, fine grained, early Proterozoic dikes which sometimes exhibit negative magnetic anomalies.

Four major faults cross the area. Starting at the north and listing them to the south, the Quetico Fault, the Baudette Fault, and the Border Fault are three essentially parallel faults trending northeast-southwest. Near the south side of the four township strip the Vermilion Fault crosses from southeast to northwest. Although Spector does not show this fault, he does show a granitic intrusive body which may have obliterated the fault in the map area. Frey and Venzke (1991) describe these in more detail.

The bedrock lithologic units have been weathered and in many places have a saprolite interval which varies from nothing on bedrock topographic highs to over 100 feet deep in zones of structural deformation, but is usually tens of feet in depth. The saprolite has very low magnetic susceptibility. Above this are deep glacial deposits usually over 100 feet in depth. The glacial deposits have a complex history. Based upon drillhole data, a major bedrock topographic high extends for more than twenty-four miles and strikes roughly parallel to the Baudette Fault. That high appears to have influenced the glacial history. East of the high, primarily late-Wisconsinan deposits are preserved, while to the west, additional older glacial deposits are also present. The glacial drift thickness is very similar on both sides of the high. The glacial drift has variable magnetic susceptibility (Martin and others, 1991).

Previous Work and Exploration History

There is very little outcrop in southern Lake of the Woods County. Maps displaying gross lithologic units and geologic features had to await completion of geophysical surveys. In 1957 the USGS and MGS published the results of an aeromagnetic survey of this area as Geophysical Investigations Maps GP 128 and GP 129 (Meuschke and others, 1957).

In the late 1960's through 1982 there were many State leases to private industry for base metals and associated minerals. Private industry flew detailed airborne magnetic and electromagnetic surveys. These

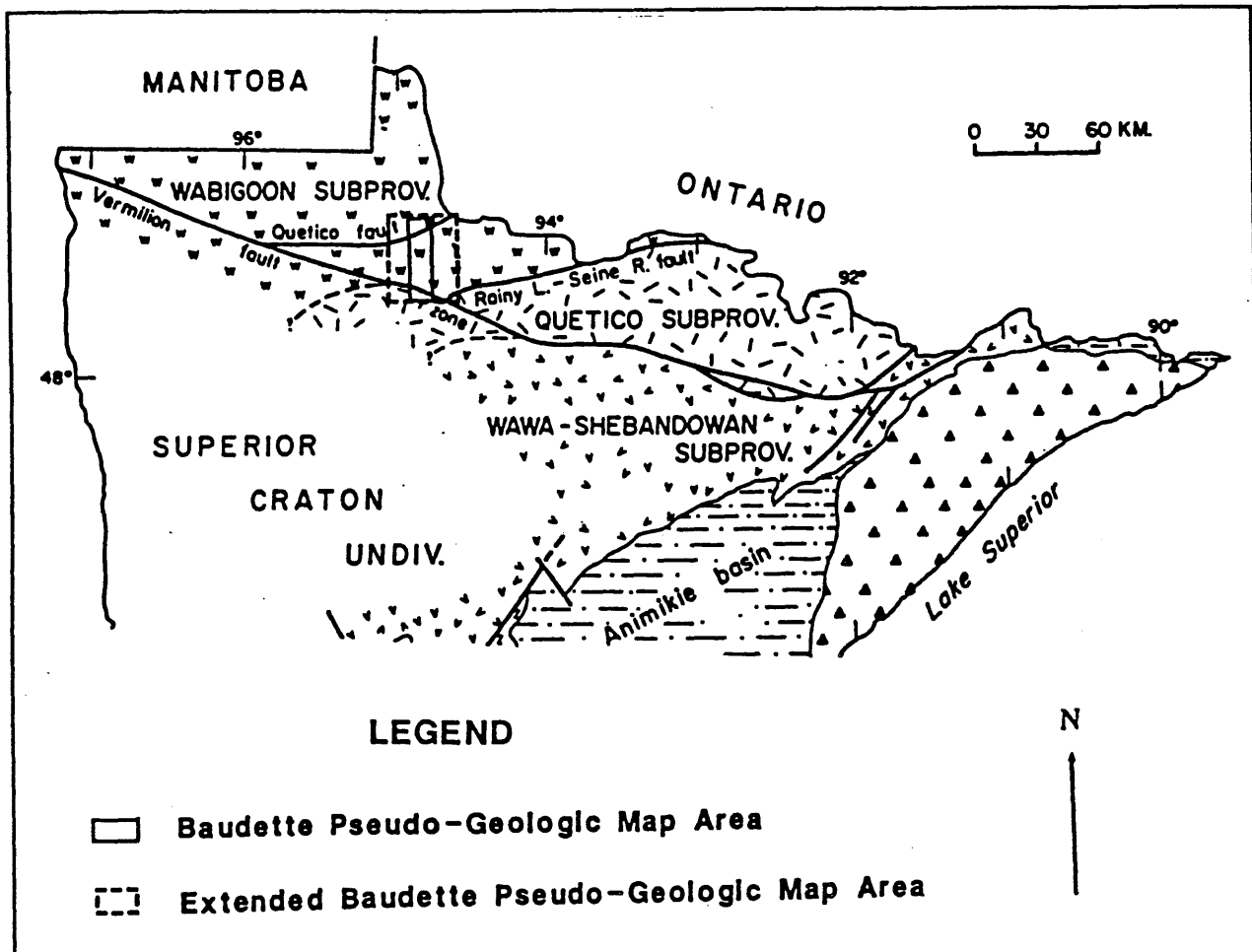


Figure 290-2. Regional geology of northern Minnesota (after Southwick and Morey, 1990) showing the original Baudette pseudo-geologic map area and the extended area.

were followed up by ground surveys and drilling where warranted. There were intersections of iron rich chemical sediments bearing magnetite, pyrrhotite, and graphite with anomalous quantities of base metals, but no economic deposits were defined. Records of this work on lands leased from the State are available in the Assessment Files of the DNR Minerals Division.

A bouguer gravity map, M-12, published by the MGS in 1973 (McGinnis and others, 1973), shows 55 gravity stations in the four township strip mapped by Spector. Twenty-three stations form one continuous traverse along the west side of the strip, the rest form five more or less east-west traverses across it. All stations are on roads. Even with this sparse coverage the gravity data helps define gross geologic features.

The MGS published a geologic map of the Roseau Sheet at 1:250,000 scale (Ojakangas and others, 1979) which was a modification of an earlier open file map (Sims and Ojakangas, 1973). The reliability index stated that the map was in an "Area

of few known bedrock exposures; cartography of Precambrian rocks based on aeromagnetic and gravity data supplemented by scattered water wells and exploration drill holes." In the four township strip (144 square miles) mapped by Spector eleven drill holes are shown, but no outcrop locations. There is also a depth to bedrock map (Olsen and Mossler, 1982) that shows expected bedrock depths to be from 80 feet to greater than 200 feet.

The DNR Division of Minerals maintains a core library in Hibbing. The most recent drill core index, published in October of 1990, lists seventy-one drill holes from Lake of the Woods County (Ruhanen and Jiran, 1990, p. 69-72). U. S. Geological Survey Open file Report 89-346 (Klein and Day, 1989) summarizes core from drill holes in this area. A mineral occurrence report of Lake of the Woods County, which included analysis from the drill core was published by the DNR Division of Minerals (Martin, 1985, p. 115-121).

For the past ten years the MGS has engaged in a program of mapping the State using high resolution airborne magnetic surveys. In the Baudette Area the airborne magnetic data was compiled by the USGS in cooperation with the MGS and the Geological Survey of Canada as a part of their Conterminous United States Mineral Resource Assessment Program (CUSMAP). Open file reports of this work are now available (Braken and others, 1991). The airborne magnetic surveys are a major part of the interpretation and formulation of the Baudette Area map. In coordination with the CUSMAP program the MGS did scientific core drilling in this area with the results published in Information Circular 24 (Mills and others, 1987, p. 19-40). The USGS also completed a sensitive reconnaissance level geochemical survey of B horizon soils in Lake of the Woods and Koochiching counties (Clark and others, 1990).

The Minnesota Department of Natural Resources, Minerals Division, has completed three projects aimed at better resolving the metallic mineral potential of the region: 1) This report on geophysical methods (Lawler and Venzke, 1991); 2) Detailed logs and lithochemical studies of bedrock drill core from the Baudette Area (Frey and Venzke, 1991); and 3) Buried overburden geochemistry (Martin and others, 1991).

Methodology - Baudette Area

The methods used by Dr. Spector in constructing the Baudette Area map (Plate 2) are explained in his report (Appendix D). Lithologic units, bedrock unit widths, faults, unit dips, and depths to magnetic source were tested using the methods described below.

Drill Hole Data

In or near the four township strip mapped by the contractor there are now twenty-six drill holes (Table 1). Only the four CUS hole logs were given to Spector, the data for the remaining holes was not provided. These holes were later used to test the accuracy of the lithologic determinations and depths to bedrock. Four holes: 508; 509; 510; and 511 were drilled through glacial drift into bedrock after the contractor's report was completed. These holes were also used to test depth to the magnetic source and bedrock lithology as mapped by the contractor.

Ground Geophysical Profile Data

A number of features shown on Spector's map were tested with ground geophysical traverses. These features, such as dikes, iron formations, and fault zones, have contrasting magnetic susceptibilities compared to the host rocks. Ground geophysical work was done using a Scintrex IGS-2, Integrated Geophysical System. Data was transferred using Scintrex IGSDUMP software in a portable Compaq computer. A hard copy was made and the data was also saved on floppy disks. This data is available on an open file basis in either format. Quattro Pro software was used to prepare the graphs displayed in this report.

On north-south traverses the total magnetic field and the very low frequency electromagnetic (vlf-em) (M), fields were measured. The vlf-em used stations NAA, Cutler, Maine, at 24.0 KHz; NLK, Seattle, Washington at 24.8 KHz; or NSS, Annapolis, Maryland, at 21.4 KHz. In this area these stations give the best response for east-west trending vertical sheet conductors. Known geology and geophysical interpretations suggested that this would be the most likely conductor orientation.

On east-west traverses the total magnetic field and magnetic gradients were measured using a one meter sensor separation. On some long traverses a base station recording magnetometer was used to correct for diurnal drift. Observations were made at fifty foot station intervals. One-hundred foot intervals

were measured with a rope and flagged, then fifty foot stations were paced between flags.

Lithologic units were checked by simply looking at the amplitude of magnetic anomalies above or below background on the profiles. For example, pyrrhotite-rich units usually have positive anomalies of less than 800 gammas amplitude, late northwest trending dikes sometimes have negative anomalies of a few hundred gammas, and oxide facies iron formations have positive anomalies of several thousand gammas.

Bedrock unit widths can be approximated using the profile width at half the anomaly amplitude height. Faults have characteristic signatures related to changes in background amplitudes, oxidation in the fault zone, or small positive anomalies on the flanks of the fault. They are also more conductive than host rocks which can be observed with very low frequency electromagnetic (vlf-em) surveys if the overburden is not too deep. Dips of units with a strong contrast in magnetic susceptibility can be estimated from changes in the slopes on the flanks of the anomaly.

Depths to the magnetic source can be estimated using various methods which utilize magnetic susceptibility profiles. Depths to a point near the upper edge of a vertical sheet vlf-em conductor approximately equals the horizontal distance between the maximum positive and negative readings, (Geonics Limited, EM 16, operating manual, p. 5). Depth estimates were checked using drill hole data not provided to Spector, along with some estimates using Peter's half slope method (Dobrin, 1960, p. 313). For an accurate estimate the traverse direction should be perpendicular to the strike of the conductor axis. The vlf-em technique was used in one place to check the estimated depth.

NOTE: Contracts with consultants and descriptions of their qualifications or product quality and the use of equipment brand names in this report is for identification purposes only and does not constitute endorsement by the Minnesota Department of Natural Resources.

Results and Discussion - Baudette Area

Dr. Spector's map of the four township strip is included in this report (Plate 2). Flight path plots, profiles of the aeromagnetic data and profiles of ground geophysical traverses are available on an open file basis. Spector's map shows lithologic units, depths to magnetic basement (usually bedrock below the nonmagnetic saprolite interval), and structural features. Tests of Spector's results found them reasonably accurate within accepted standards of practice as described in this section.

Comparison of Map and Drill Hole Data

In this section the interpretation and pseudo-geologic map made by Spector will be compared with the drill hole data not provided to him. Lithologic units will be compared first, then estimated depths to bedrock.

Table 1 compares lithologic units on the pseudo-geologic map with units intersected in drill holes as logged and summarized by Klein and Day (1989) and Frey and Venzke (1991). Plotting the twenty-six holes in or near Spector's map area on his map it is seen that: Four holes; 40917; CUS-16; CUS-17 and 511; are located on mapped granite. The dominant lithologic unit as estimated from Barry Frey's log of core from hole 40917 is quartz feldspar gneiss and schist. The dominant unit in CUS-16 is tonalite gneiss. In CUS-17 quartz gabbro. In 511 the dominant lithology was biotite quartz monzonite. The quartz gabbro is the only lithologic unit which would have a different geophysical response than granite and that is interpreted to be an intrusive body too small to respond to the scale of these surveys.

Two holes; 40918 and B58-1; are located on Spector's metavolcanic unit. The dominant lithologic units estimated from Barry Frey's log for 40918 are graywacke, with some tuffs and less iron formation. The dominant lithologies in B58-1 are tuffs, with mafic volcanics and some metasediments. For both these holes the mixture of lithologic units is interpreted to have a similar magnetic susceptibility to metavolcanics.

Twelve holes; 40919; B21-1; B21-2; B21-3; B24-1; B24-2; B24-3; CUS-27; MED-1; B5-1; 509; and 510 are located on basic metavolcanics. The dominant lithology estimated from logs for most of these holes is mafic volcanics (see Table 1). A few that have the dominant lithology as tuffs, metasediments or metavolcanics also list iron formations. (In Frey's logs these iron formations are called "SULFIDE, CHERT, OXIDE, CHEMICAL SEDIMENTS". To qualify as

iron formations they should have fifteen percent iron. However, these holes were drilled by industry to intersect conductors, usually with an associated positive magnetic anomaly which would require a fair percentage of iron either as sulfide or oxide. Therefore, in the interest of brevity on Table 1 and in this report we refer to them as iron formations, IF, whether they contain fifteen percent iron or not). Magnetic profiles show the average of the effects of small intercalated units of varying magnetic susceptibilities. The greater the distance from the magnetic source elevation to the elevation of observation the more averaging will be observed. The intercalated iron formations are interpreted to increase the overall magnetic susceptibility until the less magnetic tuffs or metasediments appear to be mafic volcanics. Holes 509 and 510 list gabbro as the dominant lithology. These are interpreted to have a similar magnetic susceptibility to Spector's mapped basic metavolcanic lithologies.

Eight holes are located on Spector's meta-sedimentary unit. These are; 40920; B24-4; CUS-18; MSD-1; MDD-1; MMD-1; 508; and 512. The dominant lithologies in holes 508 and 512 are metasediments. In hole MDD-1 The dominant lithologies are tuff, iron formation and sediments. Depending on the quantity of iron minerals and distribution, these lithologic units could have geophysical characteristics interpreted to be metasediments. The dominant lithologies in 40920, B24-4 and MMD-1 are mafic volcanics. These appear to be difficult lithologies to differentiate based on airborne magnetic surveys. A better geophysical data base with core magnetic susceptibilities would help solve this problem. Electromagnetic surveys would also help. CUS-18 dominant lithology is a plagioclase porphyry, an intrusive with geophysical responses similar to those found in metasediments. MSD-1 with dominant lithologies of metavolcanics and tuffs would be interpreted in the same way as CUS-18.

There are several depth to bedrock (magnetic interface) estimating methods using magnetic data. This means depth to unweathered rock. Most of the methods use slopes of anomaly profiles to make the estimate. The estimates vary with orientation, magnetic susceptibility, and paleomagnetism of the geologic unit. They also vary with inclination of the magnetic field. Gradational magnetic susceptibilities, interference from closely spaced units, and erratic magnetic features can cause errors. An estimate is judged to be reasonably accurate if it is within twenty percent of

Table 290-1. Comparison of Drillhole Data and Baudette Area Pseudo-Geologic Map.

Drillhole	Location S-T-R	Core Lithology	Map Lithology	Hole OB Thickness (feet)	Map Est. OB Thickness (feet)	OB Thickness Error (feet)
40917	34-157-33	Qtz Feld Gneiss & Schist	Granite	145	405	260
CUS-16	31-160-33	Tonalitic Gneiss	Granite	300	260	40
CUS-17	18-159-33	Quartz Gabbro	Granite	170	170	0
511	8-160-33	Qtz Biotite Monzonite	Granite	175	260	85
40918	8-157-33	Graywacke, Tuff IF	Meta Vol	192	190	2
B58-1	32-158-33	Tuffs, Mafic Vol, Meta Sed	Meta Vol	115	205	90
40919	25-159-33	Meta Sed, IF	Basic Meta Vol	102	180	78
B21-1	34-159-33	Mafic Vol & IF	Basic Meta Vol	82	205	123
B21-2	3-158-33	Mafic Vol	Basic Meta Vol	94	190	96
B21-3	2-158-33	Meta Vol & IF	Basic Meta Vol	92	200	108
B24-1	30-158-33	Sulf Meta Sed, Fel Int, IF	Basic Meta Vol	98	195	97
B24-2	30-158-33	Mafic Vol & IF	Basic Meta Vol	125	195	70
B24-3	30-158-33	Mafic Vol & IF	Basic Meta Vol	100	195	95
CUS-27	13-157-34	Hornblende Schist	Basic Meta Vol	30	150	120
MED-1	32-158-33	Tuff, IF	Basic Meta Vol	132	210	78
B5-1	25-158-34	Mafic Vol	Basic Meta Vol	68	200	132
509	23-158-33	Gabbro	Basic Meta Vol	92	220	128
510	36-159-33	Gabbro	Basic Meta Vol	108	210	102
B24-4	19-158-33	Mafic Vol	Meta Sed	92	190	98
CUS-18	31-159-33	Plagioclase Porphyry	Meta Sed	338*	180	158
40920	29-159-33	Mafic Vol	Meta Sed	206	180	26
MSD-1	6-158-33	Meta Vol, Tuff, Meta Sed	Meta Sed	190	180	10
MDD-1	12-158-34	Tuff IF Sed, Mafic Vol	Meta Sed	160	160	0
MMD-1	25-158-34	Mafic Vol, Tuff, Graywacke	Meta Sed	88	180	92
508	15-157-33	Meta Sed	Meta Sed	270	280	10
512	24-157-34	Graywacke	Meta Sed	107	170	63
Average Depths				140	206	83

* In Saprolite

Depth estimates are considered accurate if they are $\pm 20\%$ of altitude above causative body. At 140' average overburden depth plus 300' airplane altitude this equals $\pm 88'$ ($140' + 300' \cdot 20\% = 88'$).

the distance from the depth of burial to the observation height. For example, if the top of the unit is buried 200 feet, and the aeromagnetic survey is flown at 300 feet above ground surface (the elevation of the Baudette Area aeromagnetic survey), the total distance is 500 feet. An accurate depth estimate would be 200 feet \pm 100 feet. In his report Spector explains the method he used for estimating depth to the magnetic interface.

Using vertical depths at the drill hole locations, the average overburden thickness including saprolite where it was logged is 140 feet. An accurate estimate would be the actual depth plus or minus 88 feet for the Baudette Area where the airplane elevation was 300 feet (Chandler, pers. comm.). The average error between Spector's estimated depth and true depths is

83 feet (five feet better than what would be considered accurate). From Table 1, for sixty-nine percent of the holes the estimated overburden depth is greater than the true or drilled depth. This suggests that part of the error comes from oxidized bedrock, a saprolite interval, above the magnetic interface. Magnetic susceptibility measurements on the core could be used to determine this.

Tests of Map with Ground Geophysical Profiles

Twenty-one miles of ground geophysical profiles were run along roads in the area. These are on open file. Seven segments of the profiles in graphic format are included in this report as tests of the pseudo-geologic map. The objective was to use detailed

magnetic and very low frequency electromagnetic traverses to test: lithologic interpretation; location; structural features; and depth estimates. These profiles will be described starting at the south end of the strip and working north. These tests are summarized in Table 2.

A traverse of combined total field magnetic observations and vlf-em was run from the junction of the Faunce-Butterfield road and County Road 2 south to where the road turns west along the Rapid River, near the west quarter corner of Section 19, T157N, R33W. Twelve hundred thirty feet south of Oaks Corner in Section 18, T157N, R33W, a moderately strong conductor was observed with the vlf-em (Fig. 3). There was also an insignificant flexure of the magnetic field. Spector shows a fault zone crossing near Oaks Corner. Without support from the magnetics the vlf-em conductor could be interpreted as a surficial conductor, although a 250 foot depth is estimated to the top part of the conductor using peak amplitudes on the vlf-em profile. Spector estimates the depth to bedrock to be less than 200 feet. Thus the two estimates are in agreement.

In Section 31, T158N, R33W the same traverse observed a strong magnetic anomaly with a half width of 1,800 feet and an amplitude of 1,500 gammas extending from station 20,800S to station 22,600S (Fig. 4). Spector shows a basic metavolcanic unit in this area 1,650 feet wide, with an amplitude of 1,800 gammas. To the south of this Spector shows another basic metavolcanic unit. A profile of this anomaly was not made, but depth was calculated, using Peter's slope method to be 200 feet (Dobrin, 1960, p. 313).

To test iron formations mapped by Spector, a traverse was run along the road starting in the SW $\frac{1}{4}$, SE $\frac{1}{4}$, Section 35, T159N, R33W, thence northeasterly across Section 36 and out of the township. From station 4,150E to 4,500E in Section 36, a strong magnetic anomaly was observed with an amplitude over 5,600 gammas indicating iron formation (Fig. 5). Using Peters method the depth is calculated to be 170 feet. Spector shows a complicated structure, deformed by northwest trending faults. His iron formation units are wider than this, but the traverse could have crossed a fault segment. His depth is about 250 feet, extrapolating between the 200 and 300 foot contours.

The traverse described in the previous paragraph was run with both total field and gradient observations. Stations 5,200 to 7,050 bracket an anomaly of 2,500 gammas again indicative of iron formation. Adding this width to that of the anomaly described in the previous paragraph it would approach the width shown by Spector. Figure 6 shows part of this anomaly from station 5,900 to 7,400. From station 6,150 to

station 6,450 there is a dish shaped depression in both the total field and gradient profiles. This is interpreted as oxidation in a fault zone. Between stations 7,000 and 7,100 there is a sharp negative break in the profile, very noticeable on the gradient profile, which is also interpreted as a fault contact. These suggest that Spector's northwest trending faults are correct.

Along with the northwest trending faults are dikes with the same orientation. These often show up as negative anomalies. A traverse was run east along the road from the southwest corner of Section 17, T160N, R33W. The purpose of this traverse was to measure the influence of power lines and the northwest faults in a granite terrain. Figure 7 is a profile that crossed a dike. The feature has a half width from 3,100E to 3,600E, equal to 500 feet, and a negative amplitude of 180 gammas. There is a very slight negative swing on the gradient profile which is not shown. In this area Spector mapped a dike crossing the road at 3,960E. This is a horizontal error of about 610 feet on the airborne generated data, slightly over the 600 foot error usually accepted as reasonable for airborne surveys. The dike is there and was recognized by Spector.

To test magnetic and vlf-em responses over granite, a traverse was run south from the northeast corner of Section 1, T160N, R33W. There is a broad low amplitude, positive, magnetic anomaly from station 300S to station 1,750S, equal to 1,450 feet on the profile. The anomaly has an amplitude of about 400 gammas and a depth determination, with Peters method, of 200 feet on the south flank of the anomaly. Spector maps this as being over 400 feet. Figure 8 shows the vlf-em response over the south flank of the anomaly from station 1,500S to 3,200S. There is a strong cross over indicating a conductor at 2,400S. With the indicated depth, in a granite terrain, the conductor would normally be interpreted as surficial, but the response is both strong and very broad for a surficial conductor. There is also a small magnetic anomaly having tens of gammas amplitude coincident with the cross over (Fig. 9). In a granite terrain the magnetic anomaly might be related to a metamorphic event and the shape of the magnetic profile unreliable for depth calculations. The vlf-em profile is also erratic. Using the vlf-em peak values the estimated depth would be 1,600 feet, which is not reasonable. It is possible that the traverse crosses the conductor axis at an acute angle. However, this would likely be a structural feature of some significance to give the vlf-em response. This could be further defined with seismic work and parallel traverses.

Table 290-2. Tests with Ground Geophysical Profiles in the Baudette Area.

Profile Number	Location S-T-R	Spector's Map Data	Profile Data	Location Error (Feet)
Fig. 3	18-157-33	Fault Oaks Corner	Cross-Over Fault?	1,230' N-S
Fig. 3	18-157-33	OB Depth 180'	Cross-Over. OB Depth 250'	70' Vertical
Fig. 4	31-158-33	Basic Meta Vol 1,650' Wide	Mafic Vol 1,800' Wide	200' N-S. Contact
No Figure	30-158-33	OB Depth 180'	Magnetic Profile. OB Depth 200'	20' Vertical
Fig. 5	36-159-33	OB Depth 250'	Magnetic Profile. OB Depth 170'	80' Vertical
Fig. 5, 6	36-159-33	Fault Block Iron Fm.	Iron Fm. Faulted	± 200' N-S. Contact
Fig. 7	17-160-33	Dike	Dike	610' E-W
Fig. 8	1-160-33	Nothing Shown	Vlf-Em Cross-Over. Fault?	
Fig. 9	1-160-33	OB Depth >400'	Magnetic Profile. OB Depth 200'	200' Vertical

Summary

Dr. Spector's map (scale 1:62,500) provides much more detail than previously published maps, with more lithologic units, structural features, and depths of burial of those units. This detail helps to better identify lithological environments that are appropriate for metallic mineral exploration, especially in felsic volcanic environments. Also, detailed structural mapping is necessary for effective gold exploration. Our objective was to test the map's veracity. We acknowledge that this test required us to withhold drill hole information from Spector. By withholding it, we made the task more difficult and lowered the quality of the product. Anticipating the use of pseudo-geologic maps in areas with much less drill hole control, this is a legitimate test of the map's veracity. Both the drill data not provided to the contractor and our ground geophysical traverses indicate small scale lithologic units and structural features not observed by the aeromagnetic or gravity survey data he used. Detailed logs of drill core show numerous lithologic units intercepted within a few hundred feet. None of our tests disprove the gross dimensions of his lithologic units or structural features.

Spector's depth estimates to magnetic source are well within accepted standards of accuracy and there is some indication core logged as bedrock below saprolite could have oxidized magnetic minerals, thereby reducing their magnetic susceptibility. This would result in a deeper magnetic basement.

Using the phrase "accepted standards of accuracy" requires the author to define the criteria he used for those standards. The criteria for depth estimates is previously described in the text and on Table 1. In the Precambrian Shield of the north-central states areal location of geologic features is considered accurate if the feature as defined by

airborne data is within 600 feet of where it is defined by a ground survey or outcrop.

The criteria for determination of lithologic units by geophysical methods is more nebulous although there are characteristic signatures for many lithologic units: Magnetite-rich iron formations normally have positive linear magnetic anomalies of several thousand gammas and positive gravity features. Mafic igneous units also have positive magnetic and gravity features except for some Keweenawan dikes which have a negative, linear, magnetic signature. Pyrrhotite rich units have positive anomalies less than 800 gammas. Sedimentary units, other than iron formation, usually have bland magnetic and gravity signatures. The comparisons made in Table 1 and the text describe criteria for "accepted standards of accuracy" for determination of lithologic units in the map area.

Structural features are defined on geophysical maps by several criteria: Linear patterned offsets of lithologic units define faults. Faults may also be seen as dish shaped negative signatures on a magnetic profile. Folds are displayed as curved features of distinctive lithologic units. Certain lithologic units such as the Keweenawan dikes follow structural features. Dips are estimated from the slope on the flanks of geophysical anomalies.

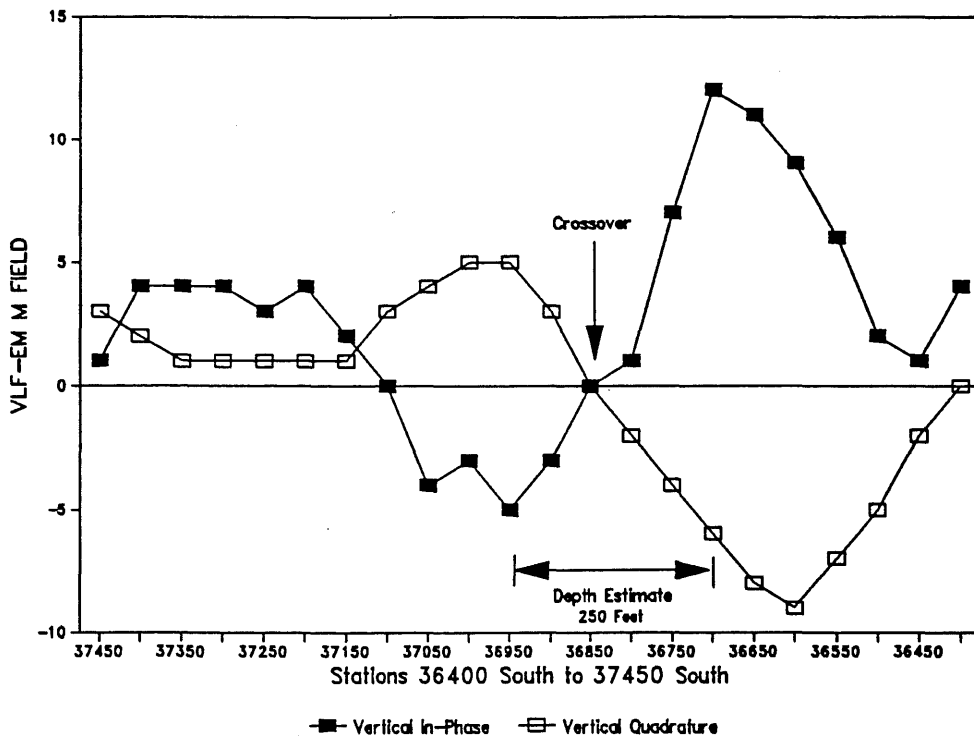


Figure 290-3. VLF-EM profile from station 36,400S to 37,450S (Section 18, T157N, R33W).

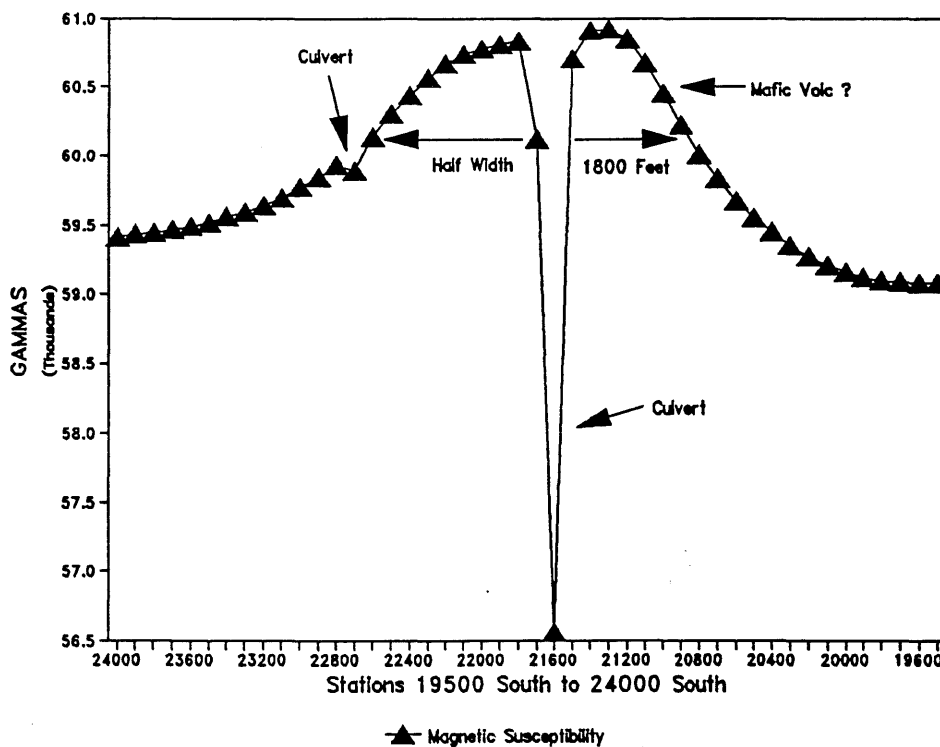


Figure 290-4. Magnetic susceptibility profile from station 20,750S to 22,600S (Section 31, T158N, R33W).

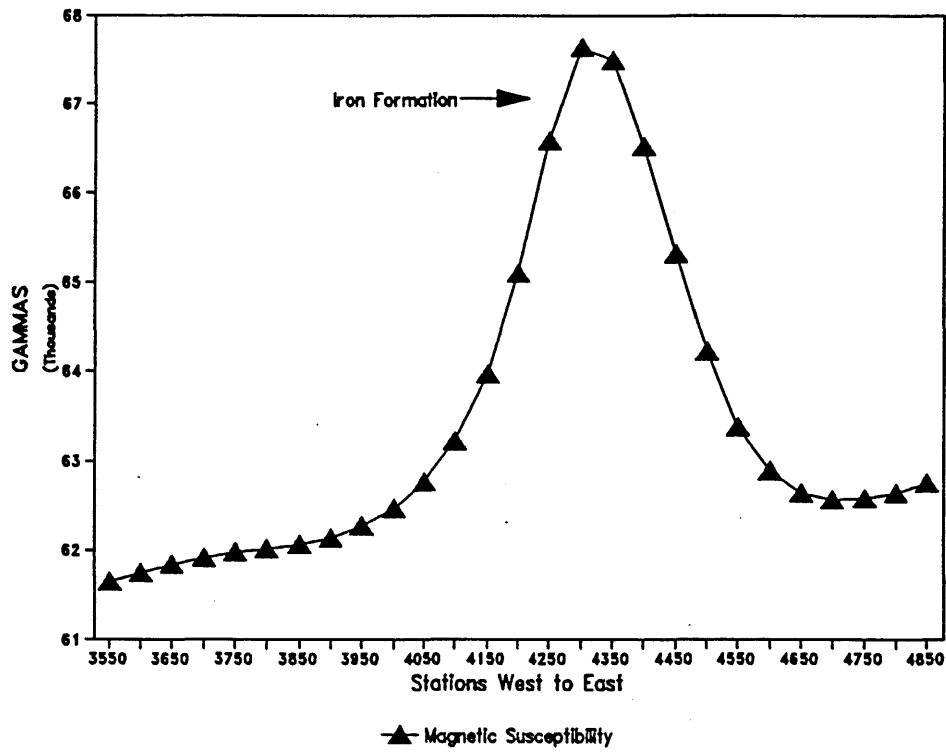


Figure 290-5. Magnetic susceptibility profile from station 4,150E to 4,500E (Section 36, T159N, R33W).

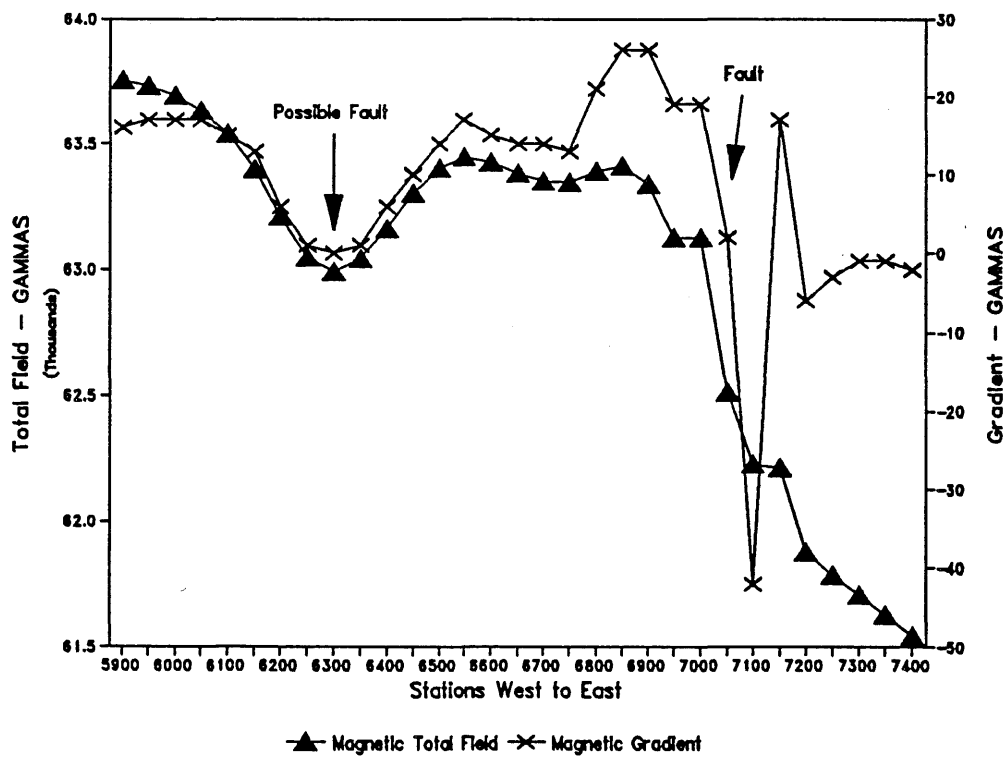


Figure 290-6. Magnetic susceptibility profile from station 5,900 to 7,400 (Section 36, T159N, R33W) showing both Magnetic Total Field and Magnetic Gradient measurements.

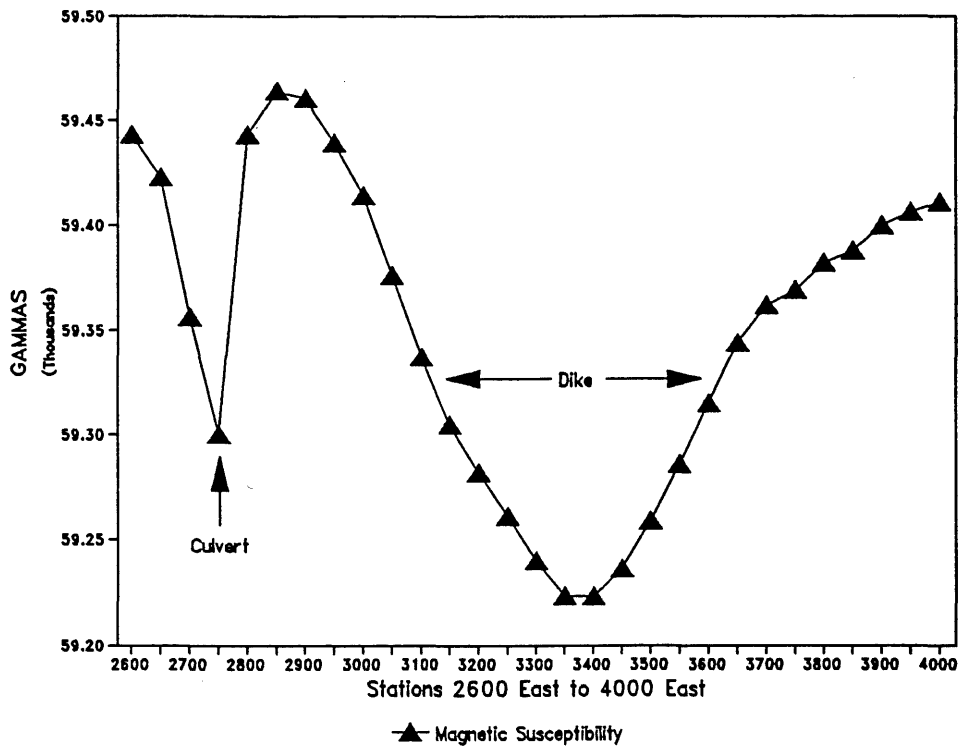


Figure 290-7. Magnetic susceptibility profile from stations 2,600E to 4,000E (Section 17, T160N, R33W).

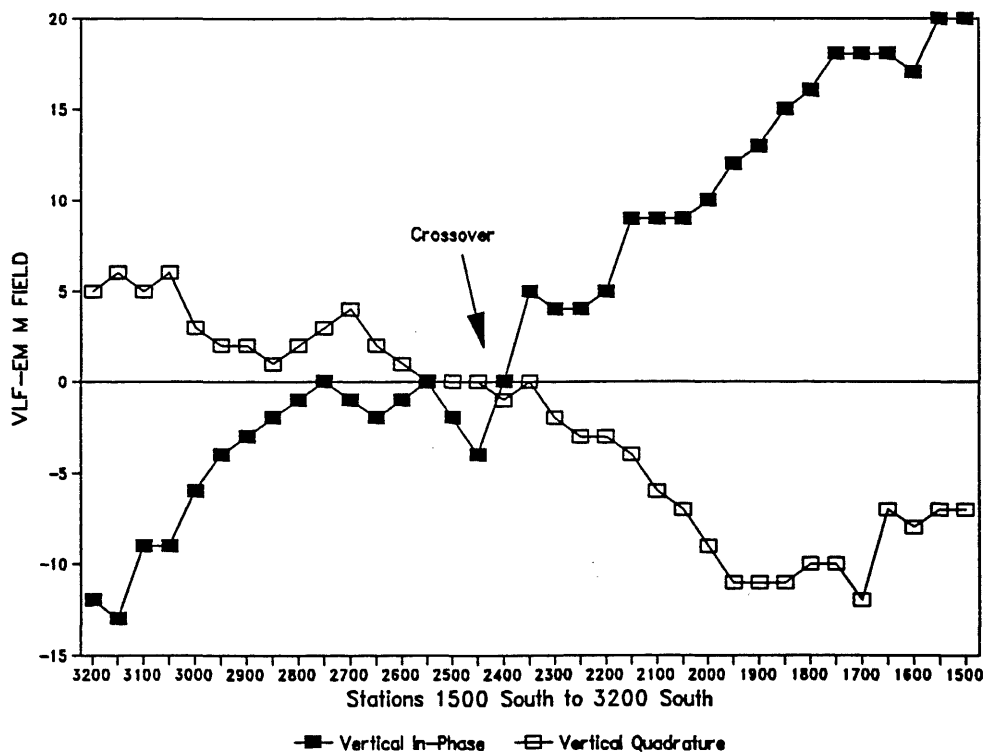


Figure 290-8. VLF-EM profile from station 1,500S to 3,200S (Section 1, T160N, R33W).

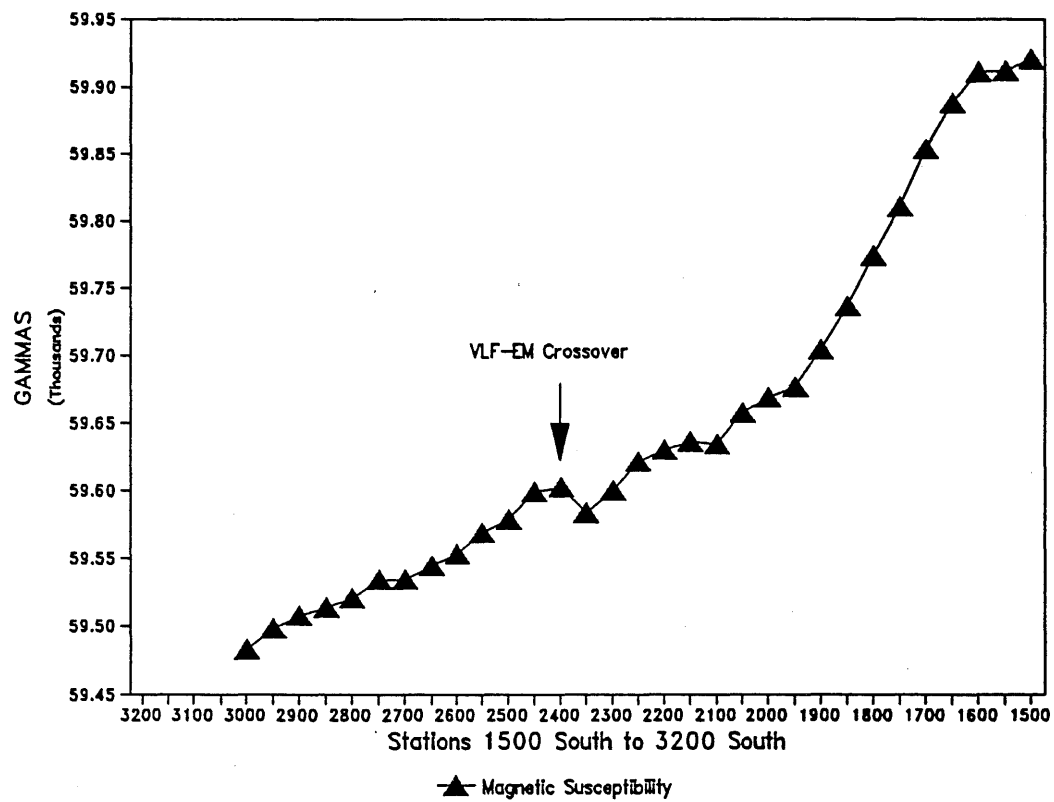


Figure 290-9. Magnetic susceptibility profile from station 1,500S to 3,200S (Section 1, T160N, R33W).

McDougal Lakes Area

Introduction

In the four township block of the McDougal Lakes area there are few outcrops, with most concentrated along the Tomahawk Trail where Olsen and Mossler (1982) show almost continuous outcrop. Only three drill holes were available before this project. Previous geochemical surveys identified encouraging high background values of strategic elements in till samples (Buchheit and others, 1989). A more definitive bedrock geologic map was needed to evaluate these analyses with respect to the local geology. The current geologic map lacked detail also resolution of lithologic units and structural features in this area of few drillholes and rare outcrops.

Dr. Robert Ferderer completed a masters thesis in this area and wrote a doctoral thesis using the Werner Deconvolution inverse magnetic modeling technique. This technique is particularly useful for computer modeling layered geologic units such as those expected in a Proterozoic intrusive complex like the Duluth Complex. Using the Werner Deconvolution technique, along with several other modeling techniques, Dr. Ferderer produced a pseudo-geologic map based on available geologic data including the three drill holes. Detailed lithologic units and structural features were inferred from airborne magnetic and ground gravity surveys. The map displays near surface bedrock structural features and lithologic units at varying depths. Gravity and broad low amplitude magnetic features define deep geologic units. Shallower units are defined by narrower, higher amplitude magnetic features. The relationships are displayed on the plan view (Fig. 10) and on ten forward modelling sections with fifteen interpretation profiles. The results and methods used are described in Ferderer's report (Appendix E).

The DNR tested Ferderer's results with four different methods: 1) Six shallow holes were drilled in lithologic units or near structural features which coincide with positive glacial drift geochemical results. Drilling of deeper lithologic units was beyond the budget limitations of this program. The drill core was logged by Dr. John C. Green, who has extensive experience with Duluth Complex lithologies. Thin sections were also described and intervals were selected for chemical analysis. In addition, magnetic susceptibility and density measurements were made on the core at five foot intervals to better understand geophysical responses. 2) Outcrops were sampled and

studied with thin sections and assays. 3) Dr. Green with the help of Ed Venzke, did a glacial drift pebble count study to compare near surface lithologic units with mapped units and test this method as a complement to maps inferred from geophysical methods. 4) Detailed ground geophysical traverses were run to test near surface structural features in the northeast quarter of the map.

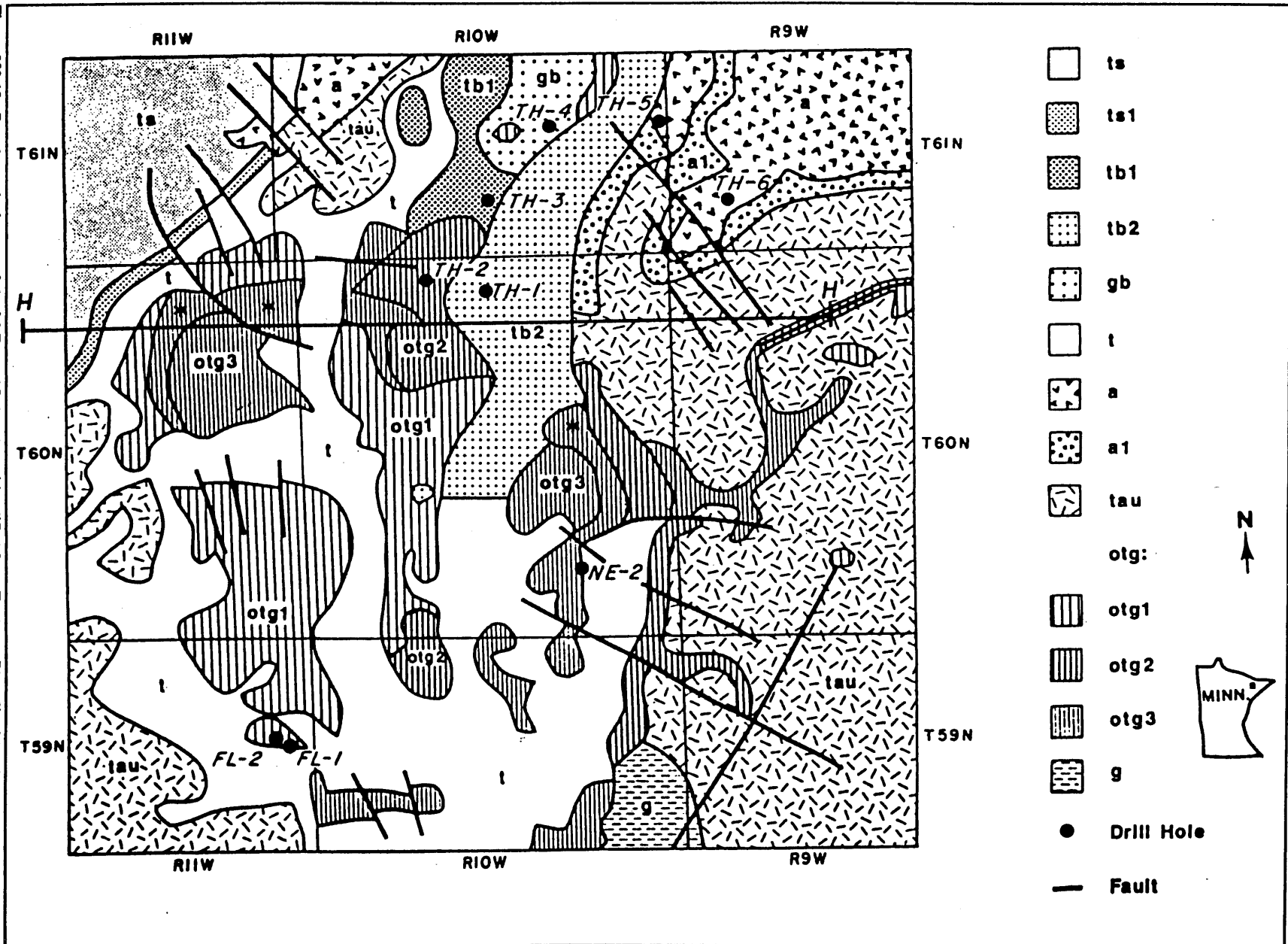
Location and Access

The McDougal Lakes Area is defined for the purposes of this report as the four township block comprising the pseudo-geologic map which is centered on T60N, R10W (Fig. 10). This area includes all or portions of the following quadrangles: Bogberry Lake, Gabbro Lake, Quadga Lake, Slate Lake West, Slate Lake East, Mitawan Lake, Greenwood Lake West, Greenwood Lake East, and Isabella Station. The north edge of the map area is about one-half mile south of the "Mineral Management Corridor" for the Boundary Waters Canoe Area (Minnesota DNR, 1991).

Access is good, with Minnesota Highway 1 passing through the area from southeast to northwest. The Tomahawk Trail (Forest Service Roads 173 and 424) provides good access in the north. Other Forest Service roads shown on the National Forest map (U. S. Forest Service, 1984) provide good access to the rest of the area. Combining these roads with trails and logging roads shown on aerial photographs puts most of the area (estimated at seventy percent) within a half mile of a road. About ten percent is more than a mile, and almost no place is more than two miles from a road. Outside of a campground at McDougal Lake, the closest facilities for food and lodging are at Babbitt, approximately twelve miles to the west.

The area of this project is within the Arrowhead Region of Minnesota. Local topography is generally gently sloping glacial features superimposed on a regional north slope, with sharp ridges formed by outcropping bedrock. Since the area is north of the Laurentian Divide, creeks and streams flow north into the Boundary Waters Canoe Area Wilderness. Numerous small lakes are located in the lowlands between the ridges and hills. Bottom lands along creeks and lakes are swampy. In places creeks and swamps form linear features with many northwest-southeast trends, in some cases making sharp angles of about ninety degrees to the northeast which suggest bedrock fault control.

Figure 290-10. Pseudo-geologic map of the McDougal Lakes Area (simplified from Ferderer, Plate 3) with drillhole locations. See Plate 3 for explanation of legend.



Forest vegetation is representative of the boreal coniferous forest that originally covered the northeastern third of Minnesota. Naturally reproduced red and white pine are in successional growth with white spruce and balsam fir, while jack pine is abundant in sandy outwash areas. Aspen, birch, balsam and spruce are the most frequent natural second-growth species. Bogs are dominated by black spruce and tamarack; with ash, willow and alder found in adjacent swampy terrains (Buchheit and others, 1989). Plantations of red and jack pine are also present.

Geologic Setting

The McDougal Lakes Area is part of the middle Proterozoic Keweenaw layered mafic intrusive Duluth Complex. Figure 11 shows the pseudo-geologic map area in relation to the regional geology and the geochemical till survey area (Buchheit and others, 1989). The Duluth Complex is intruded into and overlies the lower Proterozoic Animikie Group formations. The North Shore Volcanic Group forms the extrusive equivalent of the complex with outcrops east and south of the map area. It is expected that these Proterozoic rocks have not been extensively deformed and still retain a somewhat horizontal orientation.

The map area includes portions of the South Kawishiwi Intrusion and the Bald Eagle Intrusion, as well as rocks of the anorthositic, troctolitic, and felsic series. An excellent overall summary of the various named intrusions and divisions of the Duluth Complex can be found in Weiblen and Morey (1980). Some north-northeast trending faults have also been mapped in this area (Green, 1982).

The area not only has complicated intrusive geologic units, but also complex geophysical parameters. There are varying amounts of remanent magnetization and somewhat random units of more mafic rock as shown in the work done by Ferderer for his masters thesis (Ferderer, 1982) and in this study.

Previous Work and Exploration History

The Gabbro Lake quadrangle was mapped and described in the late 1960's (Weiblen, 1965; Green and others, 1966; and Phinney, 1966). Outcrops in the southern Duluth Complex were mapped (1:125,000) by Bonnicksen (1971). A bedrock geologic map of the Two Harbors sheet (1:250,000) was compiled by Green (1982), which is the most comprehensive map available that includes the McDougal Lakes Area. Additional mapping of the Greenwood Lake East and Greenwood Lake West quadrangles is currently in progress as part of a Master's thesis at the University

of Minnesota Duluth (Venzke, in prep.). Regional Bouguer gravity maps, station spacing of a mile or more, of the southern part of the Duluth Complex (1:125,000) (Ikola, 1968) and of the Two Harbors Sheet (1:250,000) (Ikola, 1970) published by the MGS provided the gravity database which forms a large part of Dr. Ferderer's study. An aeromagnetic map of Lake and Cook counties was completed in 1983 (Chandler, 1983). This airborne magnetic survey data was used as the main source of data for the present pseudo-geologic map. The airborne survey was funded by the Legislative Commission on Minnesota Resources (LCMR).

In the 1960's and 1970's there was leasing of State lands in the map area, during which time the New Jersey Zinc Company ran geophysical surveys in Sections 35 and 36, T61N, R11W. These are available in the Assessment Files at the DNR Minerals Division.

At the time the pseudo-geologic map contract was made there were three reported drill holes within the map area, all drilled and logged by the DNR. FL-1 and FL-2 are located near Fools Lake in Section 12, T59N, R11W (Vadis and others, 1981). The third hole, NE-2, is in Section 26, T60N, R10W (Sellner and others, 1985). Additional assay work was done on these holes in the 1988-1989 biennium (Dahlberg and others, 1989).

Ferderer (1982) completed a masters thesis on gravity and magnetic modeling of the southern half of the Duluth Complex. This thesis and his doctoral thesis (Ferderer, 1988), written on the use of the Werner deconvolution method for using airborne magnetic surveys to define geology are the most recent pertinent studies done in the area. Hinze and others (1975) have also described the use of combined magnetic and gravity data to help define geology.

Buchheit and others (1989) studied the glacial drift geochemistry of the Duluth Complex in Lake County for strategic minerals. Areas of elevated amounts of economic heavy minerals were reported which suggest good potential for copper-nickel-cobalt or platinum group mineral deposits.

Private exploration has been concentrated along the basal contact zone of the Duluth Complex, west of the map area. The basal zone has undergone extensive drilling, open pit bulk sampling, a shaft with underground workings, and a variety of geophysical and geochemical surveys. Most of this work was done trying to locate copper, nickel, and titanium deposits. More recent work has concentrated on the platinum group mineral potential that might have been missed in earlier exploration.

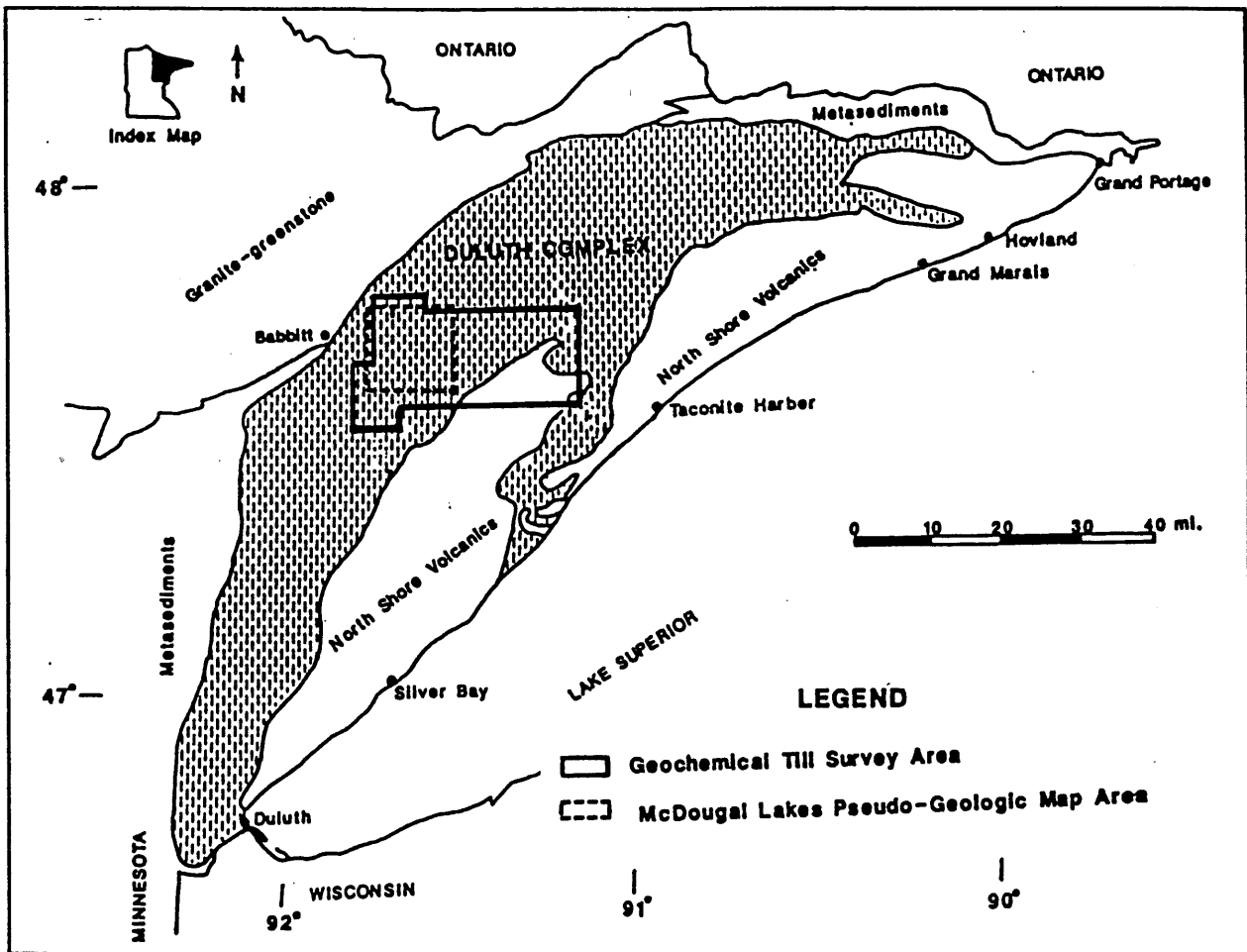


Figure 290-11. Regional geologic map of northeastern Minnesota (from Buchheit and others, 1989) showing the geochemical till survey area and the McDougal Lakes pseudo-geologic map area.

Methodology - McDougal Lakes Area

Work in the McDougal Lakes Area has produced a variety of new information. The primary product is the pseudo-geologic map of Ferderer (1989) (Plate 3). To test the accuracy of this map and the veracity of the mapping method, four types of tests were devised: 1) Drill holes; 2) Outcrop sampling; 3) Basal till pebble counts; and 4) Ground geophysical surveys.

It should be noted that although the emphasis in this report is on correlation and comparison of methods and their results, an exact match is not expected since these methods are concerned with different geologic levels and conditions. The pseudo-geologic map displays lithologic units at various depths and near surface structural features. The drill holes tested shallow lithologic units (to a depth of 193 feet) and structural features. Outcrops and pebble counts studied the surface and glacial processes.

The methods used in constructing the McDougal Lakes Area pseudo-geologic map (Plate 3) are described in Ferderer's report (Appendix E). Logs for drillholes FL-1, FL-2, and NE-2 (1,038') were available for the construction of this map. Ferderer defines geologic units with both lithologic and physical properties. For example, *otg* units are oxide-rich troctolitic and gabbroic rocks, with *otg1* being moderately magnetized, *otg2* being strongly magnetized, and *otg3* being very strongly magnetized. These and some other map units can be visualized and verified to some degree by looking at regional gravity and magnetic maps. However, most of his geologic-geophysical units cannot be visualized without the detailed, rigorous, scrutiny used to make the pseudo-geologic map.

Because there are three dimensional units involved, and many of his depths to magnetic sources are deeper within the bedrock, it becomes difficult to thoroughly evaluate the map. The magnetic source is not necessarily the depth to bedrock, but in many places represents moderately or strongly magnetized intrusive rock (rock with a strong magnetic susceptibility) lying below weakly magnetized rock (rock with a weak magnetic susceptibility). The only certain verification of these features would be deep drill holes through the magnetic source, some extending to depths of 700 meters, and perhaps averaging 250 meters, an expense far beyond the limited budget for this study.

New Drill Holes

Six new drill holes (TH-1 to TH-6) were sited to sample the bedrock over different geophysical units correlating with areas of high strategic mineral content in till samples. These holes were used to test near surface geologic units, search for evidence of mineral potential, and provide insight into deeper geologic units. Longyear Company was hired on a contract basis to drill the holes. A total of 1,036 feet was drilled, 263 feet of overburden and 773 feet of bedrock. NQ (2½") size core was recovered. The core was logged and sampled for assay and thin section studies to help with petrographic identification. Dr. John C. Green was contracted with to provide accurate petrographic logs of the core. A limited number of thin section samples helped with this task. Green's work accurately and thoroughly describes the drill core.

Magnetic susceptibility readings were taken on the core at five foot intervals using an Exploranium, G.S. Limited, KT-5, magnetic susceptibility meter. Specific gravity measurements were taken using a Jolly Balance at the same intervals.

Outcrops and Pebble Counts

Along with core logging and thin section observations, Dr. Green, with the help of Ed Venzke, conducted reconnaissance outcrop mapping and a pebble count study of glacial drift along the Tomahawk Road in the vicinity of the TH drillholes. The objective of this study was to determine the usefulness of studying glacial drift pebble compositions to determine the type of underlying bedrock in drift-covered areas.

Outcrop samples were assayed and are listed in Appendix G. These samples represent some of the major units on the McDougal Lakes Area pseudo-geologic map. A geologic map based on outcrop and assay data was then compared with Ferderer's map.

Along the Tomahawk Trail on the north side of the McDougal Lakes Area (MLA), there are several outcrops. These were included in the information Green used in making the "Two Harbors Sheet" (THS), but for this report they were re-sampled, assayed and studied with thin sections. Written locations are found in Appendix G with the assay data. Locations are shown on Plates 1 and 4 of Dr. Green and Ed Venzke's report (Appendix F).

Lithochemistry

Drill core and outcrop samples were analyzed by the DNR for both major and trace elements to help describe and correlate the lithologic units in the area. The assay work was done by Bondar-Clegg & Company Ltd., Ottawa, Ontario Canada. Analyses of samples from the TH drillholes as well as outcrops are given in Appendix G.

These analyses should be regarded as reconnaissance in nature, since only a few analyses were done on each hole and there were no duplicates or standards analyzed with them to provide a quality check. The analyses are, however, internally consistent, and do reflect the lithologic variations observed in the cores and outcrops.

In the original analytical report, the analyses for 23976 and 23977 did not agree with their lithologic descriptions. Outcrop 23977 is anorthositic, while 23976 is troctolitic. It was very obvious from the chemistry that one was an anorthosite and the other was a troctolite, but the sample numbers were reversed. The lab report even noted that sample 23976 experienced high Al interference on As, Ce, Cu, Ga, Pb, Sn, and Te. The most likely explanation is that the samples were mis-labeled at some point, so the sample numbers have been switched back in this report so the descriptions match the chemistry.

Analyses of drillholes FL-1, FL-2, and NE-2 done by the DNR in the previous biennium (Dahlberg and others, 1989) are reprinted here since those holes are within the area and were used to help construct the map. These analyses are also discussed in the geochemical interpretation and evaluation.

Ground Geophysical Surveys

Some of the structural features mapped by Dr. Ferderer respond to ground magnetic and vlf-em surveys, particularly the northwest-southeast trending faults. Seven miles of combined magnetic and vlf-em traverses were run by the DNR to evaluate these near-surface features. This work was concentrated along roads and trails in the northeast part of the McDougal Lakes Area because of high background till values (Buchheit and others, 1989) and a shortage of field assistants. Stations were measured with a one-hundred foot rope and flagged at one-hundred foot intervals. Fifty foot stations were then included by pacing the distance between 100 foot station flags. The Scintrex IGS-2 equipment was also used in this area.

Profiles of ground magnetic and vlf-em data are available on an open file basis. Short intervals of these profiles have been entered into Quattro Pro

software and graphic displays developed for this report. Some of the graphs show direct field observations of one method, while others combine vlf-em and magnetic total field data to better display a feature. For some short areas a linear regression line is developed on each side of a vlf-em cross-over to better display the structure that caused the vlf-em conductor. The vlf-em was run using the NLK station at Seattle Washington, 24.8 KHz.

NOTE: Contracts with consultants and descriptions of their qualifications or product quality and the use of equipment brand names in this report is for identification purposes only and does not constitute endorsement by the Minnesota Department of Natural Resources.

Additional Data Generated

In addition to the map and report, the following plan views and profiles made by Ferderer are available on an open file basis at the DNR Minerals Division office, Hibbing, Minnesota:

1. Bouguer Gravity Anomaly, 15 KM Bandpass Filter.
2. Second Vertical Derivative Anomaly Magnetics Upward Continued to 350 Meters and Reduced to Pole.
3. Two KM Bandpass Filter Magnetics Upward Continued to 350 M and Reduced to Pole.
4. Total Magnetic Intensity Anomaly Upward Continued to 350 M.
5. Total Magnetic Intensity Anomaly Upward Continued to 350 M and Reduced to Pole.
6. Interface - Dip (Degrees), 2 sheets.
7. Thin Sheet - Depth (Meters), 2 sheets.
8. Thin Sheet - Dip (Degrees), 2 sheets.
9. Interface - Depth (Meters), 2 sheets.
10. Thin Sheet - Susceptibility Cont. (CGS*1000), 2 sheets.
11. Interface - Susceptibility Cont. (CGS*1000), 2 sheets.
12. Plan view of location forward modeling profiles.
13. Forward Modeling Profiles, 15 sheets.

Results and Discussion - McDougal Lakes Area

Dr. Ferderer defines lithologic units with both petrographic and geophysical parameters which are shown on his plan view (Plate 3). He also maps structural features and depths to magnetic source, not necessarily the depth to bedrock. The standard bedrock geologic map plan view shows the geology either as outcrop or at the interface between overburden and bedrock. Dr. Ferderer includes the third dimension of layered rock units on his map. This is done with depth determinations on his plan view and forward modeling profiles showing the depth relationship of these units. In essence his study includes near surface glacial deposits, bedrock lithologic units with structural features, and deep lithologic units and structural features.

An expanded discussion and interpretation of the results of each method follows. The most significant result was Ferderer's pseudo-geologic map (Plate 3, scale 1:62,500) and report (Appendix E). The methods used to evaluate the pseudo-geologic map are noted here, with an expanded discussion and interpretation following. The discussion is divided into sections which compare geophysical units and geologic units, describe the geophysical core measurements, describe the lithochemistry of drillhole and outcrop analyses, and summarize significant features of the ground geophysical surveys.

Summary sheets of the six TH drill holes (Appendix B) and assay data (Appendix G) are included in this report. The drill core, logs, and thin sections are available for inspection on an open file basis at the DNR Minerals Division office in Hibbing, Minnesota. Physical measurement results on the core are described in this report.

The report by Green and Venzke (Appendix F) describes the results of the pebble count study. Samples and thin sections are available at the DNR Hibbing office.

Selected features of the ground geophysical surveys are reported here. Complete profiles are available on an open file basis as either hard copies or on computer diskettes.

Comparison of Pseudo-Geologic and Geologic Maps

Ferderer's geologic units are displayed with structural features and depths to magnetic source (Plate 3). The units are described in both lithologic terms and geophysical parameters, with depth to magnetic source given in meters. The magnetic source is not necessarily the depth to bedrock, but in many places

represents moderately or strongly magnetized intrusive rocks (rock with a strong magnetic susceptibility) which lie below weakly magnetized rocks (rocks with a weak magnetic susceptibility). Many of these estimates are much deeper than the bedrock surface. This would be expected with younger Proterozoic rocks that have not been deformed and still retain a somewhat horizontal orientation.

A comparison of the same area of Ferderer's McDougal Lakes Area map (MLA) 1:62,500 scale and the Two Harbors Sheet (THS) of Green, scale 1:250,000, (1982), shows that Ferderer's map is complicated by subdivision of lithologic units based on physical properties. On the MLA map the subdivision of units on a lithologic basis generally follows the subdivisions of Green (1982). Anorthosites, troctolites, and granophyric rocks are generally mapped in the same locations on both maps. However, it immediately becomes apparent that Dr. Ferderer further subdivides his units on the basis of magnetic susceptibility and density. Subdivisions based on geophysical parameters also occur at depth. The two dimensional plan view is somewhat deceptive since it actually represents three dimensional geology. This information is shown as dip symbols and underlined numbers showing depth to magnetic source along unit contacts.

The positions of the six TH drill holes can be located on the MLA map in Fig. 10. Detailed drill logs are available on an open file basis, with summary sheets included in this report (Appendix B). The summary log sheets include location and drilling information, assay intervals, highlights of assay data, and thin section samples, which are available on an open file basis. Table 3 summarizes and compares drillhole lithologies and the lithology and geochemical grouping of core and outcrop analyses with the geophysical map units of Ferderer.

Structure: The three dimensional composite view of the north part of the map area with the H-H' forward modelling profile (Fig. 12) is an attempt to better understand the geologic relationships and how thoroughly various pseudo-map units were evaluated. TH hole locations are plotted and the holes projected onto the H-H' profile as short vertical lines with a cross bar at the bottom of the hole. They are at the same vertical scale as the computer modelled units.

Faults trend north-northeast to northeast on the THS, whereas on the MLA they mostly trend northwest, with some north-south or east-west faults. Some

Table 290-3. Comparison of Drillholes, Core Analyses, and Outcrops with the McDougal Lakes Area Pseudo-Geologic Map.

Sample Number	Petrographic Description	Ferderer's Map		Geochemical Group
		Unit	Description	
TH-1	Troct-Picrite & Troctolite	tb2	Weakly Magnetic, Dense Troctolite	
18140	Troctolite-Picrite			Troctolite-Picrite
18142	Troctolite-Picrite			Troctolite-Picrite
18143	Troctolite-Picrite			Pyroxene Troctolite
18145	Pyroxene Troctolite			Troctolite-Picrite
18148	Pyroxene Troctolite			Pyroxene Troctolite
TH-2	Troctolite-Picrite	otg2	Strongly Magnetic Troctolite	
18131	Troctolite-Picrite			Troctolite-Picrite (TH-2)
18132	Troctolite-Picrite			Troctolite-Picrite (TH-2)
18133	Troctolite w/Dunite			Picrite/Dunite (TH-2)
18134	Picrite-Troctolite			Troctolite-Picrite (TH-2)
TH-3	Troctolite-Picrite	tb1	Moderately Magnetic, Low Density Troctolite	
18149	Troctolite-Picrite			Troctolite-Picrite
18151	Troctolite-Picrite			Troctolite-Picrite
18153	Troctolite			Pyroxene Troctolite
TH-4	Olivine Gabbro	gb	Weakly Magnetic, High Density Gabbro	
18156	Olivine Gabbro			Olivine Gabbro
18157	Olivine Gabbro			Olivine Gabbro
TH-5	Troct & Gab Anorthosite	a/a1	Weakly Magnetic, Low Density Anorthosite	
18159	Gabbroic to Troct Anorth			Anorthosite
18162	Ol-bearing Anorthosite			Anorthosite
TH-6	Troctolitic Anorthosite	a	Weakly Magnetic Anorthosite	
18165	Cpx-bearing Troct Anorth			Anorthosite
18166	Troctolitic Anorthosite			Anorthosite
FL-1	Gabbro	otg1	Moderately Magnetic Troctolite & Gabbro	
20142	Oxide Gabbro			Oxide Gabbro/Pyroxenite
20143	Oxide Melagabbro/Pyroxenite			Oxide Gabbro/Pyroxenite
20145	Oxide Gabbro			Oxide Gabbro/Pyroxenite
20146	Gabbroic Anorthosite			Anorthositic Oxide Gabbro
FL-2	Anorthositic Troctolite	otg1	Moderately Magnetic Troctolite & Gabbro	
20141	Anorth Augite Troctolite			Pyroxene Troctolite
NE-2	Troctolite & Anorthosite	otg3	Strongly Magnetic Troctolite & Gabbro	
20147	Oxide Gabbro			Oxide Gabbro
20148	Oxide Gabbro			Oxide Gabbro
20149	Oxide Gabbro			Oxide Gabbro
20150	Oxide Olivine Gabbro			Oxide Olivine Gabbro
20151	Oxide Olivine Gabbro			Oxide Olivine Gabbro
Outcrops				
18169	Olivine Anorthositic Gabbro	gb	Gabbro	Olivine Gabbro
18170	Troctolite	tb2	Troctolite	Troctolite-Picrite
18171	Anorthosite	a/a1	Anorthosite	Anorthosite
18172	Anorthosite	a	Anorthosite	Anorthosite
18192	Troctolite	tb2	Troctolite	Pyroxene Troctolite
18193	Troctolite	gb	Gabbro*	Troctolite-Picrite
18196	Anorthosite	a	Anorthosite	Anorthosite
23976	Troctolite	otg2	Troctolite & Gabbro	Pyroxene Troctolite
23977	Troctolitic Anorthosite	a	Anorthosite	Anorthosite
23978	Troctolite	gb	Gabbro*	Olivine Gabbro
23980	Anorthositic Troctolite	a1	Anorthosite	Anorthosite
24011	Olivine Melagabbro	gb	Gabbro	Olivine Melagabbro

*In gabbro but less than one-fifth mile to the mapped contact with troctolite.

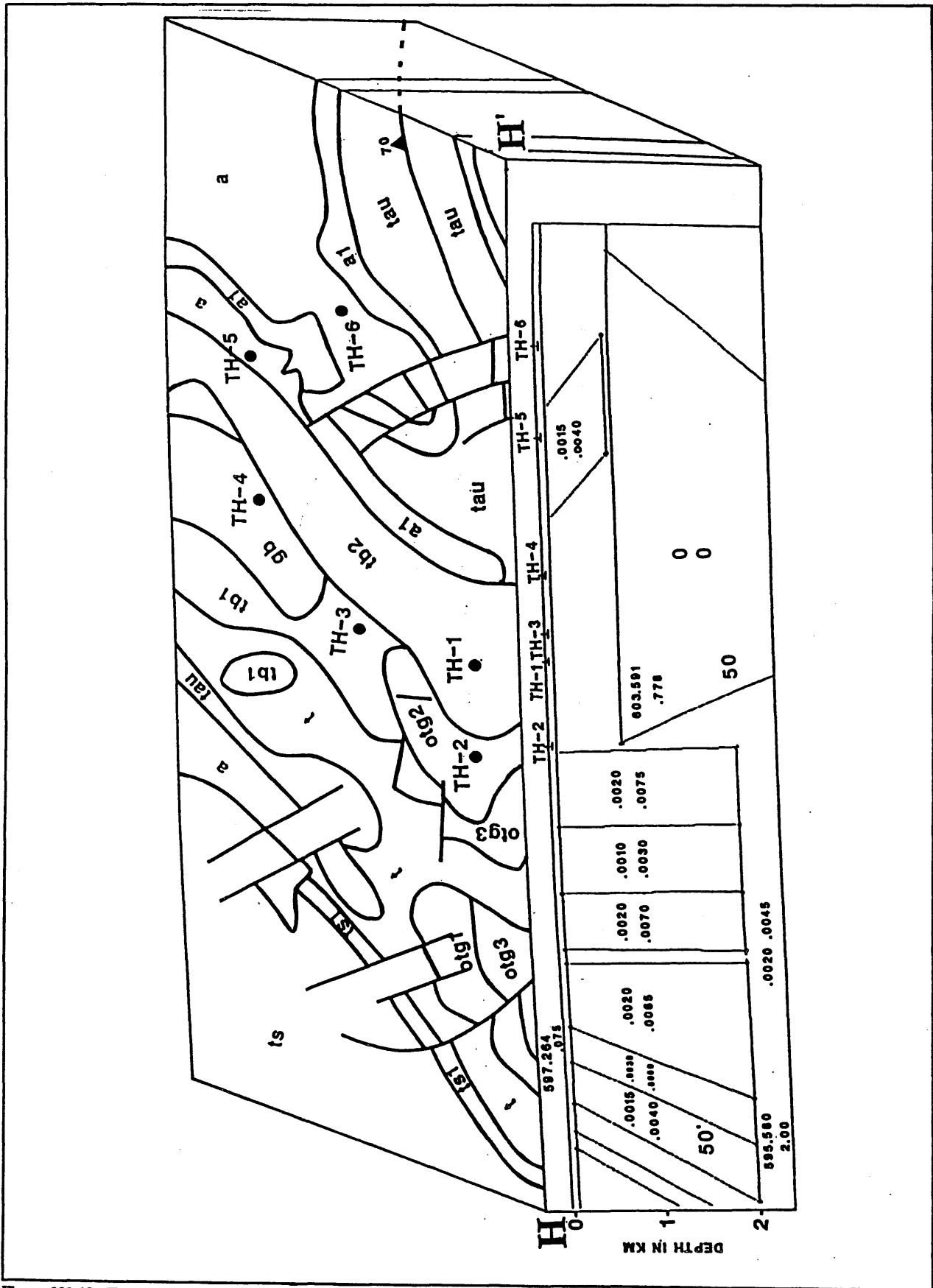


Figure 290-12. Forward modeling profile H-H' (modified from Ferderer, 1989).

northwest-southeast linear features were noted in the location and access section which suggest faults; these support the dominant fault orientation as mapped by Ferderer (1989). There are also linear features at right angles supporting Green's (1982) dominant fault orientation. It is difficult to define linear features with approximately the same orientation as the flight lines for the aeromagnetic survey, which were north-south in this area. Further evidence for the northwest-southeast trending faults will be presented in the section on ground geophysics.

South Kawishiwi Intrusion: The South Kawishiwi Intrusion (SKI) is represented on Ferderer's map by units *ts* and *ts1*. The area of these units matches the area mapped as the SKI by Green (1982) very closely. No drilling or reconnaissance mapping/sampling was done in this area.

Bald Eagle Intrusion: Three geophysical units generally correlate with the Bald Eagle Intrusion (BEI). Unit *tb1* is described as moderately magnetized, relatively low density troctolitic rocks along the western side of the BEI. The weakly magnetized and relatively dense troctolitic rocks along the eastern side of the BEI are *tb2* on the MLA map. Unit *gb* is described as the core of the BEI with weakly magnetized relatively dense gabbroic rocks.

The olivine-bearing gabbro and ferrogabbro *dg* unit of Green (1982) generally coincides with the *gb* and adjacent *otg1* unit as well as a positive gravity anomaly. The *gb* unit was penetrated by TH-4, logged primarily as olivine gabbro. The core is extensively serpentinized and shows slickensides in some places. Several small pegmatitic granite veins were intersected. At least some of the pegmatite veins have a higher magnetic susceptibility than the host rocks.

The troctolitic outer zone of the intrusion is represented by units *tb1* and *tb2*. TH-1 is located on Ferderer's *tb2* unit and TH-3 is in the *tb1* unit. Both holes contain pyroxene troctolites, troctolite-picrite, and troctolite with picrite intervals. Picrite intervals are sheared and serpentinized. Some fractures are filled with white clay or zeolite minerals, sometimes stained red from hematite or iddingsite.

The outcrop mapping did reveal some minor discrepancies from the pseudo-geologic map. Outcrop sample 18169 is described as olivine-bearing anorthositic gabbro and mapped as part of the gabbroic core of the BEI; the MLA map includes this area in the *tb2* zone rather than the *gb*. Samples 18193 and 23978 are troctolitic. On the MLA map they are located on the *gb*, gabbro unit, but they are close to the mapped

contact with the *tb1* unit which is troctolitic rock. An olivine melagabbro (24011) also falls in the *gb* unit.

Troctolite: Based on a few outcrops, Ferderer described unit *t*, found throughout most of the area, as troctolitic. The western part of the pseudo-geologic map area is shown on the THS as being *dt*, troctolite and anorthositic troctolite, with the southwest corner in a unit of *du*, undivided intrusive rocks with few or no outcrops. The MLA map has a complex mixture of troctolites, oxide rich troctolite, and gabbroic rocks, with an anorthosite unit in these areas.

Although FL-2 is located on the *otg1* unit, it was drilled along the flanks of the small anomaly penetrated by FL-1, and only to a depth of 65 feet (Vadis and others, 1981). FL-2 was logged as anorthositic augite-bearing troctolite by Vadis and others (1981) and may represent the rocks of the *t* unit in this area. An isolated anorthositic troctolite outcrop within the *t* unit was also noted by Venzke (in prep.) to the east.

Anorthosite: Relatively low density anorthositic rocks are divided into a weakly magnetized unit, *a*, and a slightly more magnetized zone within *a* labeled *a1*, although Ferderer notes that their magnetic expression is uninformative (Appendix E). These units are found in the northeast corner of the area and adjacent to a part of the South Kawishiwi Intrusion. Another anorthositic unit (*tau*) with an indistinct magnetic signature is mapped in the southeast and southwest corners of the map.

All of the anorthositic units on the eastern side of the pseudo-geologic map are included in the *da* unit of Green (1982), consisting of anorthositic gabbro, anorthosite, and gabbroic and troctolitic anorthosite. The southwestern *tau* area is included in the *du* unit noted previously.

Anorthositic rocks were described in drillholes TH-5 and TH-6. TH-5 is located near the contact of Ferderer's *a* and *a1* units, while TH-6 is completely in *a*. TH-5 was logged as a mixture of troctolitic and gabbroic anorthosite. The core displays some features associated with shearing and faulting. It could be on a fault zone, although somewhat northeast of Ferderer's map location. TH-6 was logged as anorthosite to troctolitic anorthosite, and some fractures with a thin film of serpentine were noted.

Outcrops located within the *a* unit in the vicinity of the TH-5 and TH-6 holes were all anorthositic. Within the *tau* unit just west of McDougal Lakes, Venzke (in prep.) also reports anorthosite outcrops.

Oxide-rich Rocks: A unit of oxide-rich troctolitic and gabbroic rocks (*otg*) occur as discrete lithologic units within the troctolitic series. These rocks are divided into three subunits based on relative magnetization with *otg1* being moderately magnetized, *otg2* strongly magnetized, and *otg3* very strongly magnetized. Two subunits of *otg3* were also distinguished, the more strongly magnetized denoted with an asterisk. The magnetic bodies that cause the anomalies, although all designated as *otg* units, are discussed as two different groups by Ferderer.

The three *otg* bodies within *t* in the western part of the area are thought by Ferderer to be related (see Appendix E for details). The elongate anomalies to the east adjacent to and within the *tau* unit were interpreted by Ferderer to be caused by oxide-rich gabbroic and troctolitic rocks, probably similar to those that compose the Greenwood Lake Anomaly to the south (Vadis and others, 1981), some of which may be a continuation of that body.

Venzke (in prep.) agrees that the *otg3* body west of the granophyre is probably an extension of the Greenwood Lake Anomaly, but there is no evidence beyond the continuation of the magnetic anomaly trend. The narrow *otg2* body north of the granophyre may also be a continuation of this anomaly, but must be at depth below anorthositic rocks, since anorthosite outcrops have been identified east of McDougal Lakes by Bonnicksen (1971) and Venzke (in prep.). The massive oxide gabbros intersected by NE-2 in the eastern *otg3* unit, however, are not like the well foliated cumulate oxide gabbros described by Venzke (in prep.) and thought to be related to the oxide peridotites of the Greenwood Lake Anomaly (Vadis and others, 1981, and Venzke, in prep.).

TH-2 is located on Ferderer's *otg2* unit, oxide rich troctolitic and gabbroic rocks, in the central *otg* body south of the Bald Eagle Intrusion. Logged as primarily troctolite-picrite, it has a total depth of 191 feet. Picrite intervals are sheared and serpentinized and there are numerous fractures filled with white clay.

Hole FL-1, with a depth of 125.5 feet, is located on Ferderer's *otg1* unit on an outlier of the main southwestern *otg1* body. The core was logged as being oxide-gabbro-hornfels from 13.3 to 51.5 feet, then oxide gabbro to the bottom of the hole (Vadis and others, 1981). FL-2 did not intersect oxide-rich rocks and is discussed in the section on troctolitic rocks.

Hole NE-2 was logged as dominantly a massive oxide rich, olivine-bearing gabbro with some intervals of olivine melagabbro, pyroxenite, troctolite and anorthosite (Sellner and others, 1985). On Ferderer's

map, hole NE-2 is located on the contact between his *otg3* and *t* units. The *otg3* is strongly magnetized oxide-rich troctolitic and gabbroic rock which would correlate with the core log.

Granophyre: Granophyric rocks, weakly magnetized, are found as a single body in the southeast area of the MLA map, and are represented by unit *g*. The *df* unit of granophyric granite and adamellite on the THS corresponds to this granophyric zone. Ferderer notes that the granophyre may be more extensive than shown on the pseudo-geologic map, which is shown to be the case by Venzke (in prep.) on the basis of outcrops in the area and topographic highs characteristic of the granophyre in the area.

Geophysical Measurements of Drill Core

Figures 13 and 14 summarize the results of measuring magnetic susceptibility and density at five foot intervals on the TH drill cores and relate them to lithologies. Each graph is divided into three sections: lithology, detailed lithology, and drillholes. The lithology section distinguishes between major lithologic groups (anorthosites, olivine gabbro, troctolites, and troctolite-picrites from TH-2). Further subdivisions are shown in the detailed lithology section where the anorthosites are divided into anorthosite and oxide anorthosite, and the troctolites are divided into pyroxene troctolite and troctolite-picrite. The drillhole section is simply data from each respective hole without regard for lithologic differences. These summary graphs of the geophysical parameters show the range of readings as the length of the bar, the average for that hole or unit as a solid square with the value next to it, and one standard deviation on each side of the average as a tic mark on the bar.

Magneticsusceptibility and density measurements for each hole are given in Appendix C along with diagrams showing the values measured at five foot intervals as a depth profile. Regression line data is also presented and plotted. Trends of magnetic susceptibility and density are more easily visualized when a linear regression line is added to the graph. It is not known whether these trends can be projected to Ferderer's magnetic source depths, but they do reflect the expected response from some of his units. Table 3 compares drilled lithologic units with Ferderer's mapped units and physical properties.

Drillhole TH-1 has a high average density and moderate to high average magnetic susceptibility, compared with other TH holes, with strong variations between readings or groups of readings. Linear regression lines show density increasing with depth

and magnetic susceptibility decreasing. The closest magnetic source depth estimates are 450 meters and 700 meters.

TH-2 has moderate average magnetic susceptibility and low average density compared with other TH holes. There are strong variations between readings or groups of readings in this hole. The density increases slightly with depth and magnetic susceptibility increases strongly with the closest magnetic source depth estimates ranging from 200 to 700 meters.

TH-3 has a moderately high average magnetic susceptibility and a moderate average density compared to other TH holes. These physical properties have moderate to strong variations between readings or groups of readings. Linear regression lines of core measurement data show that density is constant with depth and magnetic susceptibility is strongly decreasing. The closest magnetic source depth estimate to hole TH-3 is 450 meters.

TH-4 has a very low average magnetic susceptibility and a low to moderate average density compared to other TH holes. The magnetic susceptibility and density exhibits small variations between readings, except for a strong positive reading on a granitic pegmatite vein. Linear regression lines of core measurement data show density is decreasing with depth and magnetic susceptibility is constant. The closest magnetic source depth estimate is 450 meters.

TH-5 has a low average magnetic susceptibility and a low average density compared to other TH holes. The density and magnetic susceptibility have minor variations between readings. Linear regression lines of core measurement data show that density remains constant with depth and magnetic susceptibility increases slightly. The closest magnetic source depth estimate is 450 meters.

TH-6 has moderate average magnetic susceptibility and density compared to other TH holes. The density has minor variations between readings. The magnetic susceptibility varies strongly between groups of readings. Linear regression lines of core measurement data show density increases slightly with depth and magnetic susceptibility increases strongly. The nearest magnetic source depth estimates are 150 to 250 meters.

When using lithologic classifications as logged by normal petrographic methods there is considerable variation of average magnetic susceptibilities between lithologic units even though individual observations, within one standard deviation of the average, overlap each other on the vertical axis of the graph (Fig. 13). This suggests that at least some lithologic units can be differentiated based on their magnetic susceptibility. In density measurements only the troctolites seem to

have a significant difference from other lithologies (Fig. 14).

When more detailed petrographic descriptions separated anorthosites from oxide-bearing anorthosites, the separation for average magnetic susceptibility of most units is increased. It should be noted that all of the anorthosites observed in the cores are mixed gabbroic and troctolitic anorthosites. For this discussion, the oxide (magnetite) content is a significant variable, so the anorthosites are described either as anorthosite (oxide-poor) or oxide anorthosite (oxide-rich).

Comparing the lithology group with the detailed lithology group, the range of the standard deviation becomes smaller for the anorthositic rocks, showing that the oxide bearing intervals have been removed. With the same comparison the standard deviation range of the oxide bearing anorthosite is increased, suggesting there are both oxide-rich and oxide-poor intervals in this group. The change in averages after dividing this group is also striking; the average for all the anorthosites is 5.22, while the average for the plain anorthosites is 3.84 and the oxide anorthosites is 15.09. As can be seen in the section on the drillholes and in the profiles in Appendix C, most of the variation is found in TH-6 whereas TH-5 is relatively uniform. This is only one example with a few measurements and not a detailed study, but it does indicate that for some rock types geophysical measurements can be useful in distinguishing and naming rocks where petrographic descriptions are not definitive. Looking at the density measurements for the detailed lithologies there is a small difference between anorthosites and oxide anorthosites, but not enough to distinguish the units.

Density measurements were better able to distinguish the troctolitic lithologies. The troctolite-picrite lithology has the highest density of all the units, but the troctolite-picrite of hole TH-2 has the lowest density which reflects the lower percentage of oxides and greater percentage of olivine and associated alteration. The lower oxide content is also reflected by the lower magnetic susceptibility of the TH-2 rocks compared to the troctolites of TH-1 and TH-3 when taken as a whole. Although the differences are not as obvious for the troctolites, additional measurements may allow refinement so that more definitive statements can be made.

The olivine gabbro in TH-4 from the Bald Eagle Intrusion has a similar density to other rock types, but the magnetic susceptibility, although overlapping the low extremes of other units, averages 1.38 with very little variation (also see Appendix C).

Looking at the grouping by drill holes there is almost as much variation for both magnetic suscep-

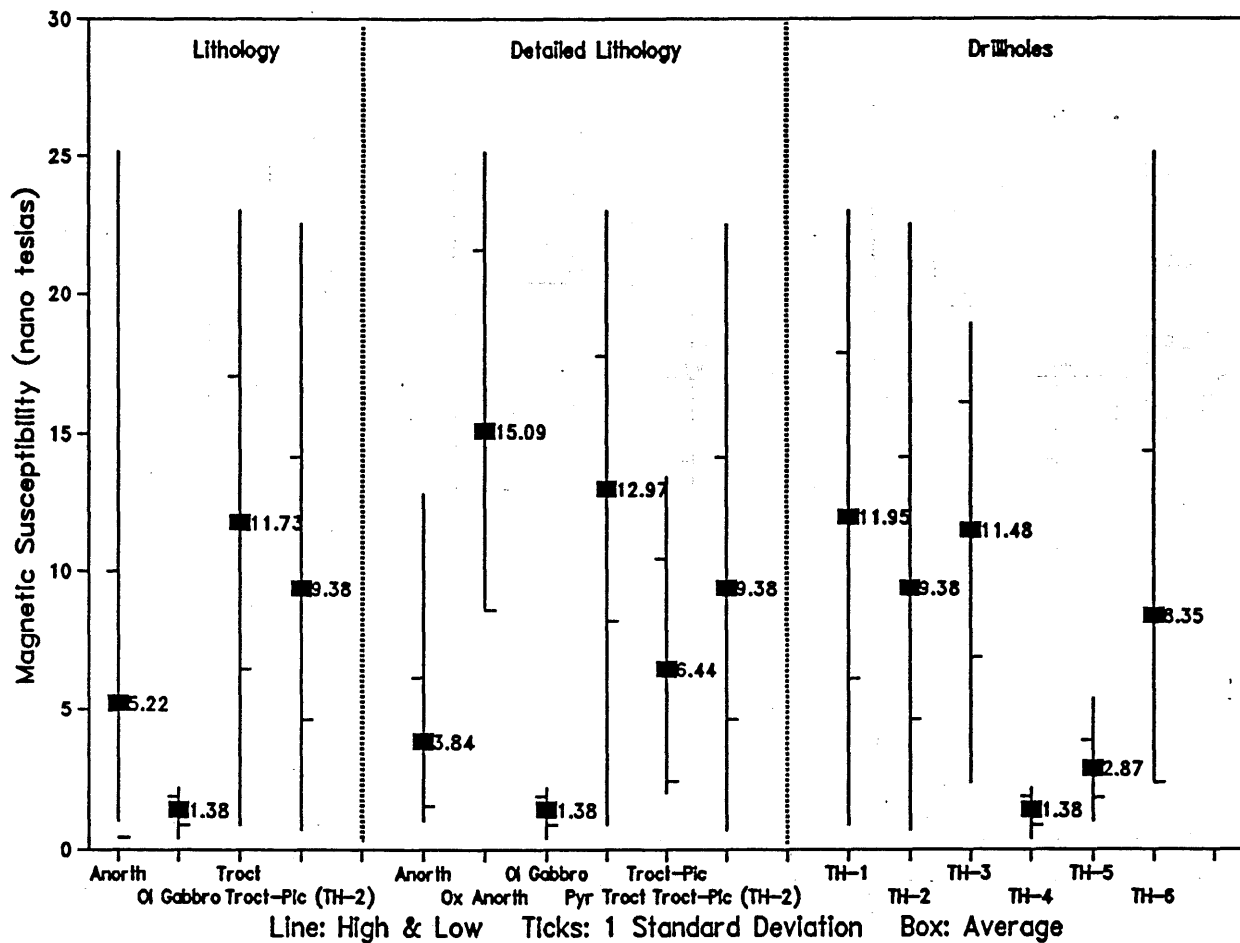


Figure 290-13. Summary of magnetic susceptibility measurements on drill core.

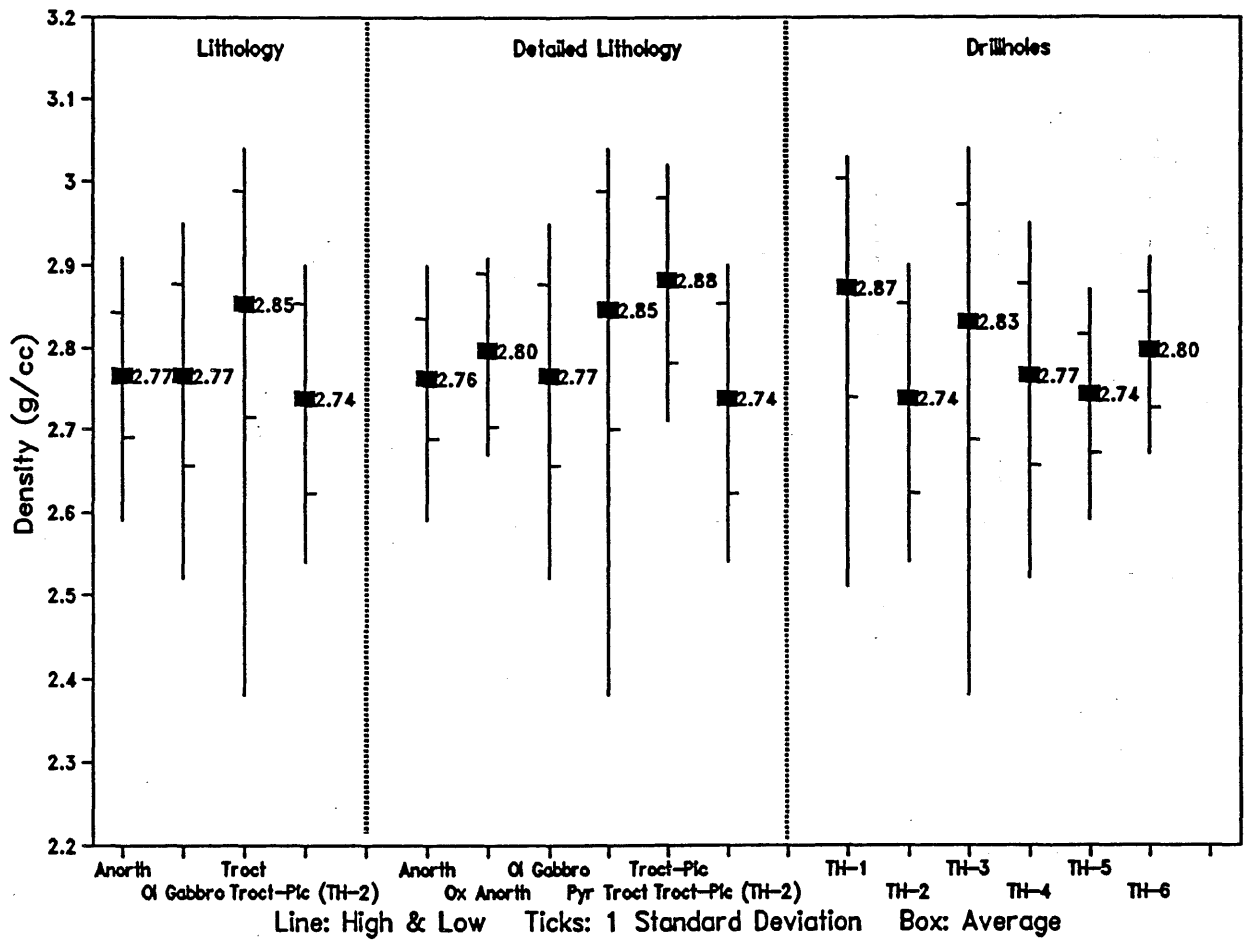


Figure 290-14. Summary of density measurements on drill core.

tibility and density between holes as there is between lithologic units. This suggests that while there are detailed variations of lithology within a hole, the overall measurements will place it in a distinct geophysical classification, and that generally this classification will follow a lithologic classification. This further suggests that classification of lithologic units based on airborne magnetic survey data is reasonable for the rocks found in this area, although the results from the three troctolitic drill holes are so close together that hole lithologies could not be differentiated based on magnetics alone. Average density measurements of lithologies also shows considerable variation, and a greater density variability in units which had small variations in magnetic susceptibility. This shows the need to use more than one geophysical method in the making of pseudo-geologic maps. It also shows the need for a physical properties database of Minnesota's lithologic units.

Lithochemistry of Drill Core and Outcrops

All assay data is included in Appendix G. This data includes new drillcore and outcrop analyses completed for this project and reprints analyses from drillholes FL-1, FL-2, and NE-2 (Dahlberg and others, 1989) located in the southern part of the McDougal Lakes Area. Outcrops are located on Plate 4 of Appendix F. Overall, this data set appears to be internally consistent and the analyses correspond well with the lithologic descriptions of outcrops and drillcore as noted below. No significant base or precious metal occurrences were found in the six new drill holes.

When plotted on variation diagrams, these rocks fall into distinct groups which generally correspond to their lithotypes. The most significant chemical variations are in MgO and FeO* (total iron), reflecting variations in olivine and magnetite content. Figure 15 is an MgO vs. FeO* variation diagram showing all of the analyses from this area. Fields are outlined and named with the general lithotype of the samples in each group. The outlines are only meant to help locate and identify the lithologies of samples analyzed in this study, and are not an interpretation of any limits or boundaries for classification purposes. This diagram distinguishes anorthositic rocks, gabbros and troctolites related to the Bald Eagle Intrusion, and four varieties of oxide-rich gabbroic rocks. These major types will be discussed below and correlated with the pseudo-geologic map. Pyroxenes are also significant minerals in these troctolitic and gabbroic rocks. The CaO vs TiO₂ variation diagram (Fig. 16) also identifies the different lithotypes, although is unable to distinguish between the troctolite-picrites.

TiO₂ is a reflection of the ilmenite content. Analyses are also plotted on a standard AFM diagram (Fig. 17).

Anorthositic Rocks: Gabbroic and troctolitic anorthosites were identified in drillholes TH-5 and TH-6 drilled into the anorthositic *a* and *a1* units and outcrops in the northeast corner of the pseudo-geologic map. This group is represented by four outcrop analyses and four drillcore analyses. These analyses are more magnesium and iron-rich than to those of the coarse-grained anorthosite (> 95% plagioclase) outcrops of Venzke (in prep.) east of McDougal Lakes in the *tau* unit.

Bald Eagle Intrusion: Six lithotypes have been identified which represent or may be related to the Bald Eagle Intrusion. These rocks have been described as olivine gabbros, melagabbros, pyroxene troctolites, troctolite-picrites, and dunites. FeO* exhibits a consistent positive correlation with MgO content from olivine gabbro to melagabbro to pyroxene troctolite to one group of troctolite-picrites (Fig. 15). These rocks all exhibit similar MG#'s (Fig. 18). A second group of troctolite-picrites and a picrite/dunite composite sample have distinctly higher MG# values.

One melagabbro outcrop from the core zone of the intrusion was sampled, which has a very similar chemistry to the Bald Eagle melagabbro sample M6505 reported by Weiblen and Morey (1980).

Olivine gabbro, also from the core zone of the intrusion, was identified in outcrop and drillhole TH-4. Two analyses from TH-4 (18156 and 18157) and one outcrop sample (18169) plot together.

A transitional rock type is thought to be represented by outcrop 23978, described in the field as a troctolite, but which has mixed chemical characteristics. MgO and FeO* values are similar to the olivine gabbros, but on variation diagrams of other elements such as CaO (Fig. 16), it plots with the pyroxene troctolites. This may be a transitional rock type such as those described by Weiblen (1965) as containing more interstitial pyroxene than typical outer zone troctolites. A greater percentage of olivine than the gabbros and more pyroxene than the troctolites could explain the chemical variations in MgO and CaO relative to the gabbros and troctolites.

Five samples from TH-1 and three samples from TH-3 were assayed and fall into two related groups on geochemical variation diagrams: troctolite-picrite and pyroxene-troctolite. These lithologic variations were noted in the cores, although the distinctions were not very great in some cases. As seen in the logs and the

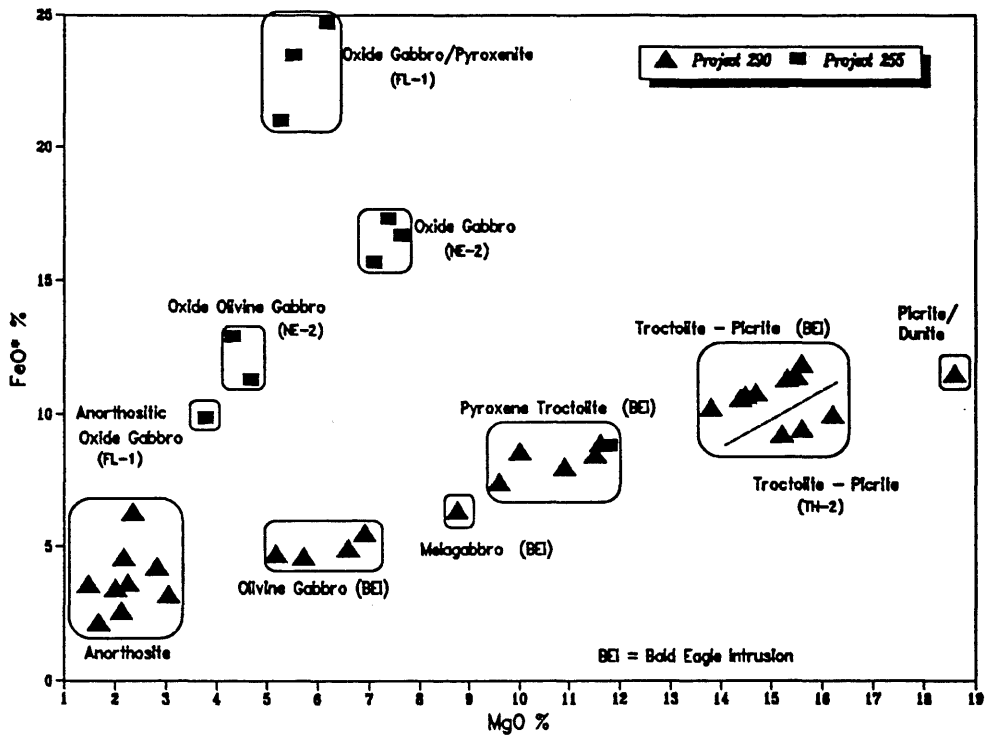


Figure 290-15. MgO vs. FeO* variation diagram showing geochemical fields with associated lithologic names of samples. Project 290 data from this study; Project 255 data from Dahlberg and others (1989).

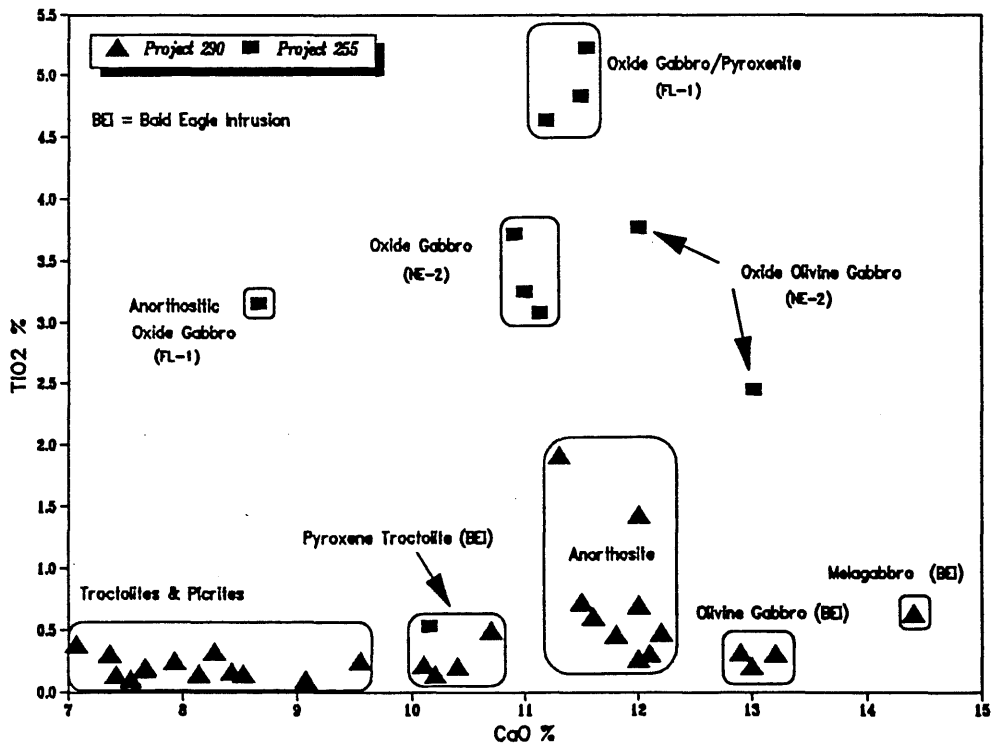


Figure 290-16. CaO vs. TiO₂ variation diagram showing geochemical fields with associated lithologic names of samples. Project 290 data from this study; Project 255 data from Dahlberg and others (1989).

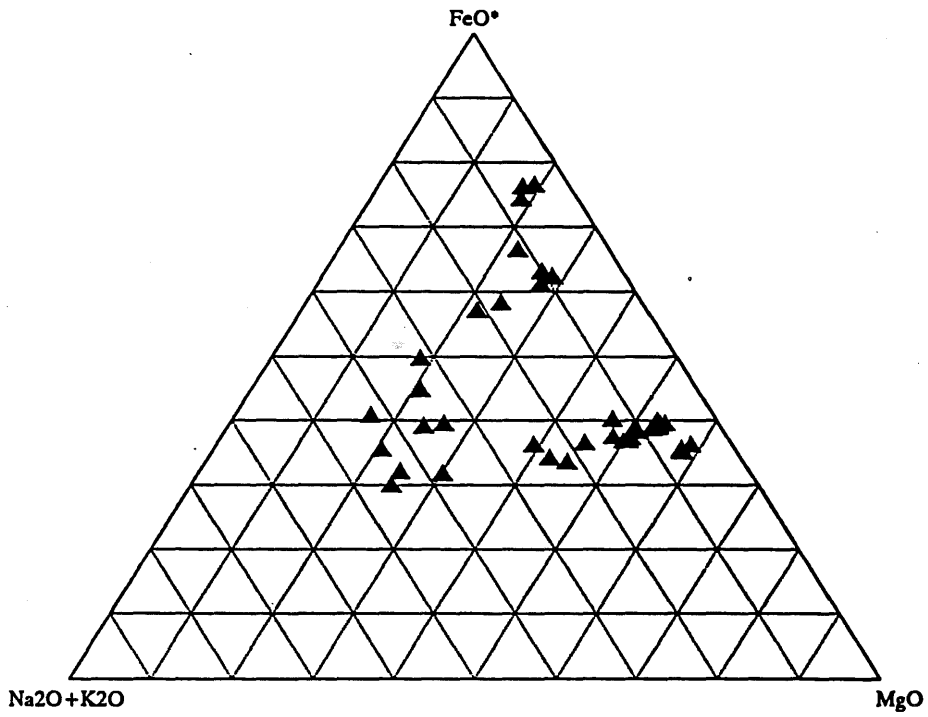


Figure 290-17. AFM diagram of McDougal Lakes Area analyses.

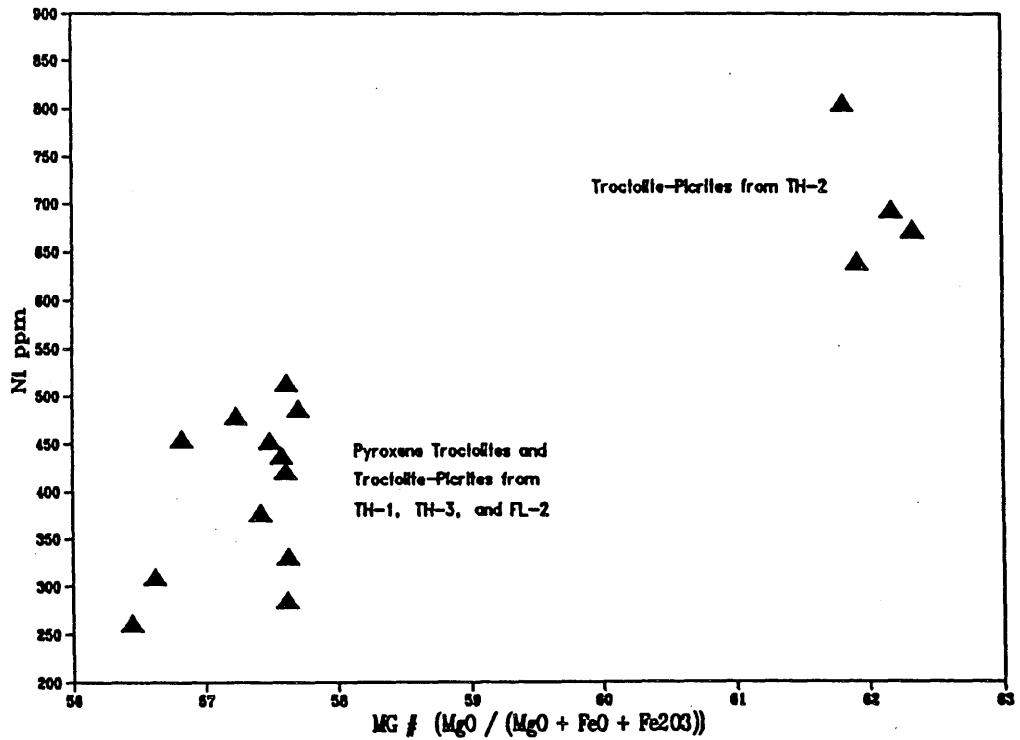


Figure 290-18. Variation diagram of MG# vs. Ni showing varieties of Troctolite-Picrite.

analyses, these units are intermixed, and may represent cyclic crystallization and accumulation. Since one hole is in *tb1* and the other in *tb2*, but both lithologies are present in each, a distinction between them is difficult to make. Portions of both of these units have been mapped as the outer zone of the Bald Eagle Intrusion by Weiblen (1965) and Green and others (1966).

FL-2 had only one assay which plotted in the field of a pyroxene troctolite. In map view, this hole is within the *otg1* unit. However, Vadis and others (1981) describe this hole as being drilled adjacent to the anomaly penetrated by FL-1, which has very different rock types and analyses. Since this hole did not reach the rocks of the *otg1* unit, these rocks and analysis can be taken as representing the unit *t* in this area. Although one short drillhole and a single analysis is not conclusive, this suggests that unit *t* may be the same as, or related to, units *tb1* and *tb2*.

A second group of troctolite-picrites was distinguished on the basis of chemistry in drillhole TH-2. This hole is in an *otg2* unit south of the Bald Eagle Intrusion, and is distinguished from the other troctolite-picrites by a higher MgO/FeO* ratio. This is most obvious on a variation diagram with the MG# (Fig. 18). The MG# ($\text{MgO} / (\text{MgO} + \text{FeO} + \text{Fe}_2\text{O}_3)$) was calculated using recalculated iron values, where $\text{FeO} = 0.8 \text{ FeO}^*$. The rocks from TH-2 all have MG#'s close to 62, compared to the pyroxene troctolites and troctolite-picrites from TH-1, TH-3, and FL-2, which are all in the 56-58 range, with most about 57.5. The TH-2 troctolites also have higher Ni values.

Oxide Gabbros: Four varieties of oxide gabbros are distinguished primarily on the basis of total iron content (FeO*). All of these samples are from drillholes FL-1 and NE-2, which were drilled on magnetic anomalies described and mapped as *otg* units on the MLA map.

Three FL-1 samples have MgO content of an olivine gabbro but very high total iron (FeO*); descriptions of these rocks from core and thin sections identify them as oxide gabbros or melagabbros and pyroxenite (Vadis and others, 1981, and Venzke, in prep.).

Less iron and slightly more MgO are evident in three analyses from NE-2, which are described as oxide gabbros. Chemically these rocks show some similarities to the oxide gabbros associated with the Greenwood Lake Anomaly to the south, however, these massive oxide gabbros are lithologically very different from the foliated oxide gabbros associated with that anomaly as described by Venzke (in prep.)

Two NE-2 analyses have a low MgO for an olivine gabbro but high FeO, and are described as oxide olivine gabbros in the log (Sellner and others, 1985). These samples plot close to the anorthositic oxide gabbro from FL-1 on Fig. 15, but are distinctly different with respect to pyroxene content, as seen on Fig. 16.

Ground Geophysical Surveys

Magnetic and vlf-em traverses provide good indications that the fault zone in the northeast quarter of the map area exists. Depths to bedrock are much shallower than estimated magnetic source depth estimates. Short intervals of vlf-em and magnetic data are presented and discussed below.

A traverse was run west on the Tomahawk Trail from the road junction in the northeast quarter of section 30, T61N, R9W. A strong cross-over is observed just east of where Snake Creek goes through a culvert under the Tomahawk Trail (Fig. 19). The orientation of the east-west road and the expected strike of the fault from the MLA map would be likely to produce the erratic cross-over observed. The magnetic profile (Fig. 20), suggests a negative magnetic feature developing between station 1,750W and 2,300W that is masked by the anomaly from the culvert. Some evidence of faulting was observed in drill hole TH-5, and a line from TH-5 through the Snake Creek cross-over parallels Ferderer's mapped faults.

Another traverse was run north from a road junction in the northeast quarter of section 25, T61N, R10W. There was a cross-over located in section 24, T61N, R10W (Fig. 21) which is close to drill hole TH-5. This is additional evidence for a fault zone in this area. On the magnetic profile, however, there is no direct evidence of a fault (Fig. 22). Linear regression lines calculated north and south of the cross-over show an increase in the slope, but no definite evidence for faulting.

On the Tomahawk Trail profile (Sec. 26, T61N, R10W) there are two cross-overs at stations 8,600W and 9,050W just east of Robin Creek (Fig. 23) which are probably two vertical sheet conductors. However, the quadrature doesn't cross to the positive side, which is interpreted as a weak, possibly surficial conductor. The total field magnetic profile (Fig. 24) shows a sharp increase in magnetic susceptibility west of the cross-over at station 9,050W. Regression lines were calculated east and west of the cross-over which clearly display the vertical offset interpreted as a fault in bedrock with the west side upthrown.

The vertical in-phase part of a vlf-em profile and the total field magnetic field profile is displayed on

Fig. 25. This profile runs south along Forest Service Road 386 from the road junction in the northwest quarter of section 32, T61N, R9W. A strong cross-over indicating a vertical sheet conductor is seen at station 2,000S, coincident with a roughly dish-shaped total field magnetic feature interpreted as being caused by oxidation in a fault zone. The cross-over is located just north of the fault on the MLA map. The sharp magnetic features are interpreted to indicate a shallow depth of overburden (about sixty feet). The vlf-em peak to peak depth estimate is 850 feet, but the shape suggests that the profile is not perpendicular to the axis of the conductor. Therefore, the sixty foot depth is probably closer to the true depth.

Figure 26 shows a strong cross-over at station 2,755S in section 3, T60N, R10W on a traverse run south from near the center of section 34, T61N, R10W. The cross-over coincides with a sharp break in the linear regression line on the total field magnetic profile. A fault is also interpreted at this location.

Summary

A variety of evaluation methods were used which confirm Dr. Ferderer's shallow lithologic units and structural features. The scale of various sampling methods must be considered in the evaluation and mapping process.

The *tb2* unit and mapped structural features correlate with encouraging geochemical results from glacial drift geochemistry (Buchheit and others, 1989). Some of the reported high metal values, such as Ni, may be related to the troctolite-picrites seen in TH-2.

Measurements of density and magnetic susceptibility on drill core started a physical properties database for Minnesota lithologies at the DNR. These properties change with depth in some holes, suggesting changes in mineral content. However, there are significant differences between holes which reflect lithologic differences between holes. Lithologies show considerable variation of physical properties between short intervals of core. These variations involve amplitude between and within lithologic units and the range of response within a unit. However, there are enough variations of response using both magnetic susceptibility and density to identify the physical properties of most lithotypes. Distinctive responses are observed over late pegmatitic veins in several core intervals.

The pebble count surveys and outcrop samples map local lithologic units where glacial drift is not too deep and the drift has not been transported a great distance. Pebble count-based drift units correlate reasonably well with units mapped from geophysical

data. The results of Green and Venzke's study is best summarized by a quote from their abstract: "In general, the most abundant pebble type in these samples corresponds to the underlying bedrock type, suggesting that this technique can be useful for 'remotely sensing' bedrock types in covered areas. However, in the eastern ¼ of the area the drift is dominated by lithologies. . . that have been transported for long distances. . . . This must have been carried by the Superior Lobe and is clearly not basal till (directly overlying bedrock). Elsewhere in the area, ice transport has produced some gradations or transition zones in the drift pebble assemblages, compared to the bedrock contacts. Also since glacial transport in the Rainy Lobe (dominant here) was primarily roughly parallel to the main bedrock contact (anorthosite vs troctolite), the pebble assemblage at any sample site may have come largely from a few km up-ice. Thus the technique will be most successful when the drift is relatively thin and its stratigraphy is known well enough to exclude the existence of an upper drift sheet that is not in contact with local bedrock, and where rock boundaries are at large angles to ice transport direction."

Geochemical analyses were able to distinguish the same units observed in drill core and outcrops. The anorthosites, generally lacking abundant oxides and mafic minerals, were easily observed on geochemical variation diagrams. Within the Bald Eagle Intrusion, four lithotypes were distinguished. A second group of troctolite-picrites and dunites was identified on the basis of the chemistry from drillhole TH-2 which may be related to the Bald Eagle troctolite-picrites. The gabbros and troctolites related to the Bald Eagle Intrusion exhibit a small but consistent iron enrichment with an increase in the MgO content, which is generally equivalent to an increase in oxides with olivine. The chemistry of the oxide-rich rocks seen in drillcore from the *otg* units also followed the lithologic descriptions. Although not extensive or tightly controlled, these analyses are consistent with lithologic descriptions and provide a good base for further geochemical interpretations of these rocks and their relationship to one another and to other units within the Duluth Complex.

Ground geophysical profiles using very low frequency electromagnetic and magnetic susceptibility measurements define some structural features. The vlf-em displays these features as conductors. The magnetics define them with negative, smooth, dish-shaped susceptibility profile features or with breaks in the profile, which are often easier to observe by using linear regression analysis on both sides of the suspected fault.

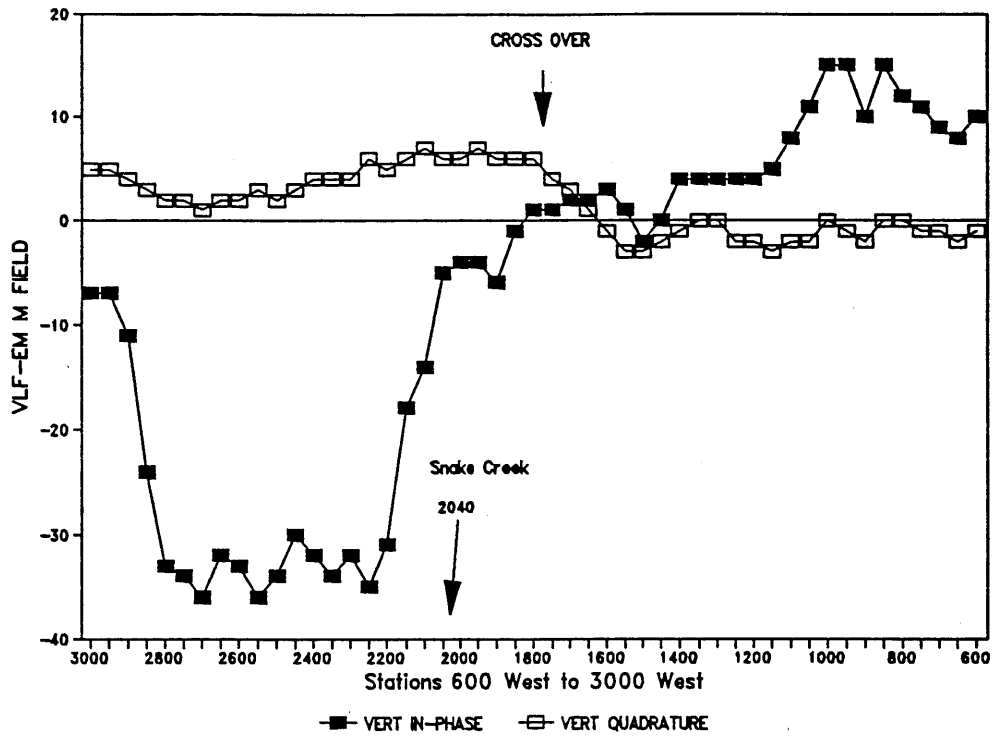


Figure 290-19. VLF-EM profile from station 600W to 3,000W (Section 30, T61N, R9W).

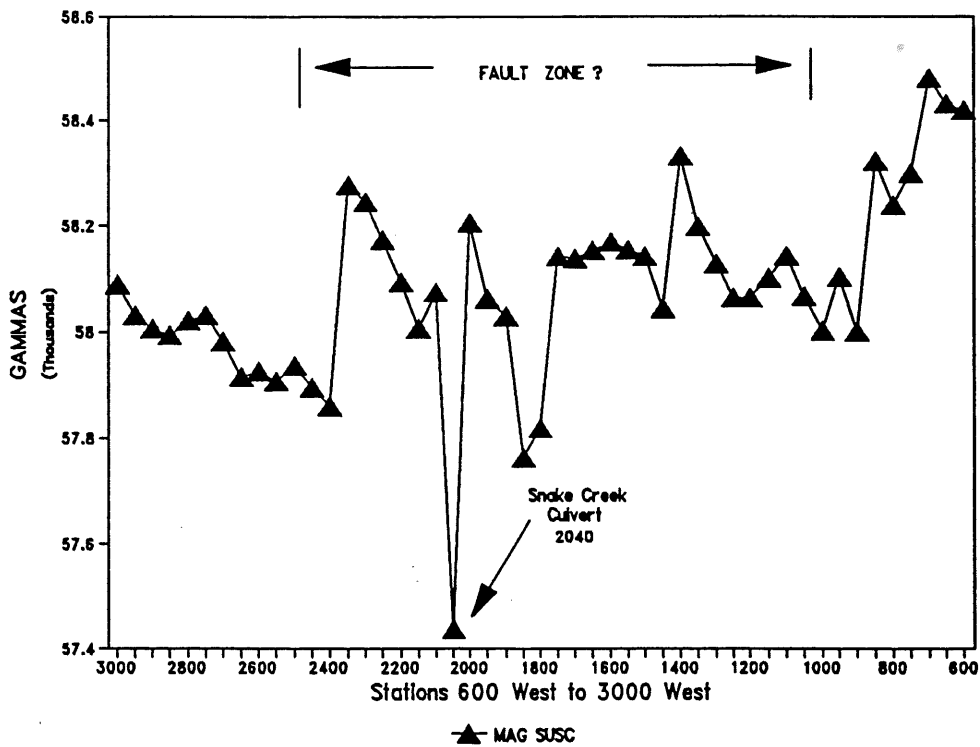


Figure 290-20. Magnetic susceptibility profile from station 600W to 3,000W (Section 30, T61N, R9W).

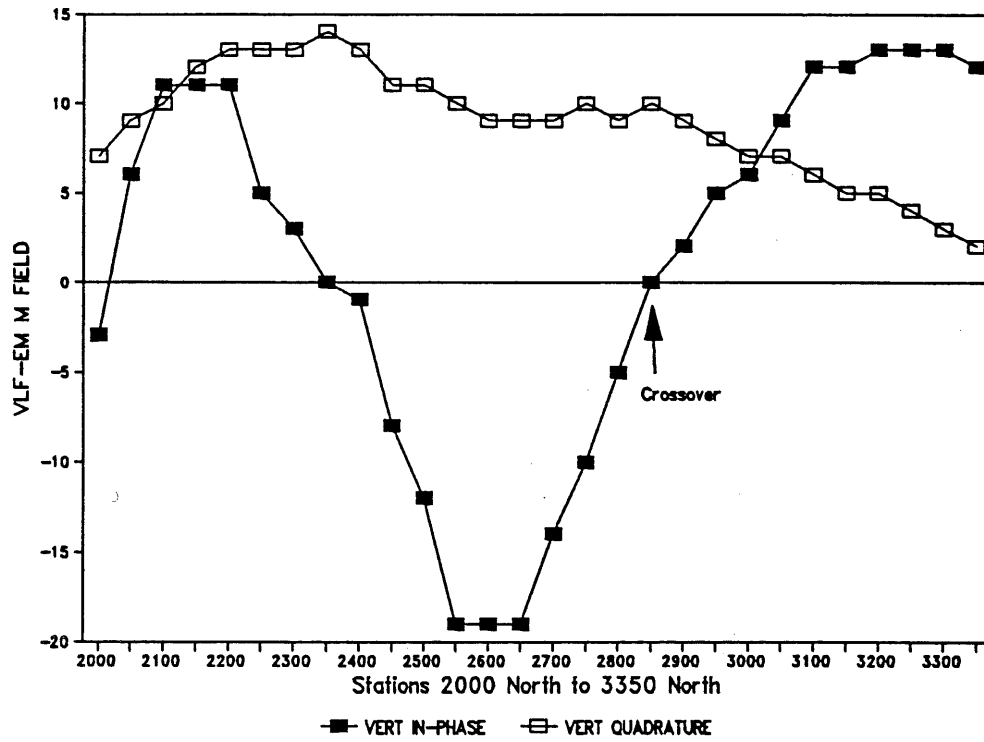


Figure 290-21. VLF-EM profile from station 2,000N to 3,350N (Section 25, T61N, R10W).

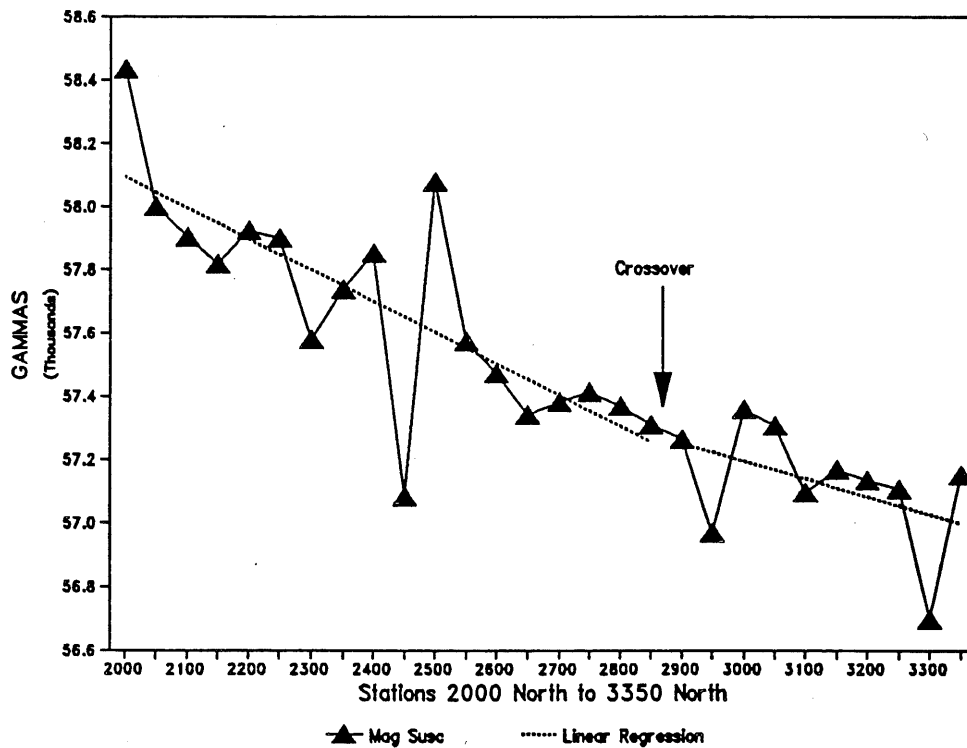


Figure 290-22. Magnetic susceptibility profile from station 2,000N to 3,350N (Section 25, T61N, R10W).

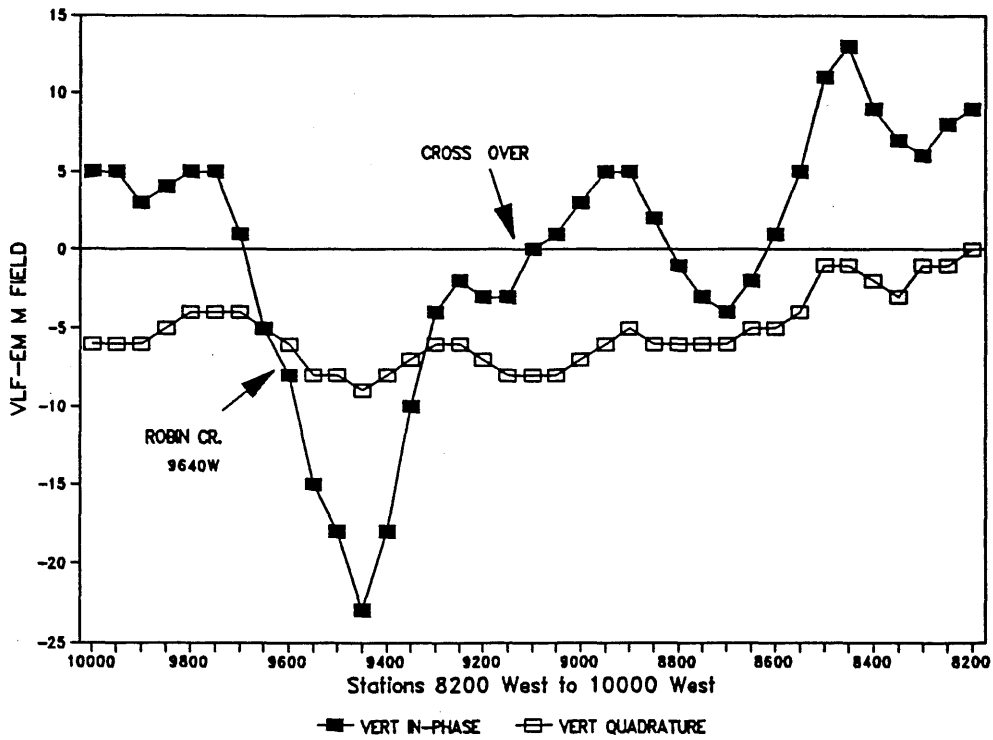


Figure 290-23. VLF-EM profile from station 8,200W to 10,000W (Section 26, T61N, R10W).

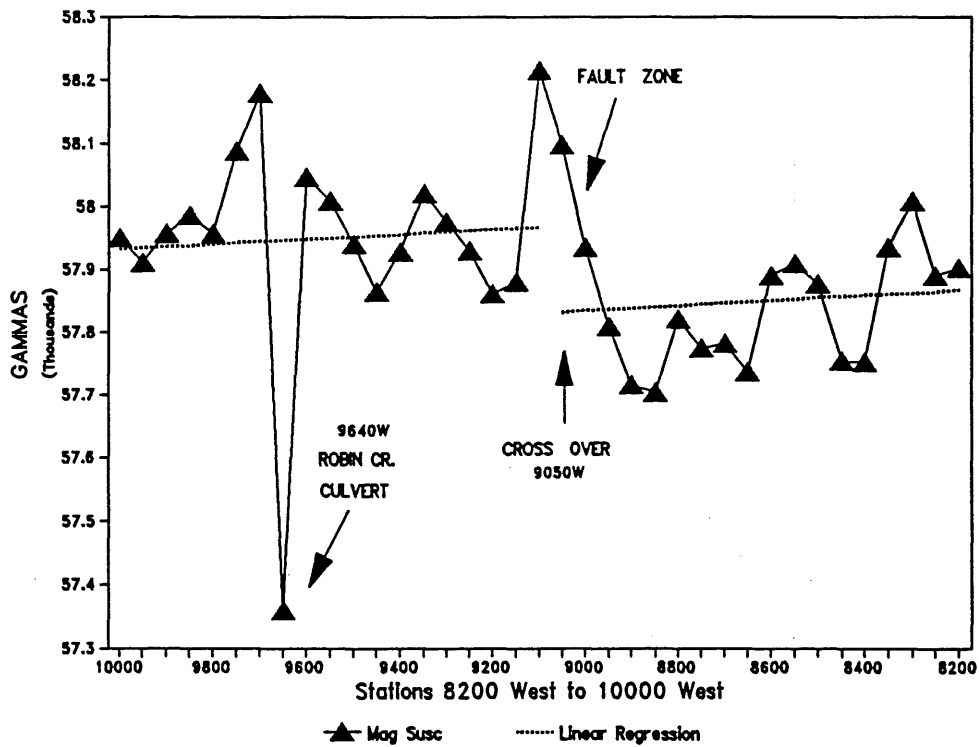


Figure 290-24. Magnetic susceptibility profile from station 8,200W to 10,000W (Section 26, T61N, R10W).

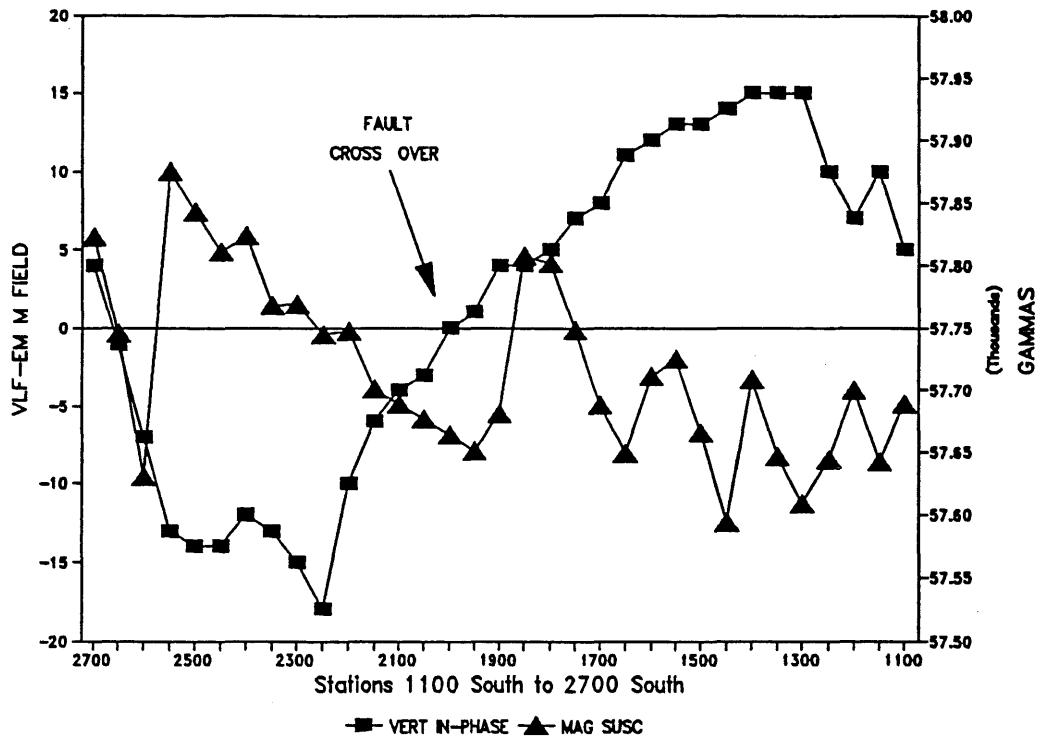


Figure 290-25. Magnetic susceptibility and VLF-EM profile from station 1,100S to 2,700S (Section 32, T61N, R9W).

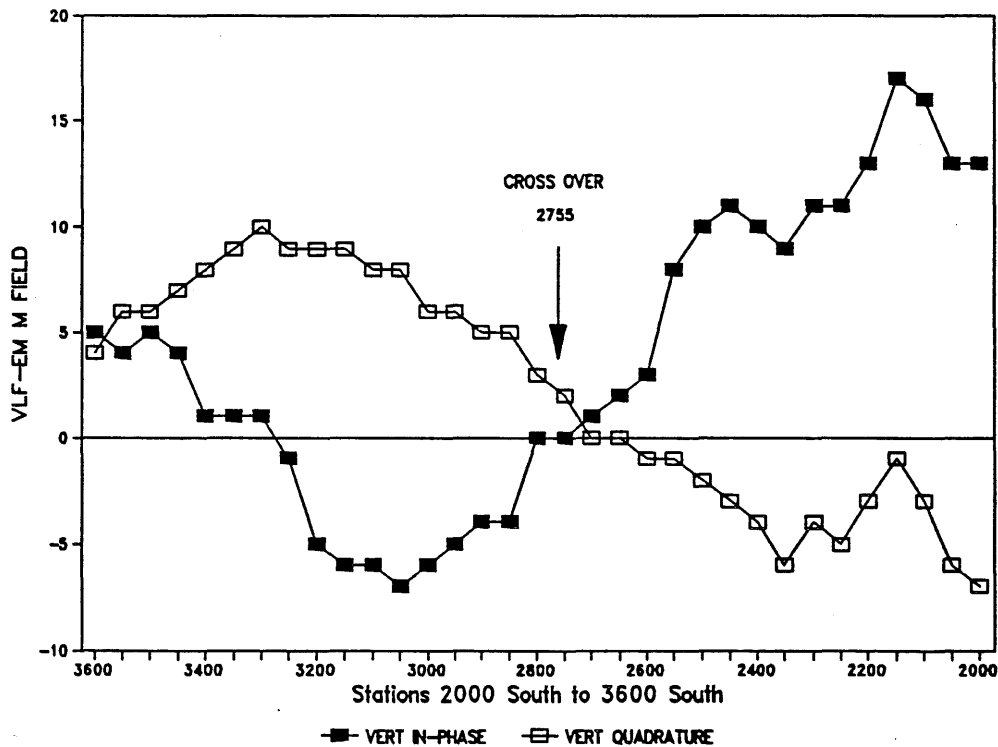


Figure 290-26. VLF-EM profile from station 2,000S to 3,600S (Section 3, T61N, R10W).

Conclusions

Baudette Area

Using data from existing regional aeromagnetic and gravity surveys, Spector has constructed a pseudo-geologic map which has greatly increased our knowledge of this four township strip in Lake of the Woods County. This is an area where there are no outcrops, deep glacial deposits, and good potential for economic Archean massive-sulfide base metal or lode gold deposits. In the past there has been considerable interest in this area and it is certain that the pseudo-geologic map will help encourage more exploration in the future. It will also be valuable as a land management tool.

McDougal Lakes Area

Using data from existing regional aeromagnetic and gravity surveys, Dr. Ferderer has constructed a pseudo-geologic map which has greatly increased our knowledge of this four township block in Lake County. Here encouraging results for strategic mineral deposits have previously been obtained from glacial drift geochemical studies. For planning mineral potential evaluations or land management it is important to know deep bedrock geology as well as that at bedrock surface.

The various sampling methods used to evaluate Ferderer's work have different scales of measurement. For example diamond drill cores or outcrop samples with thin section studies and assay data provide a very detailed examination of a small sample area of near surface bedrock. Ground geophysical surveys with a short station spacing provide a relatively less detailed examination of a larger sample area including near surface bedrock and structural features, also bedrock to shallow depths. Short interval or high-frequency variations mask lower frequency (long interval), responses from regional geologic features. Airborne magnetic surveys average the response from lithologic units over an area of several hundred feet. This reduces or eliminates the masking effect of short interval variations. The size of the integrated area depends on the airplane elevation above ground level and the time interval between observations. Gravity surveys with a one mile station spacing measure regional lithologic units. Both these methods examine a larger area to greater depth than above described methods, with less detailed interpretations of lithologic units and structures.

Combining all available data produces the most accurate geologic maps; but confidence in the results decreases with less detail and greater depth. These maps should be considered interim in nature, becoming obsolete as more detailed data is accumulated. Ferderer's work should encourage more interest in this area. His map and report will also be a valuable land management tool. Where Ferderer's lithologic units or structural features correlate with encouraging geochemical results there is a potential for economic mineral deposits. These should be followed up with more detailed studies.

In addition to proving the veracity of Dr. Ferderer's map there is a better understanding of evaluation methods used. The pebble count study done by Dr. Green and Ed Venzke showed that in portions of the MLA pebble lithologies from inexpensive surface samples are a fairly accurate representation of the gross bedrock lithology.

As geologic mapping is extended into areas with greater amounts of glacial cover and less outcrop exposure, classification of rock types will become more dependent on combinations of drill core petrography, lithochemistry, and geophysical data. If a statistically viable database of physical properties can be accumulated on known lithologies, previously characterized petrographically and chemically, this information can then help to identify and classify lithologies based on a combination of lithologic, geochemical, and geophysical properties. A data base using these combined methods will become a valuable aid to map accuracy. Such a database was started at the DNR with measurements of magnetic susceptibility and density on cores from the TH drill holes. To some extent measurements of physical properties on outcrops and near surface drill core can be extrapolated to deeper lithologic units.

Recommendations

In both the McDougal Lakes Area and the Baudette Area pseudo-geologic maps scaled at 1:62,500 are a valuable tool for encouraging and planning mineral potential evaluations and solving land management problems. They will provide a valuable interim data base until more detailed information becomes available for improvement of existing maps. The DNR should consider an ongoing program of producing such maps in areas where they are most needed.

Along with producing the maps on a contract basis, the DNR should provide the contractor with low cost ground geophysical surveys, physical measurements on drill core and overburden depth studies. This information will help make the most comprehensive map possible. In most areas airborne electromagnetic studies with flight lines oriented perpendicular to the strike of geologic features would greatly benefit the making of pseudo-geologic maps. Reflection seismic depth determinations would provide better depths to bedrock.

References

- Bonnichsen, B., 1971, Outcrop map of southern part of Duluth Complex and associated Keweenaw rocks, St. Louis and Lake counties, Minnesota: Minnesota Geological Survey, Miscellaneous Map Series M-11, 1:125,000.
- Bracken, R. E., Horton, R. J., Rohret, D. H., Krizman, R. W., Thompson, C. R., Sneddon, R. A., Pierce, H. A., and Mitchell, C. M., 1991, Aeromagnetic map of the Roseau 1° X 2° quadrangle, Minnesota and Ontario: U. S. Geological Survey, Open-File Report 89-452.
- Buchheit, R. L., Malmquist, K. L., and Niebuhr, J. R., 1989, Glacial drift geochemistry for strategic minerals, Duluth Complex, Lake County, Minnesota: Minnesota Department of Natural Resources, Division of Minerals, Report 232, 95 p.
- Chandler, V. W., 1983, Aeromagnetic map of Minnesota, Cook and Lake Counties: Minnesota Geological Survey, Aeromagnetic Map Series A-1, 1:125,000.
- Chandler, V. W., Nordstrand E., and Anderson, S., 1984, Shaded-relief aeromagnetic anomaly map of northeastern and east-central Minnesota: Minnesota Geological Survey, Miscellaneous Map Series M-53, 1:1,000,000.
- Chandler, V. W., personal communication: Minnesota Geological Survey.
- Clark, J. R., Day, W. C., and Klein, T. L., 1990, Geochemical and geological evidence for potential lode-gold deposits near Baudette, Lake of the Woods and Koochiching counties, Minnesota: U. S. Geological Survey, Executive Announcement.
- Dahlberg, E. H., 1975, Base metal exploration in a basic granulite terrain in the Bakhuis Mts. western Surinam: Contributions to the Geology of Suriname 4: Department of Development, Surinam Government Geological and Mining Service, p. 194-205.
- Dahlberg, E. H., Peterson, D., and Frey, B. A., 1989, Drill core repository sampling projects: Minnesota Department of Natural Resources, Division of Minerals, Report 255-1, 265, 266.
- Day, W. C., Klein, T. L., and Schulz, K. J., 1991, Preliminary bedrock geologic map of the Roseau 1° x 2° quadrangle, Minnesota, United States and Ontario, Canada: U. S. Geological Survey, Open-File Report OF 90-0544A, scale 1:250,000.
- Dobrin, M. B., 1960, Introduction to geophysical prospecting, 2d ed.: McGraw Hill Book Co. Inc.
- Ferderer, R. J., 1982, Gravity and magnetic modeling of the southern half of the Duluth Complex, northeastern Minnesota: Unpub. Masters thesis, Indiana University, 76 p.
- Ferderer, R. J., 1988, Application of Werner Deconvolution to the Penokean orogen, east-central Minnesota: Unpub. Ph.D. thesis, University of Minnesota.
- Ferderer, R. J., 1989, Aeromagnetic data interpretation for the McDougal Lakes Area, Duluth Complex Lake County, Minnesota: Minnesota Department of Natural Resources, Minerals Division, Open File Report 282-1-1, Hibbing, Minnesota.
- Frey, B. A. and Venzke, E. A., 1991, Archean drill core description and assay, Lake of the Woods County, Minnesota: Minnesota Department of Natural Resources, Division of Minerals, Report 278.
- Geonics Ltd., EM 16 operating manual, 2 Thorncliffe Park Drive, Toronto, 17, Ontario, Canada.
- Green, J. C., 1982, Geologic map of Minnesota, Two Harbors Sheet: Minnesota Geological Survey, 1:250,000
- Green, J. C., Phinney, W. C., and Weiblen, P. W., 1966, Geologic map of the Gabbro Lake quadrangle, Lake County, Minnesota: Minnesota Geological Survey, Miscellaneous Map Series M-2, 1:31,680.
- Hinze, W. J., Braile, L. W., Chandler, V. W., and Mazzella, F. E., 1975, Combined magnetic and gravity analysis: U. S. Geological Survey, Final Report, NASA Contract No. S-500 29A Modification No. 8, 119 p.

- Hodgson, C. J., Chapman, R. S. G., and MacGeehan, P. J., 1981, Application of exploration criteria for gold deposits in the Superior Province of the Canadian Shield to gold exploration in the Cordillera, *in* Precious metals in the northern Cordillera: Proceedings of a symposium held April 13-15, 1981, Vancouver, British Columbia, Canada, A. A. Levinson, ed.: jointly sponsored by The Association of Exploration Geochemists and the Cordilleran Section of the Geological Association of Canada.
- Ikola, R. J., 1968, Simple Bouguer gravity map of southern part of the Duluth Complex and adjacent areas, Minnesota: Minnesota Geological Survey, Miscellaneous Map Series M-4, 1:125,000.
- Ikola, R. J., 1970, Simple Bouguer gravity map of Minnesota, Two Harbors Sheet: Minnesota Geological Survey, Miscellaneous Map Series M-9, 1:250,000.
- Klein, T. L., and Day, W. C., 1989, Tabular summary of lithologic logs and geologic characteristics from diamond drill holes in the Western International Falls and the Roseau 1° by 2° quadrangles, northern Minnesota: Open-File Report 89-346, U. S. Geological Survey, Reston, Virginia.
- Listerud, W. H. and Meineke, D. G., 1977, Mineral resources of a portion of the Duluth Complex and adjacent rocks in St. Louis and Lake counties, northeastern Minnesota: Minnesota Department of Natural Resources, Division of Minerals, 49 p.
- Martin, D. P. and Gladen, L. W., 1985, A compilation of ore mineral occurrences, drill core, and test pits in the State of Minnesota: Minnesota Department of Natural Resources, Division of Minerals, Report 231.
- Martin, D. P., Dahl, D. A., and Cartwright, D., 1991, Regional survey of glacial drift, saprolite, and Precambrian bedrock, Lake of the Woods County, Minnesota: Minnesota Department of Natural Resources, Division of Minerals, Report 280, Hibbing, Minnesota.
- May, E. R. and Schmidt, P. G., 1982, The discovery, geology and mineralogy of the Crandon Precambrian massive sulfide deposit, Wisconsin, *in* Precambrian sulfide deposits, H. S. Robinson Memorial Volume, Hutchinson, R. W., Spence, C. D., and Franklin, J. M., eds.: The Geological Association of Canada, Special Paper 25, p. 447-480.
- McGinnis, L., Durfee, G., and Ikola R. J., 1973, Simple bouguer gravity map of Minnesota Roseau Sheet: Minnesota Geological Survey, Miscellaneous Map Series Map M-12, 1:250,000.
- Meuschke, J. L., Books, K. G., Henderson, J. R., Jr., and Schwartz, G. M., 1957, Aeromagnetic and geologic map of northern Lake of the Woods and northeastern Roseau Counties Minnesota: U. S. Geological Survey, Geophysical Investigations Map GP 128, 1:63,360.
- Meuschke, J. L., Books, K. G., Henderson, J. R., Jr., and Schwartz, G. M., 1957, Aeromagnetic and geologic map of northern Beltrami and southern Lake of the Woods Counties, Minnesota: U. S. Geological Survey, Geophysical Investigations Map GP 129, 1:63,360.
- Mills, S. J., Southwick, D. L., and Meyer, G. N., 1987, Scientific core drilling in north-central Minnesota: Summary of 1986 lithologic and geochemical results: Minnesota Geological Survey, Information Circular 24, University of Minnesota, p. 19-40.
- Minnesota Department of Natural Resources, 1991, Minnesota Department of Natural Resources B.W.C.A.W. Mineral Management Corridor, Division of Minerals.
- Ojakangas, R. W., Mossler, J. H., and Morey, G.B., 1979, Geologic map of Minnesota, Roseau sheet, bedrock geology: Minnesota Geological Survey, University of Minnesota.
- Olsen, B. M. and Mossler, J. H., 1982, Geologic map of Minnesota, depth to bedrock: Minnesota Geological Survey, University of Minnesota, Map S-14.
- Phinney, W. C., 1969, The Duluth Complex in the Gabbro Lake quadrangle, Minnesota: Minnesota Geological Survey, Report of Investigations 9, 20 p.

- Ruhanen, R. W. and Jiran, J. R., 1990, Drill core library index: Minnesota Department of Natural Resources, Division of Minerals.
- Sellner, J. M., Lawler, T. L., Dahlberg, E. H., Frey, B. A., and McKenna, M. P., 1985, 1984-1985 Geodrilling report: Minnesota Department of Natural Resources, Division of Minerals, Report 242, 56 p.
- Sims, P. K. and Ojakangas, R. W., 1973, Precambrian geology of the Roseau Sheet, Minnesota: Minnesota Geological Survey Open File Map, 1:250,000.
- Southwick, D. L. and Morey, G. B., 1990, Simplified tectonic map of Minnesota compiled from published sources and unpublished work in progress: Minnesota Geological Survey, U.S.-U.S.S.R.-Canada, Joint Seminar on Precambrian Geology of the Southern Canadian Shield and the Eastern Baltic Shield, p. 47-61.
- Spector, Allan, 1989, Report on Aeromagnetic Data Interpretation Baudette Area, Minnesota: Minnesota Department of Natural Resources, Minerals Division, Open File Report 281-1-2.
- Spector, Allan, 1991, Report on aeromagnetic data interpretation Baudette Area extension, Minnesota: Minnesota Department of Natural Resources, Minerals Division, Hibbing, Minnesota.
- U. S. Forest Service, 1984, Superior National Forest, Minnesota: U. S. Department of Agriculture, Forest Service.
- Vadis, M. K., Gladen, L. W., and Meineke, D. G., 1981, Geological, geophysical and geochemical surveys of Lake, St. Louis and Cook counties, Minnesota for the 1980 Drilling Project: Minnesota Department of Natural Resources, Division of Minerals, Report 201, 13 p.
- Venzke, E. A., in preparation [1991], Geology and petrogenesis of the Greenwood Lake Area, Lake County, northeastern Minnesota: Unpub. M. S. thesis, University of Minnesota Duluth.
- Weiblen, P. W., 1965, A funnel-shaped, gabbro-troctolite intrusion in the Duluth Complex, Lake County, Minnesota: Unpub. Ph.D. thesis, University of Minnesota, 155 p.
- Weiblen, P. W., and Morey, G. B., 1980, A summary of the stratigraphy, petrology, and structure of the Duluth Complex: American Journal of Science, v. 280-A, p. 88-133.
- Woodall, R., 1979, Gold-Australia and the world: Gold mineralization, Issued jointly by the Geology Department and the Extension Service, The University of Western Australia, Publication No. 3.

Appendix 290-A. Project Chronology

The project was proposed and accepted in the fall of 1988 with the maps to be made on a contract basis using funds available from the 1989 fiscal year.

April 1989: Contracts were let to Dr. Allan Spector and Dr. Robert Ferderer. Work was begun immediately.

June 1989: Both contracts were completed and the contractors came to the Hibbing office of the DNR Minerals Division to review their work.

June and July 1989: Twenty-one miles of combined magnetic and very low frequency electromagnetic traverses were completed along roads in the Baudette Area.

October 1989: Seven miles of combined magnetic and very low frequency electromagnetic traverses were completed along roads and trails in the McDougal Lakes Area.

December 1989: Drill sites for six holes were selected in the McDougal Lakes Area. Land ownership was reviewed by our legal department and special use permits obtained from the U.S. Forest Service.

January 30, 1990: Longyear Company, the drilling contractor, moved equipment onto the first hole. By the end of February six holes were completed.

March 1990: Magnetic susceptibility measurements at five foot intervals were completed on the drill core. Rough logs with cutting of samples for assays and thin sections was progressing.

May 1990: Drill sites and drill roads seeded. Scintillometer tests completed at the drill sites. No abnormal radiation observed.

June 1990: Contract in place with Dr. John Green from the University of Minnesota, Duluth, to study petrography of drill core, outcrop and glacial pebbles of the McDougal Lakes Area.

September 1990: Dr. Green and Ed Venzke submitted their report. Drill sites and roads checked for revegetation. No erosion noted.

November 1990: Outcrop sampling completed.

December 1990: Writing of final report begun.

May 1991: Final report completed.

Appendix 290-B. TH Drill Core Summary Information

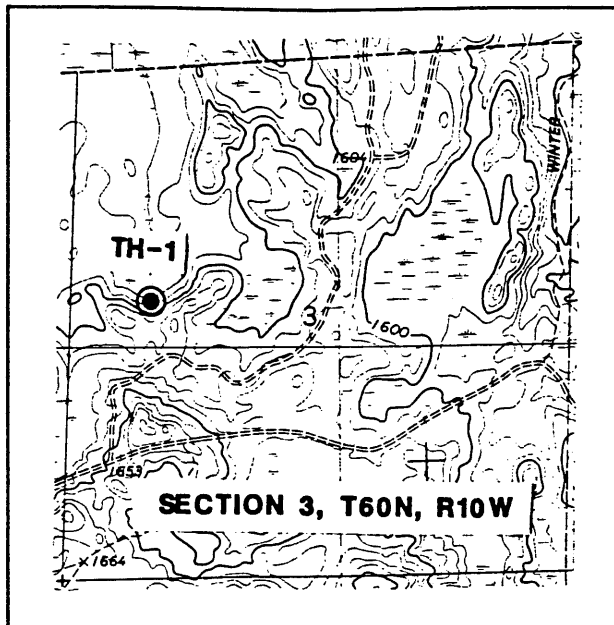
Lithologic Log for DDH TH-1

IDENTIFICATION

DNR Drill Hole Number: TH-1
DNR Unique Hole Number: 14313
Drilled: 1/30/90 - 2/2/90
Contractor: Longyear Co.

LOCATION (see map at right)

County: Lake
S-T-R: SW-NW, S3, T60N, R10W
Quadrangle: Slate Lake East, 7.5'
Reg. Survey Area: McDougal Lakes
UTM Coordinates: 605,400m E
5,285,125m N



TH-1: Drillhole Location Map.

HOLE PARAMETERS

Collar Elevation: 1590'
Total Depth: 180'
Bedrock Elevation: 1561'
Azimuth: NA Angle: 90°
Acid Tests: None Taken
Size Core: NQ - 2 3/8"
Method: Diamond Drill Core

Size Hole in Overburden: 4 1/2"
Size Casing: NW - 88.9 mm O.D.
Casing Left in Hole: 0
Hole Cemented: 2/2/90

INFORMATION SUMMARY AND HIGHLIGHTS

Interval in Feet:

- 0- 29 Overburden, glacial drift.
- 29- 180 Intrusive, primarily troctolite-picrite or troctolite with picrite intervals.
- 180 Bottom of hole.

Structure and Alteration: Olivine rich intervals (picrites) are sheared and serpentinized. Some fractures are filled with a white clay, possibly zeolite.

Assay Sample Depths in Feet and (Sample Number): 43-48 (18140); 94-99 (18142); 104-109 (18143); 135-140 (18145); 168-173 (18148).

Highlights of Sample Assays: Comparing eighteen samples from the TH holes, TH-1 had low SiO₂, high Fe₂O₃, above average MgO, and average CaO. It also has average nickel and above average chrome.

Thin Sections at Footage and (Sample Number): 41.5 (18139); 67 (18174); 93.5 (18141); 109.2 (18144); 133.6 (18175); 140 (18146); 146 (18176); 167.6 (18147).

Highlights of Core Geophysical Measurements: Magnetic susceptibility has large variations around a decreasing regression line with depth. Density has moderate variations around an increasing regression line. Geophysical map unit *tb2*.

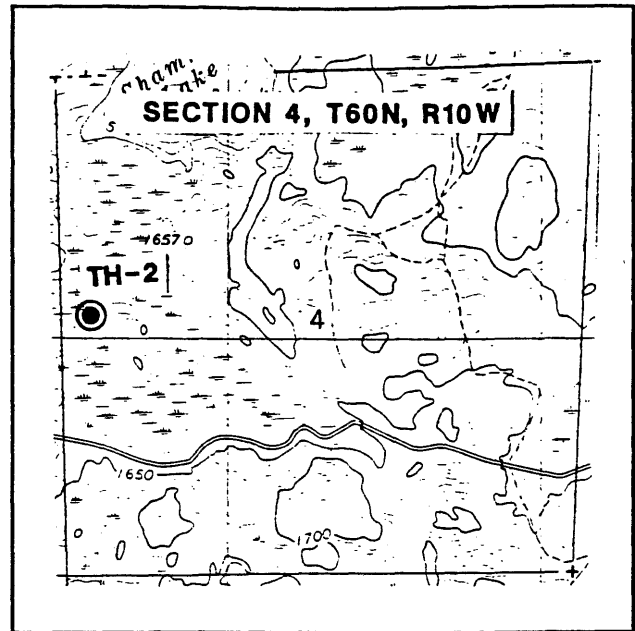
Lithologic Log for DDH TH-2

IDENTIFICATION

DNR Drill Hole Number: **TH-2**
DNR Unique Hole Number: **14314**
Drilled: **2/3/90 - 2/5/90**
Contractor: **Longyear Co.**

LOCATION (see map at right)

County: **Lake**
S-T-R: **SW-NW, S4, T60N, R10W**
Quadrangle: **Slate Lake East, 7.5'**
Reg. Survey Area: **McDougal Lakes**
UTM Coordinates: **603,590m E**
5,285,120m N



TH-2: Drillhole Location Map.

HOLE PARAMETERS

Collar Elevation:	1618'		
Total Depth:	191'		
Bedrock Elevation:	1557'		
Azimuth:	NA	Angle:	90°
Acid Tests:	None Taken		
Size Core:	NQ - 2 3/8"	Size Hole in Overburden:	4 1/2"
Method:	Diamond Drill Core	Size Casing:	NW - 88.9 mm O.D.
		Casing Left in Hole:	0
		Hole Cemented:	2/4/90

INFORMATION SUMMARY AND HIGHLIGHTS

Interval in Feet:

0- 61 Overburden, glacial drift.
61- 191 Intrusive, primarily troctolite-picrite.
191 Bottom of hole.

Structure and Alteration: Olivine rich intervals are sheared and serpentinized. Numerous fractures with white or red stained clay, (iddingsite?) possibly zeolite.

Assay Sample Depths in Feet and (Sample Number): 71-76 (18131); 90-95 (18132); 142-147 (18133); 170-175 (18134).

Highlights of Sample Assays: Comparing eighteen samples from the TH holes, TH-2 had below average SiO₂, above average Fe₂O₃, a high MgO content including sample 18133 which had the highest MgO of the eighteen samples, 18.6%, CaO was low. TH-2 also had the highest nickel assays of the group with the four samples averaging 703 ppm against the eighteen sample average of 350 ppm. Chrome assays were below average.

Thin Sections at Footage and (Sample Number): 70.5 (18135); 75.5 (18177); 86.2 (18136); 92 (18178); 147 (18179); 147.8 (18137); 169.5 (18138).

Highlights of Core Geophysical Measurements: Magnetic susceptibility varies around a regression line showing a strong increase with depth, the density regression line increases slightly. Geophysical map unit *otg2*.

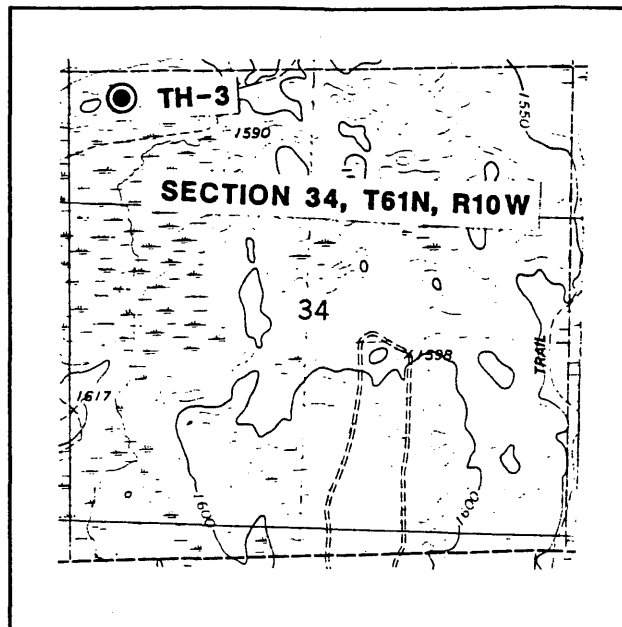
Lithologic Log for DDH TH-3

IDENTIFICATION

DNR Drill Hole Number: TH-3
DNR Unique Hole Number: 14315
Drilled: 2/5/90 - 2/6/90
Contractor: Longyear Co.

LOCATION (see map at right)

County: Lake
S-T-R: NW-NW, S34, T61N, R10W
Quadrangle: Slate Lake East, 7.5'
Reg. Survey Area: McDougal Lakes
UTM Coordinates: 605,360m E
5,287,340m N



TH-3: Drillhole Location Map.

HOLE PARAMETERS

Collar Elevation: 1590'
Total Depth: 161'
Bedrock Elevation: 1561'
Azimuth: NA Angle: 90°
Acid Tests: None Taken
Size Core: NQ - 2 3/8"
Drilling Method: Diamond Drill Core

Size Hole in Overburden: 4 1/2"
Size Casing: NW - 88.9 mm O.D.
Casing Left in Hole: 0
Hole Cemented: 2/6/90

INFORMATION SUMMARY AND HIGHLIGHTS

Interval in Feet:

0- 29 Overburden, glacial drift.
29- 161 Intrusive, primarily troctolite-picrite.
161 Bottom of hole.

Structure and Alteration: Olivine-rich intervals (picritic composition) are strongly sheared and serpentinized. Numerous fractures often filled with white clay, possibly a zeolite. In some places the clay is stained red with hematite or iddingsite.

Assay Sample Depths in Feet and (Sample Number): 53-58 (18149); 105.5-111 (18151); 155-160 (18153).

Highlights of Sample Assays: Sample 18149 (53-58') had the highest Fe₂O₃ content of the eighteen samples assayed, 13.20%. Iron content then decreased going down the hole; sample 18151 (105-111') 12.60%, sample 18153 (155-160') 8.25%. The MgO, chrome and nickel all follow this same pattern of decreasing content with depth. The CaO values reverse this pattern: 18149 7.41%, 18151 7.54%, and 18153 10.20%.

Thin Sections at Footage and (Sample Number): 29 (18180); 58.2 (18150); 105.2 (18152); 152.3 (18181); 160.7 (18154).

Highlights of Core Geophysical Measurements: Magnetic susceptibility observations are fairly uniform and decrease with depth, density varies somewhat around a constant regression line. Geophysical map unit *tb1*.

Lithologic Log for DDH TH-4

IDENTIFICATION

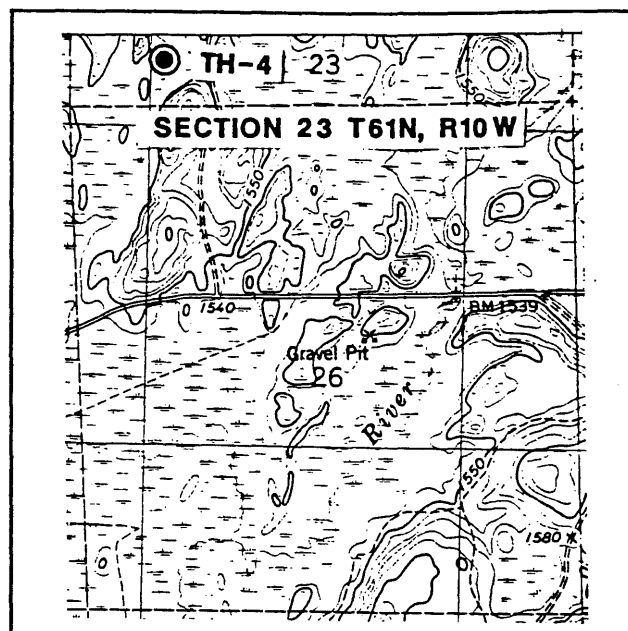
DNR Drill Hole Number: TH-4
DNR Unique Hole Number: 14316
Drilled: 2/6/90 - 2/8/90
Contractor: Longyear Co.

LOCATION (see map at right)

County: Lake
S-T-R: SW-SW, S23, T61N, R10W
Quadrangle: Slate Lake East, 7.5'
Reg. Survey Area: McDougal Lakes
UTM Coordinates: 607,045m E
5,289,215m N

HOLE PARAMETERS

Collar Elevation: 1542'
Total Depth: 151'
Bedrock Elevation: 1510'
Azimuth: NA Angle: 90°
Acid Tests: None Taken
Size Core: NQ - 2 3/8"
Drilling Method: Diamond Drill Core



TH-4: Drillhole Location Map.

Size Hole in Overburden: 4 1/2"
Size Casing: NW - 88.9 mm O.D.
Casing Left in Hole: 0
Hole Cemented: 2/7/90

INFORMATION SUMMARY AND HIGHLIGHTS

Interval in Feet:

0- 32 Overburden, glacial drift.
32- 151 Intrusive, olivine gabbro.
151 Bottom of hole.

Structure and Alteration: Some shearing with serpentine, highly fractured with chlorite, white clay and serpentine. Slickensides observed at 92-93', also 97 and 134'. Small granitic pegmatite veinlets; 70, 111, 122, 123.6, and 133'.

Assay Sample Depths in Feet and (Sample Number): 80-85 (18156); 140-145 (18157).

Highlights of Sample Assays: Comparing eighteen samples from the TH holes, TH-4 had high SiO₂ content 49.10% and 49.70%. The highest SiO₂ is 50.80%, and the eighteen sample average 45.18%. It had below average Fe₂O₃ and MgO, with the highest CaO contents of the samples, 12.90% and 13.20%. The hole had low nickel assays, but also the highest chrome values of the eighteen samples, 507 and 548 ppm against an average of 225 ppm.

Thin Sections at Footage and (Sample Number): 37 (18182); 61 (18183); 70.2 (18155); 83.5 (18184); 145.2 (18158).

Highlights of Core Geophysical Measurements: Magnetic susceptibility measurements are uniformly low with one large increase on a pegmatite vein, density decreases with depth. Geophysical map unit *gb*.

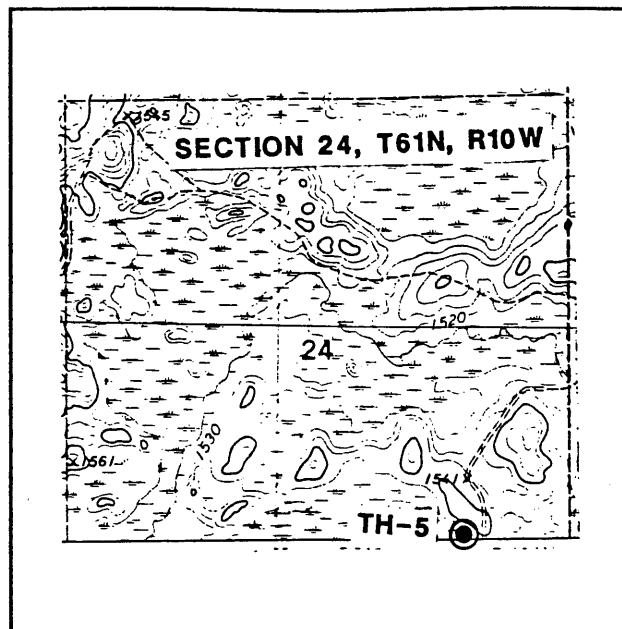
Lithologic Log for DDH TH-5

IDENTIFICATION

DNR Drill Hole Number: TH-5
DNR Unique Hole Number: 14317
Drilled: 2/12/90 - 2/15/90
Contractor: Longyear Co.

LOCATION (see map at right)

County: Lake
S-T-R: SE-SE, S24, T61N, R10W
Quadrangle: Slate Lake East, 7.5'
Reg. Survey Area: McDougal Lakes
UTM Coordinates: 609,640m E
5,289,355m N



TH-5: Drillhole Location Map.

HOLE PARAMETERS

Collar Elevation: 1545'
Total Depth: 193'
Bedrock Elevation: 1493'
Azimuth: NA Angle: 90°
Acid Tests: None Taken
Size Core: NQ - 2 3/8"
Drilling Method: Diamond Drill Core

Size Hole in Overburden: 4 1/2"
Size Casing: NW - 88.9 mm O.D.
Casing Left in Hole: 20'
Hole Cemented: 2/14/90

INFORMATION SUMMARY AND HIGHLIGHTS

Interval in Feet:

- 0- 52 Overburden, glacial drift.
- 52- 193 Intrusive, mixture of troctolite, gabbro and anorthosite.
- 193 Bottom of hole.

Structure and Alteration: Moderate to minor shearing and foliation some serpentinization. Considerable fractured or broken core, chloritized and serpentinized. Some fractures contain white clay seams, possibly a zeolite. Slickensides observed at 70-73' The interval 92.5-93.4' is a medium grained pink granite.

Assay Sample Depths in Feet and (Sample Number): 80-85 (18159); 165-170 (18162).

Highlights of Sample Assays: Comparing eighteen samples from the TH holes, TH-5 had high SiO₂. It also had low Fe₂O₃ including the lowest assay in sample 18162, 2.88%. MgO was very low and CaO high. Chrome and nickel were also very low.

Thin Sections at Footage and (Sample Number): 74 (18185); 85 (18160); 90 (18161); 91 (18186); 94 (18168); 170 (18163).

Highlights of Core Geophysical Measurements: TH-5 core has a low magnetic susceptibility variation. With depth the regression line increases slightly. Density has little variation around a slightly increasing regression line with depth. Geophysical unit *a/a1*.

Lithologic Log for DDH TH-6

IDENTIFICATION

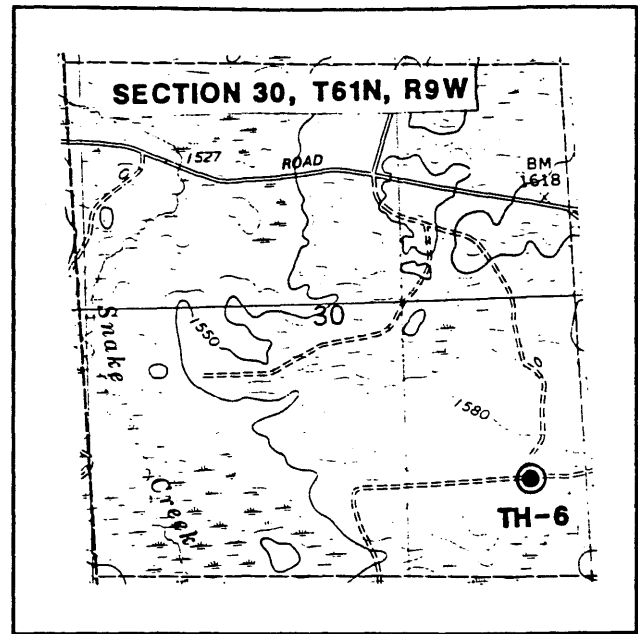
DNR Drill Hole Number: TH-6
DNR Unique Hole Number: 14318
Drilled: 2/15/90 - 2/16/90
Contractor: Longyear Co.

LOCATION (see map at right)

County: Lake
S-T-R: SE-SE, S30, T61N, R9W
Quadrangle: Slate Lake East, 7.5'
Reg. Survey Area: McDougal Lakes
UTM Coordinates: 611,410m E
5,287,430m N

HOLE PARAMETERS

Collar Elevation: 1583'
Total Depth: 160'
Bedrock Elevation: 1523'
Azimuth: NA Angle: 90°
Acid Tests: None Taken
Size Core: NQ - 2 3/8"
Drilling Method: Diamond Drill Core



TH-6: Drillhole Location Map.

Size Hole in Overburden: 4 1/2"
Size Casing: NW - 88.9 mm O.D.
Casing Left in Hole: 0
Hole Cemented: 2/16/90

INFORMATION SUMMARY AND HIGHLIGHTS

Interval in Feet:

- 0- 41 Overburden, glacial drift.
- 41- 45 Boulder, one foot of core recovered, olivine-bearing anorthosite.
- 45- 60 Overburden, glacial drift.
- 60- 160 Intrusive, anorthosite to troctolitic anorthosite.
- 160 Bottom of hole.

Structure and Alteration: Some fractures with thin films of serpentine on fracture planes. At 118.3' broken core, chloritic.

Assay Sample Depths in Feet and (Sample Number): 75-80 (18165); 138-143 (18166).

Highlights of Sample Assays: Comparing eighteen samples from the TH holes, TH-6 has high SiO₂ including the highest assay, 50.80% in sample 18165. It has very low Fe₂O₃ and MgO including the lowest MgO assay, 2.00% in sample 18165. It has high CaO. Chrome and nickel are also very low.

Thin Sections at Footage and (Sample Number): 74.8 (18164); 107.5 (18187); 143.2 (18167).

Highlights of Core Geophysical Measurements: Magnetic susceptibility has a strong increase with depth, density shows minor variation around a slightly increasing regression line. Geophysical unit *a*.

Appendix 290-C. Density and Magnetic Susceptibility Measurements on TH Drillholes

Drillhole TH-1

Measured Values:

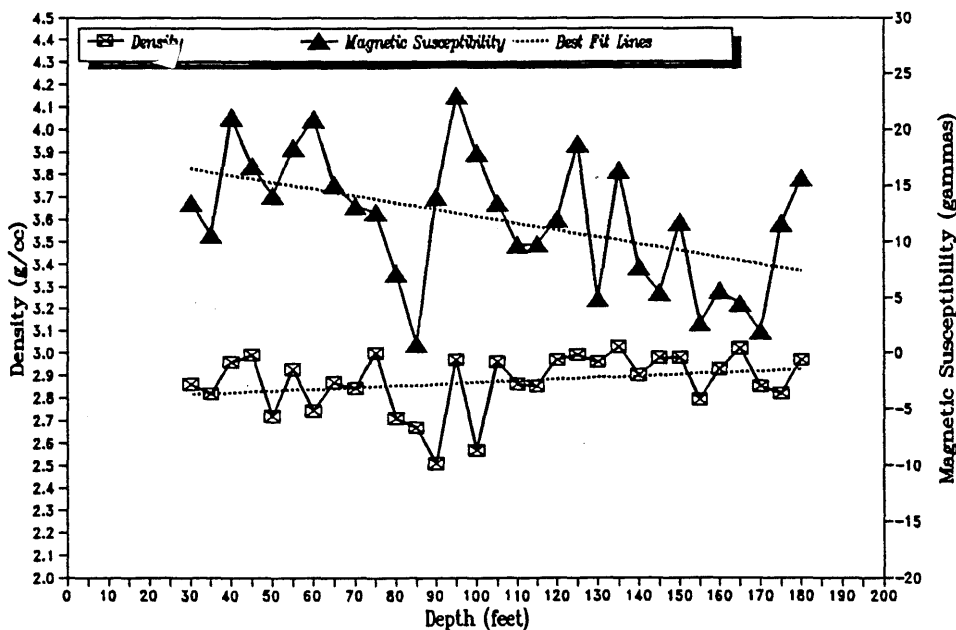
Regression Output:

Best Fit Line:

Depth (feet)	Density (g/cc)	Magnetic Susceptibility (gammas)		Density (g/cc)	Magnetic Susceptibility (gammas)
30	2.86	13.40	<div style="border: 1px solid black; padding: 5px; width: fit-content; margin: auto;"> <p>Specific Gravity</p> <p>Constant 2.795</p> <p>Std Err of Y Est 0.129</p> <p>R Squared 0.064</p> <p>No. of Observations 31</p> <p>Degrees of Freedom 29</p> <p>X Coefficient(s) 0.00073</p> <p>Std Err of Coef. 0.00052</p> </div>	2.82	16.52
35	2.82	10.60		2.82	16.21
40	2.96	21.06		2.82	15.91
45	2.99	16.74		2.83	15.60
50	2.72	14.04		2.83	15.30
55	2.93	18.41		2.83	14.99
60	2.74	20.89		2.84	14.69
65	2.87	15.06		2.84	14.39
70	2.84	13.17		2.85	14.08
75	3.00	12.62		2.85	13.78
80	2.71	7.13	2.85	13.47	
85	2.67	0.85	2.86	13.17	
90	2.51	14.00	2.86	12.86	
95	2.97	23.01	2.86	12.56	
100	2.57	17.88	2.87	12.25	
105	2.96	13.43	2.87	11.95	
110	2.86	9.68	2.88	11.65	
115	2.85	9.75	2.88	11.34	
120	2.97	12.00	2.88	11.04	
125	2.99	18.76	2.89	10.73	
130	2.96	4.90	2.89	10.43	
135	3.03	16.37	2.89	10.12	
140	2.90	7.73	2.90	9.82	
145	2.98	5.43	2.90	9.52	
150	2.98	11.70	2.90	9.21	
155	2.79	2.64	2.91	8.91	
160	2.93	5.58	2.91	8.60	
165	3.02	4.43	2.92	8.30	
170	2.85	1.98	2.92	7.99	
175	2.82	11.63	2.92	7.69	
180	2.97	15.59	2.93	7.38	

Best Fit Line Calculation:

$$Y = \text{Constant} + (\text{X Coeff.} \cdot \text{Depth})$$



Drillhole TH-2

Measured Values:

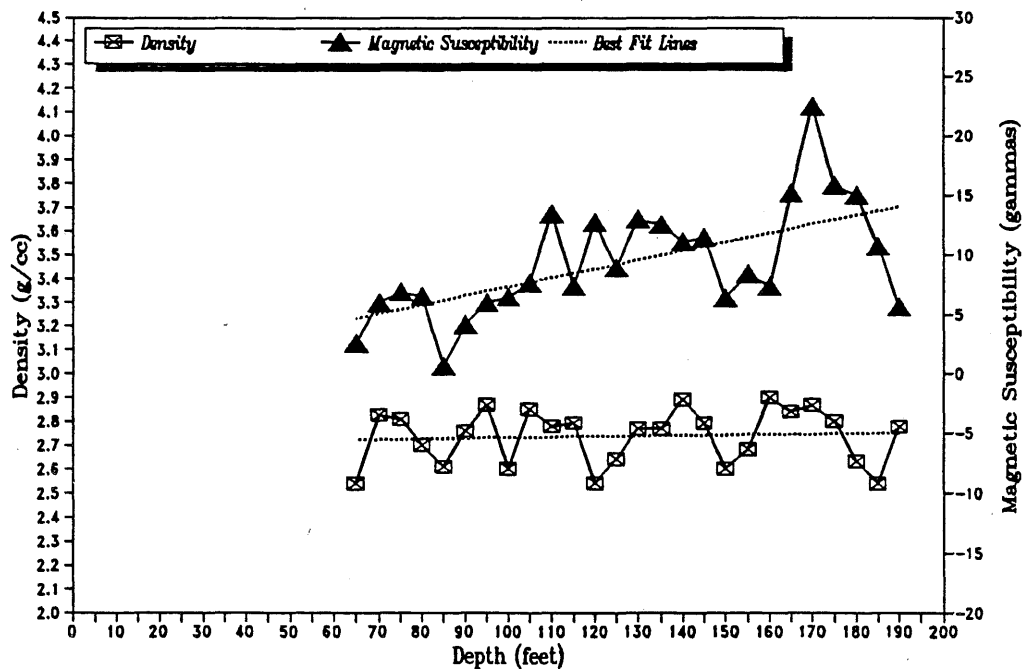
Regression Output:

Best Fit Line:

Depth (feet)	Density (g/cc)	Magnetic Susceptibility (gammas)			Density (g/cc)	Magnetic Susceptibility (gammas)
65	2.54	2.62	Specific Gravity Constant 2.707 Std Err of Y Est 0.118 R Squared 0.006 No. of Observations 26 Degrees of Freedom 24 X Coefficient(s) 0.00024 Std Err of Coef. 0.00062		2.72	4.67
70	2.83	6.00			2.72	5.04
75	2.81	6.83			2.73	5.42
80	2.70	6.53			2.73	5.80
85	2.61	0.67			2.73	6.18
90	2.76	4.09			2.73	6.55
95	2.87	6.00			2.73	6.93
100	2.60	6.43			2.73	7.31
105	2.85	7.58			2.73	7.68
110	2.78	13.40			2.73	8.06
115	2.79	7.33			2.73	8.44
120	2.54	12.67			2.74	8.81
125	2.64	8.87			2.74	9.19
130	2.77	13.02			2.74	9.57
135	2.77	12.56			2.74	9.94
140	2.89	11.08			2.74	10.32
145	2.79	11.45			2.74	10.70
150	2.60	6.32			2.74	11.07
155	2.68	8.37			2.74	11.45
160	2.90	7.31			2.75	11.83
165	2.84	15.15			2.75	12.20
170	2.87	22.48			2.75	12.58
175	2.80	15.85			2.75	12.96
180	2.63	14.97			2.75	13.34
185	2.54	10.67			2.75	13.71
190	2.78	5.59			2.75	14.09

Best Fit Line Calculation:

$$Y = \text{Constant} + (\text{X Coeff.} * \text{Depth})$$

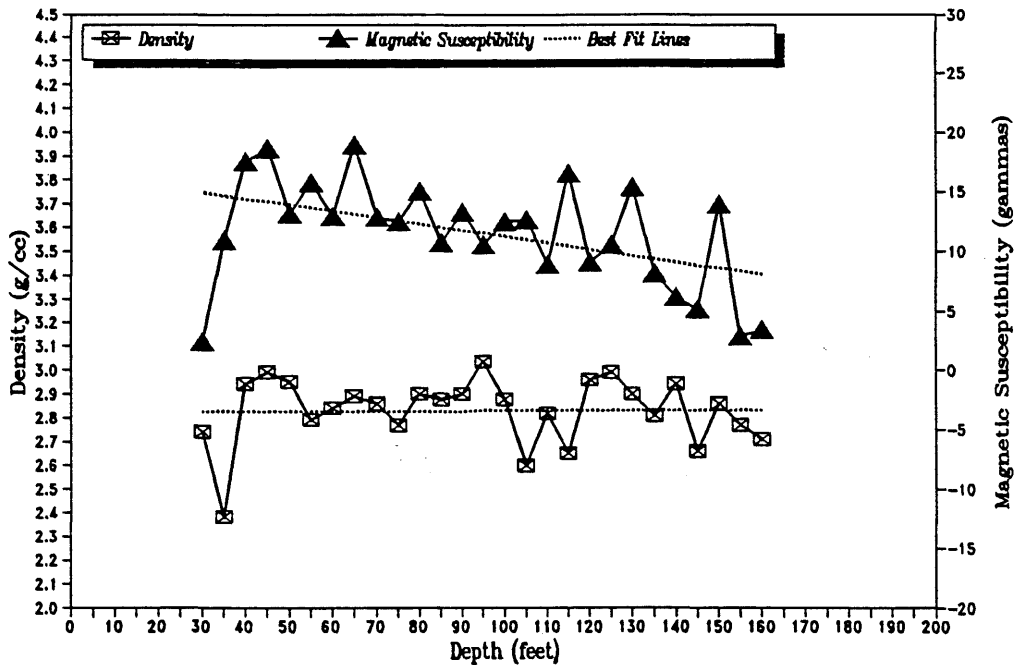


Drillhole TH-3

Measured Values:			Regression Output:	Best Fit Line:	
Depth (feet)	Density (g/cc)	Magnetic Susceptibility (gammas)		Density (g/cc)	Magnetic Susceptibility (gammas)
30	2.74	2.37	<div style="border: 1px solid black; padding: 5px; margin-bottom: 10px;"> Specific Gravity Constant 2.826 Std Err of Y Est 0.145 R Squared 0.000 No. of Observations 27 Degrees of Freedom 25 X Coefficient(s) 0.00005 Std Err of Coef. 0.00072 </div> <div style="border: 1px solid black; padding: 5px;"> Magnetic Susceptibility Constant 16.515 Std Err of Y Est 4.188 R Squared 0.208 No. of Observations 27 Degrees of Freedom 25 X Coefficient(s) -0.05299 Std Err of Coef. 0.02070 </div>	2.83	14.93
35	2.38	10.92		2.83	14.66
40	2.94	17.58		2.83	14.40
45	2.99	18.67		2.83	14.13
50	2.95	13.08		2.83	13.87
55	2.79	15.72		2.83	13.60
60	2.84	12.89		2.83	13.34
65	2.89	18.94		2.83	13.07
70	2.86	12.83		2.83	12.81
75	2.77	12.46		2.83	12.54
80	2.90	15.03		2.83	12.28
85	2.88	10.67		2.83	12.01
90	2.90	13.28		2.83	11.75
95	3.04	10.55		2.83	11.48
100	2.88	12.46		2.83	11.22
105	2.60	12.64		2.83	10.95
110	2.82	8.87		2.83	10.69
115	2.65	16.58		2.83	10.42
120	2.96	9.08		2.83	10.16
125	2.99	10.51		2.83	9.89
130	2.90	15.38		2.83	9.63
135	2.81	8.11		2.83	9.36
140	2.94	6.11		2.83	9.10
145	2.66	5.12		2.83	8.83
150	2.86	13.88		2.83	8.57
155	2.77	2.90	2.83	8.30	
160	2.71	3.36	2.83	8.04	

Best Fit Line Calculation:

$$Y = \text{Constant} + (\text{X Coeff.} * \text{Depth})$$



Drillhole TH-4

Measured Values:

Regression Output:

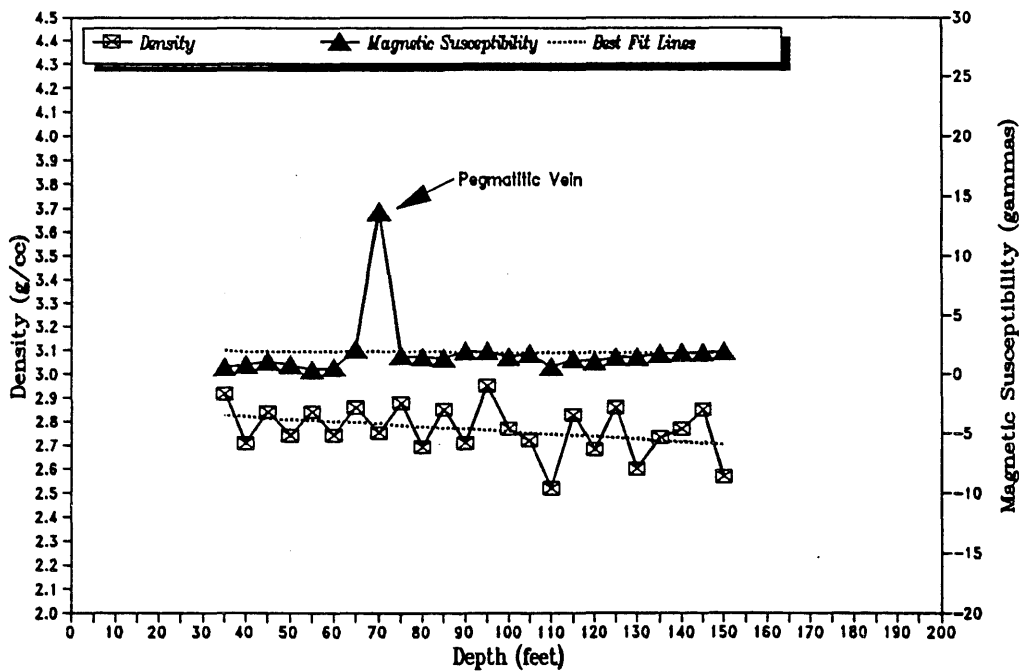
Best Fit Line:

Depth (feet)	Density (g/cc)	Magnetic Susceptibility (gammas)			Density (g/cc)	Magnetic Susceptibility (gammas)
35	2.92	0.69			2.83	2.00
40	2.71	0.87			2.82	1.99
45	2.84	1.10			2.82	1.98
50	2.74	0.89			2.81	1.97
55	2.84	0.39			2.81	1.96
60	2.74	0.57			2.80	1.95
65	2.86	2.16			2.80	1.94
70	2.75	13.70			2.79	1.93
75	2.88	1.59			2.78	1.92
80	2.69	1.45			2.78	1.91
85	2.85	1.36			2.77	1.90
90	2.71	1.96			2.77	1.90
95	2.95	1.93			2.76	1.89
100	2.77	1.52			2.76	1.88
105	2.72	1.73			2.75	1.87
110	2.52	0.71			2.75	1.86
115	2.83	1.29			2.74	1.85
120	2.68	1.08			2.74	1.84
125	2.86	1.49			2.73	1.83
130	2.60	1.52			2.73	1.82
135	2.73	1.77			2.72	1.81
140	2.77	1.88			2.72	1.80
145	2.85	1.81			2.71	1.79
150	2.57	1.91			2.70	1.78

Specific Gravity	
Constant	2.865
Std Err of Y Est	0.103
R Squared	0.122
No. of Observations	24
Degrees of Freedom	22
X Coefficient(s)	-0.00107
Std Err of Coef.	0.00061

Magnetic Susceptibility	
Constant	2.062
Std Err of Y Est	2.620
R Squared	0.001
No. of Observations	24
Degrees of Freedom	22
X Coefficient(s)	-0.00186
Std Err of Coef.	0.01545

Best Fit Line Calculation:

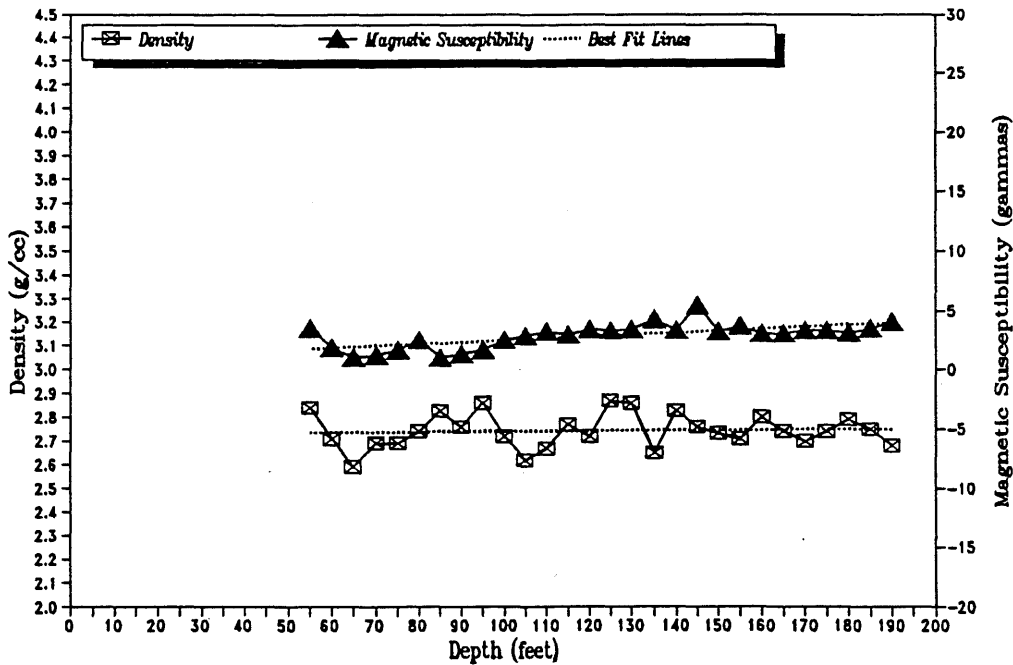


Drillhole TH-5

Measured Values:			Regression Output:	Best Fit Line:	
Depth (feet)	Density (g/cc)	Magnetic Susceptibility (gammas)		Density (g/cc)	Magnetic Susceptibility (gammas)
55	2.84	3.49	<div style="border: 1px solid black; padding: 5px; margin-bottom: 10px;"> Specific Gravity Constant 2.729 Std Err of Y Est 0.074 R Squared 0.004 No. of Observations 28 Degrees of Freedom 26 X Coefficient(s) 0.00012 Std Err of Coef. 0.00035 </div> <div style="border: 1px solid black; padding: 5px;"> Magnetic Susceptibility Constant 0.861 Std Err of Y Est 0.795 R Squared 0.429 No. of Observations 28 Degrees of Freedom 26 X Coefficient(s) 0.01644 Std Err of Coef. 0.00372 </div>	2.74	1.77
60	2.71	1.89		2.74	1.85
65	2.59	1.01		2.74	1.93
70	2.69	1.19		2.74	2.01
75	2.69	1.70		2.74	2.09
80	2.74	2.50		2.74	2.18
85	2.83	1.06		2.74	2.26
90	2.76	1.33		2.74	2.34
95	2.86	1.63		2.74	2.42
100	2.72	2.46		2.74	2.50
105	2.62	2.89		2.74	2.59
110	2.67	3.22		2.74	2.67
115	2.77	2.92		2.74	2.75
120	2.72	3.36		2.74	2.83
125	2.87	3.31		2.74	2.92
130	2.86	3.38		2.74	3.00
135	2.65	4.25		2.75	3.08
140	2.83	3.33		2.75	3.16
145	2.76	5.40		2.75	3.24
150	2.73	3.22		2.75	3.33
155	2.71	3.65		2.75	3.41
160	2.80	3.01		2.75	3.49
165	2.74	3.01		2.75	3.57
170	2.70	3.29		2.75	3.66
175	2.74	3.33		2.75	3.74
180	2.79	3.15		2.75	3.82
185	2.75	3.47	2.75	3.90	
190	2.68	4.04	2.75	3.98	

Best Fit Line Calculation:

$$Y = \text{Constant} + (\text{X Coeff.} * \text{Depth})$$



Drillhole TH-6

Measured Values:

Regression Output:

Best Fit Line:

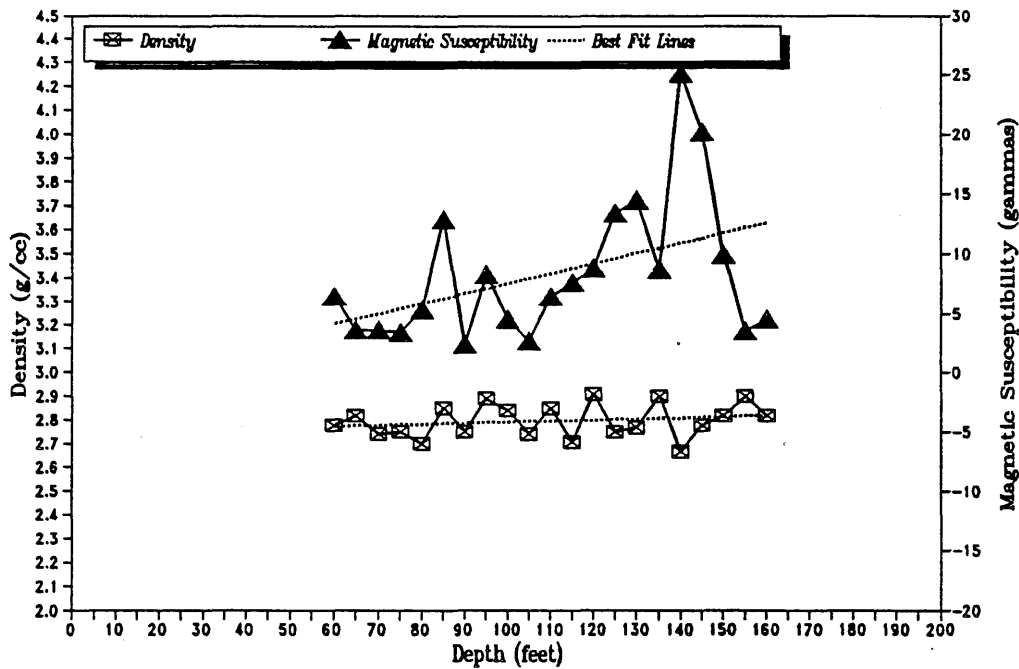
Depth (feet)	Density (g/cc)	Magnetic Susceptibility (gammas)			Density (g/cc)	Magnetic Susceptibility (gammas)
60	2.78	6.39			2.77	4.15
65	2.82	3.56			2.78	4.57
70	2.74	3.59			2.78	4.99
75	2.75	3.40			2.78	5.41
80	2.70	5.36			2.78	5.83
85	2.85	12.78			2.79	6.25
90	2.75	2.44			2.79	6.67
95	2.89	8.23			2.79	7.09
100	2.84	4.46			2.79	7.51
105	2.74	2.69			2.79	7.93
110	2.85	6.39			2.80	8.35
115	2.71	7.58			2.80	8.77
120	2.91	8.76			2.80	9.18
125	2.75	13.36			2.80	9.60
130	2.77	14.44			2.81	10.02
135	2.90	8.69			2.81	10.44
140	2.67	25.13			2.81	10.86
145	2.78	20.18			2.81	11.28
150	2.82	9.86			2.82	11.70
155	2.90	3.47			2.82	12.12
160	2.82	4.50			2.82	12.54

Specific Gravity	
Constant	2.745
Std Err of Y Est	0.071
R Squared	0.043
No. of Observations	21
Degrees of Freedom	19
X Coefficient(s)	0.00047
Std Err of Coef.	0.00051

Magnetic Susceptibility	
Constant	-0.882
Std Err of Y Est	5.518
R Squared	0.190
No. of Observations	21
Degrees of Freedom	19
X Coefficient(s)	0.08389
Std Err of Coef.	0.03977

Best Fit Line Calculation:

$$Y = \text{Constant} + (\text{X Coeff.} * \text{Depth})$$



**Appendix 290-D. Report on Aeromagnetic Data Interpretation,
Baudette Area, Minnesota**

June 1989

For the Minnesota Department of Natural Resources

by

Allan Spector and Associates Limited

Toronto, Canada

Available as Open File Report 281-1-2

Table of Contents

	Page
1. Introduction	3
1.1 The Project Area	3
1.2 Aeromagnetic Data and Its Analysis	3
1.3 Geological Setting	8
1.4 Correlation with Gravity Data	8
2. Geological Interpretation	9
2.1 Magnetic/Lithological Units	9
2.2 Structures	10
2.3 Depth to Magnetic Basement	10
2.4 Summary and Recommendations for Follow-up Investigation	10
3. References	11

List of Figures

Figure 1.	Location Map	3
Figure 2.	Flight Path Plot	*
Figure 3a.	Prism Anomaly Profiles	3
Figure 3b.	Dipping Prism Anomalies	3
Figure 3c.	Prism Model Anomaly	3
Figure 3d.	Magnetic susceptibility and magnetite content	3
Figure 4.	Aeromagnetic Interpretation	*

* = in pocket

1. INTRODUCTION

1.1 The Project Area

This report contains the results of an analysis of aeromagnetic data in an area located in Lake of the Woods county, as shown in Figure 1. Four townships are included; T157 to T160N, R33W; an area of 216 square miles. The area is mainly covered by swamp, with elevations ranging from 1100 to just over 1300 feet.

Principal objective of this work is geological mapping; to analyze and interpret aeromagnetic data in conjunction with all other available data, to elucidate the geology of buried Precambrian crystalline rocks with regard to structure, depth of burial and lithology.

1.2 The Aeromagnetic Data and Its Analysis

Aeromagnetic data analyzed in this study were taken from a relatively detailed survey conducted by the USGS in 1985. The survey replaces a previous 1949 USGS survey described by Meuschke et al (1957). That survey consisted of north-south lines at one mile spacing and 1000 foot altitude. The 1985 survey consisted of north-south lines at 1/4 mile spacing and 300 foot altitude.

A 9-track digital tape recording of the 'new' aeromagnetic data was supplied for this study by Dr. Bruce Smith of the USGS.

Figure 2 [Plate 290-1] shows the location of the survey lines, as plotted from the digital tape recording, that cross the project area; lines 3471 to 3723. No east-west cross/tie lines were flown in the vicinity of the project area. According to the USGS, some difficulty was encountered in positioning of the survey lines because of the featureless topography.

A 1:50,000 scale contour map compilation of the data was also supplied.

For purposes of this study, profiles of the magnetic survey data (minus Geomagnetic Gradient) and aircraft altimeter data were constructed at 1" = 50 and 500 gammas and 1" = 600 feet scales.

About 650 line miles of aeromagnetic data were analyzed in this study.

The magnetic data analysis was done with reference to model anomaly profiles, shown in Figures 3a and 3b. The profiles simulate anomalies created by prismatic bodies as seen in north-south lines. Magnetic field characteristics for the area in 1985 are described as follows (see USGS Geophys. Invest. Maps 9P-986-D, I and F);

Declination: 5% E
Inclination: 76% N
Intensity: 59,800 gammas

The model curves have been generated for a declination of 5%E and inclination of 76%. They provide a basis for determining the location of magnetic contacts, magnetic bedding attitude, and depth of burial of a magnetized unit.

In Figure 3c, a plan view is given of a typical anomaly in contour form. This figure is taken from Vacquier et al (1951) who give a series of model anomaly maps for various model shapes and orientations. They also provide methods for magnetic susceptibility estimation. From susceptibility determinations, estimates of magnetite content may be obtained using an empirical relationship derived by Mooney and Bleifuss (1953) using a suite of 75 rock samples from Minnesota. The least squares relationship is shown in graphical form in Figure 3d.

The analysis included a correlation with the radar altimeter data to determine which magnetic features had been amplified or attenuated by variations in aircraft/ground clearance.

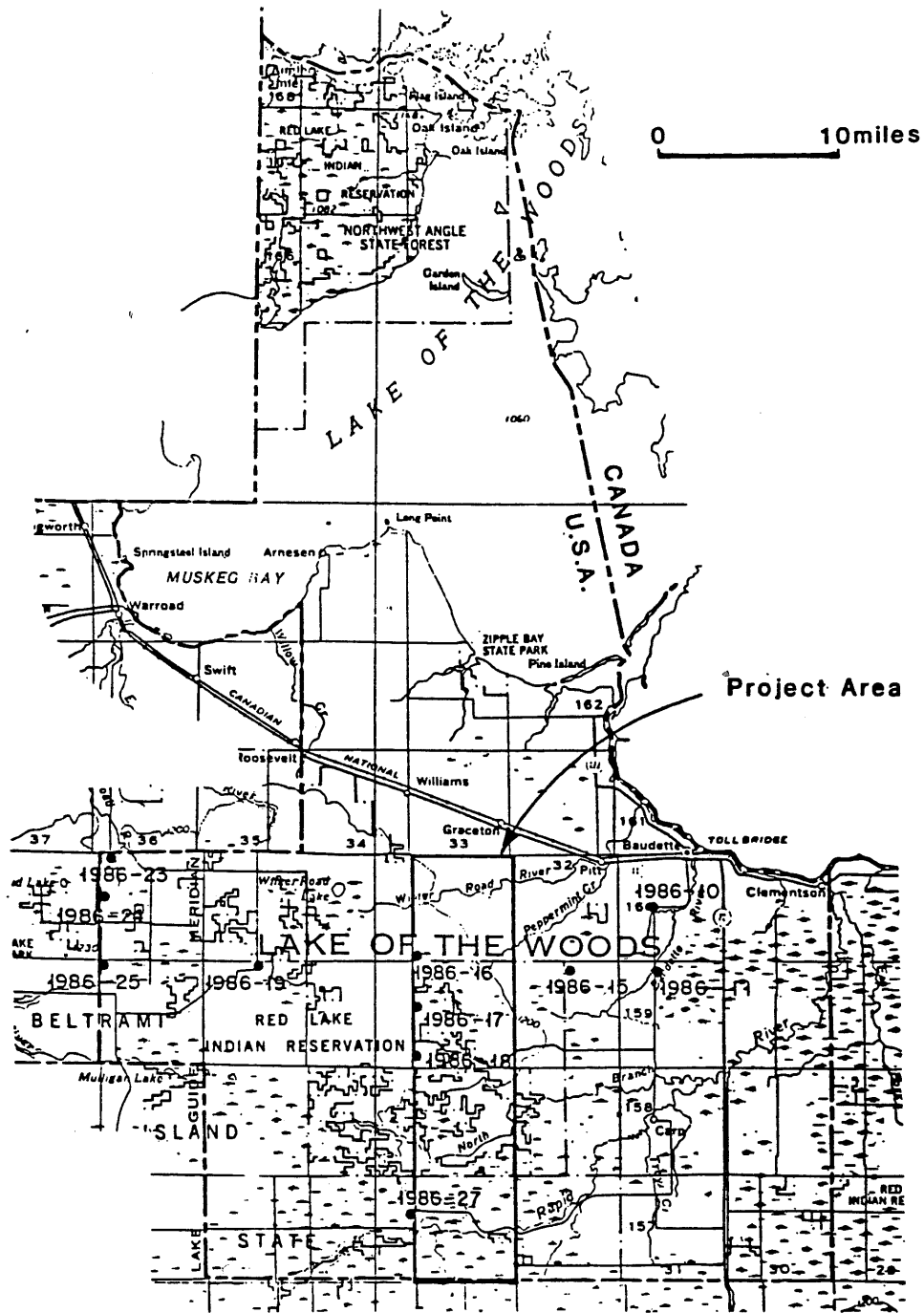
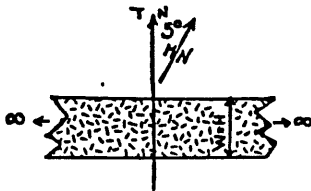


Figure 1. Location Map.

DIPPING PRISM ANOMALIES



field inclination: 76°
 field intensity: 69800γ
 prism depth: 10Δ ($\Delta=50'$)
 susceptibility: 1000×10^6 cgs

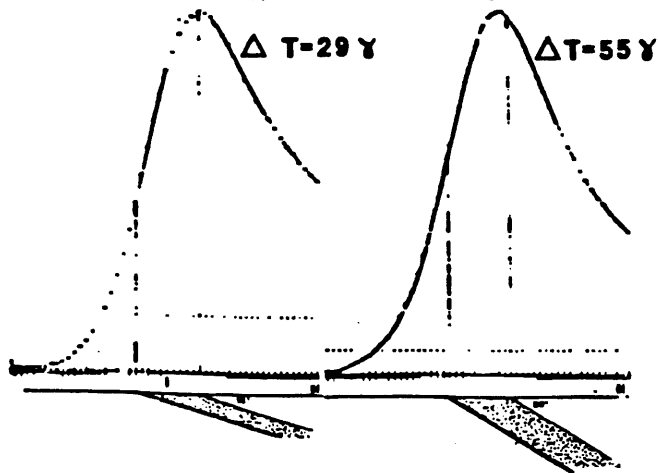
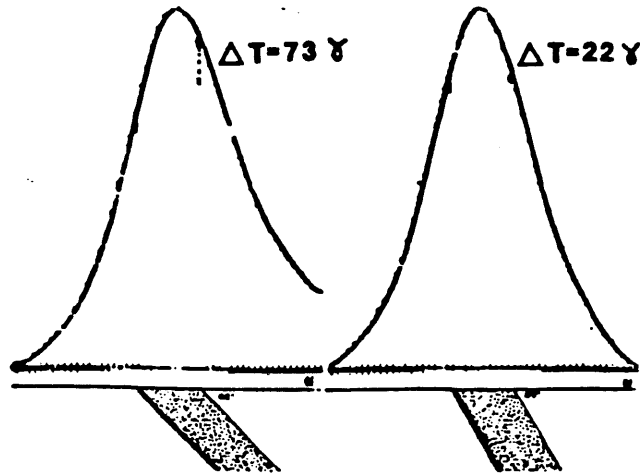
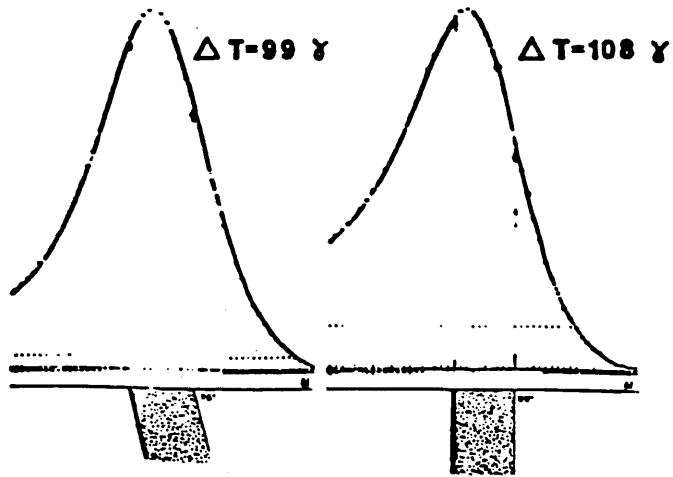


Figure 3b. Dipping Prism Anomalies.

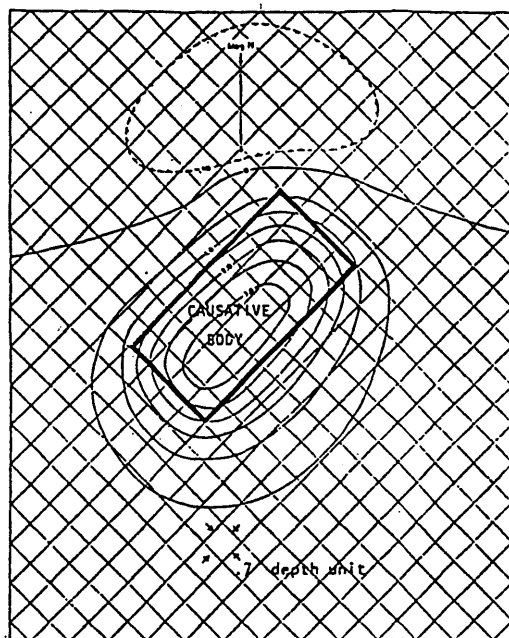


Figure 3c. Prism Model Anomaly.

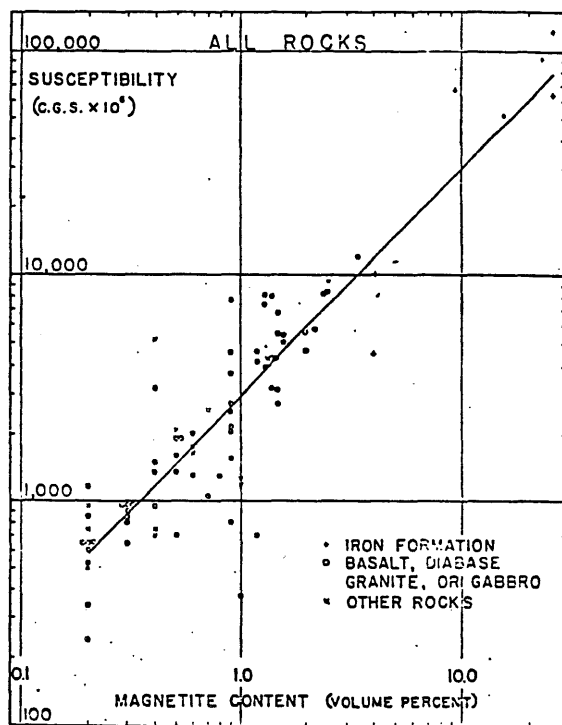
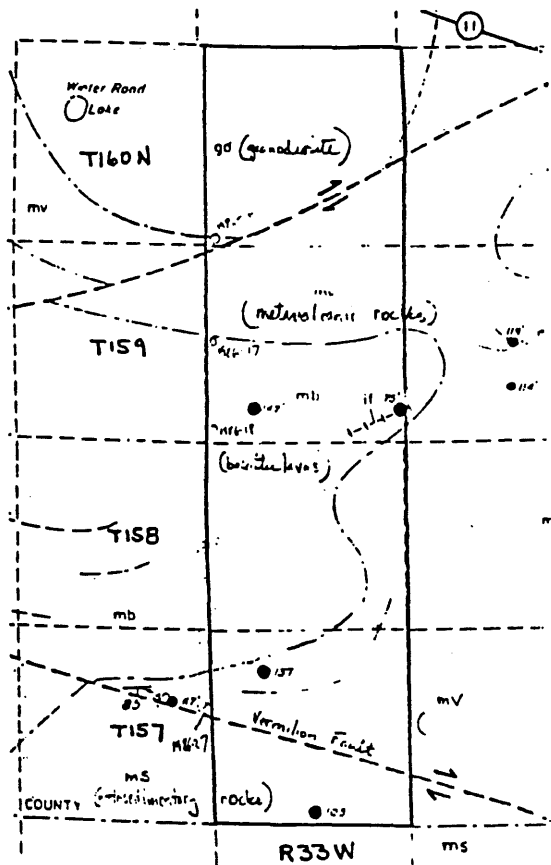


Figure 3d. Magnetite and Magnetic Susceptibility.

1.3 Geological Setting



According to Sims and Ojakangas (1975) there are no known bedrock exposures in the project area. They produced a pseudo-geological map of the area using some rather widely scattered drill hole data and the 1949 aeromagnetic data supplemented by gravity data published by McGinnis et al (1973). Their map is seen across. Three principal lithologic units were discerned;

- granodiorite to the north,
- metavolcanic rocks (mv) and mafic units (mb), and iron formation.
- metasedimentary rocks (ms) to the south.

Right-lateral faults are shown to cross the southern part of the area.

As part of Minnesota's contribution to the USGS CUSMAP project in the Roseau Quadrangle, four drill holes were completed in 1986 (1986-16,17,18 and 27). Their locations are shown in Figures 1 and 2, in relation to the aeromagnetic survey. A summary of the logging, taken from Mills et al (1987) is given below;

Drill Hole	Depth to Bedrock	Bedrock	Comments
1986-16	300'	Gneissic Tonalite	
1986-17	190'	Gabbro	Magnetic rock
1986-18	335'	Plagioclase Porphyry	Highly weathered
1986-17	30'	Hornblende Schist	

Prospecting interest is directed to metavolcanic or 'greenstone' rocks because they host massive sulfide basemetal deposits, particularly to the northeast, in Canada. For example, the Mattabi orebody at Sturgeon Lake consists of 13 million tons of 0.9% copper and 7.6% zinc. The orebody is associated with a conspicuous 300 gamma aeromagnetic anomaly observed at 500 foot altitude.

1.4 Correlation With Gravity Data

The gravity map of the area (McGinnis et al, 1973) shows -30 mgal gravity anomalies in the north and south halves of the area. These negative effects may be attributed to the lower density of granitic rocks and metasedimentary rocks, respectively. The metavolcanic rocks occupying the central part of the area are associated with a relatively positive effect.

This gravity data was collected in the course of a reconnaissance survey of Minnesota, involving measurements at one mile intervals along roads or section corners where elevations were known from published topographic maps. Further gravity surveying is necessary to detail many of the features that are prominent in the data.

2. GEOLOGICAL INTERPRETATION

The results of the analysis and geological interpretation of the aeromagnetic data are presented at 1:62500 scale as Figure 4. [Plate 290-2]

The map shows the location of magnetized rocks, their depth below ground and their structure.

2.1 Magnetic/Lithological Units

Areas of similar magnetization were distinguished and outlined in the interpretation map as 'magnetic units.' On the basis of drill hole data and recognized characteristics of rock units in published geological mapping the magnetic units are given a lithological identity.

Metavolcanic and associated units: 10 to 3000 gamma anomalies that reflect long, rather linear, mainly west-trending magnetic zones. These rather narrow zones are separated by non-magnetic intervals. Metavolcanic rocks are associated with these anomalies that occupy a 10 mile wide interval that extends across the map area in an arcuate-shaped pattern. The metavolcanic rock interval is also marked in the published gravity map as a 30 mgal. increase over areas underlain by granitic or metasedimentary rocks.

We may further divide this interval into 3 sub-units, in addition to the non-magnetic intervals which probably reflect volcanoclastic and/or felsic volcanic units, e.g., rhyolite.

- mv Moderately magnetic zones are associated with relief of from 10 to 200 gammas. From modelling, the susceptibility contrast of these units is in the range 100 to 1000 x 10⁻⁶ cgs units and according to Mooney and Bleifuss, these rocks have 0.1 to 0.3% minimum magnetite content.
- m vb A much more magnetic volcanic facies is evident by magnetic relief of from 300 to 3000 gammas (1 to 10% minimum magnetite content). Two or three of these zones appear to be involved in a west-trending synclinal structure near the boundary of T157 and T158. Probable lithology is metabasalt.
- IF A 4000 to 7000 gamma anomaly dominates the central part of the map. According to Sims and Ojakangas (1973), the anomaly is due to iron formation. Estimated magnetite content is 20 to 30%. The iron formation is seen to be intimately associated with the mafic metavolcanics.

Metasedimentary Rocks:

- ms metasedimentary rocks are associated with depressed levels in magnetic intensity in the aeromagnetic data. Drill hole 1986-27 encountered hornblende schist (with high copper and zinc grades). These rocks also appear to have lower bulk density as compared to the metavolcanic sequence to the north.

Intrusive Rocks:

- g Magnetic intensity levels in the north third of the area which is underlain by granodiorite, are observed as much more uniform or less erratic than levels over the metavolcanics. In comparison to metasedimentary rocks, the granodiorite is associated with a 50 to 250 gamma increase in magnetic intensity. This is indicative of a 0.1 to 0.3% increase in magnetite content. The south contact of the granodiorite with the metavolcanics appears to be fairly well definable. A stock-like granitic intrusive is outlined in T157N, in contact with metasedimentary rocks. It exhibits magnetization quite similar to that associated with the granodioritic rocks.

Narrow, dyke-like anomalies are conspicuous in the north half of the area against the uniform magnetic background of the granodiorite. The anomalies are mostly negative in polarity; -50 to -200 gammas in amplitude. A NNW-trending swarm of these dykes appears to cross the area, apparently in association with a parallel fault zone.

2.2 Structures

A number of structures may be deduced from the aeromagnetic data;

- (a) Synclinal fold structure. Magnetic anomalies linked to the metavolcanic assemblage, invariably display asymmetry indicative of northerly dipping, as opposed to vertically dipping attitude. A synclinal structure is deduced from the distribution of the mafic metavolcanic units. The axial plane of the syncline appears to have been rotated and is now dipping northerly. This rotation may help to explain the 1 to 2 mile displacement between the synclinal axis and the gravity anomaly peak.
- (b) West-trending faults. The contact between the metavolcanic and the metasedimentary rocks to the south appears to be a fault zone as judged by the linearity of the contact and the strong gravity gradient across it. A second west-trending fault may be coincident with the contact between the metavolcanic rocks and the granodioritic rocks to the north.
- (c) NNW-trending faults. Granodioritic rocks and metavolcanic units appear to have been dislocated or sheared by NNW-trending faults. This structure appears to be associated with a dyke swarm. Similar deformation appears to have affected the granitic stock in T157N.
- (d) Other faults. The WSW-trending Quetico Fault is associated with a magnetic contact that is located in granodioritic rocks. A major northerly-trending fault zone is suggested by the abrupt termination or dislocation of magnetic anomalies near the east border of the project area.

2.3 Depth to Magnetic Basement

Magnetic basement in this area is covered by unconsolidated surficial deposits of Quaternary age and highly weathered non-magnetic Precambrian rocks or regolith. Contours of depth to magnetic basement below ground are included in Figure 4, at 100 foot interval. Depth determinations were made at most magnetic contact locations. The determinations are considered to have an accuracy of $\pm 20\%$. Thus a determination of 200 feet (plus 300 feet aircraft height) would have a reliability of ± 100 feet.

To avoid obscuration of other aspects of the aeromagnetic interpretation, individual depth determinations were not included in Figure 4. [Plate 290-2]

Depth determinations were found to vary from less than 100 to over 400 feet. Two basement depressions (depths greater than 400 feet) are expressed;

- in the northeast part of the map, over granodiorite,
- near the south border of the area.

Elsewhere, magnetic basement, for the most part, appears to be at depths of 200 ± 100 feet.

2.4 Summary and Recommendations for Follow-Up Investigation

A 10 mile wide 'greenstone' belt is delineated from the aeromagnetic and gravity data. The belt includes magnetized volcanic members of intermediate and mafic composition and iron formation. Intervening non-magnetic, possibly felsic members attract interest as preferred mediums for massive sulfide, base metals mineralization.

Certain structural environments may be attractive in terms of potential gold mineralization;

- (1) The axial part of the synclinal fold structure involving mafic metavolcanic units,
- (2) Along west trending fault zones that border the metavolcanic belt on its north and south flanks,
- (3) Along the NNW-trending fault zone that crosses the metavolcanic belt.

VLF electromagnetic surveying may be considered as an economical means for testing for conductivity anomalies along some of these structures. However the thick cover of Quaternary and regolith cover may make it difficult to achieve penetration by this prospecting method.

Additional gravity surveying is necessary in the area. There is a good correlation between some of the aeromagnetic structures and gravity features, but the gravity coverage to date must only be considered as reconnaissance in scope.

The analysis of the survey data embodied in this report is essentially a geophysical appraisal of the area. As such, it can incorporate only as much geological and geophysical information as the interpreter has available at the time. It should be judiciously used therefore as a guide only by geologists thoroughly familiar with the area and who are in a better position to evaluate the significance of any particular feature. With additional information, such as that provided by other surveys and eventually drilling, it may be possible to revise the significance of features identified in this study.

Respectfully submitted,

ALLAN SPECTOR AND ASSOCIATES LIMITED

Allan Spector Ph.D., P. Eng.

3. REFERENCES

- McInnis L., Durfee G. and Ikola R.J. (1973) Simple Bouguer gravity map of Minnesota, Roseau Sheet USGS Misc. Map M-12.
- Meuschke J.L., Books K.G., Henderson J.R. and Schwartz G.M. (1957) Aeromagnetic and geological maps of Northern Beltrami and Southern Lake of the Woods Counties/Northern Lake of the Woods and NE Roseau Counties. USGS Geophys. Invest. Maps GP129 and 128.
- Mills S.J., Southwick D.L. and Meyer G.N. (1987) Scientific core drilling in Northcentral Minnesota. Summary of 1986 lithologic and geochemical results. Minnesota Geological Survey Information Circular #24. 48 p.
- Mooney H.M. and Bleifuss R. (1953) Magnetic susceptibility measurements in Minnesota. Geophysics, v. 18, pp. 383-393.
- Sims P.K. and Ojakangas R.W. (1973) Precambrian geology of Roseau sheet, Minnesota. Minnesota Geological Survey open file map.
- Vacquier V., Steenland N.C., Henderson, R.G. and Zeitz I. (1951) Interpretation of aeromagnetic maps. Geological Society of America Memoir 47, 151 p.

**Appendix 290-E. Aeromagnetic Data Interpretation for the McDougal Lakes Area,
Duluth Complex, Lake County, Minnesota**

June 1989

For the Minnesota Department of Natural Resources

by

Robert J. Ferderer

Eagan, Minnesota

Available as Open File Report 282-1-1

Table of Contents

	Page
Objective	3
Data	3
Approach	6
Discussion	9
Recommendations	11
References Cited	13

List of Figures

	Page
Figure 1. Location map	3
Figure 2. Remanent magnetization example	3
Figure 3. Ideal Werner deconvolution anomaly sources	6
Figure 4. Real anomaly sources that may be represented by Werner deconvolution results	6

Objective

In this study, aeromagnetic and to a lesser degree, gravity data are analyzed for a four-township sized area in the block T59-61N, R9-11W, Lake County, Minnesota (Fig. 1). Techniques utilized include: Werner deconvolution-based inverse modeling, Talwani-based forward modeling and frequency-domain filtering. The objective of this study is to define geologic structures and lithologic units within the Duluth Complex, based on information provided by these techniques.

Data

Digital aeromagnetic and gravity data were taken from magnetic tapes owned by the Minnesota Geological Survey.

Aeromagnetic Data

The high-resolution aeromagnetic survey used in this study was flown in 1979-80, and consists of flight lines oriented south-north, spaced 400 m apart, and sampled at a 50 m interval. Tie lines are oriented west-east, spaced 2000 m apart and sampled every 50 m. Both flight and tie lines were flown at a mean terrain clearance of 150 m.

Aeromagnetic anomalies in the study area have amplitudes ranging from < -2000 to > 1000 gammas. The anomaly expression is complicated by strong remanent magnetization, having an average declination and inclination of (290° , 40°) (Halls and Pesonen, 1982). Induced magnetization is assumed to be aligned along the main geomagnetic field which has an approximate declination and inclination of (3° , 75°). The Koenigsberger (Q) ratio, or ratio of remanent to induced magnetization generally ranges between 1 and 10 throughout the study area (Holst and others, 1986).

The strong remanent magnetization described above results in magnetic anomalies that are significantly asymmetrical. For a west-east (south-north) profile, and a vertical prism anomaly source, an anomaly minimum occurs near the western (northern) contact and a maximum occurs near the eastern (southern) contact (Fig. 2).

Gravity Data

Gravity coverage over the study area is poor, as measurements have been taken at less than one hundred stations. Bouguer gravity anomaly data indicate a strong near-linear gradient, with anomaly values increasing from northwest to southeast. This regional anomaly is interpreted to be related to eastward thickening of the Duluth Complex (Ferderer, 1982). Superimposed on the regional anomaly are shorter-wavelength anomalies that are more indicative of the near-surface geology in the study area. The strongest of these anomalies has an amplitude of about 20 milligals.

Rock Property Data

Rock property data pertinent to this study are summarized in Table 1. NRM is the intensity of natural remanent magnetization.

Table 1. Rock property information for Duluth Complex rocks. Taken from Holst and others (1986), and V. W. Chandler (personal communication). Asterisks denote values based on less than 5 measurements.

	Avg. Density (gm/cc)	Avg. Susc. (cgs)	Avg. NRM (cgs)	Avg. Q (cgs)	Avg. NRM decl.	Avg. NRM incl.
Ferrogabbro	3.18*	.0050*	.0058*	1.9*	304*	32*
B. Eagle Ring Troctolite	2.97	.0007	.0012	2.8	303	55
B. Eagle Core Gabbro	2.98	.003	.0038	21.0	291	30
Anorthositic Rocks	2.80	.0010*	.0006*	1.0*	296*	37*
Basal Troctolites	2.91	.0013	.0033	4.2	284	44

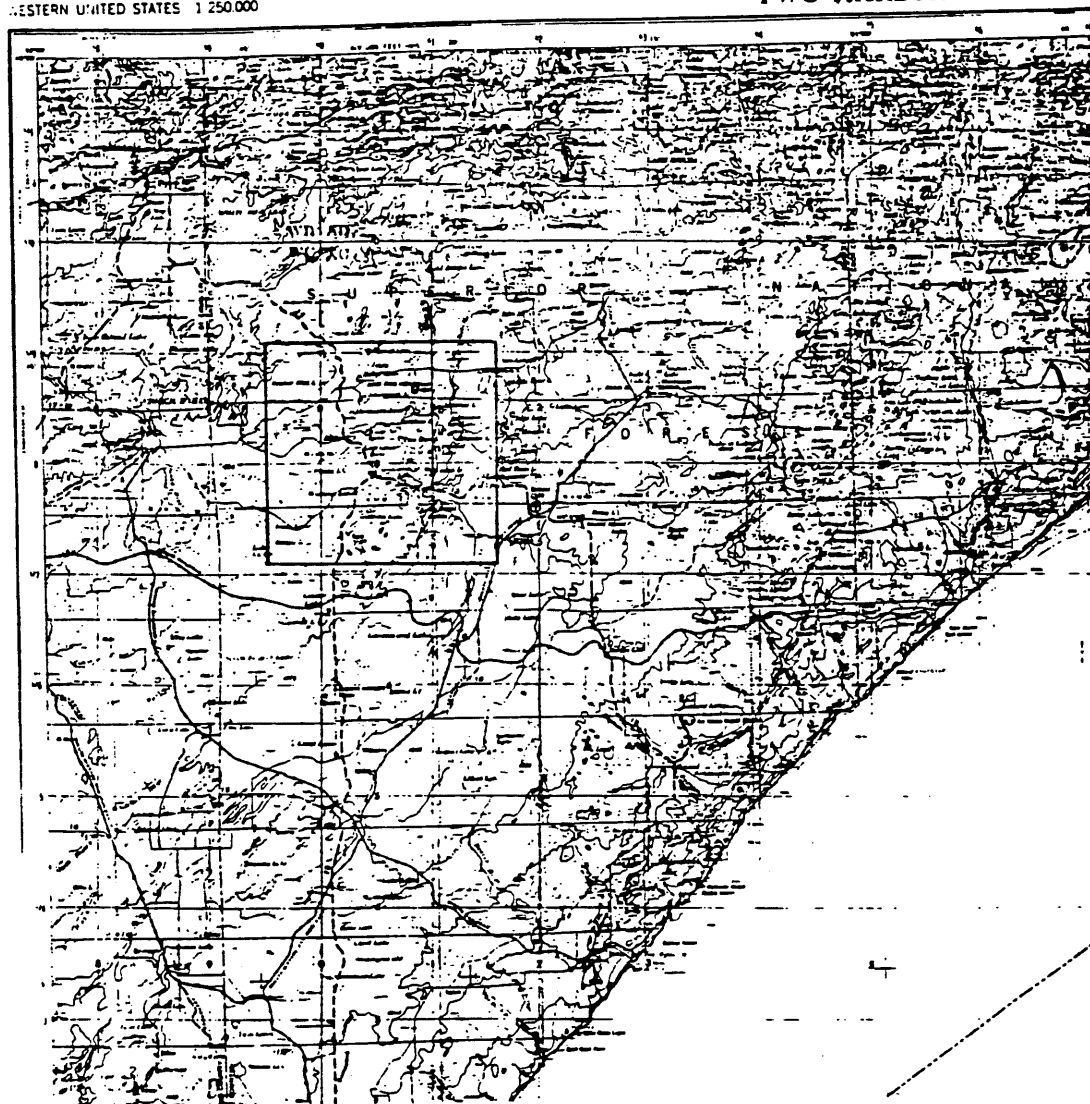


Figure 1. Location Map.

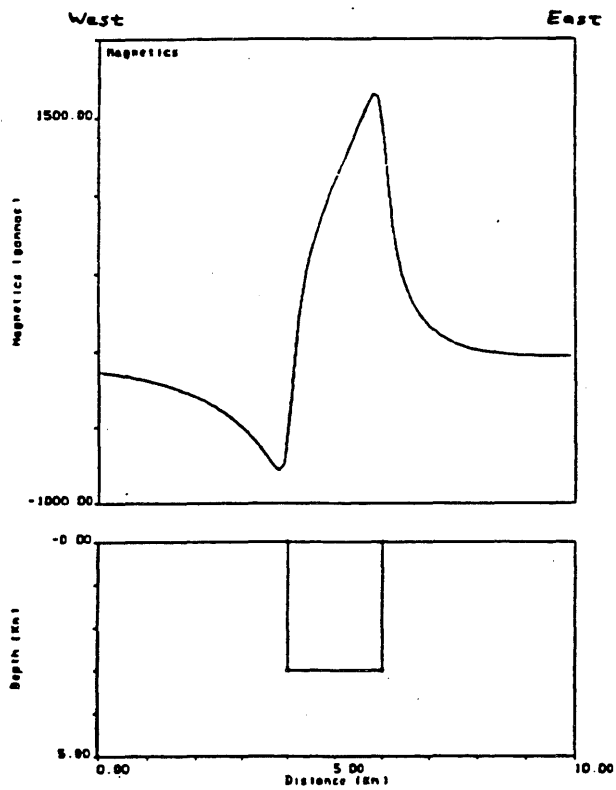
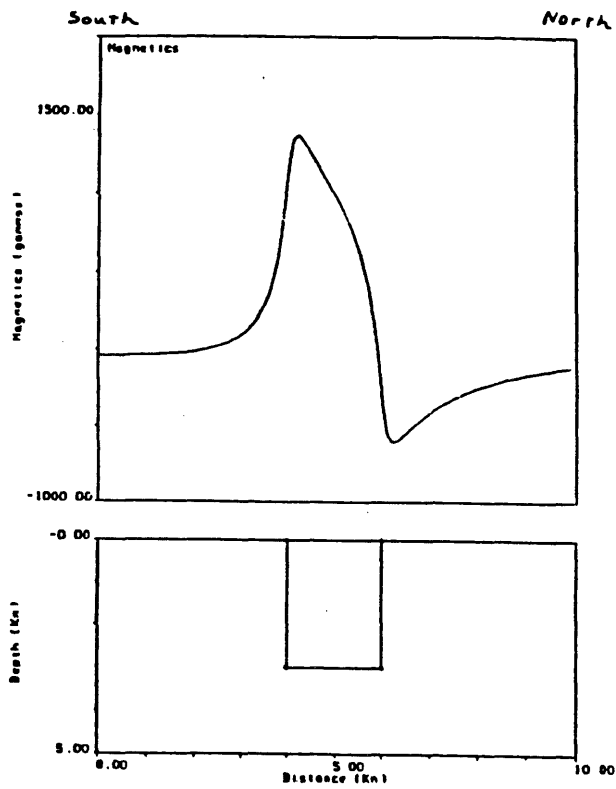


Figure 2. Magnetic anomalies along (a) west-east and (b) south-north profiles, over a vertical prism that has a strong remanent magnetization (inc., dec. = 40° , 290°).

The majority of the Bald Eagle ring troctolite samples used for Table 1 were obtained along the eastern side of the intrusion.

Weakly magnetized rocks in the study area include anorthositic, troctolitic, gabbroic and granophyric rocks. The magnetic properties of these rocks are not generally distinctive. If outcrop or drill hole information exists, rock types may be assigned to weakly magnetized zones that have been defined through modeling, filtering and imaging.

Rock magnetization measurements indicate that many of the stronger magnetic anomalies observed over the Duluth Complex are produced by troctolitic and gabbroic rocks that are enriched in magnetite.

Approach

The processing and interpretation approach applied in the study utilizes three techniques, each having particular strengths. These techniques include:

- Werner deconvolution-based inverse modeling.
- Talwani-based forward modeling.
- Frequency-domain filtering and data enhancement.

Werner Deconvolution

This inverse magnetic modeling technique is based on the assumption that anomaly sources may be approximated by thin sheets and interfaces of arbitrary dip and infinite strike and depth extents (Fig. 3). The assumption of polynomial-like anomaly interference allows a wide variety of geologic features (Fig. 4) to be accurately characterized, even when severe interference occurs.

Information provided by Werner deconvolution includes source location (x_0), depth (z_0), dip (d) and susceptibility contrast (k) estimates. These results are presented in map form so that they may be overlain on aeromagnetic maps. For more detailed information and references, see Ferderer (1988).

Because geologic strike varies considerably in the study area, the aeromagnetic data were gridded prior to deconvolution. The resulting 100 m grid, was broken into south-north and west-east oriented profiles which were upward continued and deconvolved. When data are gridded, smoothing occurs. As a result, gridding prior to deconvolution may result in slight parameter estimate errors. Upward continuation is used to minimize the effects of noise.

Information was obtained for anomaly sources having a wide variety of strike directions. The effects of geologic strike on depth estimates were accounted for during across-profile correlation of results.

Remanent magnetization was accounted for during deconvolution.

Forward Modeling

Forward modeling was performed along four south-north, and six west-east oriented grid lines. This technique assumes uniformly magnetized, two-dimensional, polygonal-shaped bodies, and is based on the technique of Talwani and Heirtzler (1965). Remanent magnetization was accounted for during modeling.

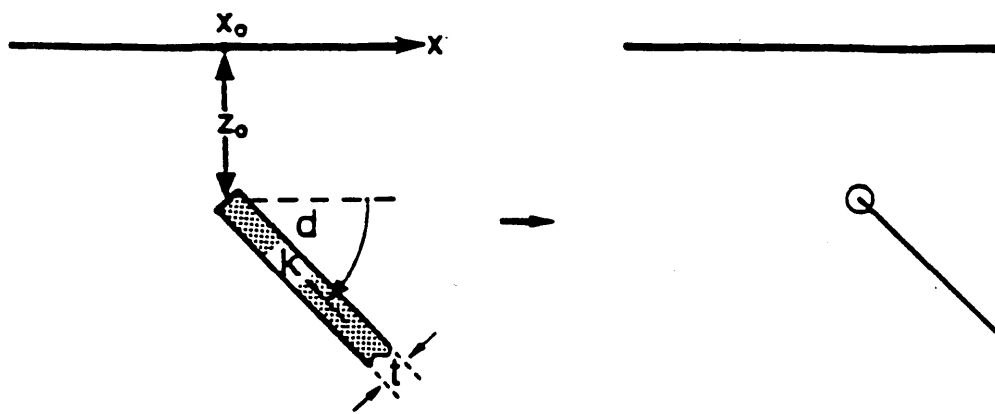
Forward modeling was also applied to one northwest-southeast oriented Bouguer gravity profile.

Frequency Domain Filtering

Four frequency domain filtering techniques were applied to the above mentioned 100 m grid. These techniques include:

- **Reduction to the pole:** The total magnetization vector, comprised of induced and remanent magnetization components, was reduced.

THIN SHEET



INTERFACE

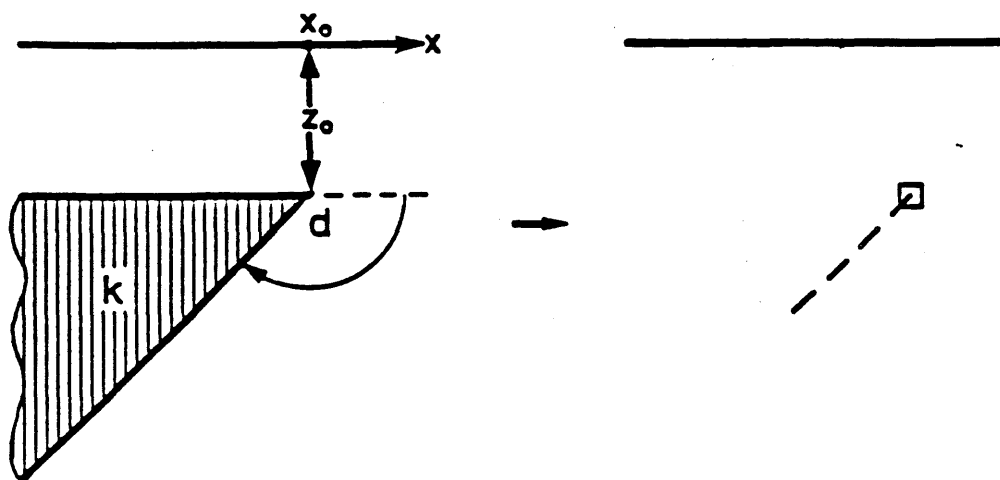


Figure 3. Ideal thin sheet and interface sources. The position, depth and dip of the stick symbols shown on the right-hand side correspond directly to those features of the actual sources. Thin sheets are indicated by circles, and interfaces by squares. Stick length is proportional to the reciprocal logarithm of the magnitude of k and is not related to the depth extent of the sheet. Negative k values are designated by a dashed stick and, for the case of an interface, indicate a susceptibility decrease in the positive x -direction.

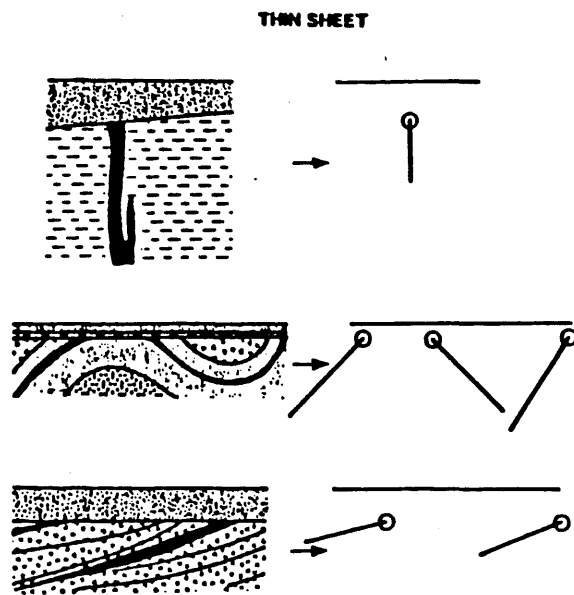


Figure 4a. Geological features that can be approximated by thin sheets: (top) dike, (center) magnetic unit (i.e. iron-formation, etc.) contained in the limbs of a truncated fold, (bottom) magnetic lens (i.e. magnetic lava flow, pyrrhotite body, etc.) surrounded by non-magnetic rock. Corresponding stick symbols are shown on the right hand side.

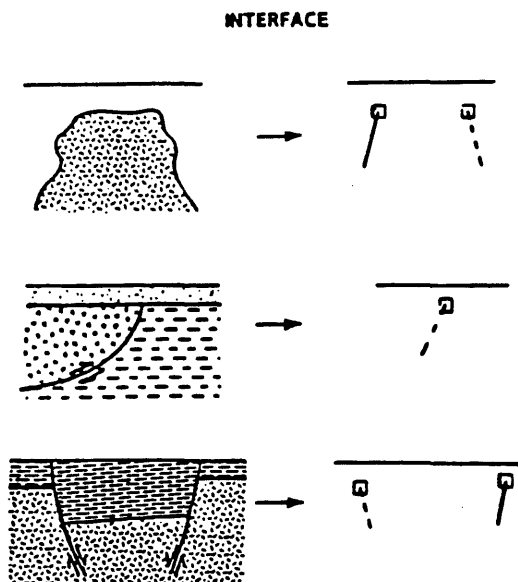


Figure 4b. Geological features that can be approximated by dipping interfaces: (top) edges of a plutonic body, (center) leading edge of a thrust fault, (bottom) normal faults. Corresponding stick symbols are shown on the right hand side.

- **Upward continuation:** Data were calculated at levels of 350 m, 500 m and 1000 m. Werner deconvolution was applied to test profiles for each of these three levels, and the 500 m level was chosen for production processing.
- **Second vertical derivative filter.**
- **Bandpass filters:** Wavelengths less than or equal to 2, 5, 10 and 15 km were passed. The 15 km bandpass filter was found to be quite useful for isolating shorter-wavelength gravity anomalies. This technique was not heavily relied on for magnetic interpretation.

Filtering operations were performed in the following sequences:

- 1) Red. to pole
- 2) Red. to pole > upward contin. > 2nd vert. deriv.
- 3) Red. to pole > upward contin. > bandpass filter
- 4) Upward contin. > Werner deconvolution

Color and shaded relief maps were used to present the raw and filtered data.

Interpretation

Results obtained using each of the three processing techniques described above were plotted at a scale of 1:62,500.

The derived aeromagnetic interpretation is given on Plate 1. [Plate 290-3].

Where Werner deconvolution solutions are strong, contacts were drawn based on these results. In areas of weak or no solutions, results of forward modeling and second vertical derivative data were used to extrapolate contact positions.

Parameter estimates indicated on Plate 1 [Plate 290-3] are average values, obtained from groups of clustered Werner deconvolution solutions. A small number of these estimates are based on the results of forward modeling.

In most cases, interpreted faults are based on evidence provided by Werner deconvolution. This technique is especially useful for locating strike-slip faults, based on sharp offsets in source position estimates. Normal faults are often indicated by offsets in depth estimates.

Depth estimates represent the depth to a magnetic source. This is not necessarily the depth to bedrock. In some cases, deep estimates may represent moderately or strongly magnetized intrusive rocks which lie below more weakly magnetized rocks. Depth estimates are rounded to the nearest 25 m for depths less than 100 m, and to the nearest 50 m for depths greater than 100 m.

In most cases, depth and dip estimates are assigned to mapped contacts and layering. In a few instances, isolated sets of parameter estimates which represent unmapped structures, are given.

Discussion

The study area is located in the west-central portion of the 1.1 Ga Duluth Complex.

Bedrock throughout most of this area is poorly exposed, and with the exception of the northwest corner and the northern margin, mapping has only been performed at a regional scale (1:250,000) (Green, 1982).

The South Kawishiwi Intrusion (SKI) occurs in the northwest corner of the study area. The SKI is relatively well exposed and has been studied by Foose and Cooper (1982), and Foose and Weiblen (1986). On average, the dominantly troctolitic rocks (ts) of the SKI strike N40-50° E and dip between 5 and 20° SE.

Rocks of the SKI are weakly magnetized and have little aeromagnetic expression. Measurements taken from these rocks were included with those of the basal troctolite group of Table 1.

A number of faults have been mapped in the SKI, only one of which appears to be strongly reflected in the aeromagnetic data. Four additional northwest trending faults that intersect the SKI are mapped based on the results of this study.

The Bald Eagle Intrusion (BEI) (Weiblen, 1965; Chandler, 1985) is a second, well studied structure occurring in the study area. The southern end of this intrusion intersects the northern margin of the study area. The BEI is a funnel-shaped intrusion, consisting of a core gabbro surrounded by troctolitic rocks.

Anomaly data suggest that the magnetizations and densities of troctolitic rocks on the western and eastern sides of the intrusion differ significantly. Troctolitic rocks on the western side (tb1) are moderately magnetized and have a relatively low density (two samples of this rock have a density 2.73 gm/cc, Holst and others, 1986). Those on the eastern side (tb2) are weakly magnetized and quite dense (several samples have an average density of 3.03 gm/cc). The magnetization of the core gabbro (gb) is intermediate to those of the western and eastern troctolites, and it is also quite dense.

A magnetic high occurs near the mapped contact (Green and others, 1966) between the core gabbro and the eastern troctolitic rocks. Model studies suggest that this high is related to two factors, a zone of more magnetic gabbro or troctolite (otg1), in contact with, or located near the weakly magnetized eastern troctolitic rocks.

Immediately west of the BEI, rocks are weakly to moderately magnetized. Both troctolitic and anorthositic rocks have been mapped in this area by Green and others (1966).

Due to lack of exposure, the geology of the remainder of the study area is much more poorly understood.

A unit denoted ts1, interpreted along the southeast margin of the SKI and striking approximately N45° E, is slightly more magnetic than surrounding ts and t units. This unit may be a reaction zone, produced when younger rocks were intruded to the southeast of the SKI. Rocks of the t unit, mapped just south of the SKI, may actually belong to the SKI, in which case the ts1 unit would likely represent an internal structure of the SKI.

Three large, oblong to circular shaped anomalies occur in the western half of the study area. The units otg1-3 have been assigned to the magnetic bodies that produce these anomalies, referred to as the northwestern, southwestern and eastern bodies. At least two of these bodies appear to be magnetically zoned, which may reflect further petrologic zoning. The three bodies are separated by rocks of the t unit.

The weakly magnetized zone to which the t unit has been assigned is widespread throughout the study area and more poorly defined to the southeast. A small number of outcrops indicate that rocks in this zone are troctolitic. Possible relationships between the t unit and rocks that produce the three large anomalies include the following:

- 1) A single, moderately to very strongly magnetized intrusion was forcibly injected by rocks of the t unit, possibly along faults, and its parts were spread apart.
- 2) Three separate intrusions of moderately to very strongly magnetized rock were emplaced into the weakly magnetized t unit.
- 3) The three anomalies are produced by large inclusions of the Lower Proterozoic Biwabik Iron Formation, in the t unit. This possibility seems least likely based on geometries and magnetizations derived through modeling.

The western and northern contacts of the northwestern body are indicated to dip moderately to steeply to the northwest. This is evidence that this body is discordant with rocks of the SKI.

Modeling indicates that the southwestern body has a deep root which may represent a feeder. It is further implied that this root rises from the east and from depths in excess of 5 km. Large depth estimates obtained along this anomaly suggest that the mapped otg1 unit is covered by weakly magnetized rocks along the northern and western sides of the anomaly.

Thin ledges of the otg1 unit, which extend and thin to the south, are interpreted for both the southwestern and eastern bodies. These ledges may have been shaped when the original body or bodies were intruded by rocks of the t unit. Alternatively, they may represent an original funnel shape for the magnetic body or bodies.

Offsets in Werner deconvolution solutions indicate that strike-slip faults occur within each of the three bodies.

Gravity and magnetic expressions just east of the eastern body (near UTM's 606,5285) are especially interesting. The anomaly source in this area is weakly magnetized, yet quite dense. Forward modeling was applied to a residual Bouguer gravity anomaly along a northwest-southeast trending profile in this area. The residual anomaly was obtained by subtracting values calculated assuming a linear gradient, from data of Ikola

(1970). The model suggests a source rock density of 3.15 gm/cc, and it is implied that the source rock contains weakly-magnetic oxides or considerable olivine. Although these rocks appear to be denser than the relatively dense troctolitic rocks of the eastern BEI to the north, it is likely that the two rocks are related. Accordingly, both of these dense rocks are assigned to the unit **tb2**. Werner deconvolution results suggest that this unit may form the core of the moderately magnetic eastern body at depth.

Outcrops of anorthositic rocks (**a**) occur in the northwest, northeast and southeast portions of the study area. Consistent with rock property data, these rocks appear to be weakly magnetized and have a low density. Their magnetic expression is generally uninformative.

A unit denoted **a1**, located in the northeast portion of the study area is slightly more magnetic than surrounding rocks. Anorthositic rocks outcrop on both sides of this unit near the northern margin of the study area. It is therefore likely that this unit reflects an original structure within the anorthositic rocks.

East of the study area, a major eastward trending aeromagnetic lineament splits into two lineaments which transect the **tau** unit as they enter the northeast portion of the study area, trending about N70° E. Strong Werner deconvolution interface solutions, were obtained along the northern lineament, and the anomaly source is interpreted to be a fault. Magnetization decreases from south to north across this fault, which appears to have been refaulted by strike-slip faults that trend about N45° W.

Thin sheet solutions are strongest along the southern lineament. This lineament is interpreted to correspond to a second fault which has been intruded by moderately magnetic material so that it generates a sheet-like anomaly. Both of these lineaments are truncated by rocks in the west-central portion of the study area, implying that they are older than these rocks, or that they originated with the intrusion of these rocks.

Several strong, elongate and plug shaped anomalies occur in the western and southern parts of the study area. These anomalies are interpreted to be produced by oxide-rich troctolitic and gabbroic rocks, similar to those thought to be responsible for the "Snake" or "Greenwood Lake Anomaly", in the Greenwood Lake area (Vadis and others, 1981). It is likely that the longest of these bodies is a continuation of the source of the Snake Anomaly.

Dip estimates obtained along the contacts of these intrusions indicate that they are wedge-shaped, their contacts dipping outwards at moderate to steep angles. Magnetizations estimated for these rocks are similar to those for the rocks responsible for the three oblong to circular shaped anomalies in western portion of the study area. This does not necessarily imply a genetic relationship.

Rocks occurring in the southeast portion of the study area are magnetically indistinct. Anorthositic rocks are observed at a small number of outcrops, and it is likely that troctolitic rocks are also present in this area. The unit **tau** is used to represent these rocks. It is also likely that granophyric rocks are more widespread than is indicated on Plate 1. [Plate 290-3]

Forward modeling was performed along a south-north oriented profile, near the southeastern corner of the study area. The modeled bodies were all assigned depths greater than 500 m. This implies that more strongly magnetized rocks in the southeast corner of the area are located at depth, beneath less magnetic rocks.

Faulting does not always produce a magnetization contrast, and it is likely that faulting is significantly more widespread than indicated on Plate 1. [Plate 290-3]

Recommendations

Drilling should be performed to test and refine the interpretations that have been made here. Some of the interpreted structures may have implications for mineral exploration. Possible targets include:

- The dense, weakly magnetized **tb2** unit, along the northeastern side of the large anomaly in the north central portion of the study area (near UTM's 606,5285). It is likely that this unit does not intersect the bedrock surface everywhere it has been mapped. Further geophysical studies may be helpful in this regard.
- The series of intersecting faults interpreted near (611,5284). Ground-geophysical surveys should be used to more precisely locate these faults before drilling is performed.
- The units **ts1** and **a1**, to determine how they differ from surrounding rocks.

- The unit **t**, at different locations, to more specifically define its character.
- Rocks of the units **otg1-3**, which produce large, oblong to circular shaped anomalies in the western half of the study area, to verify that petrologic zoning occurs in these rocks.

The analysis performed in this study is almost entirely geophysical in nature. The resulting interpretation should therefore be regarded as a first approximation of the geology in the study area, and be used judiciously by geologists working in the area.

Respectfully submitted,

Robert J. Ferderer, Ph.D.

References Cited

- Chandler, V. W., 1985, Interpretation of Precambrian geology in Minnesota using low-altitude, high-resolution aeromagnetic data, *in* Hinze, W. J., ed., *The utility of regional gravity and magnetic anomaly maps*: Tulsa, Oklahoma, Society of Exploration Geophysicists, p. 375-391.
- Ferderer, R. J., 1982, Gravity and magnetic modeling of the southern half of the Duluth Complex, northeastern Minnesota: Unpublished M.S. thesis, Indiana University, Bloomington, 99 p.
- Ferderer, R. J., 1988, Werner deconvolution and its application to the Penokean orogen, east-central Minnesota: Unpublished Ph.D. thesis, University of Minnesota, Minneapolis, 284 p.
- Foose, M. P., and Cooper, R. W., 1981, Faulting and fracturing in part of the Duluth Complex, northeastern Minnesota: *Canadian Journal of Earth Sciences*, v. 18.
- Foose, M. P., and Weiblen, P. W., 1986, The physical and petrologic setting and textural and compositional characteristics of sulfides from the South Kawishiwi Intrusion, Duluth Complex, Minnesota, USA: *in* Friedrich, G. H., ed., *Geology and Metallogeny of Copper Deposits*.
- Green, J. C., 1982, Geologic Map of Minnesota, Two Harbors sheet: Minnesota Geological Survey.
- Green, J. C., Phinney, W. C., and Weiblen, P. W., 1966, Gabbro Lake quadrangle, Lake County, Minnesota: Minnesota Geological Survey Miscellaneous Map Series M-2.
- Halls, H. C., and Pesonen, L. J., 1982, Paleomagnetism of Keweenawan rocks, *in* Wold, R. J., and Hinze, W. J., eds., *Geology and Tectonics of the Lake Superior Basin*: Geological Society of America Memoir 156, p. 173-202.
- Holst, T. B., Mullenmeister, E. E., Chandler, V. W., Green, J. C., and Weiblen, P. W., 1986, Relationship of structural geology of the Duluth Complex to economic mineralization: Minnesota Dept. of Natural Resources Report 241-2.
- Ikola, R. J., 1970, Simple Bouguer gravity map of Minnesota, Two Harbors sheet: Minnesota Geological Survey Miscellaneous Map Series M-9, scale 1:250,000.
- Talwani, M., and Heirtzler, J. R., 1965, Computation of magnetic anomalies caused by two-dimensional structures of arbitrary shape: *Computers in the Mineral Industries*, part 1, Stanford University Publication, Geological Sciences, v. 9, p. 464-480.
- Vadis, M. K., Gladen, L. W., and Meineke, D. G., 1981, Geological, geophysical, and geochemical surveys of Lake, St. Louis, and Cook counties, Minnesota for the 1980 drilling project: Minnesota Dept. of Natural Resources, Division of Minerals Report 201, 13 p.
- Weiblen, P. W., 1965, A funnel-shaped gabbro-troctolite intrusion in the Duluth Complex, Lake County, Minnesota: Unpublished Ph.D. dissertation, University of Minnesota, Minneapolis.

**Appendix 290-F. Drift Pebble Lithology of the Tomahawk Road Area,
Lake County, Minnesota: Can it be used to infer local bedrock?**

August 1990

For the Minnesota Department of Natural Resources

by

John C. Green and Edward A. Venzke

University of Minnesota Duluth

Table of Contents

	Page
Abstract	4
Introduction	4
Outline of the Project	4
Previous Work	4
Assumptions Involved	5
Methods	5
Bedrock Geology	6
Drift Pebble Analysis	7
Criteria for Identification of Pebble Lithology	7
Results of Pebble Counts	8
Drift Pebble Assemblages	8
Provenance of the Pebble Types	9
Conclusions	17
Glacial Drift Units	17
Bearing of this study on Ferderer's Aeromagnetic Interpretation	17
Evaluation of the Method	18
References	19

List of Figures

	Page
Figure 1. Simplified Rock Classification Diagram for Duluth Complex Pebbles	23
Figure 2. Bar Chart Showing Pebble Types of Representative Troctolitic (Tr) Assemblages	24
Figure 3. Bar Chart Showing Pebble Types of Representative Anorthositic (An) Assemblages	25
Figure 4. Bar Chart Showing Pebble Types of Representative Mixed Troctolite and Anorthosite (MTA) Assemblages	26
Figure 5. Bar Chart Showing Pebble Types of Representative Mixed Anorthosite and Troctolite (MAT) Assemblages	27
Figure 6. Bar Chart Showing Pebble Types of Representative Mixed Archean (MAr) Assemblages	28
Figure 7. Bar Chart Showing Pebble Types of Representative Mixed Anorthosite (MAAn) Assemblages ..	29
Figure 8. Bar Chart Showing Pebble Types of Representative Mixed Volcanic (MV) Assemblages	30

List of Tables

	Page
Table 1. Basic Data for Drift Samples, Tomahawk Road Area	20
Table 2. Results of Duplicate Counts of Samples	22
Table 3. Numerical Pebble Counts for the 81 Drift Samples	23
Table 4. Results of the Pebble Counts, in Percent	26
Table 5. Petrographic Descriptions of Pebble Thin Sections	29

List of Plates

	Page
Plate 1. Map of Sample Locations	30
Plate 2. Map of Samples Showing their Relationship to Surficial Units of Hobbs (1988)	31
Plate 3. Map of Outcrops and Drill Holes and Their Relationship to the Aeromagnetic Interpretation Map of Ferderer (1989)	32
Plate 4. Geologic Map, Tomahawk Road area, from this Study	33
Plate 5. Map of Samples Showing their Assignment to Glacial Drift Units	34

Abstract

This MDNR project was aimed at testing the usefulness of using glacial drift pebble composition to determine the type of underlying bedrock in drift-covered areas. Pebbles $> 1/4"$ in 81 surface drift samples from west-central Lake County were separated and examined, and each was assigned to one of 19 rock types (12 Keweenawan, 3 Animikie, 3 Archean, 1 "unknown"). The 50 (or more) largest pebbles were counted in each sample; this number was found to give reproducible results. Each sample was then assigned to one of seven Drift Pebble Assemblages, which were plotted on a digitized map. No significant differences were found between samples classed as subglacial (basal) and "reworked" (supraglacial, meltout) till.

Meanwhile rock outcrops and the six DDH cores from the area were examined both megascopically and in thin section, and a revised geologic map was constructed. Four (and possibly 5) bedrock units are discernible: anorthosite in the eastern 2/5, olivine gabbro and troctolite of the Bald Eagle Intrusion in the north-central part, and one or two troctolite units (including the South Kawishiwi troctolite) in the western half of the area. Some large gaps in outcrop control, however, make some contacts poorly constrained.

In general, the most abundant pebble type in these samples corresponds to the underlying bedrock type, suggesting that this technique can be useful for "remotely sensing" bedrock types in covered areas. However, in the eastern 1/4 of the area the drift is dominated by lithologies (Archean, Animikie, Keweenawan lavas, granophyre) that have been transported for long distances (several 10's of km) from the E, ENE, or ESE. This must have been carried by the Superior Lobe and is clearly not basal till (directly overlying bedrock). Elsewhere in the study area, ice transport has produced some gradations or transition zones in the drift pebble assemblages, compared to the bedrock contacts. Also, since glacial transport in the Rainy Lobe (dominant here) was primarily roughly parallel to the main bedrock contact (anorthosite vs troctolite), the pebble assemblage at any sample site may have come largely from a few km up-ice. Thus the technique will be most successful when the drift is relatively thin and its stratigraphy is known well enough to exclude the existence of an upper drift sheet that is not in contact with local bedrock, and where rock boundaries are at large angles to ice transport direction.

Introduction

Outline of the Project

The main purpose of this project was to test the idea that the pebble composition of glacial drift can be used to infer bedrock types in drift-covered areas in northern Minnesota, especially the central Duluth Complex. This concept is based on the general principles that continental glaciers pick up their sediment load from the base of the ice, and that the greatest proportion of this sediment load is derived from the most recently overridden bedrock. This test was focused on a 20 square mile E-W strip (10 x 2 miles) in west-central Lake County between the McDougal Lakes and the South Kawishiwi River, including Secs. 25-36 of T.61 N., R.10 W. and Secs. 27-34 of T. 61 N., R. 9 W. (?) Personnel included John C. Green, Principal Investigator, and Edward A. Venzke, Research Assistant. The work was carried out between June 20 and early September, 1990.

Previous Work

Compilation of published work and field reconnaissance led to the 1:250,000 Two Harbors bedrock geologic map (Green, 1982). The area immediately to the north of the study area (Gabbro Lake quadrangle) was mapped in the early 1960's (Green et al., 1966), and the area to the south (Greenwood Lake area) is currently under study as an M. S. thesis at UMD by E. A. Venzke.

H. Hobbs recently completed a regional surficial geology map, based mostly on air photo interpretation, and developed an interpretation of the Late Pleistocene geologic history (Hobbs, 1988) (?). Buchheit et al. (1989) studied the geochemistry of the glacial drift over a large area of central Lake County, and P. Morton and J. Reichhoff (1989) have studied the heavy mineral suite (especially chromite and chrome spinels) in drift as a part of that work. Ferderer (1989) has developed an interpretation of the aeromagnetic data for the wider McDougal Lakes area (?), and Venzke (1990) studied the magnetic properties of rock units in the Greenwood Lake area just to the south of the study area.

Assumptions Involved

The project involved data and assumptions of several kinds, relating to both the bedrock and the glacial deposits.

In order to establish correlation between drift lithology and bedrock, the test assumes that the bedrock geology is known; the aim is to use the drift-pebble technique to infer bedrock in other areas of poor or non-exposure. A revised bedrock geologic map is presented (?), but because of some wide local gaps in outcrop, considerable uncertainty about bedrock contacts exists in some areas.

Another assumption is that there is an adequate density of drift samples. This assumption is met in this study by the collection of about 94 drift samples by R. Buchheit from the 10 x 2 mile study area, at approximately ¼ mile intervals along roads. Sample density is good along the Tomahawk Road (US Forest Service 173) but some large gaps exist in some sections to the south. Of these 94 samples, 81 were studied, well distributed throughout the area (Appendix A).

A third assumption is that these drift samples were deposited by ice regimes that were comparable throughout the area. Different correlations between pebbles and local bedrock would be expected for each of the following situations, among others: a) ice movement in different directions (perhaps different lobes, Rainy vs. Superior) in different parts of the area; b) "basal" till deposited on bedrock from debris carried in the lower part of the glacier; c) "supraglacial" till deposited by meltout of upper parts of the ice sheet, perhaps several hundreds of feet or more above bedrock, and redistributed somewhat by meltwater; d) glaciofluvial action as in an esker (tunnel valley) or kame in which the pebbles may have been transported by meltwater from several kilometers away; and e) drift from a glacial advance later than and over-riding that which deposited a lower drift sheet. The existence of all of these possibilities will lead to uncertainty in interpretation of the drift lithology. On the other hand, drift sample lithology in the local context can in turn be used to infer various aspects of the glacial history.

Hobbs (1988) recently presented a Surficial Geologic Map of the Greenwood Lake, Isabella, and Cramer 15 minute quadrangles, which includes the study area at its northern edge. Hobbs's study also includes a report on the glacial history of the same area. The drift samples have each been assigned to one of the glacial drift units on Hobbs's surficial map, as closely as possible considering the relatively small scale of the glacial map (?). The map units involved were all interpreted to be derived from the Rainy Lobe, with apparent derivation from the north, northwest, and northeast. The units in the Hobbs study are "till", apparently basal, showing little evidence of reworking by meltwater; "reworked till", which is probably dominantly supraglacial or meltout till; "ice-contact deposits" which are moderately well-sorted and rounded and deposited by meltwater beneath and adjacent to ice; and "outwash", similar to the latter but deposited beyond the ice margin. General evaluations of the roundness of the clasts were made for most of the samples to aid in inferring the glacial origin of the sample.

Methods

Study proceeded along two lines: bedrock geologic mapping and petrographic study of thin sections from outcrops and drill core; and study of the drift samples.

One day of bedrock reconnaissance was spent in the area by both JCG and EAV, and three other days by EAV. JCG logged the drill core at MDNR Hibbing and examined about 60 thin sections at the Geology Department, University of Minnesota, Duluth.

Each drift sample was sieved and the clasts $> \frac{1}{4}$ " were separated into three size classes: $\frac{1}{4}$ " to $\frac{5}{8}$ "; $\frac{5}{8}$ " to 1"; and > 1 ". These were washed thoroughly before examination, but many pebbles retained a partial coating of weakly cemented silt. Pebbles were examined and assigned to a lithologic type using naked eye and hand lens; most were broken to expose a fresh surface. Because the smaller the pebble the less representative it is of its source and the more difficult it may be to identify, the largest pebbles (> 1 ") were examined first, then smaller classes until the desired sample size was attained. The pebbles were drawn from a container in such a way as to avoid bias in selection. All pebbles studied (at least parts of them) were subsequently retained. The optimum sample size (number of pebbles to count) was unknown at the beginning of the project, and several experiments were run to compare duplicate samples and samples of different sizes. One hundred-pebble samples were found to give reproducible results, and many samples of this size were counted. To speed the process it was hoped that a brief visual survey of a sample could eliminate some from detailed study if many non-Duluth Complex

clasts were obviously present, but this was deemed too subjective. Eventually it was found that 50-pebble counts gave valid, reproducible results adequate for the purposes of the study, and the remainder were counted at this size. Appendix B gives the results of duplicate analyses. A few counts were made with over 50 pebbles if there remained only a few more pebbles in the size class being studied when 50 had been identified.

The pebble lithologies were tabulated and entered into a Lotus 1-2-3 spreadsheet. Maps were developed using AutoCAD showing geographic coordinates, sample locations and numbers, earlier surficial and aeromagnetic geologic maps, new bedrock geology, and data derived from the pebble counts.

Bedrock Geology

Exposures of bedrock in the study area are unevenly distributed and not abundant; they probably constitute well under 1% of the area. They have been augmented by 6 diamond drill holes located in covered areas. These have been logged, with thin sections made from both outcrops and drill core (Appendices C, D, E). The map of the Gabbro Lake quadrangle just to the north (Green et al., 1966) is useful for extrapolation of units. There remain, however, some large areas where there is essentially no control for the bedrock geologic map, so that placement of some of the contacts has a large uncertainty (?).

Five bedrock units were found in the study area: anorthositic rocks, three troctolite units, and an olivine gabbro unit.

The anorthositic unit (mainly troctolitic anorthosite) is believed to underlie the eastern 2/5 (approximately) of the area, but no outcrops were found in the several easternmost sections. The rock is medium- to coarse-grained, brown to gray, foliated (expressed by subparallel plagioclase laths), and contains 6 to 13% of relatively small cumulus olivine along with minor interstitial augite and opaque minerals. Orthopyroxene reaction rims are common around olivine, and many other reaction and exsolution textures and products are present, perhaps produced by a metamorphic event. These include exsolution/oxidation needles and rods in plagioclase and clinopyroxene, biotite rims on opaque minerals, and symplectic intergrowths of orthopyroxene in plagioclase and of opaques in orthopyroxene.

Two lithologic units represent the extension to the south of the Bald Eagle Intrusion in the adjacent Gabbro Lake quadrangle. The outer zone (BEt) is a fine- to medium-grained, weakly to moderately foliated troctolite containing cumulate plagioclase (40-75%) and olivine (20-46%) and intercumulate orthopyroxene, augite, and opaques (mostly magnetite according to its habit). In thin section the rock appears somewhat granoblastic, suggesting that it may have been recrystallized. The augite contains abundant microscopic exsolution/oxidation platelets which give it the luster of orthopyroxene in hand specimen.

The inner zone of the Bald Eagle Intrusion (BEog) is a medium-grained, adcumulate olivine gabbro showing a moderately well-developed cumulate foliation and weak lineation expressed by the augite prisms. It contains cumulate plagioclase (50-63%), augite (25-33%), and olivine (10-20%) with minor intercumulate orthopyroxene and opaques.

Two other troctolite units are distinguished in the western part of the area. The first (Tx) is rather similar to the outer, troctolite zone of the Bald Eagle Intrusion and may be an extension of it, but since no outcrops were found there are no structural observations to guide such a correlation. It is represented only by DDH's TH-1 and TH-3. The rock is fine- to medium-grained with discontinuous, streaky concentrations of olivine grains and a somewhat granoblastic texture. It appears to have been recrystallized. It contains cumulate plagioclase (50-65%) and slightly smaller olivine (20-40%), and in a few samples augite (0 to 20%), with intercumulate orthopyroxene, augite, opaques, biotite, and hornblende. A few thin olivine anorthosite bands are intersected in TH-3.

The last troctolite unit (SKt) is probably part of the South Kawishiwi Intrusion. It crops out in the western part of the area and is intersected by DDH TH-2. It is a moderately well-foliated, medium-grained adcumulate troctolite to picrite, and is not granoblastic. A few thin dunite to peridotite zones were intersected in the drill core, but no lengthy sections. Cumulate minerals are restricted to plagioclase (40-60%) and relatively large, oval olivine (35-60%, but more in the peridotitic bands), with intercumulate orthopyroxene, augite, biotite, and opaques. Partial to complete serpentinization of olivine has led to expansion fracturing of adjacent plagioclase.

Drift Pebble Analysis

Criteria for Identification of Pebble Lithology

Nineteen categories were established for identification/assignment of the pebbles: 12 Keweenaw lithologies, 3 Animikie types, 3 Archean groups, and one "unknown" or otherwise unassignable class.

For Keweenaw mafic intrusive rocks (Duluth Complex) a simplified version of the modal Ol/Plag/Cpx triangular diagram used by the DNR (after Phinney, 1972) was used (?). The troctolite/picrite group includes non-anorthositic rocks with olivine the dominant ferromagnesian mineral. A few pebbles are rich enough in olivine to be feldspathic dunite or peridotite; these were not counted separately but were noted on the original data sheets. Aside from these obvious mineralogic criteria in phaneritic rocks, several more subtle characteristics were used which will be mentioned below. A hand lens was used routinely.

Keweenaw volcanic rocks (North Shore Volcanic Group, NSVG - but some could possibly be from the Osler Group east and southeast of Thunder Bay) were classed as either basalt, rhyolite, or intermediate. The basalts generally have a decussate meshwork of small plagioclase laths with black, dark green or dark brown (if weathered) interstices, visible with a hand lens. Grain size is generally finer than for diabase but these overlap; fresher, coarser rocks were called diabase. Still coarser (medium-grained) rocks with similar texture and mineralogy were called gabbros, along with a few cumulate-textured rocks of gabbroic composition.

NSVG rhyolites: light gray, tan, red, or brown, aphanitic dense to grainy, commonly with blocky feldspar phenocrysts (mostly orthoclase) with or without quartz. Many are vesicular/amygdaloidal, some show flow lamination and/or hydrothermal veining.

NSVG intermediate rocks (andesite, icelandite): typically light to dark brown, grainy-aphanitic, nearly all with sparse plagioclase phenocrysts, some oxidized ferromagnesian phenocrysts. Abundant in the eastern part of the area.

Keweenaw red granite: mostly medium-grained; with or without abundant visible quartz; dominated by blocky red feldspar; altered ferromagnesian minerals; no biotite; non-foliated; micrographic texture common. Commonly weather to very rough surface by physical disintegration.

Keweenaw intermediate plutonic rocks: generally red to brown, intermediate between red granite and gabbro or diabase mineralogically; some have prismatic Fe silicates. Uncommon in these samples.

Keweenaw hornfels: fine-grained, granoblastic, massive, polymineralic rocks.

Animikie rocks represent sources such as the Rove and Gunflint Formations. Sandstone/graywacke/argillite pebbles are abundant: mostly light to dark gray, a few tan, brown, or black; massive to faintly bedded; well sorted; well lithified fine sandstones and siltstones and black shales and mudstones. With a hand lens, small, dark, roundish quartz grains are commonly visible, as well as equant feldspar clasts, whereas in massive, fine-grained basalts or intermediate volcanics no such quartz is present and at least some lath-shaped feldspars and/or needles of apatite are present. Some graywackes also contain a few muscovite clasts. The Animikie graywackes are among the hardest and toughest pebbles in this drift, and tend to be more rounded than other pebble types.

Iron-formation pebbles are mostly slightly recrystallized chert with vague granule structure (1-2 mm across), and weathered (rusty, dissolved-out) spots are common. Some are magnetic.

Animikie quartzites: tan orthoquartzites; may possibly be derived from the Middle Proterozoic (Sibley, Osler, or Puckwunge). Rare.

Archean pebbles were classed in three categories, and included all dynamically metamorphosed rocks. Granite and gneiss: pink, tan, or pale gray, phaneritic, quartzofeldspathic rocks with or without a metamorphic fabric; typically contain biotite and/or hornblende.

Greenstone and amphibolite: aphanitic to phaneritic; schistose, gneissic, or massive; chloritic or amphibole-rich metamorphic rocks. Relatively rare.

Felsic or intermediate metavolcanic rocks and metasediments. These have at least some metamorphic foliation or lineation and most contain either phenocrysts (volcanic) or clasts (graywackes) of feldspar (mostly plagioclase) and/or quartz. Colors are highly variable but most are off-white, to green to gray. Pyrite is moderately common as an accessory. Rarely vesicular.

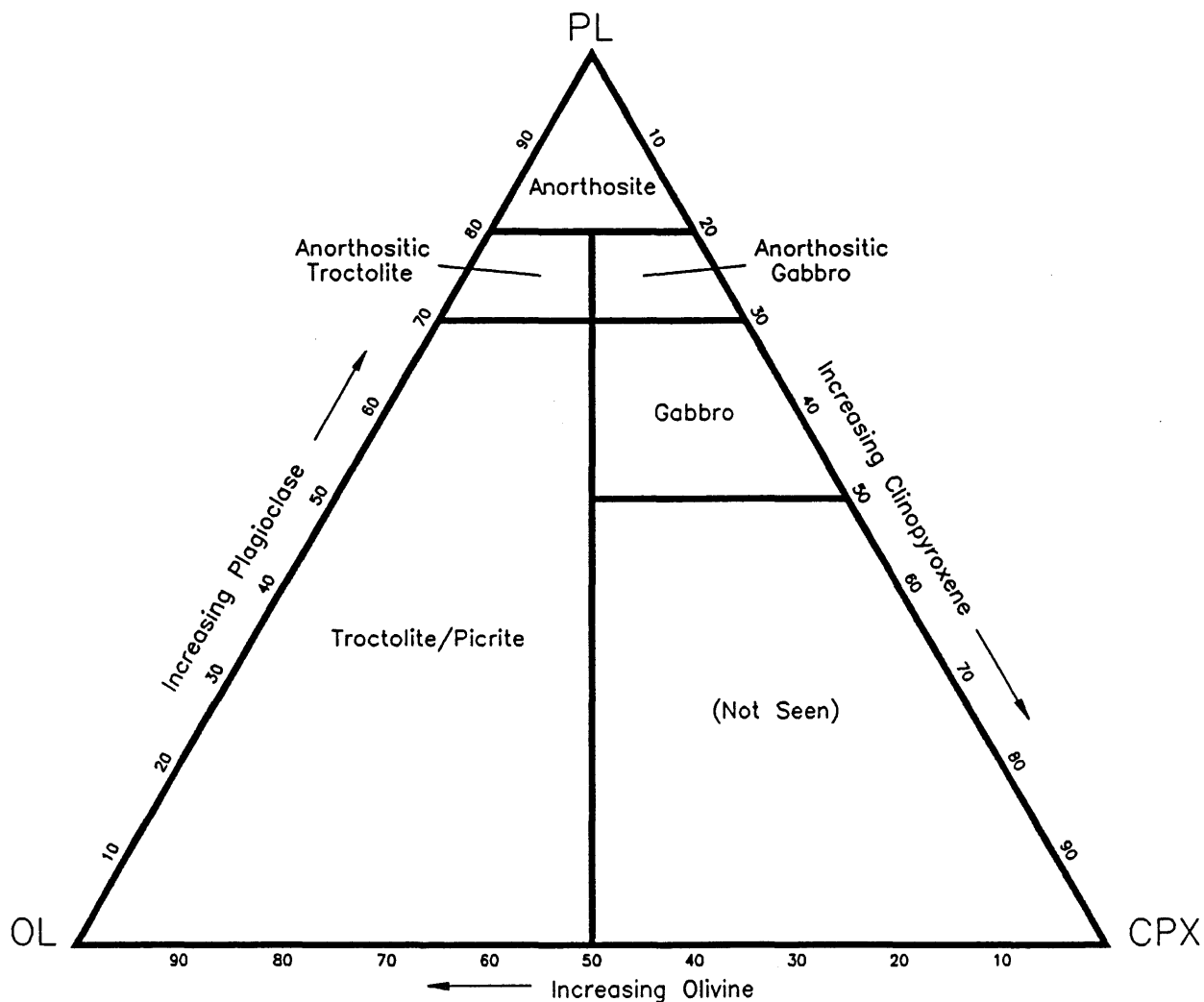


Figure 1. Simplified Rock Classification Diagram for Duluth Complex Pebbles. (after Phinney, 1972)

Finally, a few pebbles could not be confidently assigned to any of the above categories and were classed as "unknown". These were typically aphanitic, structureless rocks with no visible fabric, phenocrysts, clasts, etc.. Except for two samples of non-basal drift (21741, 21222) these never amounted to more than 2% of any sample counted, and most samples contained none.

Results of Pebble Counts

Appendix F gives the raw data from pebble identification of the 81 samples, and Appendix G presents the results in percentages.

Drift Pebble Assemblages

After examination of the pebbles, each sample was assigned to a category based on the relative abundances of the different lithologic types. These are briefly described in this section.

- A. Duluth Complex rocks dominant. Because there is a complete gradation between troctolitic anorthosite, anorthositic troctolite, and troctolite, there is some uncertainty in assigning samples with respect to these

dominant Duluth Complex lithologies. As a rule, "Anorthositic Gabbro" pebbles were generally included with "Anorthosite", and "Anorthositic Troctolite" pebbles were generally added to whichever was otherwise dominant, Troctolite or Anorthosite, for the final sample assignment.

1. Tr: Troctolitic: troctolitic and picritic rocks dominant
2. An: Anorthositic: anorthositic rocks dominant
3. MTA: a mixture of troctolitic and anorthositic pebbles, with troctolitic somewhat more abundant
4. TAR: dominantly troctolitic but with a large minority of Archean pebbles present
5. MAT: both anorthositic and troctolitic pebbles abundant, anorthositic dominant

B. Rocks of Duluth Complex not dominant; mixed provenance

1. MAr: Archean rocks most abundant (a plurality)
2. MAn: Archean, Animikie, and NSVG pebbles dominant but a significant representation (30-48%) of anorthositic rocks present
3. MV: Archean, Animikie, and especially Keweenawan volcanic rocks (NSVG) and red granites (granophyres) abundant. These samples also contain anorthositic pebbles as the most abundant Duluth Complex component, but fewer than in MAn samples.

Figures 2 through 8 illustrate pebble assemblages in representative samples.

Provenance of the Pebble Types

The Archean rocks in this drift could have come from anywhere in the Vermilion District in the footwall of the Duluth Complex, or its extension to the northeast into Canada. The closest source is the Giants Range batholith, about 14 km to the northwest of the study area, but most of the glacial transport (Hobbs, 1988) is thought to have come from the north or northeast. All metamorphic rocks would have been derived from a considerably greater distance to the NW, N, or NE. No pebbles were specifically identified as coming from the Giants Range or Saganaga batholiths.

The Animikie pebbles could not have come from the Virginia or Biwabik Formations because that would require ice movement from the southwest. They must instead have come from the Rove and Gunflint Formations, the nearest exposures of which are in the Gunflint Lake area about 75 km to the northeast of the study area. Even there, much of these formations is contact-metamorphosed by the basal Duluth Complex, so the (visibly) unmetamorphosed pebbles must have come from farther along strike to the east, perhaps twice that distance.

The NSVG pebbles, and Keweenawan diabase and red granites, must have been transported to this site from the east or southeast. The nearest significant zone of red felsic and intermediate plutonic rocks in a conceivable up-ice direction is exposed between 27 and 42 km to the ESE (Wanless Lookout area), E, and ENE (Grace Lake area), with others still farther to the E and ENE. There is however a broad region of covered bedrock closer than Wanless that may possibly be underlain by such rocks.

Keweenawan volcanic rocks must also have come from a considerable distance to the SE, E, or ESE, generally beyond the areas of granophyre outcrop mentioned above. The nearest known NSVG area is north of Dumbbell Lake (both rhyolites and basalts), about 20 km to the ESE of the study area, but most of the NSVG lies at distances of 35 to 135 km away.

The Keweenawan hornfels pebbles are not traceable to any particular source, but hornfels is especially abundant in the Complex near its base (e.g. 25 km to the north) and in its roof zone (e.g. 40 km to the ENE).

Some pebbles are of medium-grained, foliated and lineated cumulate olivine gabbro with prismatic pyroxenes, which strongly resembles the core of the Bald Eagle intrusion in the Gabbro Lake quadrangle adjoining the north side of the study area.

The troctolitic and anorthositic pebbles could be local but many could also have come from considerable distances to the NW, N, or NE (for troctolite) or from the N, NE, E, or SE (for anorthositic rocks).

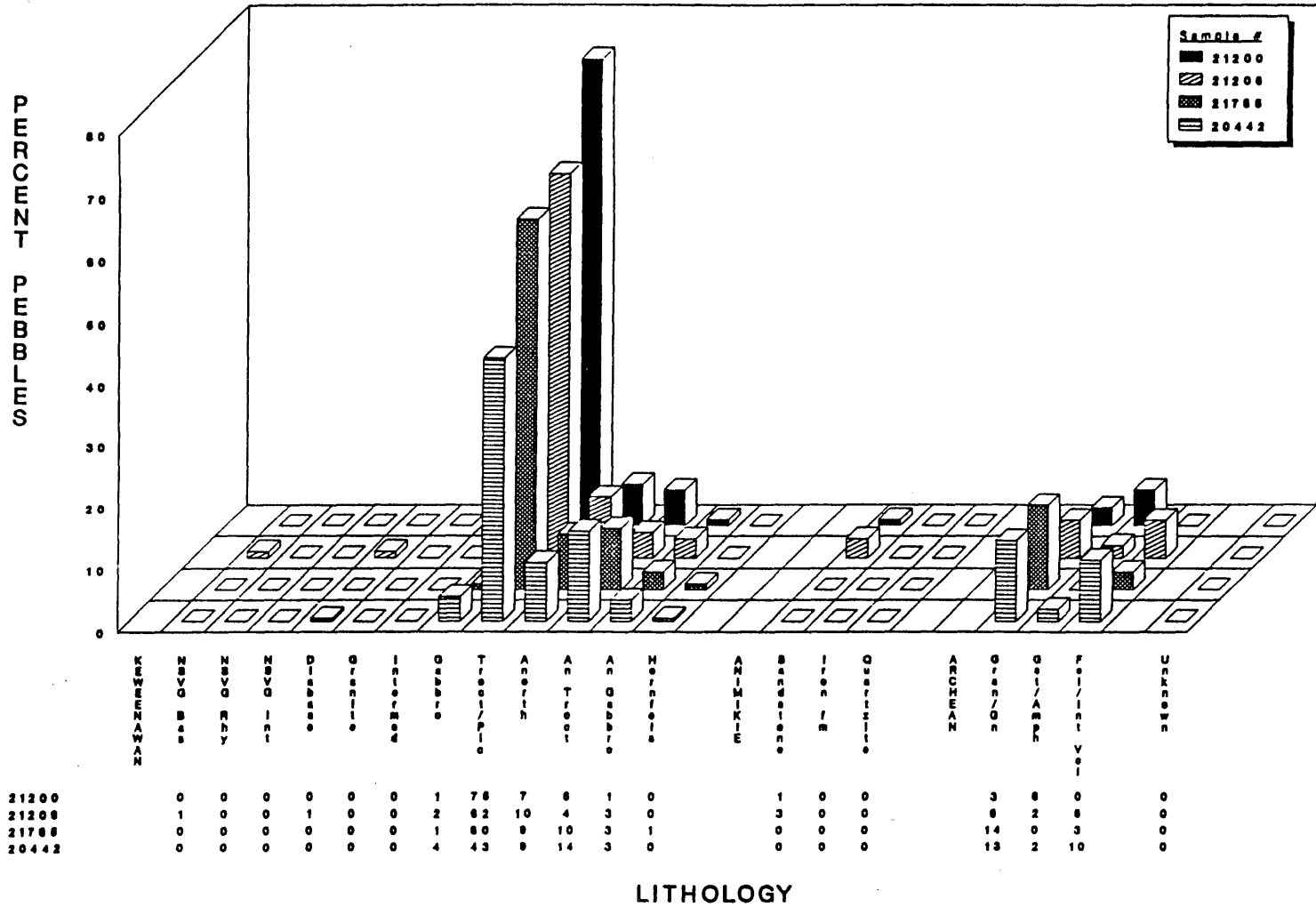


Figure 2. Bar Chart Showing Pebble Types of Representative Troctolitic (Tr) Assemblages

F-11

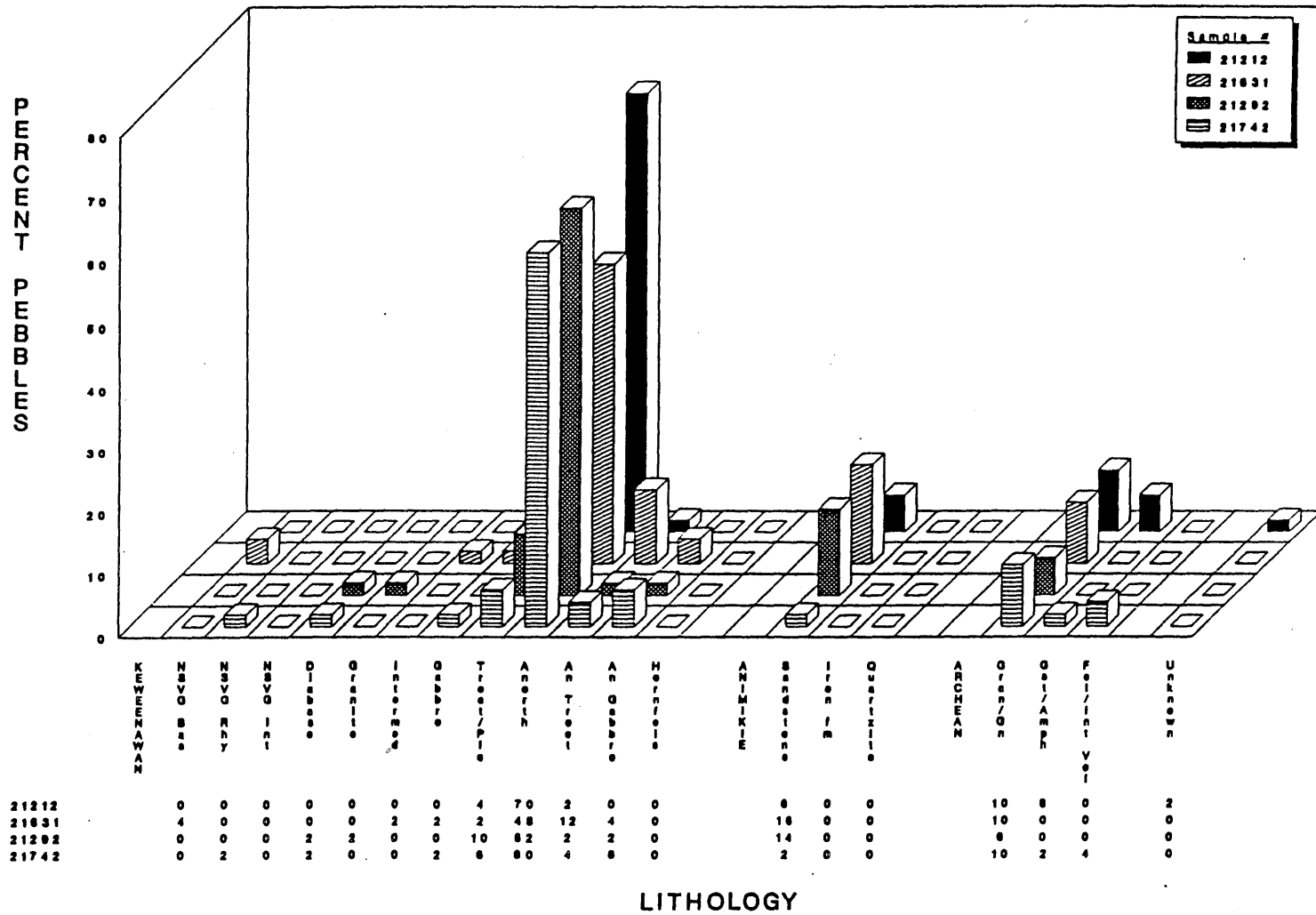


Figure 3. Bar Chart Showing Pebble Types of Representative Anorthositic (An) Assemblages

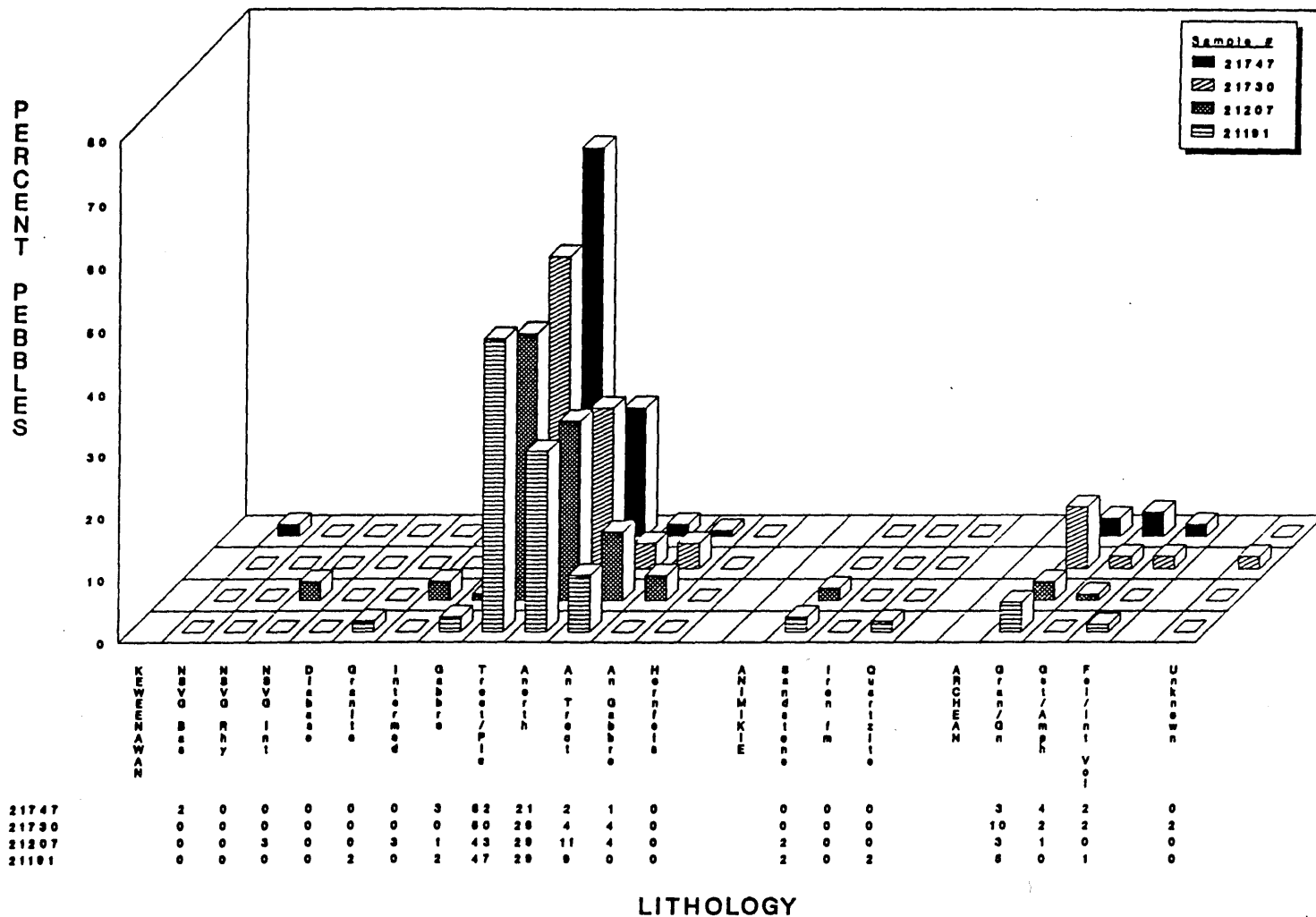


Figure 4. Bar Chart Showing Pebble Types of Representative Mixed Troctolite and Anorthosite (MTA) Assemblages

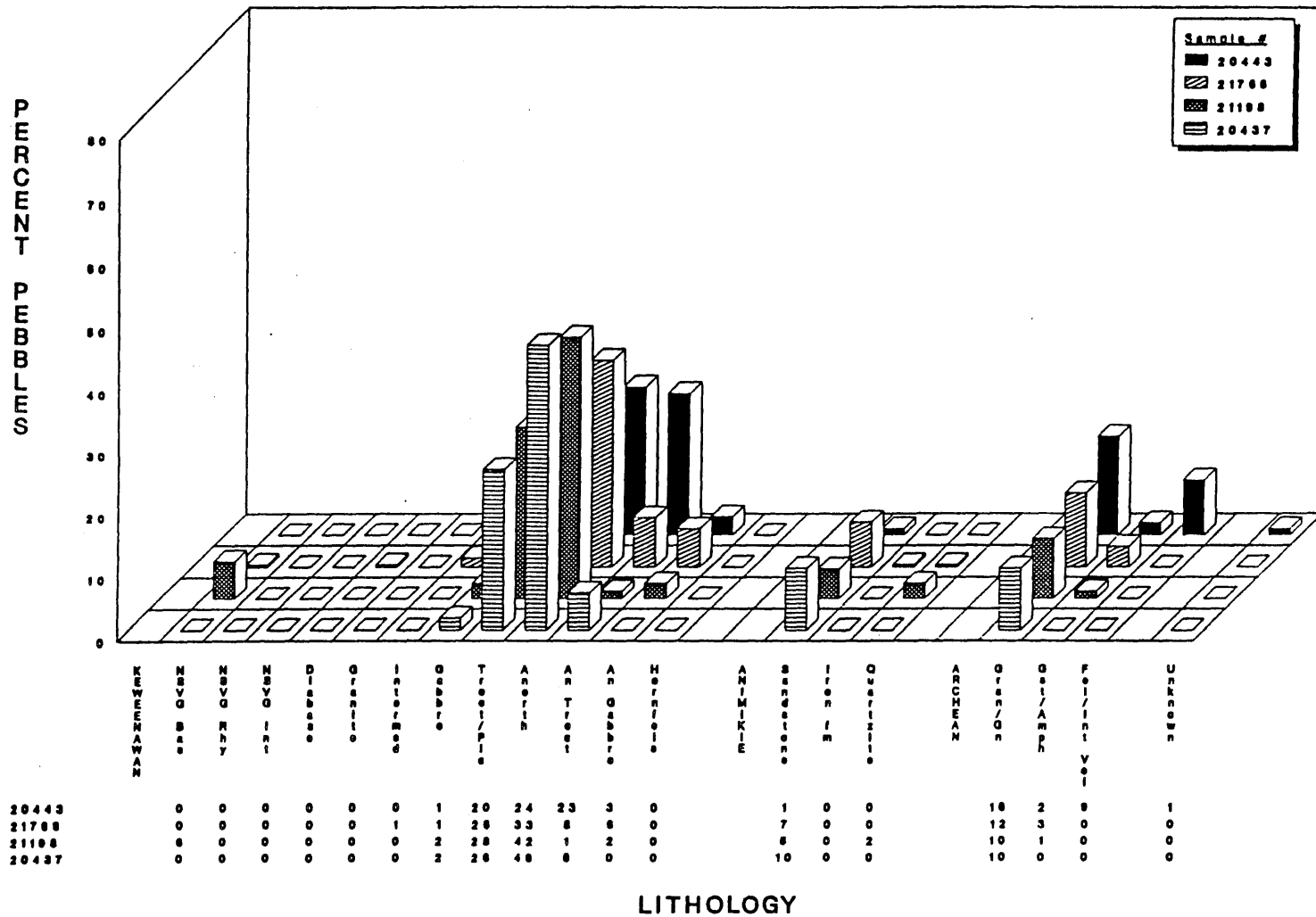


Figure 5. Bar Chart Showing Pebble Types of Representative Mixed Anorthosite and Troctolite (MAT) Assemblages

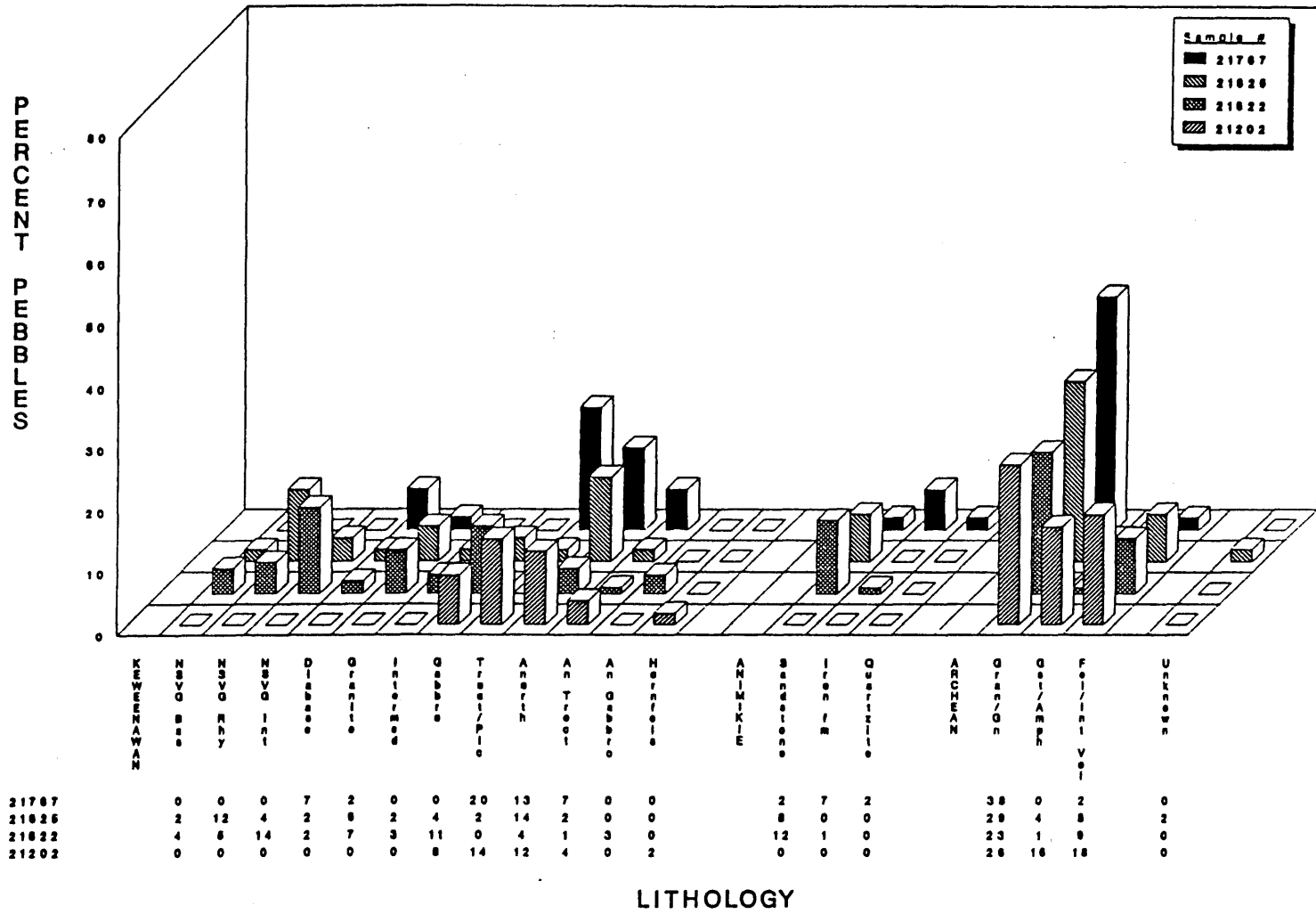


Figure 6. Bar Chart Showing Pebble Types of Representative Mixed Archean (MAr) Assemblages

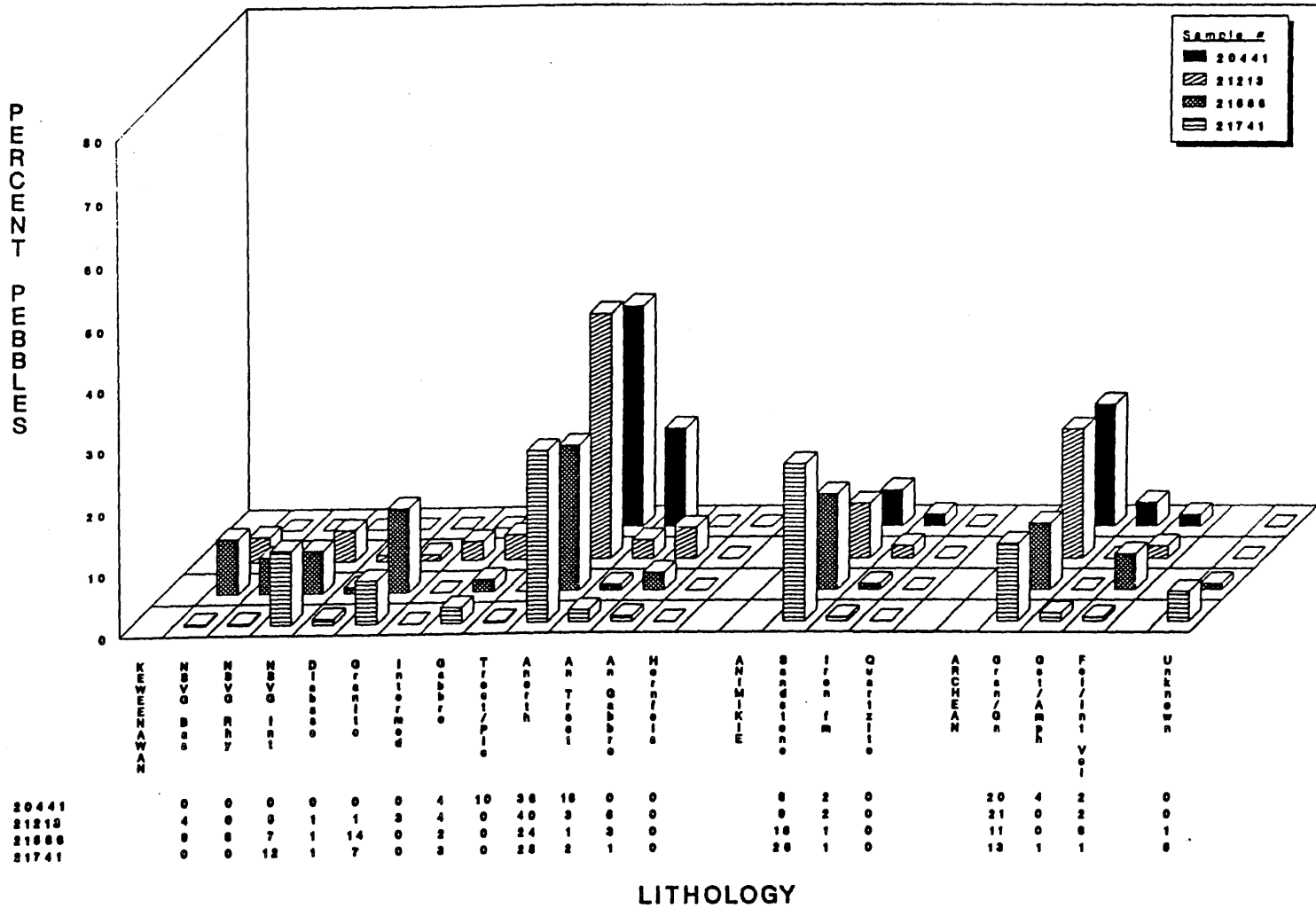


Figure 7. Bar Chart Showing Pebble Types of Representative Mixed Anorthosite (MA) Assemblages

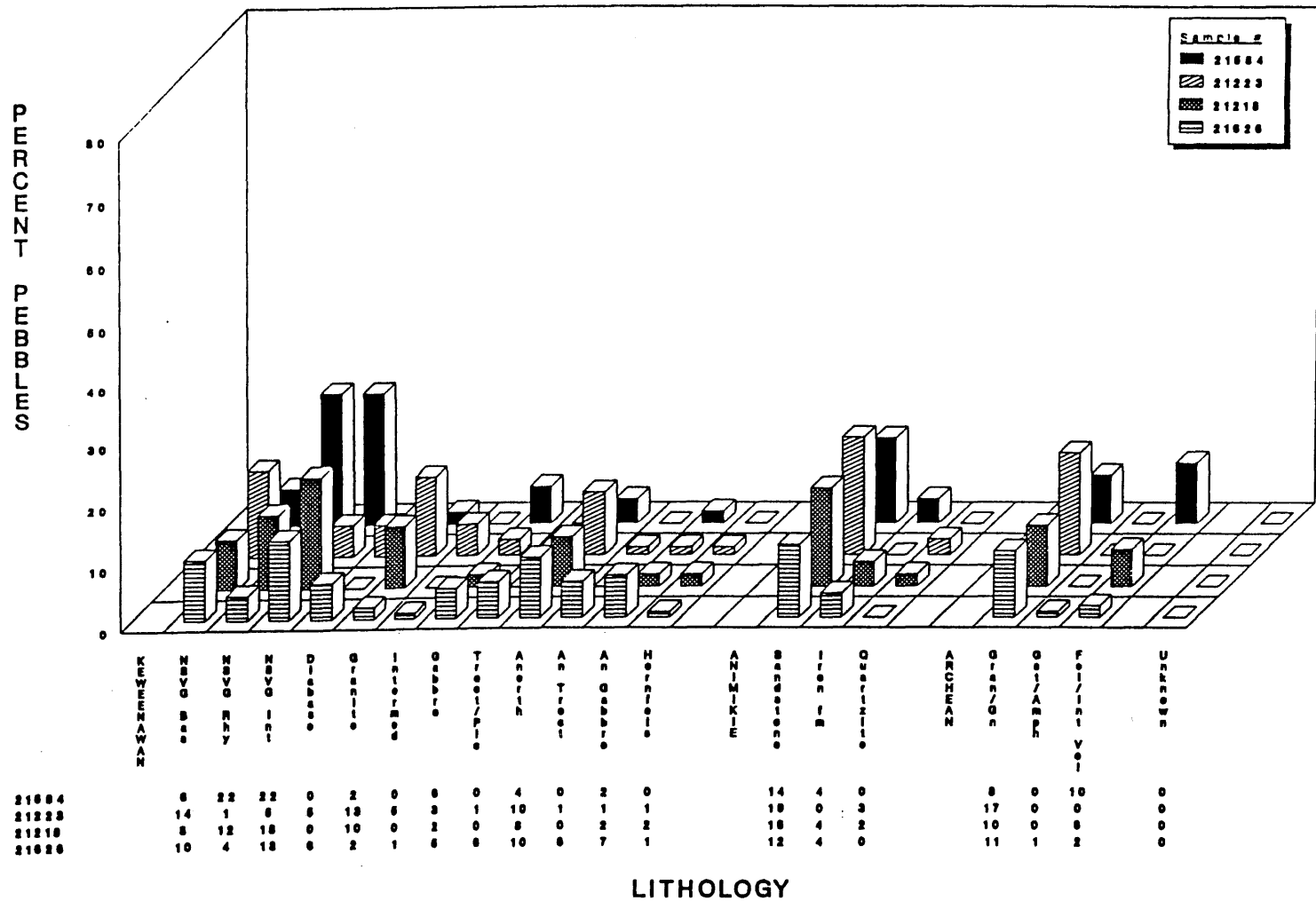


Figure 8. Bar Chart Showing Pebble Types of Representative Mixed Volcanic (MV) Assemblages

Conclusions

Glacial Drift Units

Roundness estimations of sample pebbles correspond fairly well with the glacial process units of Hobbs (1988), in that samples classed in the current study as dominantly subrounded fall in the areas mapped as outwash, ice-contact deposits (eskers, etc.) and to some extent, "reworked till". All "till" areas of Hobbs's map produced samples with angular to subangular pebbles prevalent. Most of the samples determined to consist predominantly of subrounded pebbles contained approximately the same lithologic assemblage as nearby samples consisting of more angular pebbles, implying that the provenance of the pebbles was local till. Others, however, especially in the western part of the area, contained a higher proportion of pebbles not derived from the local till: *e.g.*, Archean and anorthositic rocks. These samples are from units classed as ice-contact deposits by Hobbs, and are probably eskers with a more distant source up-ice.

No significant differences were seen among the remaining samples (till and reworked till): they all appeared to be dominated by angular to subangular pebbles and the same local pebble assemblage. Four such lithologic drift units are discernible. From east to west, they are a Mixed Volcanic unit, an Anorthositic unit, a Transition zone, and a Troctolitic unit (?).

The Mixed Volcanic unit occurs from the eastern edge of the area westward to the Little Isabella River (just east of U.S. Forest Service Road 386). It consists predominantly of MV with lesser MAn and MAr assemblages, and thus most of the pebbles must have been carried for a great distance from the SE, E, or ENE, probably by the Superior Lobe at least at some stage. (Hobbs's 1988 interpretation shows Superior Lobe outwash but not ice extending this far to the west.) Although this drift unit contains some anorthositic clasts, which could have been derived locally, it is predominantly the product of long-distance transport and may actually overlie a lower drift sheet that contains more of the local material. This unit is clearly not a "basal till" and is unreliable as a source of information on the character of local bedrock. However, despite the long transport distance, most of the samples do not contain a predominance of subrounded to rounded pebbles.

The Anorthositic unit extends from the Little Isabella River (Secs. 29,32) west to the eastern part of Sec. 25. It includes all the samples taken along USFS 386. All of the 18 samples but one in this unit have either anorthositic or MAn (mixed, with abundant anorthosite) assemblages. The percentage of NSVG, diabase and red granite pebbles decreases westward across this unit to a general range of 0 to 4%, for the remainder of the study area. The boundary between this drift unit and the Mixed Volcanic unit to the east is also a topographic break, and may represent an ice front position. Rock outcrops and a drill hole in the area of this drift unit are also anorthositic, and it appears that the dominant pebbles are locally derived. One sample, however (21210) is dominantly troctolitic. Assuming no mislabeling of the sample, its composition is not readily explainable.

A Transition zone unit occurs between the Anorthositic drift unit and the Troctolitic unit to the west, in Secs. 25, 35, and 36 (and possibly including sample 21730 at the south edge of Sec. 34). These samples are dominated by troctolite but several have significant percentages of anorthositic pebbles as well (MTA). Some pebbles in this zone are lithologically identifiable with the central olivine gabbro core of the Bald Eagle intrusion to the north). This drift unit was probably deposited by southward or SE-moving ice of the Rainy Lobe bringing troctolite and olivine gabbro debris over local anorthositic bedrock.

The Troctolitic drift unit occupies nearly the entire western half of the area. Although the great majority of samples are troctolite-dominated, several contain significant anorthosite (*e.g.* MTA) and a few contain a large Archean element (*e.g.* MAr, TAr) implying transport from the NW, N, or NE. NSVG pebbles are rare or absent. Some but not all of such anorthosite- and Archean-rich samples are from ice-contact deposits according to Hobbs (1988); see ?.

Bearing of this study on Ferderer's Aeromagnetic Interpretation

Ferderer (1989) used various methods of filtering and modeling of aeromagnetic data, combined with some gravity and density data, to arrive at an interpretation of the bedrock lithology and structure in this area. A portion of his map (?) includes several "pseudogeologic" rock units that were not discernible or resolvable in the present study. For instance, Ferderer mapped two anorthositic units in the eastern part of the area but neither

outcrops nor drift pebbles suggest the necessity for more than one anorthositic rock unit (although the outcrops at Jackpine Mountain may represent his "a1" unit).

The contact between the anorthositic and troctolitic rocks mapped in this project is closely parallel to that in Ferderer's interpretation, but slightly offset to the (north)west. The geologic contact is closely constrained by an outcrop in Sec. 35, T. 61 N., R. 10 W. and a drill hole (TH-5) in Sec. 24. This offset could indicate either a minor problem with the aeromagnetic modeling or that the troctolite/anorthosite contact dips gently to the southeast.

Ferderer also shows three "oxide-rich troctolitic and gabbroic" rock units of different magnetic signature in the southwestern part of the area; although there is a magnetic anomaly here, these rock units were not discerned in outcrop (which is scarce), drill core, or pebbles. His "gabbro" unit corresponds reasonably closely with the olivine gabbro core of the Bald Eagle Intrusion, but the troctolitic outer part of that intrusion is represented on Ferderer's map by two troctolitic units, not one. The southerly trend of his "tb2" troctolite unit suggests that the "Tx" troctolite unit mapped in the present study (on the basis of two drill cores) may be the southern extension of the Bald Eagle Intrusion. Our geologic evidence does not enable us to distinguish between Ferderer's four troctolitic units *ts*, *ts1*, *t*, and *tau*. The contact mapped between the SKt and Tx troctolites is poorly constrained geologically, and may actually correspond better with the contact between Ferderer's tb1 and t units.

Finally, no geologic evidence was seen for the NW-trending faults shown on the aeromagnetic interpretation in this area. Although there are some heavily serpentinized and locally sheared portions of some of the troctolite drill cores, these did not appear to coincide with displacement of rock types. This lack of definitive evidence does not imply that faults do not exist.

Evaluation of the Method

Pebble lithology was found in general to reflect underlying bedrock, and thus the method has some promise for use in more completely drift-covered areas. Even in the eastern part of the study area, where the drift is largely exotic, the few Duluth Complex clasts are nearly exclusively anorthositic, corresponding to the (inferred) underlying bedrock.

However, a few considerations, outlined below, act to lessen the usefulness of this method:

- a) Contacts between bedrock units in this area run generally N-S or NE-SW. This is also the inferred direction of transport by the various phases of the Rainy Lobe of the Late Wisconsinan ice sheet. Thus the drift lithology at any one point could have been derived from some distance (a few km) up-ice (though still within the Duluth Complex) without changing the composition. A better test of the method would involve a geologic contact at nearly a right angle to the (known) ice movement.
- b) Aside from the above consideration, knowing the direction of ice movement would be very useful in evaluating the results of such a clast analysis. In the present case, it became obvious that the eastern drift unit came from the Superior Lobe (from the E or SE) at some stage, but this was not known before the study was done. Even in the case of the Rainy Lobe drift, Hobbs's (1988) interpretation of the glacial history involves ice movement from the NW at one stage, as well as the dominant flow from the N or NNE. This further restricts the confidence of interpretations based on pebble types.
- c) If the drift sheet is too thick or overlies a separate, basal drift sheet from another advance or lobe, it will clearly not give information about local bedrock. The method should be used only where there is some indication as to drift thickness and stratigraphy.
- d) Detecting subtle differences in pebble lithology, perhaps to separate different troctolite units, etc., would be more challenging and would take a longer time per sample, but with practice could probably be done.

References

- Buchheit, R. L., Malmquist, K. L., and Niebuhr, J. R., 1989, Glacial Drift Geochemistry for Strategic Minerals; Duluth Complex, Lake County, Minnesota: Report 262, Minnesota Department of Natural Resources, Division of Minerals, Parts I, II.
- Ferderer, R. J., 1989, Aeromagnetic Data Interpretation for the McDougal Lakes Area, Duluth Complex, Lake County, Minnesota: Minnesota Department of Natural Resources, Division of Minerals, 18 p., map.
- Green, J. C., 1982, Two Harbors Sheet, Geologic Map of Minnesota: Minnesota Geological Survey, St. Paul.
- Green, J. C., Phinney, W. C., and Weiblen, P. W., 1966, Gabbro Lake Quadrangle, Lake County, Minnesota: Miscellaneous Map Series M-2, Minnesota Geological Survey, St. Paul.
- Hobbs, H. C., 1988, Glacial History of the Greenwood Lake, Isabella, and Cramer Quadrangles, Minnesota: Minnesota Geological Survey, St. Paul, 9 p., map.
- Morton, P., and Reichhoff, J., 1989, Analysis of opaque oxides in partial heavy mineral concentrates from glacial drift samples, Lake County, Minnesota, p. 53-78 in Buchheit et al., 1989 (see above).
- Phinney, W. C., 1972, Duluth Complex, History and Nomenclature, p. 333-334 in Sims, P. K. and Morey, G. B., eds., 1972, Geology of Minnesota, A Centennial Volume: Minnesota Geological Survey, Minneapolis.
- Venzke, E. A., 1990, Preliminary report on the magnetic properties of rock units in the Greenwood Lake area, Lake County, northeastern Minnesota: prepared for Minnesota Dept of Natural Resources, Division of Minerals.

Table 1: Basic Data for Drift Samples, Tomahawk Road Area

Sample Locations: Buchheit et al., 1989

Geologic Units

- Bedrock: Green, J. C., 1982
- Magnetic: Ferderer, R. J., 1989
- Glacial: Hobbs, H. C., 1988
- New Geology: Based on Green et al., 1966, and this study.

Sample	Location		Geologic Units				Dominant Lithologies
	S-T-R	Forty	Bedrock	Magnetic	Glacial	New Geol	
20437	31-61-10	NE-SW	dt	otg1	ri	SKt	Mixed Anorthosite/Troctolite
20438	31-61-10	SW-NE	dt	t	rt	SKt	Not Counted
20439	31-61-10	SE-NE	dt	t	rt	SKt	Not Counted
20440	30-61-10	SW-NE	dt	tau	ri	SKt	Mixed Troctolite/Anorthosite
20441	30-61-10	SW-NE	dt	tau	ri	SKt	Mixed Anorthosite
20442	30-61-10	SE-NW	dt	tau	rt	SKt	Troctolite
20443	30-61-10	SW-NW	dt	t/tau	rt	SKt	Mixed Anorthosite/Troctolite
21190	31-61-10	SE-NE	dt	t	ri	SKt	Not Counted
21191	32-61-10	SW-NW	dt	t	ri	SKt	Mixed Troctolite/Anorthosite
21192	32-61-10	SW-NE	dt	t	ra	SKt	Mixed Troctolite/Anorthosite
21193	32-61-10	SE-NE	dt	t	ra	SKt	Not Counted
21194	32-61-10	NE-NE	dt	tb1/t	ra	Tx	Troctolite
21195	28-61-10	SE-SW	dg	tb1	ra/rt	Tx	Troctolite
21196	28-61-10	SW-SE	dg	tb1	ri	Tx	Troctolite
21197	28-61-10	SE-SE	dg	tb1	ra	Tx	Troctolite
21198	28-61-10	NE-SE	dg	tb1	ra	BEt	Mixed Anorthosite/Troctolite
21199	27-61-10	NW-SW	dt	tb1/gb	ra	BEt	Troctolite
21200	27-61-10	SE-NW	dt	gb	ra	BEt	Troctolite
21201	27-61-10	NW-SE	dt	gb	ra	BEt	Troctolite
21202	26-61-10	SW-NW	dt	tb2	ra	BEt	Mixed Archean
21203	26-61-10	SE-NW	dt	tb2	ra	BEt	Troctolite
21204	26-61-10	SW-NE	dt	tb2	ri	BEt	Troctolite
21205	26-61-10	SE-NE	dt	tb2	ra	BEt/An	Troctolite
21206	25-61-10	SW-NW	da	tb2	ra	An	Troctolite
21207	25-61-10	SE-NW	da	a1	ra	An	Mixed Troctolite/Anorthosite
21208	25-61-10	SW-NE	da	a1	ra	An	Troctolite
21209	25-61-10	SE-NE	da	a1/a	ra	An	Anorthosite
21210	30-61-9	NE-NW	da	a1	ra	An	Troctolite
21211	30-61-9	NW-NE	da	a1	ra	An	Anorthosite
21212	30-61-9	NE-NE	da	a1/a	ra	An	Anorthosite
21213	30-61-9	SE-NE	da	a	ra	An	Mixed Anorthosite
21214	29-61-9	SW-NW	da	a	ra	An	Not Counted - Missing
21215	29-61-9	SW-NE	da	a	ra	An	Mixed Anorthosite
21216	29-61-9	SE-NE	da	a	rt	An	Not Counted - Missing
21217	29-61-9	SE-NE	da	a	rt	An	Mixed Volcanics
21218	28-61-9	SE-NW	da	a	ro	An	Mixed Volcanics
21219	28-61-9	SW-NE	da	a	ro	An	Mixed Volcanics
21220	28-61-9	NE-NE	da	a	rt	An	Mixed Anorthosite
21221	27-61-9	NW-NW	da	a	rt	An	Mixed Volcanics
21222	27-61-9	NE-NW	da	a	rt	An	Mixed Anorthosite
21223	27-61-9	NW-NE	da	a	rt	An	Mixed Volcanics
21224	27-61-9	NE-NE	da	a	rt	An	Not Counted
21264	22-61-9	SE-SW	da	a	rt	An	Not Counted
21265	22-61-9	NW-SE	da	a	rt	An	Anorthosite

Table 1: Basic Data for Drift Samples, Tomahawk Road Area (cont.)

Sample	Location		Geologic Units				Dominant Lithologies
	S-T-R	Forty	Bedrock	Magnetic	Glacial	New Geol	
21277	29-61-9	NE-NE	da	a	rt	An	Mixed Volcanics
21278	19-61-9	SW-SE	da	a	ra	An	Anorthosite
21279	19-61-9	NE-SE	da	a	ra	An	Anorthosite
21292	25-61-10	NE-NE	da	a1/a	ra	An	Anorthosite
21295	26-61-10	NW-NW	dt	tb2	ra	BEog	Troctolite
21296	23-61-10	SE-SW	dt	gb	ra	BEog	Not Counted
21301	27-61-10	SE-NW	dt	gb	ra	BEt	Mixed Troctolite/Anorthosite
21302	27-61-10	NE-NW	dt	gb/otg1	ra	BEt	Troctolite
21309	28-61-10	NW-SE	dg	tb1	ri	Tx	Troctolite
21310	28-61-10	SW-NE	dg	t/tb1	ri	BEt	Troctolite
21311	28-61-10	NW-NE	dg	t/tb1	ra	BEt	Not Counted - Missing
21581	27-61-9	NE-SW	da	a1	rt	An	Mixed Volcanics
21582	27-61-9	NE-SW	da	a1	rt	An	Not Counted
21583	27-61-9	SE-SW	da	tau	rt	An	Not Counted
21584	34-61-9	SE-NW	da	tau	rt/ro	An	Mixed Volcanics
21585	33-61-9	SE-NE	da	tau	rt	An	Not Counted
21586	27-61-9	SW-SW	da	tau	rt	An	Mixed Anorthosite
21619	32-61-9	NE-SW	da	tau	rt	An	Not Counted
21620	32-61-9	NW-SE	da	tau	rt	An	Mixed Volcanics
21621	32-61-9	SE-NE	da	tau	rt	An	Mixed Volcanics
21622	29-61-9	SE-SE	da	tau	rt	An	Mixed Archean
21623	28-61-9	NW-SW	da	a1	rt	An	Mixed Volcanics
21624	29-61-9	SE-NW	da	a	ra	An	Mixed Volcanics
21625	29-61-9	NW-SE	da	a/a1	ra	An	Mixed Archean
21626	29-61-9	SW-SE	da	a1	rt	An	Mixed Volcanics
21627	29-61-9	SW-NW	da	a	ra	An	Anorthosite
21628	29-61-9	NW-SW	da	a	ra	An	Mixed Anorthosite
21629	29-61-9	SW-SW	da	a1/a	ra	An	Anorthosite
21630	32-61-9	SE-SW	da	tau/a1	ra	An	Anorthosite
21631	32-61-9	NE-SW	da	tau	ra	An	Anorthosite
21730	34-61-10	SE-SW	dt	tb2	ra	Tx	Mixed Troctolite/Anorthosite
21736	32-61-10	SE-SE	dg	otg2	rt	SKt	Troctolite
21737	32-61-10	NE-SE	dt	t	rt	SKt	Not Counted
21738	30-61-9	SW-SE	da	a	ra	An	Mixed Anorthosite
21739	30-61-9	SE-NE	da	a1/a	ra	An	Mixed Anorthosite
21740	30-61-9	SW-NE	da	a1/a	ra	An	Anorthosite
21741	30-61-9	NE-SW	da	a1	ra	An	Mixed Anorthosite
21742	25-61-10	NE-SE	da	a1	ra	An	Anorthosite
21743	25-61-10	NW-SE	da	tau/a1	ra	An	Anorthosite
21744	25-61-10	NE-SW	da	a1	ra	An	Troctolite
21745	25-61-10	SW-SE	da	tau	ra	An	Troctolite
21746	36-61-10	SW-NE	da	tau	ra	An	Mixed Troctolite/Anorthosite
21747	25-61-10	NW-SW	da	a1	ra	An	Mixed Troctolite/Anorthosite
21748	35-61-10	NE-NE	da	a1	ra	An	Troctolite
21749	35-61-10	SE-NE	da	a1	ra	An	Not Counted
21750	35-61-10	NE-SE	da	a1	ra	An	Mixed Troctolite/Anorthosite
21751	25-61-10	NW-SW	da	tb2	ra	An	Troctolite
21752	26-61-10	SE-SE	dt	tb2	ra	An	Troctolite
21753	27-61-10	SW-SE	dt	tb2/tb1	ra	BEt	Troctolite/Archean
21764	29-61-10	NW-SW	dt	tau	rt	SKt	Troctolite
21765	29-61-10	SE-NW	dt	tau	rt	SKt	Troctolite
21766	29-61-10	NW-NE	dt	tau	ri	Tx	Mixed Anorthosite/Troctolite
21767	29-61-10	NE-NE	dt	t	ri	Tx	Mixed Archean

Table 2: Results of Duplicate Counts of Pebble Samples

Sample #	20442		21220		21766		21741	
	#1	#2	#1	#2	#1	#2	#1	#2
KEWEENAWAN								
NSVG Basalt	0.0	0.0	3.8	6.9	1.0	0.0	1.0	0.0
NSVG Rhyolite	0.0	0.0	3.8	6.9	0.0	0.0	1.0	0.0
NSVG Intermediate	0.0	0.0	11.4	10.9	0.0	0.0	13.0	11.5
K. Diabase	0.0	1.0	3.8	9.9	0.0	0.6	2.0	0.5
K. Red Granite	0.0	0.0	7.6	5.0	0.0	0.0	7.0	7.2
K. Intermediate	0.0	0.0	2.9	1.0	0.0	2.3	0.0	0.0
K. Gabbro	4.0	4.0	4.8	4.0	1.0	1.7	2.0	2.9
K. Troctolite/Picrite	43.0	42.6	0.0	0.0	27.0	25.0	1.0	0.0
K. Anorthosite	8.0	10.9	14.3	17.8	31.0	34.7	24.0	29.7
K. Anorth. Troctolite	16.0	12.9	1.0	0.0	9.0	7.4	3.0	1.4
K. Anorth. Gabbro	3.0	4.0	18.1	11.9	7.0	5.7	3.0	0.0
K. Hornfels	1.0	0.0	0.0	0.0	0.0	0.0	0.0	0.0
ANIMIKIE								
Sst/grwcke/argillite	4.0	0.0	17.1	15.8	8.0	6.8	22.0	27.3
Fe-Formation	2.0	0.0	1.0	1.0	0.0	0.6	2.0	0.0
Quartzite	0.0	0.0	1.0	0.0	1.0	0.0	0.0	0.0
ARCHEAN								
Granite & Gneiss	7.0	12.9	6.7	5.9	10.0	13.1	17.0	10.5
Gst & Amphibolite	4.0	2.0	1.0	0.0	5.0	2.3	1.0	1.4
Fel/Int vol & metased	7.0	9.9	1.9	3.0	0.0	0.0	1.0	0.5
Unknown	1.0	0.0	0.0	0.0	0.0	0.0	0.0	7.2
Total Pebbles Counted:	100	101	105	101	100	176	100	209
Dominant Lithology:	Tr	Tr	MAn	MAn	MAT	MAT	MAn	MAn

Sample #	21209		21586		21738		21747		21191	
	#1	#2	#1	#2	#1	#2	#1	#2	#1	#2
KEWEENAWAN										
NSVG Basalt	0.0	0.0	6.0	12.0	8.0	2.0	4.0	0.0	0.0	0.0
NSVG Rhyolite	0.0	0.0	8.0	4.0	8.0	24.0	0.0	0.0	0.0	0.0
NSVG Intermediate	0.0	0.0	4.0	10.0	12.0	6.0	0.0	0.0	0.0	0.0
K. Diabase	0.0	0.0	0.0	2.0	0.0	0.0	0.0	0.0	0.0	0.0
K. Red Granite	0.0	0.0	14.0	14.0	6.0	2.0	0.0	0.0	4.0	0.9
K. Intermediate	0.0	2.0	0.0	0.0	0.0	0.0	0.0	0.0	0.0	0.0
K. Gabbro	0.0	2.0	2.0	2.0	2.0	2.0	2.0	4.0	4.0	1.7
K. Troctolite/Picrite	20.0	8.0	0.0	0.0	2.0	0.0	60.0	64.0	48.0	47.0
K. Anorthosite	60.0	74.0	32.0	12.0	24.0	26.0	16.0	26.0	32.0	27.8
K. Anorth. Troctolite	8.0	8.0	0.0	2.0	2.0	4.0	4.0	0.0	10.0	8.7
K. Anorth. Gabbro	2.0	0.0	6.0	0.0	2.0	2.0	2.0	0.0	0.0	0.0
K. Hornfels	2.0	2.0	0.0	0.0	0.0	0.0	0.0	0.0	0.0	0.0
ANIMIKIE										
Sst/grwcke/argillite	0.0	0.0	12.0	20.0	4.0	6.0	0.0	0.0	2.0	2.6
Fe-Formation	0.0	0.0	2.0	0.0	4.0	6.0	0.0	0.0	0.0	0.0
Quartzite	2.0	0.0	0.0	0.0	0.0	0.0	0.0	0.0	0.0	2.6
ARCHEAN										
Granite & Gneiss	6.0	4.0	8.0	14.0	20.0	16.0	6.0	0.0	0.0	7.0
Gst & Amphibolite	0.0	0.0	0.0	0.0	0.0	0.0	6.0	2.0	0.0	0.0
Fel/Int vol & metased	0.0	0.0	4.0	8.0	4.0	2.0	0.0	4.0	0.0	1.7
Unknown	0.0	0.0	2.0	0.0	2.0	2.0	0.0	0.0	0.0	0.0
Total Pebbles Counted:	50	50	50	50	50	50	50	50	50	115
Dominant Lithology:	An	An	MAn	MAn	MAn	MAn	MTA	MTA	MTA	MTA

Table 3: Numerical Pebble Counts for the 81 Drift Samples

Sample #	20437	20440	20441	20442	20443	21191	21192	21194	21195	21196	21197	21198	21199	21200	21201
KEWEENAWAN															
NSVG Basalt												5			
NSVG Rhyolite															
NSVG Intermediate															
K. Diabase				1											
K. Red Granite						3							1		
K. Intermediate									1						
K. Gabbro	1		2	8	1	4				3		2	2	1	1
K. Troctolite/Picrite	13	17	5	86	20	78	38	39	34	74	30	23	98	75	39
K. Anorthosite	23	10	18	19	24	48	1	10	9	21	11	35	25	7	5
K. Anorth. Troctolite	3	6	8	29	23	15	2	3	4	2	3	1	2	6	1
K. Anorth. Gabbro				7	3			1	1			2		1	
K. Hornfels				1											
ANIMIKIE															
Sst/grwcke/argillite	5	1	3		1	4	2					4	3	1	
Fe-Formation			1												
Quartzite						3						2	1		
ARCHEAN															
Granite & Gneiss	5	13	10	26	16	8	6	3	1		4	8	4	3	2
Gst & Amphibolite		1	2	4	2		1					1	1	6	
Fel/Int vol & metased		2	1	20	9	2		4			2				2
Unknown					1										
Total Pebbles Counted:	50	50	50	201	100	165	50	60	50	100	50	83	137	100	50
Dominant Lithology:	MAT	MTA	MAn	Tr	MAT	MTA	MTA	Tr	Tr	Tr	Tr	MAT	Tr	Tr	Tr

Sample #	21202	21203	21204	21205	21206	21207	21208	21209	21210	21211	21212	21213	21215	21217	21218
KEWEENAWAN															
NSVG Basalt			2		1					3		4	6	9	4
NSVG Rhyolite													1	3	6
NSVG Intermediate		1				3						5	1	3	9
K. Diabase					1					1		1	1	2	
K. Red Granite		1										1	3	7	5
K. Intermediate						3	1	1		1		3		1	
K. Gabbro	4	4	1	1	2	1	1	1	1	1		4	1	6	1
K. Troctolite/Picrite	7	30	53	66	62	43	41	14	35	15	2		3		
K. Anorthosite	6	2	6	12	10	29	3	67	4	50	35	40	16	4	4
K. Anorth. Troctolite	2		4	15	4	11	3	8	2	6	1	3	1	1	
K. Anorth. Gabbro				2	3	4		1		1		5	2		1
K. Hornfels	1		1					2					1	1	1
ANIMIKIE															
Sst/grwcke/argillite			6	2	3	2			1	6	3	9	7	9	8
Fe-Formation												2			2
Quartzite			1	1				1						1	1
ARCHEAN															
Granite & Gneiss	13	6	4	1	6	3	1	5	3	14	5	21	5	5	5
Gst & Amphibolite	8	4			2	1			1	3	3				
Fel/Int vol & metased	9	5			6				3			2	3		3
Unknown											1			1	
Total Pebbles Counted:	50	53	78	100	100	100	50	100	50	101	50	100	51	50	50
Dominant Lithology:	MAR	Tr	Tr	Tr	Tr	MTA	Tr	An	Tr	An	An	MAn	MAn	MV	MV

Table 3: Numerical Pebble Counts for the 81 Drift Samples (cont.)

Sample #	21219	21220	21221	21222	21223	21265	21277	21278	21279	21292	21295	21301	21302	21309	21310
KEWEENAWAN															
NSVG Basalt	7	11	24	3	11	1	7				2		1		
NSVG Rhyolite	3	11	13	2	1		19							1	
NSVG Intermediate	2	23	12	2	4	3	13					1			
K. Diabase		14	9		4		1			1					1
K. Red Granite	6	13	8	6	10	3	14			1					
K. Intermediate	2	4	3	1	4	1	5				1				
K. Gabbro	2	9		3	2	1	1	1			2	3	1		
K. Troctolite/Picrite	2		1	1	1	7		1		5	57	31	38	32	60
K. Anorthosite	8	33	12	9	8	22	6	30	35	31	15	13	8	10	22
K. Anorth. Troctolite	2	1	1	2	1			3		1	9	1	1	1	6
K. Anorth. Gabbro	1	31	2		1		1			1					2
K. Hornfels				1	1										
ANIMIKIE															
Sst/grwcke/argillite	6	34	33	14	15	8	15	1	6	7	8		2		3
Fe-Formation	1	2	4					3	1						
Quartzite		1			2										2
ARCHEAN															
Granite & Gneiss	4	13	13	4	13	4	11	7	8	3	2	1	6	3	3
Gst & Amphibolite	2	1	4				1	1			4		1		1
Fel/Int vol & metased	2	5	8				6	6	1				4	3	
Unknown			2	2			1								
Total Pebbles Counted:	50	206	149	50	78	50	104	51	50	50	100	50	62	50	100
Dominant Lithology:	MV	MAn	MV	MAn	MV	An	MV	An	An	An	Tr	MTA	Tr	Tr	Tr

Sample #	21581	21584	21586	21620	21621	21622	21623	21624	21625	21626	21627	21628	21629	21630	21631
KEWEENAWAN															
NSVG Basalt	6	3	9	6	5	4	11	10	1	10	1	1	1		2
NSVG Rhyolite	7	11	6	4	8	5	6	15	6	4		2	1	2	
NSVG Intermediate	4	11	7	6	2	14	21	12	2	13		6		5	
K. Diabase			1		1	2	1	4	1	6	2	2			
K. Red Granite	2	1	14	2	4	7	3	13	3	2	1	4	3		
K. Intermediate				1		3	2	2	1	1		1			1
K. Gabbro	1	3	2	5		11	2	22	2	5	2				1
K. Troctolite/Picrite	1				1		1		1	6	1		1	1	1
K. Anorthosite	7	2	24	5	9	4	3	4	7	10	24	12	26	20	24
K. Anorth. Troctolite	3		1			1			1	6	3	2	3	1	6
K. Anorth. Gabbro	1	1	3	1		3	2			7	1	4	3	2	2
K. Hornfels							1			1	4		1		
ANIMIKIE															
Sst/grwcke/argillite	8	7	16	11	10	12	7	16	4	12		11	3	3	8
Fe-Formation	1	2	1			1	4	2		4				1	
Quartzite												3			
ARCHEAN															
Granite & Gneiss	3	4	11	7	10	23	20	5	15	11	6	7	7	10	5
Gst & Amphibolite	1				1	1	1	1	2	1	2			1	
Fel/Int vol & metased	5	5	6	2		9	14	14	4	2	2		1	4	
Unknown			1				2		1		1			1	
Total Pebbles Counted:	50	50	102	50	51	100	101	120	51	101	50	55	50	51	50
Dominant Lithology:	MV	MV	MAn	MV	MV	MAn	MV	MV	MAn	MV	An	MAn	An	An	An

Table 3: Numerical Pebble Counts for the 81 Drift Samples (cont.)

Sample #	21730	21736	21738	21739	21740	21741	21742	21743	21744	21745	21746	21747	21748	21750	21751
KEWEENAWAN															
NSVG Basalt			5	5		1						2	1		
NSVG Rhyolite			16	4	1	1	1						1		
NSVG Intermediate			9	5		37							1		
K. Diabase				1		3	1								
K. Red Granite			4	4	2	22									
K. Intermediate				2									1		
K. Gabbro		1	2	5		8	1		1		1	3	3	2	
K. Troctolite/Picrite	25	112	1	2		1	3	2	41	75	25	62	26	28	49
K. Anorthosite	13	23	25	25	22	86	30	47	3	9	20	21	4	10	
K. Anorth. Troctolite	2	7	3	2	1	6	2	1	2	2		2	2	4	1
K. Anorth. Gabbro	2		2	9	4	3	3			2		1			
K. Hornfels				2	1					1				1	
ANIMIKIE															
Sst/grwcke/argillite			5	11	4	79	1		2				1	1	
Fe-Formation			5	1	2	2							1		
Quartzite															
ARCHEAN															
Granite & Gneiss	5	5	18	16	11	39	5		1	2	3	3	4	1	
Gst & Amphibolite	1	6		4		4	1					4	2		
Fel/Int vol & metased	1		3	3	5	2	2				8	2	4	3	
Unknown	1		2	1	1	15									
Total Pebbles Counted:	50	154	100	102	54	309	50	50	50	91	57	100	51	50	50
Dominant Lithology:	MTA	Tr	MAAn	MAAn	An	MAAn	An	An	Tr	Tr	MTA	MTA	Tr	MTA	Tr

Sample #	21752	21753	21764	21765	21766	21767
KEWEENAWAN						
NSVG Basalt	1				1	
NSVG Rhyolite						
NSVG Intermediate						
K. Diabase				1	3	
K. Red Granite					1	
K. Intermediate				4		
K. Gabbro		2	7	1	4	
K. Troctolite/Picrite	40	25	45	61	71	9
K. Anorthosite	2	3	14	9	92	6
K. Anorth. Troctolite	3	2	8	10	22	3
K. Anorth. Gabbro		1	4	3	17	
K. Hornfels				1		
ANIMIKIE						
Sst/grwcke/argillite	1	1	1		20	1
Fe-Formation			1		1	3
Quartzite					1	1
ARCHEAN						
Granite & Gneiss	2	9	15	14	33	17
Gst & Amphibolite	1	2			9	
Fel/Int vol & metased		5	5	3		1
Unknown						
Total Pebbles Counted:	50	50	100	102	276	45
Dominant Lithology:	Tr	TAr	Tr	Tr	MAT	MAr

Table 4: Results of the Pebble Counts, in Percent

Sample #	20437	20440	20441	20442	20443	21191	21192	21194	21195	21196	21197	21198	21199	21200	21201
KEWEENAWAN															
NSVG Basalt	0.0	0.0	0.0	0.0	0.0	0.0	0.0	0.0	0.0	0.0	0.0	6.0	0.0	0.0	0.0
NSVG Rhyolite	0.0	0.0	0.0	0.0	0.0	0.0	0.0	0.0	0.0	0.0	0.0	0.0	0.0	0.0	0.0
NSVG Intermediate	0.0	0.0	0.0	0.0	0.0	0.0	0.0	0.0	0.0	0.0	0.0	0.0	0.0	0.0	0.0
K. Diabase	0.0	0.0	0.0	0.5	0.0	0.0	0.0	0.0	0.0	0.0	0.0	0.0	0.0	0.0	0.0
K. Red Granite	0.0	0.0	0.0	0.0	0.0	1.8	0.0	0.0	0.0	0.0	0.0	0.0	0.7	0.0	0.0
K. Intermediate	0.0	0.0	0.0	0.0	0.0	0.0	0.0	0.0	2.0	0.0	0.0	0.0	0.0	0.0	0.0
K. Gabbro	2.0	0.0	4.0	4.0	1.0	2.4	0.0	0.0	0.0	3.0	0.0	2.4	1.5	1.0	2.0
K. Troctolite/Picrite	26.0	34.0	10.0	42.8	20.0	47.3	76.0	65.0	68.0	74.0	60.0	27.7	71.5	75.0	78.0
K. Anorthosite	46.0	20.0	36.0	9.5	24.0	29.1	2.0	16.7	18.0	21.0	22.0	42.2	18.2	7.0	10.0
K. Anorth. Troctolite	6.0	12.0	16.0	14.4	23.0	9.1	4.0	5.0	8.0	2.0	6.0	1.2	1.5	6.0	2.0
K. Anorth. Gabbro	0.0	0.0	0.0	3.5	3.0	0.0	0.0	1.7	2.0	0.0	0.0	2.4	0.0	1.0	0.0
K. Hornfels	0.0	0.0	0.0	0.5	0.0	0.0	0.0	0.0	0.0	0.0	0.0	0.0	0.0	0.0	0.0
ANIMIKIE															
Sst/grwcke/argillite	10.0	2.0	6.0	0.0	1.0	2.4	4.0	0.0	0.0	0.0	0.0	4.8	2.2	1.0	0.0
Fe-Formation	0.0	0.0	2.0	0.0	0.0	0.0	0.0	0.0	0.0	0.0	0.0	0.0	0.0	0.0	0.0
Quartzite	0.0	0.0	0.0	0.0	0.0	1.8	0.0	0.0	0.0	0.0	0.0	2.4	0.7	0.0	0.0
ARCHEAN															
Granite & Gneiss	10.0	26.0	20.0	12.9	16.0	4.8	12.0	5.0	2.0	0.0	8.0	9.6	2.9	3.0	4.0
Gst & Amphibolite	0.0	2.0	4.0	2.0	2.0	0.0	2.0	0.0	0.0	0.0	0.0	1.2	0.7	6.0	0.0
Fel/Int vol & metased	0.0	4.0	2.0	10.0	9.0	1.2	0.0	6.7	0.0	0.0	4.0	0.0	0.0	0.0	4.0
Unknown	0.0	0.0	0.0	0.0	1.0	0.0	0.0	0.0	0.0	0.0	0.0	0.0	0.0	0.0	0.0
Total Pebbles Counted:	50	50	50	201	100	165	50	60	50	100	50	83	137	100	50
Dominant Lithology:	MAT	MTA	MAAn	Tr	MAT	MTA	MTA	Tr	Tr	Tr	Tr	MAT	Tr	Tr	Tr

Sample #	21202	21203	21204	21205	21206	21207	21208	21209	21210	21211	21212	21213	21215	21217	21218
KEWEENAWAN															
NSVG Basalt	0.0	0.0	2.6	0.0	1.0	0.0	0.0	0.0	0.0	3.0	0.0	4.0	11.8	18.0	8.0
NSVG Rhyolite	0.0	0.0	0.0	0.0	0.0	0.0	0.0	0.0	0.0	0.0	0.0	0.0	2.0	0.0	12.0
NSVG Intermediate	0.0	1.9	0.0	0.0	0.0	3.0	0.0	0.0	0.0	0.0	0.0	5.0	2.0	6.0	18.0
K. Diabase	0.0	0.0	0.0	0.0	1.0	0.0	0.0	0.0	0.0	1.0	0.0	1.0	2.0	4.0	0.0
K. Red Granite	0.0	1.9	0.0	0.0	0.0	0.0	0.0	0.0	0.0	0.0	0.0	1.0	5.9	14.0	10.0
K. Intermediate	0.0	0.0	0.0	0.0	0.0	3.0	2.0	1.0	0.0	1.0	0.0	3.0	0.0	2.0	0.0
K. Gabbro	8.0	7.5	1.3	1.0	2.0	1.0	2.0	1.0	2.0	1.0	0.0	4.0	2.0	12.0	2.0
K. Troctolite/Picrite	14.0	56.6	67.9	66.0	62.0	43.0	82.0	14.0	70.0	14.9	4.0	0.0	5.9	0.0	0.0
K. Anorthosite	12.0	3.8	7.7	12.0	10.0	29.0	6.0	67.0	8.0	49.5	70.0	40.0	31.4	8.0	8.0
K. Anorth. Troctolite	4.0	0.0	5.1	15.0	4.0	11.0	6.0	8.0	4.0	5.9	2.0	3.0	2.0	2.0	0.0
K. Anorth. Gabbro	0.0	0.0	0.0	2.0	3.0	4.0	0.0	1.0	0.0	1.0	0.0	5.0	3.9	0.0	2.0
K. Hornfels	2.0	0.0	1.3	0.0	0.0	0.0	0.0	2.0	0.0	0.0	0.0	0.0	2.0	2.0	2.0
ANIMIKIE															
Sst/grwcke/argillite	0.0	0.0	7.7	2.0	3.0	2.0	0.0	0.0	2.0	5.9	6.0	9.0	13.7	18.0	16.0
Fe-Formation	0.0	0.0	0.0	0.0	0.0	0.0	0.0	0.0	0.0	0.0	0.0	2.0	0.0	0.0	4.0
Quartzite	0.0	0.0	1.3	1.0	0.0	0.0	0.0	1.0	0.0	0.0	0.0	0.0	0.0	2.0	2.0
ARCHEAN															
Granite & Gneiss	26.0	11.3	5.1	1.0	6.0	3.0	2.0	5.0	6.0	13.9	10.0	21.0	9.8	10.0	10.0
Gst & Amphibolite	16.0	7.5	0.0	0.0	2.0	1.0	0.0	0.0	2.0	3.0	6.0	0.0	0.0	0.0	0.0
Fel/Int vol & metased	18.0	9.4	0.0	0.0	6.0	0.0	0.0	0.0	6.0	0.0	0.0	2.0	5.9	0.0	6.0
Unknown	0.0	0.0	0.0	0.0	0.0	0.0	0.0	0.0	0.0	0.0	2.0	0.0	0.0	2.0	0.0
Total Pebbles Counted:	50	53	78	100	100	100	50	100	50	101	50	100	51	50	50
Dominant Lithology:	MAR	Tr	Tr	Tr	Tr	MTA	Tr	An	Tr	An	An	MAAn	MAAn	MV	MV

Table 4: Results of the Pebble Counts, in Percent (cont.)

Sample #	21219	21220	21221	21222	21223	21265	21277	21278	21279	21292	21295	21301	21302	21309	21310
KEWEENAWAN															
NSVG Basalt	14.0	5.3	16.1	6.0	14.1	2.0	6.7	0.0	0.0	0.0	2.0	0.0	1.6	0.0	0.0
NSVG Rhyolite	6.0	5.3	8.7	4.0	1.3	0.0	18.3	0.0	0.0	0.0	0.0	0.0	0.0	2.0	0.0
NSVG Intermediate	4.0	11.2	8.1	4.0	5.1	6.0	12.5	0.0	0.0	0.0	0.0	2.0	0.0	0.0	0.0
K. Diabase	0.0	6.8	6.0	0.0	5.1	0.0	1.0	0.0	0.0	2.0	0.0	0.0	0.0	0.0	1.0
K. Red Granite	12.0	6.3	5.4	12.0	12.8	6.0	13.5	0.0	0.0	2.0	0.0	0.0	0.0	0.0	0.0
K. Intermediate	4.0	1.9	2.0	2.0	5.1	2.0	4.8	0.0	0.0	0.0	1.0	0.0	0.0	0.0	0.0
K. Gabbro	4.0	4.4	0.0	6.0	2.6	2.0	1.0	2.0	0.0	0.0	2.0	6.0	1.6	0.0	0.0
K. Troctolite/Picrite	4.0	0.0	0.7	2.0	1.3	14.0	0.0	2.0	0.0	10.0	57.0	62.0	61.3	64.0	60.0
K. Anorthosite	16.0	16.0	8.1	18.0	10.3	44.0	5.8	58.8	70.0	62.0	15.0	26.0	12.9	20.0	22.0
K. Anorth. Troctolite	4.0	0.5	0.7	4.0	1.3	0.0	0.0	5.9	0.0	2.0	9.0	2.0	1.6	2.0	6.0
K. Anorth. Gabbro	2.0	15.0	1.3	0.0	1.3	0.0	1.0	0.0	0.0	2.0	0.0	0.0	0.0	0.0	2.0
K. Hornfels	0.0	0.0	0.0	2.0	1.3	0.0	0.0	0.0	0.0	0.0	0.0	0.0	0.0	0.0	0.0
ANIMIKIE															
Sst/grwcke/argillite	12.0	16.5	22.1	28.0	19.2	16.0	14.4	2.0	12.0	14.0	8.0	0.0	3.2	0.0	3.0
Fe-Formation	2.0	1.0	2.7	0.0	0.0	0.0	2.9	2.0	0.0	0.0	0.0	0.0	0.0	0.0	0.0
Quartzite	0.0	0.5	0.0	0.0	2.6	0.0	0.0	0.0	0.0	0.0	0.0	0.0	0.0	0.0	2.0
ARCHEAN															
Granite & Gneiss	8.0	6.3	8.7	8.0	16.7	8.0	10.6	13.7	16.0	6.0	2.0	2.0	9.7	6.0	3.0
Gst & Amphibolite	4.0	0.5	2.7	0.0	0.0	0.0	1.0	2.0	0.0	0.0	4.0	0.0	1.6	0.0	1.0
Fel/Int vol & metased	4.0	2.4	5.4	0.0	0.0	0.0	5.8	11.8	2.0	0.0	0.0	0.0	6.5	6.0	0.0
Unknown	0.0	0.0	1.3	4.0	0.0	0.0	1.0	0.0	0.0	0.0	0.0	0.0	0.0	0.0	0.0
Total Pebbles Counted:	50	206	149	50	78	50	104	51	50	50	100	50	62	50	100
Dominant Lithology:	MV	MAAn	MV	MAAn	MV	An	MV	An	An	An	Tr	MTA	Tr	Tr	Tr

Sample #	21581	21584	21586	21620	21621	21622	21623	21624	21625	21626	21627	21628	21629	21630	21631
KEWEENAWAN															
NSVG Basalt	12.0	6.0	8.8	12.0	9.8	4.0	10.9	8.3	2.0	9.9	2.0	1.8	2.0	0.0	4.0
NSVG Rhyolite	14.0	22.0	5.9	8.0	15.7	5.0	5.9	12.5	11.8	4.0	0.0	3.6	2.0	3.9	0.0
NSVG Intermediate	8.0	22.0	6.9	12.0	3.9	14.0	20.8	10.0	3.9	12.9	0.0	10.9	0.0	9.8	0.0
K. Diabase	0.0	0.0	1.0	0.0	2.0	2.0	1.0	3.3	2.0	5.9	4.0	3.6	0.0	0.0	0.0
K. Red Granite	4.0	2.0	13.7	4.0	7.8	7.0	3.0	10.8	5.9	2.0	2.0	7.3	6.0	0.0	0.0
K. Intermediate	0.0	0.0	0.0	2.0	0.0	3.0	2.0	1.7	2.0	1.0	0.0	1.8	0.0	0.0	2.0
K. Gabbro	2.0	6.0	2.0	10.0	0.0	11.0	2.0	18.3	3.9	5.0	4.0	0.0	0.0	0.0	2.0
K. Troctolite/Picrite	2.0	0.0	0.0	0.0	2.0	0.0	1.0	0.0	2.0	5.9	2.0	0.0	2.0	2.0	2.0
K. Anorthosite	14.0	4.0	23.5	10.0	17.6	4.0	3.0	3.3	13.7	9.9	48.0	21.8	52.0	39.2	48.0
K. Anorth. Troctolite	6.0	0.0	1.0	0.0	0.0	1.0	0.0	0.0	2.0	5.9	6.0	3.6	6.0	2.0	12.0
K. Anorth. Gabbro	2.0	2.0	2.9	2.0	0.0	3.0	2.0	0.0	0.0	6.9	2.0	7.3	6.0	3.9	4.0
K. Hornfels	0.0	0.0	0.0	0.0	0.0	0.0	1.0	0.0	0.0	1.0	8.0	0.0	2.0	0.0	0.0
ANIMIKIE															
Sst/grwcke/argillite	16.0	14.0	15.7	22.0	19.6	12.0	6.9	13.3	7.8	11.9	0.0	20.0	6.0	5.9	16.0
Fe-Formation	2.0	4.0	1.0	0.0	0.0	1.0	4.0	1.7	0.0	4.0	0.0	0.0	0.0	2.0	0.0
Quartzite	0.0	0.0	0.0	0.0	0.0	0.0	0.0	0.0	0.0	0.0	0.0	5.5	0.0	0.0	0.0
ARCHEAN															
Granite & Gneiss	6.0	8.0	10.8	14.0	19.6	23.0	19.8	4.2	29.4	10.9	12.0	12.7	14.0	19.6	10.0
Gst & Amphibolite	2.0	0.0	0.0	0.0	2.0	1.0	1.0	0.8	3.9	1.0	4.0	0.0	0.0	2.0	0.0
Fel/Int vol & metased	10.0	10.0	5.9	4.0	0.0	9.0	13.9	11.7	7.8	2.0	4.0	0.0	2.0	7.8	0.0
Unknown	0.0	0.0	1.0	0.0	0.0	0.0	2.0	0.0	2.0	0.0	2.0	0.0	0.0	2.0	0.0
Total Pebbles Counted:	50	50	102	50	51	100	101	120	51	101	50	55	50	51	50
Dominant Lithology:	MV	MV	MAAn	MV	MV	MAr	MV	MV	MAr	MV	An	MAAn	An	An	An

Table 4: Results of the Pebble Counts, in Percent (cont.)

Sample #	21730	21736	21738	21739	21740	21741	21742	21743	21744	21745	21746	21747	21748	21750	21751
KEWEENAWAN															
NSVG Basalt	0.0	0.0	5.0	4.9	0.0	0.3	0.0	0.0	0.0	0.0	0.0	2.0	2.0	0.0	0.0
NSVG Rhyolite	0.0	0.0	16.0	3.9	1.9	0.3	2.0	0.0	0.0	0.0	0.0	0.0	2.0	0.0	0.0
NSVG Intermediate	0.0	0.0	9.0	4.9	0.0	12.0	0.0	0.0	0.0	0.0	0.0	0.0	2.0	0.0	0.0
K. Diabase	0.0	0.0	0.0	1.0	0.0	1.0	2.0	0.0	0.0	0.0	0.0	0.0	0.0	0.0	0.0
K. Red Granite	0.0	0.0	4.0	3.9	3.7	7.1	0.0	0.0	0.0	0.0	0.0	0.0	0.0	0.0	0.0
K. Intermediate	0.0	0.0	0.0	2.0	0.0	0.0	0.0	0.0	0.0	0.0	0.0	0.0	2.0	0.0	0.0
K. Gabbro	0.0	0.6	2.0	4.9	0.0	2.6	2.0	0.0	2.0	0.0	1.8	3.0	5.9	4.0	0.0
K. Troctolite/Picrite	50.0	72.7	1.0	2.0	0.0	0.3	6.0	4.0	82.0	82.4	43.9	62.0	51.0	56.0	98.0
K. Anorthosite	26.0	14.9	25.0	24.5	40.7	27.8	60.0	94.0	6.0	9.9	35.1	21.0	7.8	20.0	0.0
K. Anorth. Troctolite	4.0	4.5	3.0	2.0	1.9	1.9	4.0	2.0	4.0	2.2	0.0	2.0	3.9	8.0	2.0
K. Anorth. Gabbro	4.0	0.0	2.0	8.8	7.4	1.0	6.0	0.0	0.0	2.2	0.0	1.0	0.0	0.0	0.0
K. Hornfels	0.0	0.0	0.0	2.0	1.9	0.0	0.0	0.0	0.0	1.1	0.0	0.0	0.0	2.0	0.0
ANIMIKIE															
Sst/grwcke/argillite	0.0	0.0	5.0	10.8	7.4	25.6	2.0	0.0	4.0	0.0	0.0	0.0	2.0	2.0	0.0
Fe-Formation	0.0	0.0	5.0	1.0	3.7	0.6	0.0	0.0	0.0	0.0	0.0	0.0	2.0	0.0	0.0
Quartzite	0.0	0.0	0.0	0.0	0.0	0.0	0.0	0.0	0.0	0.0	0.0	0.0	0.0	0.0	0.0
ARCHEAN															
Granite & Gneiss	10.0	3.2	18.0	15.7	20.4	12.6	10.0	0.0	2.0	2.2	5.3	3.0	7.8	2.0	0.0
Gst & Amphibolite	2.0	3.9	0.0	3.9	0.0	1.3	2.0	0.0	0.0	0.0	0.0	4.0	3.9	0.0	0.0
Fel/Int vol & metased	2.0	0.0	3.0	2.9	9.3	0.6	4.0	0.0	0.0	0.0	14.0	2.0	7.8	6.0	0.0
Unknown	2.0	0.0	2.0	1.0	1.9	4.9	0.0	0.0	0.0	0.0	0.0	0.0	0.0	0.0	0.0
Total Pebbles Counted:	50	154	100	102	54	309	50	50	50	91	57	100	51	50	50
Dominant Lithology:	MTA	Tr	MAAn	MAAn	An	MAAn	An	An	Tr	Tr	MTA	MTA	Tr	MTA	Tr

Sample #	21752	21753	21764	21765	21766	21767
KEWEENAWAN						
NSVG Basalt	2.0	0.0	0.0	0.0	0.4	0.0
NSVG Rhyolite	0.0	0.0	0.0	0.0	0.0	0.0
NSVG Intermediate	0.0	0.0	0.0	0.0	0.0	0.0
K. Diabase	0.0	0.0	0.0	0.0	0.4	6.7
K. Red Granite	0.0	0.0	0.0	0.0	0.0	2.2
K. Intermediate	0.0	0.0	0.0	0.0	1.4	0.0
K. Gabbro	0.0	4.0	7.0	1.0	1.4	0.0
K. Troctolite/Picrite	80.0	50.0	45.0	59.8	25.7	20.0
K. Anorthosite	4.0	6.0	14.0	8.8	33.3	13.3
K. Anorth. Troctolite	6.0	4.0	8.0	9.8	8.0	6.7
K. Anorth. Gabbro	0.0	2.0	4.0	2.9	6.2	0.0
K. Hornfels	0.0	0.0	0.0	1.0	0.0	0.0
ANIMIKIE						
Sst/grwcke/argillite	2.0	2.0	1.0	0.0	7.2	2.2
Fe-Formation	0.0	0.0	1.0	0.0	0.4	6.7
Quartzite	0.0	0.0	0.0	0.0	0.4	2.2
ARCHEAN						
Granite & Gneiss	4.0	18.0	15.0	13.7	12.0	37.8
Gst & Amphibolite	2.0	4.0	0.0	0.0	3.3	0.0
Fel/Int vol & metased	0.0	10.0	5.0	2.9	0.0	2.2
Unknown	0.0	0.0	0.0	0.0	0.0	0.0
Total Pebbles Counted:	50	50	100	102	276	45
Dominant Lithology:	Tr	TAr	Tr	Tr	MAT	MAr

Table 5: Petrographic Descriptions of Pebble Thin Sections

Sample Description

- 22708 Pebble A; Drift Sample 21626 Graywacke Sandstone (Rove formation)
Fine-grained, moderate sorting, angular to subangular grains, very well cemented.
- Clasts: Quartz; feldspars, especially plagioclase (some sericitized), rare microcline, rare muscovite, biotite
Rock Fragments: Siltstone, minor chert, etc.
Matrix: Very fine-grained, grungy intergranular; chlorite, sericite, quartz?
- 22709 Pebble; Drift Sample 21200 Amphibolite (Archean)
Fine-grained, gneissic to schistose, cut by many fine veinlets, fractures. Matrix of actinolite/hornblende, with rare amphibole euhedra (small porphyroblasts). Scattered scraps of opaques along parallel foliations, few epidote granules. Veinlets etc. made of very fine-grained quartzofeldspathic material and epidote granules \pm amphibole needles.
- 22710 Pebble; Drift Sample 21739 Mela-Andesite
Fine-grained, somewhat quench textured
- Plagioclase (?): Elongate sprays and parallel mesh crystals
Quartz: Interstitial to feldspar, some in micrographic intergrowths
Actinolite: Anhedra and subhedra prisms, pseudomorphs after cpx?
Epidote (?): Small, high-relief granules
- 18199 Pebble A; Drift Sample 21221 Hornblende-Biotite Tonalite (Archean)
Fine-grained, weakly foliated.
- Plagioclase; Hornblende; Apatite; Ilmenite; Magnetite; Pyrite
Biotite: Some alteration to chlorite
Orthoclase: Dusty, altered, interstitial
Quartz: Interstitial, some poikilitic, rarely micrographic

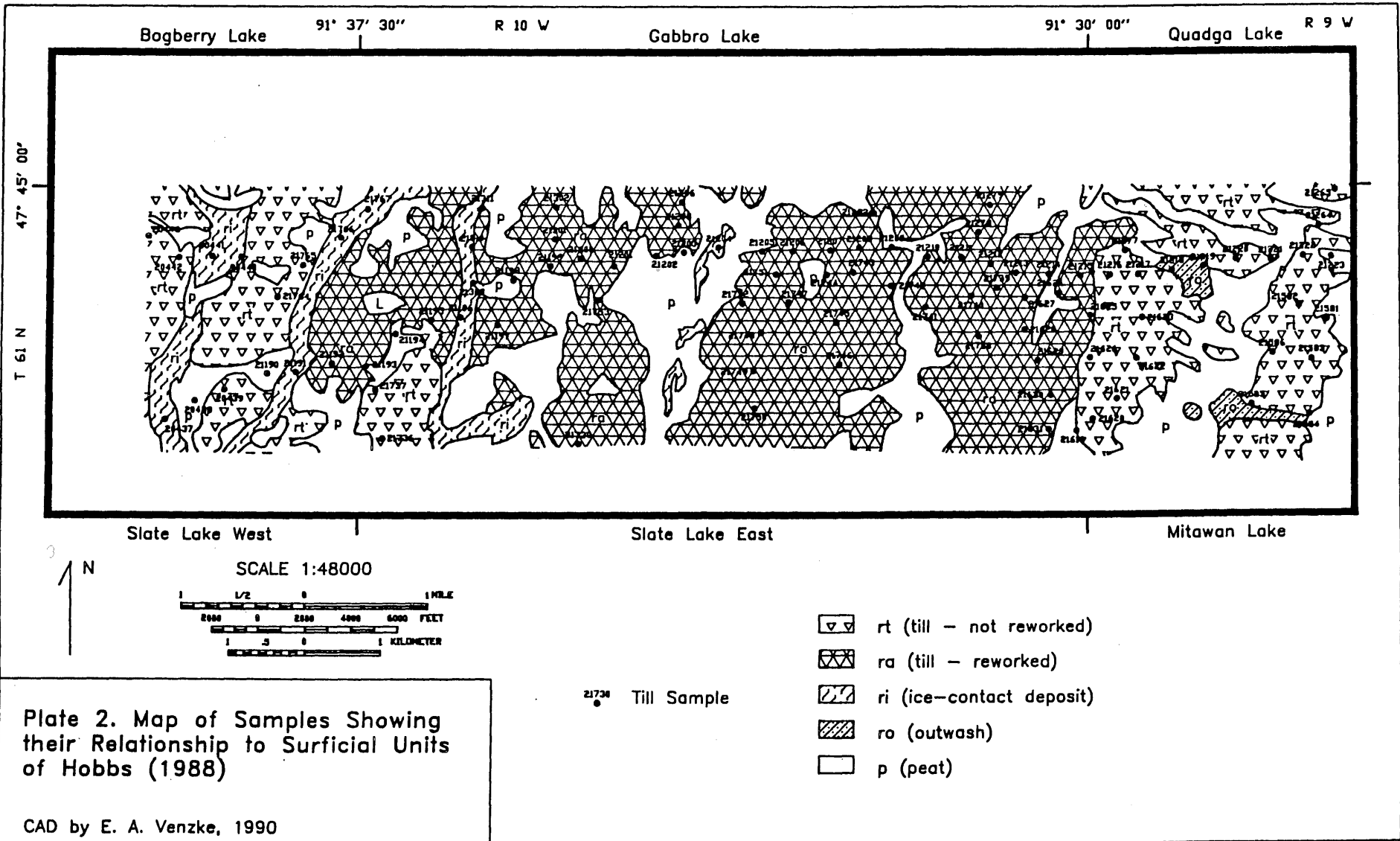


Plate 2. Map of Samples Showing their Relationship to Surficial Units of Hobbs (1988)

CAD by E. A. Venzke, 1990

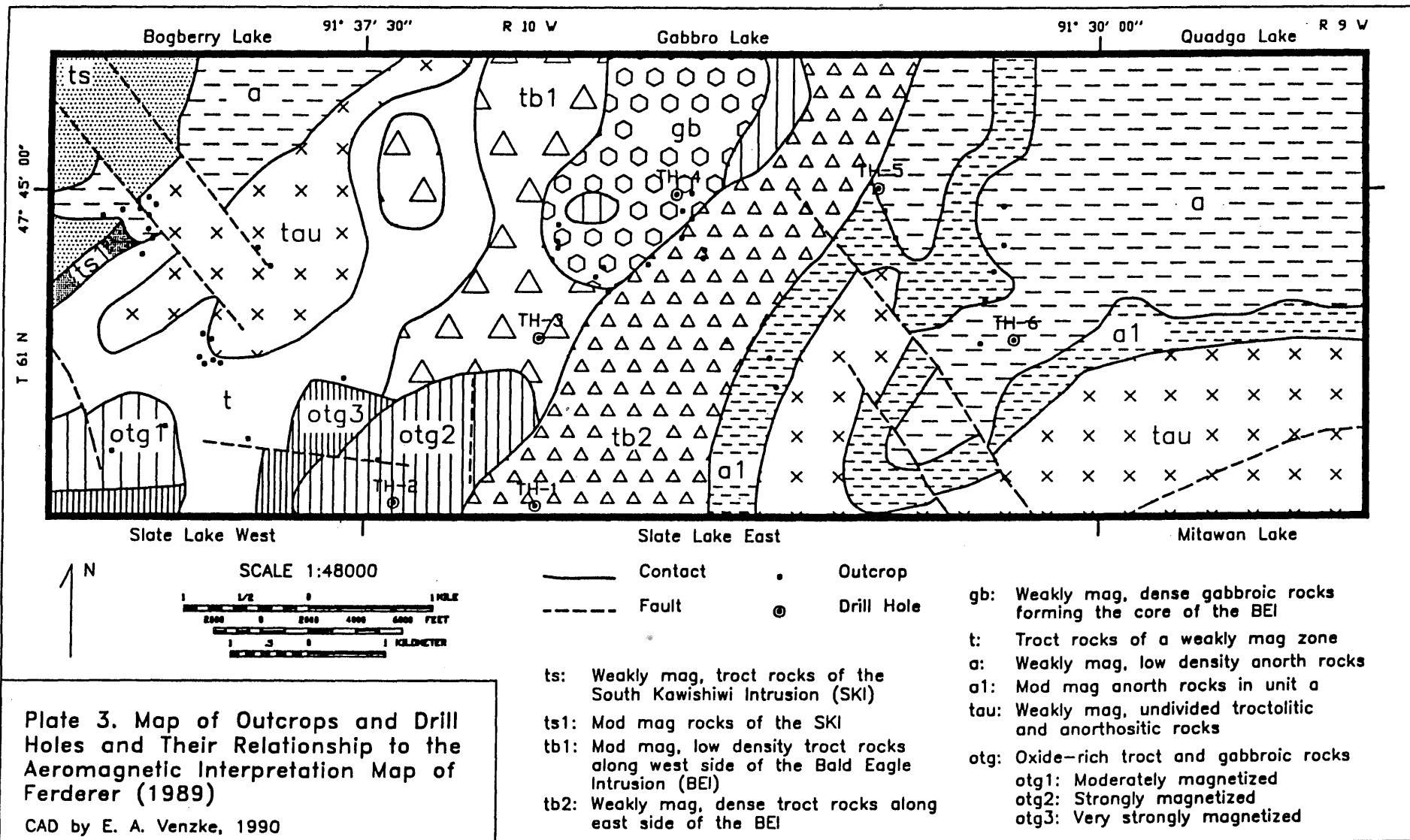


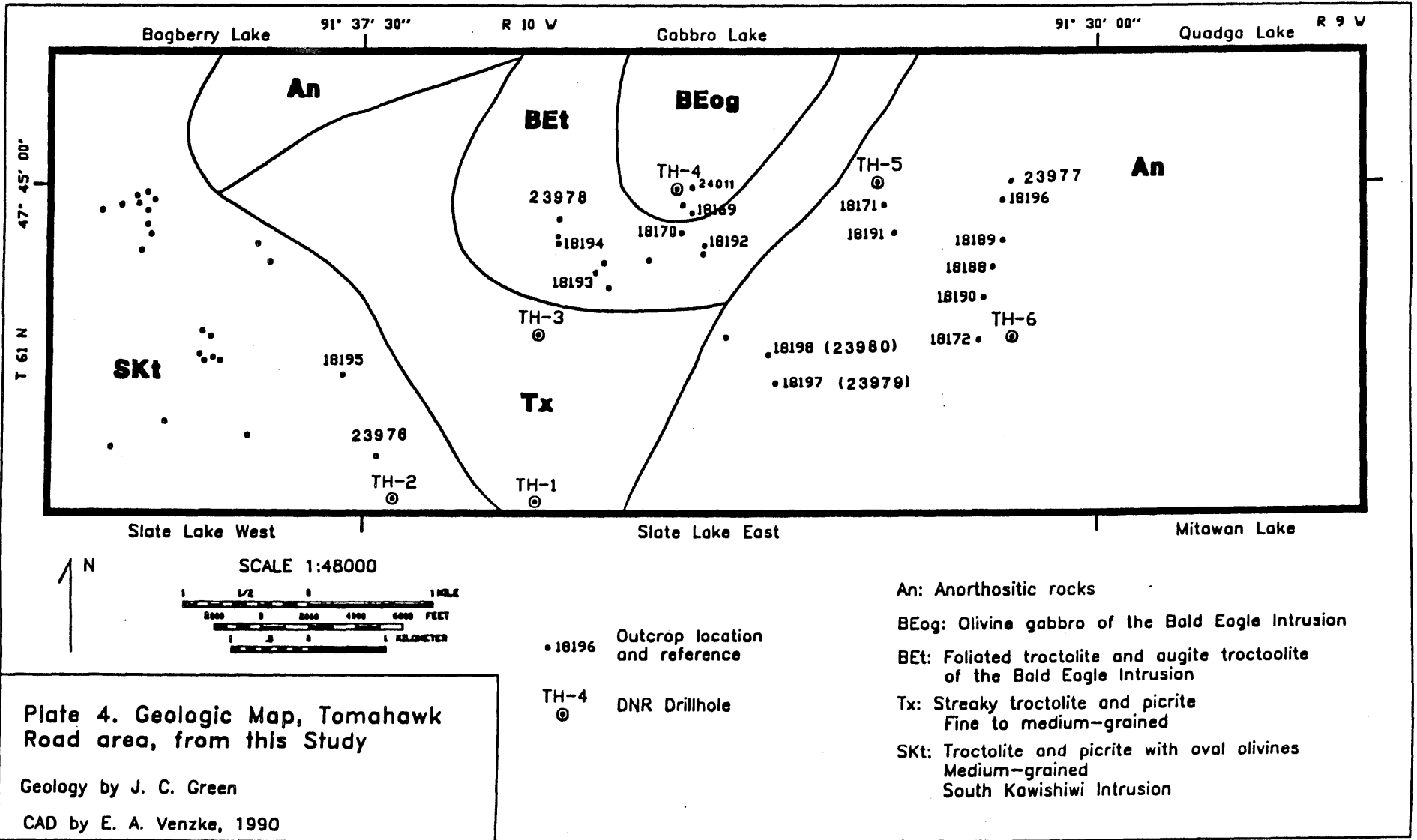
Plate 3. Map of Outcrops and Drill Holes and Their Relationship to the Aeromagnetic Interpretation Map of Ferderer (1989)

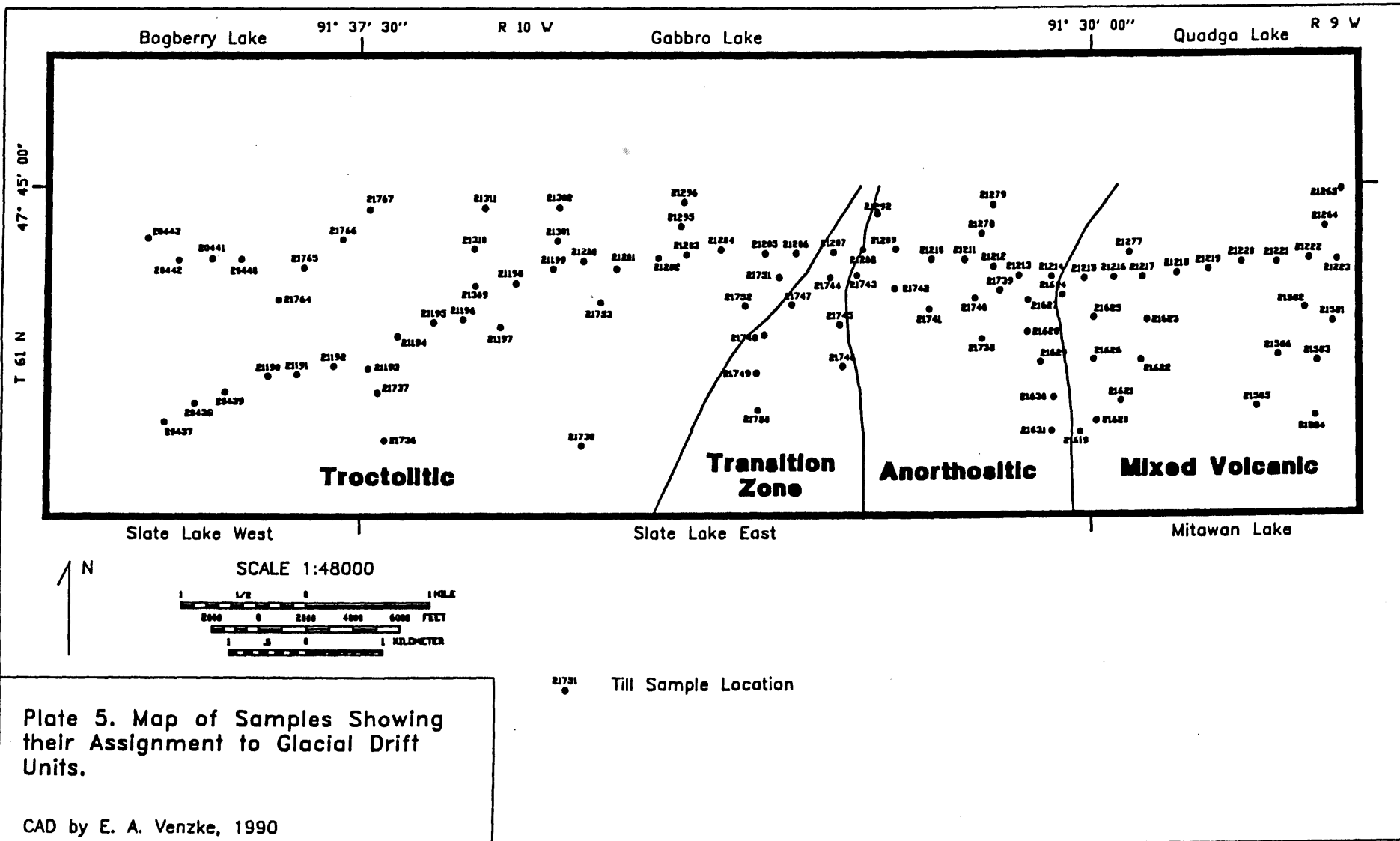
CAD by E. A. Venzke, 1990

- Contact
- - - Fault
- Outcrop
- ⊙ Drill Hole

- ts: Weakly mag, troct rocks of the South Kawishiwi Intrusion (SKI)
- ts1: Mod mag rocks of the SKI
- tb1: Mod mag, low density troct rocks along west side of the Bald Eagle Intrusion (BEI)
- tb2: Weakly mag, dense troct rocks along east side of the BEI

- gb: Weakly mag, dense gabbroic rocks forming the core of the BEI
- t: Troct rocks of a weakly mag zone
- a: Weakly mag, low density anorth rocks
- a1: Mod mag anorth rocks in unit a
- tau: Weakly mag, undivided troctolitic and anorthositic rocks
- otg: Oxide-rich troct and gabbroic rocks
 - otg1: Moderately magnetized
 - otg2: Strongly magnetized
 - otg3: Very strongly magnetized





Appendix 290-G. Drill Core and Outcrop Assay Data

Appendix 290-G. Drill Core and Outcrop Assay Data.

Sample	DDH	Footage		SiO ₂ %	Al ₂ O ₃ %	Fe ₂ O ₃ %	MnO %	MgO %	CaO %	Na ₂ O %	K ₂ O %	TiO ₂ %	P ₂ O ₅ %	LOI %	TOTAL %	S %
		Top	Bottom													
18140	TH-1	43.0	48.0	43.10	16.30	12.00	0.15	14.70	7.66	2.01	0.15	0.18	0.07	3.17	99.49	0.012
18142	TH-1	94.0	99.0	43.40	16.70	11.90	0.15	14.50	8.13	2.23	0.16	0.15	0.14	3.69	101.15	<0.002
18143	TH-1	104.0	109.0	46.00	18.40	9.42	0.12	11.50	10.10	2.53	0.16	0.22	0.16	2.32	100.93	<0.002
18145	TH-1	135.2	140.2	44.30	15.60	11.80	0.15	14.40	8.42	1.94	0.20	0.17	0.06	3.06	100.10	<0.002
18148	TH-1	168.0	173.0	46.30	18.70	8.93	0.12	10.90	10.40	2.69	0.15	0.21	0.10	2.49	100.99	0.025
18131	TH-2	71.0	76.0	40.50	15.50	11.10	0.13	16.20	8.27	1.70	0.15	0.33	0.13	6.09	100.10	<0.002
18132	TH-2	90.0	95.0	41.20	15.10	10.50	0.13	15.60	7.36	1.61	0.22	0.31	0.21	7.42	99.66	0.024
18133	TH-2	142.0	147.0	39.00	12.70	12.80	0.15	18.60	7.07	1.49	0.14	0.39	0.21	7.96	100.51	0.011
18134	TH-2	170.0	175.0	41.20	15.20	10.30	0.13	15.20	7.92	1.63	0.15	0.25	0.14	6.60	98.72	0.023
18149	TH-3	53.0	58.0	42.00	15.80	13.20	0.15	15.60	7.41	2.07	0.12	0.14	0.15	4.06	100.70	0.020
18151	TH-3	105.5	111.0	42.80	15.70	12.60	0.15	15.30	7.54	1.96	0.11	0.11	0.09	3.20	99.56	0.015
18153	TH-3	155.0	160.0	45.20	21.30	8.25	0.11	9.60	10.20	2.58	0.18	0.14	0.12	1.96	99.64	<0.002
18156	TH-4	80.0	85.0	49.10	21.90	5.16	0.07	5.71	12.90	2.93	0.26	0.32	0.30	1.26	99.91	<0.002
18157	TH-4	140.0	145.0	49.70	21.30	5.51	0.08	6.59	13.20	2.81	0.39	0.31	0.04	1.33	101.26	0.027
18159	TH-5	80.0	85.0	49.20	27.40	3.57	0.05	3.04	12.00	3.54	0.29	0.27	0.14	0.86	100.36	0.014
18162	TH-5	165.0	170.0	50.40	27.30	2.88	0.04	2.12	12.10	3.58	0.31	0.31	0.14	0.59	99.77	0.013
18165	TH-6	75.0	80.0	50.80	26.20	3.84	0.05	2.00	11.80	3.83	0.40	0.46	0.22	0.50	100.10	0.048
18166	TH-6	138.0	143.0	49.10	24.20	7.00	0.09	2.35	12.00	3.44	0.56	1.43	0.10	0.20	100.47	0.038
18169	OC	10-61-10	NE-NW	50.70	23.10	5.32	0.08	5.15	12.20	2.98	0.24	0.48	0.09	0.35	100.69	0.02
18170	OC	26-61-10	NW-NE	46.20	14.20	11.40	0.15	13.80	9.54	1.97	0.14	0.25	0.11	1.29	99.05	0.02
18171	OC	25-61-10	NE-NE	49.00	26.00	4.73	0.05	2.83	11.50	3.23	0.41	0.73	0.15	0.65	99.28	<0.02
18172	OC	30-61-09	SW-SE	49.00	28.00	4.03	0.05	1.48	11.60	3.30	0.44	0.61	0.17	0.34	99.02	0.02
18192	OC	26-61-10	SE-NW	45.60	17.90	9.90	0.13	11.60	8.52	2.30	0.18	0.15	0.11	2.45	98.84	0.02
18193	OC	27-61-10	Center	45.00	15.60	12.70	0.16	15.50	7.67	1.80	0.15	0.20	0.12	0.19	99.09	<0.02
18196	OC	19-61-09	SE	47.40	27.60	5.13	0.06	2.17	11.30	3.06	0.45	1.92	0.25	0.67	100.01	<0.02
23976	OC	5-60-10	NE-NE	46.70	19.80	9.55	0.12	10.00	9.07	2.56	0.17	0.10	0.08	0.48	98.63	<0.02
23977	OC	19-61-09	NE-SE	47.80	30.00	2.43	0.03	1.69	13.00	2.75	0.18	0.21	0.11	0.30	98.50	<0.02
23978	OC	27-61-10	NW-NW	45.50	25.00	6.18	0.07	6.90	10.70	2.47	0.28	0.50	0.12	1.02	98.74	0.06
23980	OC	35-61-10	NE-NE	48.30	27.50	4.05	0.05	2.26	12.00	3.02	0.39	0.70	0.16	0.40	98.83	<0.02
24011	OC	23-61-10	SE-SE	50.80	14.20	7.12	0.12	8.76	14.40	2.01	0.17	0.63	0.19	0.54	98.94	0.03
20141	FL-2	52.1	61.3	46.28	18.44	9.81	0.12	11.79	10.14	2.31	0.11	0.53	0.08		99.61	0.080
20142	FL-1	43.2	50.7	37.18	16.15	23.32	0.17	5.27	12.00	1.95	0.02	3.77	0.08		99.91	0.160
20143	FL-1	92.6	95.5	34.49	13.48	27.43	0.21	6.18	11.55	1.33	0.05	5.22	0.05		99.99	0.010
20145	FL-1	100.0	110.0	35.89	14.18	26.08	0.21	5.50	11.49	1.75	0.01	4.83	0.04		99.98	0.010
20146	FL-1	115.5	125.5	41.52	21.32	14.35	0.13	4.31	13.01	2.21	0.06	2.45	0.06		99.42	0.010
20147	NE-2	269.0	275.0	41.84	15.20	17.46	0.18	7.09	11.13	2.61	0.21	3.08	0.28		99.08	0.020
20148	NE-2	287.0	289.0	40.42	15.07	19.26	0.18	7.37	10.90	2.63	0.12	3.72	0.38		100.05	0.110
20149	NE-2	303.0	306.0	42.74	15.48	18.57	0.22	7.65	8.66	2.46	0.01	3.16	0.28		99.23	0.020
20150	NE-2	554.0	564.0	47.38	19.93	10.97	0.12	3.77	10.99	3.43	0.21	3.25	0.11		100.16	0.030
20151	NE-2	746.0	756.0	45.85	17.46	12.56	0.14	4.67	11.18	3.11	0.27	4.64	0.15		100.03	0.030

Appendix 290-G. Drill Core and Outcrop Assay Data.

Sample	DDH	Footage		Au ppb	Pt ppb	Pd ppb	Ag ppm	Cl ppm	F ppm	Cu ppm	Ni ppm	Zn ppm	Pb ppm	Cr (XRF) ppm	Cr (ICP) ppm	Co ppm	V ppm	Rb ppm	Cs ppm	Sr ppm	Ba ppm
		Top	Bottom																		
18140	TH-1	43.0	48.0	<1	<5	<1	<0.5	170	28	23	487	71	9	353	157	74	12	56		159	33
18142	TH-1	94.0	99.0	<1	<5	1	<0.5	290	23	20	438	65	13	302	145	68	10	29		157	38
18143	TH-1	104.0	109.0	<1	<5	<1	<0.5	190	30	19	332	51	7	337	166	52	14	<20		154	39
18145	TH-1	135.2	140.2	<1	<5	<1	<0.5	170	67	15	422	64	7	351	118	67	10	<20		111	30
18148	TH-1	168.0	173.0	<1	<5	<1	<0.5	160	31	12	286	45	5	443	181	47	15	<20		139	30
18131	TH-2	71.0	76.0	4	<5	1	<0.5	310	54	61	639	73	13	93	83	66	13	<20		181	39
18132	TH-2	90.0	95.0	1	<5	2	<0.5	210	47	55	673	67	14	145	76	68	14	<20		201	38
18133	TH-2	142.0	147.0	1	<5	2	<0.5	260	56	58	807	80	11	153	85	81	18	<20		154	36
18134	TH-2	170.0	175.0	1	<5	4	<0.5	380	39	84	694	65	9	148	98	69	14	<20		168	35
18149	TH-3	53.0	58.0	<1	<5	<1	<0.5	330	21	19	455	71	9	224	136	82	10	71		185	37
18151	TH-3	105.5	111.0	<1	<5	1	<0.5	160	<20	18	453	73	13	199	98	81	8	21		160	35
18153	TH-3	155.0	160.0	<1	<5	<1	<0.5	160	<20	22	262	52	4	62	91	46	9	<20		194	44
18156	TH-4	80.0	85.0	<1	<5	<1	<0.5	100	32	18	83	24	<2	507	263	16	27	<20		141	39
18157	TH-4	140.0	145.0	<1	<5	1	0.5	70	29	16	88	25	5	548	269	18	26	57		133	36
18159	TH-5	80.0	85.0	1	<5	2	<0.5	70	45	34	72	25	3	50	117	13	11	<20		193	61
18162	TH-5	165.0	170.0	<1	<5	1	<0.5	90	47	22	36	18	6	50	102	8	13	<20		207	66
18165	TH-6	75.0	80.0	1	<5	8	<0.5	50	45	48	43	23	5	26	111	10	17	<20		163	60
18166	TH-6	138.0	143.0	<1	<5	4	<0.5	150	45	102	37	28	3	52	119	11	91	<20		156	77
18169	OC	10-61-10	NE-NW	2	<5	14	<0.5		64	94	85	20	6	391	209	15	28	<20		139	36
18170	OC	26-61-10	NW-NE	<1	<5	<1	0.7		51	17	378	47	9	854	252	61	22	79		110	23
18171	OC	25-61-10	NE-NE	<1	<5	2	<0.5		48	93	68	25	9	48	123	15	60	64		184	45
18172	OC	30-61-09	SW-SE	<1	<5	2	<0.5		85	75	28	23	9	49	150	8	65	73		218	61
18192	OC	26-61-10	SE-NW	<1	<5	<1	<0.5		40	15	310	45	8	444	151	56	11	46		156	29
18193	OC	27-61-10	Center	<1	<5	<1	0.8		162	24	515	63	10	404	231	75	20	78		132	31
18196	OC	19-61-09	SE	<1	<5	1	<0.5		90	72	41	28	8	42	112	11	47	<20		210	74
23976	OC	5-60-10	NE-NE	<1	<5	<1	0.8		37	14	269	48	11	61	96	55	7	86		143	29
23977	OC	19-61-09	NE-SE	<1	5	3	<0.5		34	43	62	18	<2	22	65	9	7	36		304	42
23978	OC	27-61-10	NW-NW	<1	<5	<1	<0.5		65	58	249	31	9	626	199	28	17	71		201	55
23980	OC	35-61-10	NE-NE	<1	<5	2	<0.5		64	68	37	17	12	52	124	7	31	80		222	65
24011	OC	23-61-10	SE-SE	<1	<5	<1	0.5		56	20	54	19	3	863	202	12	31	95		69	24
20141	FL-2	52.1	61.3	3	<10	11	<0.5	100	140	173	480	61		500		69	85	1	19	229	73
20142	FL-1	43.2	50.7	2	<10	18	<0.5	110	100	67	85	84		200		92	364	<1	41	245	28
20143	FL-1	92.6	95.5	<1	<10	11	<0.5	110	360	36	140	102		195		120	500	1	48	181	29
20145	FL-1	100.0	110.0	2	<10	6	<0.5	185	<20	45	100	100		185		110	433	<1	45	224	21
20146	FL-1	115.5	125.5	<1	<10	11	<0.5	200	<20	38	120	58		230		64	233	<1	26	300	43
20147	NE-2	269.0	275.0	5	<10	15	<0.5	160	100	392	200	63		1200		87	312	2	34	221	104
20148	NE-2	287.0	289.0	5	<10	9	<0.5	110	540	1200	200	88		1400		97	370	<1	38	230	99
20149	NE-2	303.0	306.0	2	<10	5	<0.5	160	<20	99	265	133		5250		103	445	<1	34	219	103
20150	NE-2	554.0	564.0	<1	<10	<2	<0.5	105	<20	265	55	56		150		58	286	2	21	338	145
20151	NE-2	746.0	756.0	2	<10	5	<0.5	145	<20	249	70	80		80		69	396	2	25	301	174

G-3

Appendix 290-G. Drill Core and Outcrop Assay Data.

Sample	DDH	Footage		Zr ppm	Bi ppm	As ppm	Sb ppm	Se ppm	Te ppm	Mo ppm	Sn ppm	Sc ppm	Y ppm	Li ppm	Be ppm	B ppm	La ppm	Ce ppm	Nb ppm	Ta ppm	W ppm
		Top	Bottom																		
18140	TH-1	43.0	48.0	<1	<5	<0.5	<0.2	<1	<10	<1	<20	1	1	4	<0.5	<10	3	<5	10	<3	<10
18142	TH-1	94.0	99.0	<1	<5	<0.5	<0.2	<1	<10	<1	<20	<1	1	5	<0.5	<10	2	<5	10	<3	<10
18143	TH-1	104.0	109.0	<1	<5	<0.5	<0.2	<1	<10	<1	<20	<1	1	4	<0.5	<10	1	<5	9	<3	<10
18145	TH-1	135.2	140.2	<1	<5	<0.5	<0.2	<1	<10	<1	<20	<1	1	6	<0.5	<10	<1	<5	9	<3	<10
18148	TH-1	168.0	173.0	<1	<5	<0.5	<0.2	<1	<10	<1	<20	<1	<1	4	<0.5	<10	<1	<5	8	<3	<10
18131	TH-2	71.0	76.0	<1	<5	0.5	<0.2	<1	<10	<1	<20	1	2	4	<0.5	<10	4	<5	10	<3	<10
18132	TH-2	90.0	95.0	<1	<5	<0.5	<0.2	<1	<10	<1	<20	1	2	5	<0.5	26	4	<5	11	<3	<10
18133	TH-2	142.0	147.0	<1	<5	<0.5	<0.2	<1	<10	<1	<20	2	2	4	<0.5	15	4	<5	11	<3	<10
18134	TH-2	170.0	175.0	<1	8	<0.5	<0.2	<1	<10	<1	<20	1	2	5	<0.5	<10	4	<5	11	<3	<10
18149	TH-3	53.0	58.0	<1	<5	<0.5	2.0	1	<10	<1	<20	1	1	4	<0.5	<10	2	<5	11	<3	<10
18151	TH-3	105.5	111.0	<1	<5	<0.5	0.9	<1	<10	<1	<20	1	1	4	<0.5	<10	2	<5	11	<3	<10
18153	TH-3	155.0	160.0	<1	<5	<0.5	0.6	<1	<10	<1	<20	<1	1	4	<0.5	<10	2	<5	9	<3	<10
18156	TH-4	80.0	85.0	<1	<5	<0.5	0.4	<1	<10	<1	<20	<1	1	7	<0.5	24	1	<5	5	<3	<10
18157	TH-4	140.0	145.0	<1	<5	<0.5	0.2	<1	<10	<1	<20	<1	1	10	<0.5	26	1	<5	6	<3	<10
18159	TH-5	80.0	85.0	<1	<5	<0.5	0.2	<1	<10	<1	<20	<1	2	6	<0.5	<10	2	<5	5	<3	<10
18162	TH-5	165.0	170.0	<1	<5	<0.5	0.2	<1	<10	<1	<20	<1	2	6	<0.5	<10	2	<5	5	<3	<10
18165	TH-6	75.0	80.0	<1	<5	<0.5	<0.2	<1	<10	<1	<20	<1	3	3	<0.5	<10	3	<5	4	<3	<10
18166	TH-6	138.0	143.0	<1	<5	0.5	0.2	<1	<10	<1	<20	<1	10	4	<0.5	<10	8	<5	5	<3	<10
18169	OC	10-61-10	NE-NW	<1	<5	2.0	<0.2	<1	<10	<1	<20	2	1	3	<0.5	10	3	9	<1	<3	<10
18170	OC	26-61-10	NW-NE	1	6	1.0	<0.2	<1	<10	<1	<20	3	<1	2	<0.5	<10	2	5	3	27	<10
18171	OC	25-61-10	NE-NE	1	<5	1.0	<0.2	<1	<10	1	<20	1	2	5	<0.5	<10	4	10	<1	<3	<10
18172	OC	30-61-09	SW-SE	2	<5	1.0	<0.2	<1	<10	<1	<20	<1	5	5	<0.5	<10	7	13	<1	<3	<10
18192	OC	26-61-10	SE-NW	1	<5	1.0	<0.2	<1	<10	<1	<20	3	<1	3	<0.5	<10	2	<5	2	<3	<10
18193	OC	27-61-10	Center	2	<5	1.0	<0.2	<1	<10	1	<20	3	1	4	<0.5	<10	3	6	4	<3	<10
18196	OC	19-61-09	SE	2	<5	1.0	<0.2	<1	<10	<1	<20	1	4	5	<0.5	10	6	15	<1	<3	<10
23976	OC	5-60-10	NE-NE	<1	<5	<1	<0.2	<1	<10	<1	<20	3	<1	3	<0.5	<10	3	6	3	<3	<10
23977	OC	19-61-09	NE-SE	2	<5	1.0	<0.2	<1	<10	<1	<20	<1	2	5	<0.5	<10	3	<5	<1	<3	<10
23978	OC	27-61-10	NW-NW	2	<5	<1	<0.2	<1	<10	<1	<20	2	3	4	<0.5	<10	6	11	<1	<3	<10
23980	OC	35-61-10	NE-NE	<1	<5	<1	1.5	<1	<10	1	<20	1	3	5	<0.5	10	5	10	<1	<3	<10
24011	OC	23-61-10	SE-SE	1	<5	<1	<0.2	<1	<10	<1	<20	3	<1	1	<0.5	<10	2	11	<1	14	<10
20141	FL-2	52.1	61.3	7	<1	2	<1	<1	1			14	3								
20142	FL-1	43.2	50.7	7	<1	1	<1	1	<1			39	4								
20143	FL-1	92.6	95.5	16	1	1	<1	3	<1			43	8								
20145	FL-1	100.0	110.0	13	1	2	<1	2	1			40	2								
20146	FL-1	115.5	125.5	9	<1	2	<1	1	1			22	5								
20147	NE-2	269.0	275.0	28	<1	1	<1	<1	<1			32	21								
20148	NE-2	287.0	289.0	19	<1	2	<1	3	1			30	16								
20149	NE-2	303.0	306.0	33	<1	1	<1	<1	1			21	16								
20150	NE-2	554.0	564.0	14	<1	3	<1	<1	<1			25	3								
20151	NE-2	746.0	756.0	48	1	3	<1	2	1			35	11								

Appendix 290-G. Drill Core and Outcrop Assay Data.

Sample	DDH	Footage		Ga ppm	Cd ppm	Hg ppb	FeO* %	Recalculated Iron		MG#
		Top	Bottom					Fe ₂ O ₃ %	FeO %	
18140	TH-1	43.0	48.0	7	<1	<5	10.80	2.40	8.64	57.65
18142	TH-1	94.0	99.0	7	<1	<5	10.71	2.38	8.57	57.52
18143	TH-1	104.0	109.0	5	<1	<5	8.48	1.88	6.78	57.57
18145	TH-1	135.2	140.2	8	<1	<5	10.62	2.36	8.49	57.56
18148	TH-1	168.0	173.0	5	1.0	<5	8.04	1.79	6.43	57.56
18131	TH-2	71.0	76.0	5	<1	<5	9.99	2.22	7.99	61.86
18132	TH-2	90.0	95.0	8	<1	<5	9.45	2.10	7.56	62.28
18133	TH-2	142.0	147.0	9	<1	<5	11.52	2.56	9.21	61.76
18134	TH-2	170.0	175.0	6	<1	<5	9.27	2.06	7.41	62.12
18149	TH-3	53.0	58.0	9	<1	<5	11.88	2.64	9.50	56.77
18151	TH-3	105.5	111.0	7	<1	<5	11.34	2.52	9.07	57.44
18153	TH-3	155.0	160.0	<2	<1	<5	7.42	1.65	5.94	56.39
18156	TH-4	80.0	85.0	3	<1	<5	4.64	1.03	3.71	55.15
18157	TH-4	140.0	145.0	4	<1	<5	4.96	1.10	3.97	57.07
18159	TH-5	80.0	85.0	<2	<1	<5	3.21	0.71	2.57	48.62
18162	TH-5	165.0	170.0	<2	<1	<5	2.59	0.58	2.07	45.00
18165	TH-6	75.0	80.0	2	<1	<5	3.46	0.77	2.76	36.66
18166	TH-6	138.0	143.0	3	<1	<5	6.30	1.40	5.04	27.17
18169	OC	10-61-10	NE-NW	9	<1	<5	4.79	1.06	3.83	51.83
18170	OC	26-61-10	NW-NE	8	2.0	<5	10.26	2.28	8.21	57.36
18171	OC	25-61-10	NE-NE	11	1.0	<5	4.26	0.95	3.40	39.94
18172	OC	30-61-09	SW-SE	11	<1	<5	3.63	0.81	2.90	28.98
18192	OC	26-61-10	SE-NW	10	1.0	<5	8.91	1.98	7.13	56.56
18193	OC	27-61-10	Center	9	<1	<5	11.43	2.54	9.14	57.56
18196	OC	19-61-09	SE	11	<1	<5	4.62	1.03	3.69	31.98
23976	OC	5-60-10	NE-NE	10	<1	<5	8.59	1.91	6.87	53.78
23977	OC	19-61-09	NE-SE	10	<1	<5	2.19	0.49	1.75	43.60
23978	OC	27-61-10	NW-NW	11	<1	<5	5.56	1.24	4.45	55.37
23980	OC	35-61-10	NE-NE	11	<1	<5	3.64	0.81	2.92	38.28
24011	OC	23-61-10	SE-SE	5	<1	<5	6.41	1.42	5.13	57.76
20141	FL-2	52.1	61.3				8.83	1.96	7.06	57.19
20142	FL-1	43.2	50.7				20.98	4.66	16.79	20.07
20143	FL-1	92.6	95.5				24.68	5.49	19.75	20.02
20145	FL-1	100.0	110.0				23.47	5.22	18.77	18.99
20146	FL-1	115.5	125.5				12.91	2.87	10.33	25.03
20147	NE-2	269.0	275.0				15.71	3.49	12.57	31.10
20148	NE-2	287.0	289.0				17.33	3.85	13.86	29.84
20149	NE-2	303.0	306.0				16.71	3.71	13.37	31.40
20150	NE-2	554.0	564.0				9.87	2.19	7.90	27.64
20151	NE-2	746.0	756.0				11.30	2.51	9.04	29.24

